UNIVERSITY OF LONDON THESIS

Degree PhD Year 2006 Name of Author SIMMGEN Marcus

The role of liver insulin signalling pathways in carbohydrate and lipid homeostasis

---

Marcus Simmgen

Centre for Diabetes & Endocrinology
Rayne Institute
University College London
London WC1E 6JJ

Thesis submitted to the University of London
for the degree of Doctor of Philosophy 2006

ProQuest LLC
789 East Eisenhower Parkway
P.O. Box 1346
Ann Arbor, MI 48106-1346

ACKNOWLEDGEMENTS

The Wellcome Trust made this work possible and I am extremely thankful for its generosity. Beyond the financial support, the Trust's grant has allowed me to work in two first-class research institutions, Imperial College and University College London. Their environment and facilities have greatly stimulated and enabled my interest in scientific research.

Many people helped me in the course of this project, and I would like to thank first and foremost my supervisor Professor Dominic Withers for his encouragement, trust, and support. Without his help and backing I would not have been able to undertake this fellowship. Furthermore, his guidance was instrumental to my success to complete the presented work in time, when after two years my initial project had to be abandoned.

The growing team of dear colleagues taught me the nuts and bolts of research, and I much hope that a fraction of their brightness and enthusiasm might have rubbed off on me. I am very grateful indeed to David Bedford for being an ideal companion in the animal house and for sharing his expertise in protein work. Munim Choudhury, as well as Marika Charalambous and Colin Selman were the fountain of much knowledge and advice throughout this research, and they also inspired many enjoyable scientific discussions and philosophical debates. I owe much of the fun of these three years, however, to all members of the lab who kept up a warm-hearted atmosphere through the ups and downs of this time.

My particular thanks go to the collaborators in Cambridge and Toulouse I was very fortunate to work with. In particular, I would like to thank Miguel López in Dr Antonio Vidal-Puig's lab at Addenbrooke's Hospital who taught me the art of real-time PCR and its data analysis. His clear and systematic approach to any work made it rather easy for me to follow, and he, too, inspired many fruitful conversations.

At the Hôpital Rangueil in Professor Remy Burcelin's lab I learned much about mouse surgery and the conduct of clamp studies in conscious animals, despite my limited fluency in French. Miguel Iglesias and Claude Knauf answered my questions with ease and I am very grateful for their goodwill and patience.

Throughout this work I have been conscious that mice, sentient animals, were central to answering the scientific questions posed. I believe that such research remains vital to advance our understanding of disease, yet at the same time I would like to acknowledge this fact, since without the essential specimens they provided this research would not have been possible.

ABSTRACT

The prevalence of type 2 diabetes mellitus is rapidly rising worldwide, despite an increasing awareness of the problem. Hepatic insulin resistance is a key factor in the pathogenesis of type 2 diabetes. The liver is central to the maintenance of glucose homeostasis, but the role of intrinsic liver insulin signalling *versus* indirect effects on the regulation of hepatic metabolism remains under debate. Insulin receptor substrate-2 is a major signalling molecule downstream of the insulin receptor. Global gene targeting in mice and *in vitro* studies have suggested that Irs2 mediates most metabolic insulin effects in the liver. I hypothesised that the liver-specific deletion of *Irs2* would lead to a significant dysregulation of glucose homeostasis, thus further clarifying its role in the development of type 2 diabetes. The work presented in this thesis describes the characterisation of mice with a selective deletion of the *Irs2* gene in the liver (*LivIrs2KO*), generated using the Cre/*loxP* technique. Hepatocyte-specific *Irs2* excision was achieved by an albumin promoter-driven recombination event. The animals bred and survived normally into adulthood. Hepatic insulin signalling events were investigated by immunoblotting and found to be normal. Glucose and lipid metabolism was also unaltered in *LivIrs2KO* mice, except for a mild rise in fasted glucose following a period on a high fat diet. Hyperinsulinaemic-euglycaemic clamp studies revealed a small reduction in glucose utilisation, accounted for by reduced glycogen synthesis. Quantitative gene expression analysis showed elevated *G6pc* and reduced *Gck* levels in *LivIrs2KO* mice after a prolonged fast, but appropriate gene regulation when feeding. Glycogen synthase expression was comparable to controls, as were genes of lipid metabolism. The liver function remained normal in *LivIrs2KO* animals except for a mild rise in transaminases. In summary, surprisingly, only mild abnormalities resulted from hepatic *Irs2* deletion. This suggests that Irs2-associated intrinsic insulin signalling in the liver is not required for long-term glucose and lipid homeostasis and that extra-hepatic Irs2-dependent mechanisms are involved in the regulation of these processes.

CONTENTS

ABBREVIATIONS AND GENE SYMBOLS

Symbols for mouse genes and corresponding proteins were used in accordance to the rules set out by the International Committee on Standardized Genetic Nomenclature for Mice (1). The National Center for Biotechnology Information (NCBI) databases 'Entrez Gene' and the 'Entrez Protein' were accessed in May 2006 [http://www.ncbi.nlm.nih.gov/]. Mouse gene symbols generally begin with an uppercase letter, followed by lower case letters and numbers and are *italicised*, whereas gene products are shown in regular typefont.

Abbreviation	**Full name**
4EBP1	4E-binding protein-1
Acc	acetyl-CoA carboxylase
Acox1	acetyl-CoA oxidase-1, peroxisomal isoform
ADP	adenosine diphosphate
AGC kinases	protein kinases regulated by cAMP (A), cGMP (G), or Ca^{2+} (C)
ALT	alanine transaminase
AS160	Akt substrate of 160kDa
AST	aspartate transaminase
ATP	adenosine triphosphate
AUC	area-under-the-curve
Bad	Bcl2-associated death agonist
Bcl2	B-cell lymphoma-associated protein-2
cDNA	complementary DNA
ChREBP	carbohydrate response element-binding protein
Cpt1a	carnitine palmitoyl transferase-1, liver isoform
Cre	loxP-specific recombinase enzyme
eIF2B	eukaryotic initiation factor 2 B
ELISA	enzyme-linked immuno-sorbent assay

Abbreviation	Full name
ERK	extracellular signal-regulated kinase
Fasn	fatty acid synthase
FBG	fasted blood glucose
FIRKO	fat-specific insulin receptor knockout
Fox	forkhead box-containing protein
G6pc	glucose 6-phosphatase
Gab1	Grb2-associated binder-1
GABA	gamma-aminobutyric acid
Gck	glucokinase
GDP	guanine diphosphate
Glut	glucose transporter
Grb2	growth factor receptor-bound protein-2
Gsk3	glycogen synthase kinase-3
GTP	guanine triphosphate
GTT	glucose tolerance test
Gys2	glycogen synthase, liver isoform
HFD	high fat diet
HGP	hepatic glucose production
Hnf4a	hepatocyte nuclear factor-4 alpha
HPO	horseradish peroxidase
i.p.	intraperitoneal
Igf1	insulin-like growth factor-1
Igf1r	insulin-like growth factor-1 receptor
Igfbp1	insulin-like growth factor-binding protein-1
Insr	insulin receptor
IRKO	insulin receptor knockout
Irr	insulin receptor-related receptor
Irs	insulin receptor substrate
ITT	insulin tolerance test

Abbreviation	Full name
IU	international units
IVC	inferior vena cava
K_{ATP} channel	ATP-activated potassium channel
LIRKO	liver-specific insulin receptor knockout
loxP	locus of 'cross(x)-over'
MAPK	mitogen-activated protein kinase
MEK	MAPK- and ERK-related kinase
MIRKO	muscle-specific insulin receptor knockout
mRNA	messenger RNA
mTOR	mammalian target of rapamycin
NEFA	non-esterified fatty acid
NIRKO	neuron-specific insulin receptor knockout
p70S6K	protein-70 S6 kinase
Pck1	phospho*enol*pyruvate carboxykinase, cytosolic isoform
PCR	polymerase chain reaction
Pdk1	phosphoinositide-dependent kinase-1
Pfkfb1	phosphofructokinase/fructose biphosphatase-1
Pgc1	peroxisome proliferator-activated receptor-gamma coactivator-1
PH	pleckstrin homology
PI3K	phosphatidylinositol-3 kinase
PIP3	phosphatidylinositol triphosphate
PKA	protein kinase A
PKB	protein kinase B
PKC	protein kinase C
Pklr	pyruvate kinase, liver and red cell isoform
Ppara	peroxisome proliferator-activated receptor-alpha
Pparg	peroxisome proliferator-activated receptor-gamma
PTB	phosphotyrosine binding

Abbreviation	Full name
rictor	rapamycin-insensitive companion of mTOR
RIP	rat insulin promoter
RNAi	RNA interference
Ser	serine
SH2	src homology-2
Shc	SH2-containing protein
Shp2	SH2 domain phosphatase-2
Sos	son of sevenless
Srebp/f	sterol regulatory element-binding protein/factor
TG	triglycerides
Thr	threonine
TSC1	tuberous sclerosis complex 1, hamartin
TSC2	tuberous sclerosis complex 2, tuberin
UCL	University College London
VLDL	very low density lipoprotein

FIGURES

Chapter 1

Chapter 2

Chapter 3

Chapter 4

Chapter 5

Chapter 6

Chapter 7

Chapter 8

Chapter 9

TABLES

Chapter 2

Chapter 1 INTRODUCTION

1.1 Diabetes mellitus

Diabetes mellitus is a chronic progressive disease characterised by the failure of glucose homeostasis, due to an absolute or relative deficiency in circulating insulin, leading to elevated plasma glucose levels.

Two main forms of diabetes are recognised that differ in their aetiology and relative frequency: Type 1 diabetes constitutes around 10% of cases and is a result of immune-mediated destruction of the pancreatic β-cells, thus causing severe insulin deficiency (2). Type 2 diabetes comprises more than 85% of cases and is a consequence of several pathophysiological events: Insulin resistance in the classic target organs of skeletal muscle and adipose tissue, increased glucose output from the liver, and a failure of insulin secretion (3).

1.1.1 The burden of type 2 diabetes

The global rise in the prevalence of diabetes that has been observed during the recent decades is almost entirely due to the increased prevalence of type 2 diabetes, driven by rising levels of obesity (4). Diabetes affects 1.8 million people In the UK with a further, hidden prevalence estimated at 1.5 - 3.1% (5). A predicted 366 million people world-wide will be affected by 2030 (6). The majority of future cases are expected to occur in developing countries, adding a heavy burden to their healthcare costs (7).

The care for patients with diabetes costs more than twice as much as for non-diabetic patients (8). In the UK the annual expenditure associated with type 2 diabetes is expected to reach 9.4% of the NHS budget in 2011 (9). The disease-associated burden to the individual patient is related to the risk of micro- and

macrovascular complications. In the developed world, diabetes is the most important single reason for visual loss (10), the leading cause of end-stage renal failure (11), and also responsible for the majority of non-traumatic amputations (12). Diabetes equally is a main risk factor for atherosclerosis, and hence for myocardial infarction, stroke and peripheral vascular disease (13).

Lifestyle changes leading to physical inactivity and obesity are mainly responsible for the rise in type 2 diabetes, with a strong genetic component long being established through epidemiological studies. Lifetime risk for offspring to develop diabetes is an estimated 40% and 70% with one or both parents affected, respectively. Whilst in the past type 2 diabetes was predominantly a disease of the elderly, recent evidence shows the disorder is now developing at a younger age, with even adolescents and children being diagnosed with type 2 diabetes (14).

1.1.2 Insulin resistance and pathogenesis of type 2 diabetes

Insulin resistance is characterised by the body's failure to respond appropriately to normal levels of circulating insulin. This central metabolic abnormality precedes the development of type 2 diabetes by an estimated five to ten years. This is because pancreatic β-cells initially respond to insulin resistance by increasing insulin secretion, which is achieved by both an increase in overall β-cell mass and a rise of the individual β-cell insulin output. In most circumstances the resulting hyperinsulinaemia at least in part overcomes insulin resistance and maintains normoglycaemia. In susceptible individuals, however, the β-cell secretory capacity begins to fail over time and overt diabetes ensues (15). This second pathological event is necessary for the development of hyperglycaemia (**Figure 1.1**).

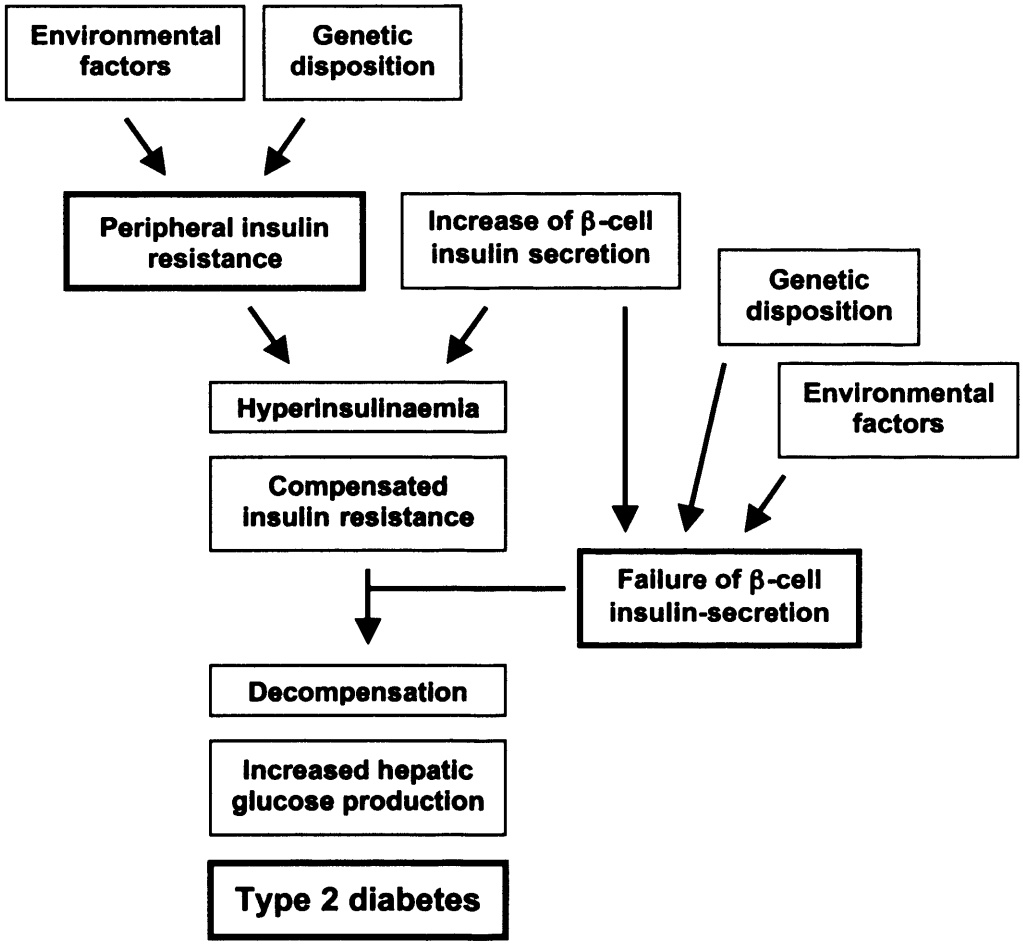

Figure 1.1 Pathogenesis of type 2 diabetes

Environmental factors as well as a genetic disposition determine the development of insulin resistance. The β-cells respond with compensatory insulin hypersecretion to maintain euglycaemia. Their capacity to sustain hyperinsulinaemia is influenced by genetic and environmental factors, too. Once β-cell failure ensues, increased hepatic glucose production due to decompensated liver insulin resistance contributes to the hyperglycaemia of type 2 diabetes.

1.1.3 Factors contributing to insulin resistance

A spectrum of progressive severity of insulin resistance can be observed: From the mild degree found in lean relatives of patients with type 2 diabetes to the pre-diabetic state of impaired glucose tolerance, which is associated with an annual risk of approximately 5% of progression to established type 2 diabetes.

Insulin sensitivity decreases with age and the prevalence of insulin resistance in the UK has been estimated to be 15-20% in the over 65-year-old population. Most other factors that induce insulin resistance are potentially modifiable or transient. These include intra-abdominal adiposity with increased waist-hip ratio, lack of physical activity, infection and inflammation, administration of certain drugs (in particular corticosteroids), and stress-induced activation of the hypothalamic-pituitary-adrenal axis. Single gene disorders causing severe insulin resistance early in life have been discovered but are rare (16). In contrast, despite intensive research, detailed molecular understanding of the underlying polygenic disposition to 'common' insulin resistance remains limited (3, 17).

1.1.4 Insulin resistance and cardiovascular risk

Even at an early stage, when euglycaemia is still maintained despite established insulin resistance, the compensatory hyperinsulinaemia is associated with dyslipidaemia and hypertension (18). In the presence of visceral obesity, this clustering of cardiovascular risk factors is commonly referred to as the 'metabolic syndrome' in recognition of the interrelated pathophysiology. The International Diabetes Federation recently issued criteria for the metabolic syndrome (19), although the usefulness of its definition as a 'syndrome' has been called into question (20, 21). Hyperinsulinaemia also leads

to endothelial dysfunction (15), abnormalities in platelet aggregation (22), a prothrombotic state (23), and hyperandrogenic infertility in women (24, 25).

Insulin resistance and the associated risk factors contribute to atherosclerosis before the potential subsequent development of type 2 diabetes. Vascular atherosclerotic disease is the leading cause of morbidity and mortality in affluent countries (26). Thus the long period of preceding insulin resistance offers an opportunity for therapeutic intervention to reduce the cardiovascular risk associated with insulin resistance, as well as that of progression to overt diabetes (**Figure 1.2**).

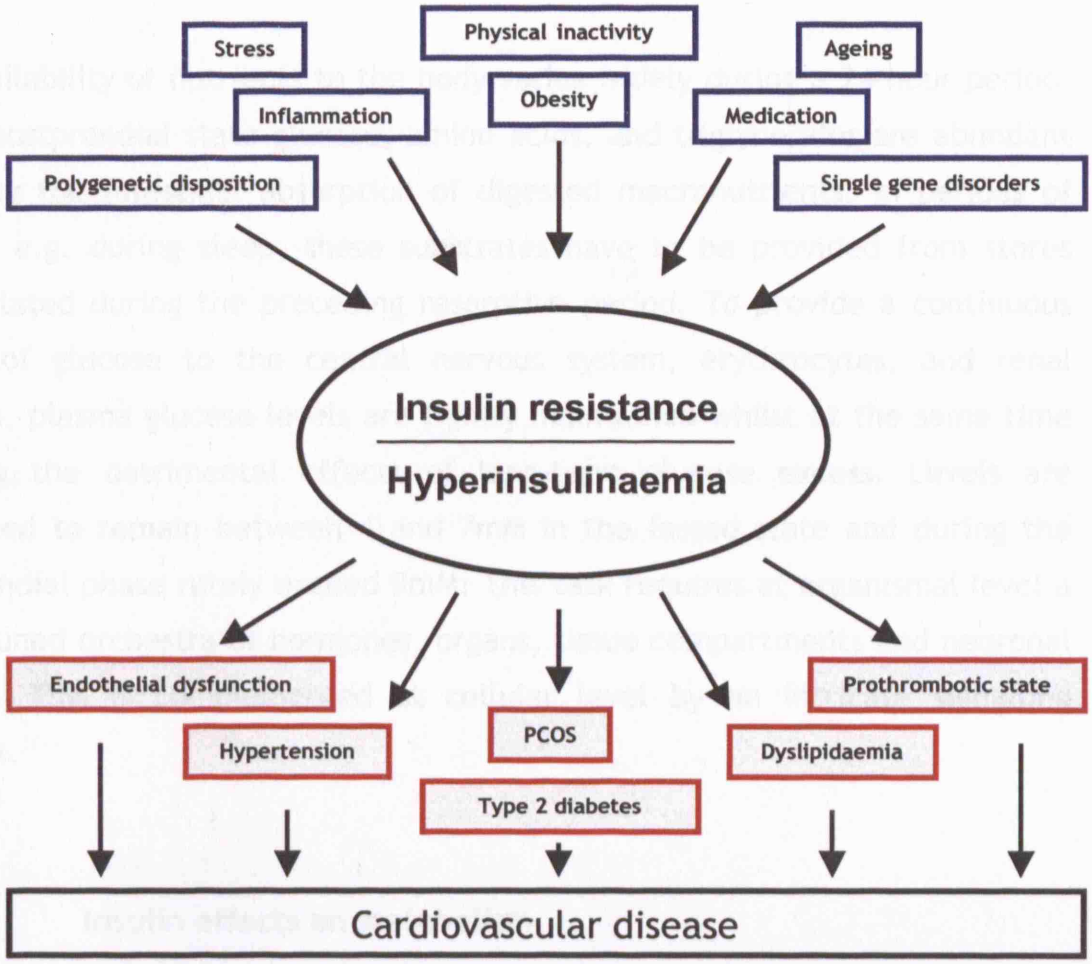

Figure 1.2 Insulin resistance and cardiovascular risk

A range of modifiable and non-modifiable risk factors contributes to insulin resistance (**blue boxes**). Insulin secretion subsequently increases to maintain glucose homeostasis. The resulting hyperinsulinaemia is associated with a cluster of atherogenic risk factors that contribute to the development of cardiovascular disease (**red boxes**). PCOS denotes polycystic ovary syndrome.

1.2 Energy substrate flow and glucose homeostasis

The availability of nutrients to the body varies widely during a 24-hour period. In the postprandial state glucose, amino acids, and triglycerides are abundant following the intestinal absorption of digested macronutrients. In periods of fasting, e.g. during sleep, these substrates have to be provided from stores accumulated during the preceding resorptive period. To provide a continuous supply of glucose to the central nervous system, erythrocytes, and renal medulla, plasma glucose levels are tightly maintained whilst at the same time avoiding the detrimental effects of long-term glucose excess. Levels are controlled to remain between 4 and 7mM in the fasted state and during the postprandial phase rarely exceed 9mM. This task requires at organismal level a finely tuned orchestra of hormones, organs, tissue compartments and neuronal circuits. This is complemented at cellular level by an intricate signalling network.

1.2.1 Insulin effects on metabolism

Insulin and glucagon are central for the acute regulation of energy substrate flow during the resorptive and fasting phase, respectively, in conjunction with autonomic nervous system activation. Both hormones are produced within the islets of Langerhans and following their release from the pancreas they exert receptor-mediated effects in the liver, which at the same time receives all nutrients via the portal circulation (27, 28). Whilst in most tissues, including the liver, glucose uptake is insulin-independent, both skeletal muscle and adipose tissue increase their glucose import significantly in response to insulin stimulation. There is no rate limit to the cellular flux of amino acids and fatty acids, although insulin regulates their flow into or from tissue compartments that store these substrates in keeping with the overall prandial state.

Neuronal influences on glucose homeostasis are mediated by autonomic fibres innervating both pancreas and liver, as well as by circulating adrenaline. The latter also has effects on adipose tissue and lipolysis. The activation of motor fibres in skeletal muscle directly affects glucose metabolism in this tissue compartment with subsequent effects on systemic glucose levels.

1.2.2 Insulin effects on cellular growth and differentiation

In addition to the acute effects on substrate flow, which are predominantly mediated through alterations in enzyme activity by regulating phosphorylation status, insulin has intermediate and longer-term effects on gene transcription and cellular protein turnover. This influences the abundance of key metabolic proteins, but also of structural cellular components and thus of growth and differentiation.

1.2.3 Insulin and glucagon synthesis and release

Insulin is the only hormone that in physiological concentrations is capable of lowering plasma glucose levels, and thus it has a central role in the postprandial regulation of carbohydrate metabolism.

Insulin is synthesised in the rough endoplasmatic reticulum of pancreatic β-cells as the precursor molecule pro-insulin. Pro-insulin is packaged into clathrin-coated secretory vesicles, in which the further processing to mature insulin occurs by proteolytic cleavage. During this process the vesicles lose their coating and become mature secretory granules, in which insulin is stored as a hexameric insulin-zinc complex (29). Glucose is the main secretagogue for insulin release with modulating influences by amino acids, fatty acids, entero-pancreatic hormones and the autonomic nervous system (30). The glucose

influx into β-cells is directly linked to circulating plasma levels. The glucose transporter protein-2 (Glut2) largely mediates uptake and the first step of β-cell glucose metabolism involves phosphorylation by glucokinase. Both molecules have a high K_m for glucose and are central in its sensing process (31, 32). The subsequent mitochondrial glucose oxidation raises the intracellular ATP/ADP ratio, which triggers the sequence of K_{ATP} channel closure, β-cell membrane depolarisation, Ca^{2+} influx and ultimately the exocytosis of stored insulin vesicles. Whilst this mechanism is well established to mediate the 'first phase' of insulin release, the sustained 'second phase' secretion requires additional, K_{ATP} channel-independent mechanisms (33). Insulin release is limited by α-adrenergic stimulation, by somatostatin released from islet δ-cells, and importantly by glucagon, whilst insulin appears to have a positive regulatory effect on its own gene transcription and on insulin secretion (34).

Glucagon stimulates hepatic glucose release through activation of glycogenolysis and gluconeogenesis, whilst reducing glycolysis and glycogenesis (35). Thus it acts as the main insulin-antagonistic hormone during fasting. Glucagon is synthesised in the α-cells of the pancreatic islets as a pro-hormone, in a similar fashion to insulin, and following processing is stored in cytoplasmic vesicles. The primary stimulus for glucagon release is a low plasma glucose concentration, whilst circulating amino acids, entero-pancreatic hormones and sympathetic innervation further enhance secretion. Hyperglycaemia and somatostatin inhibit glucagon release. Co-secretion of insulin and the inhibitory neurotransmitter γ-aminobutyric acid (GABA) from β-cells by Ca^{2+}-dependent exocytosis mediate the somatostatin effect (36), since the activation of $GABA_A$ receptors on glucagon-secreting α-cells inhibits glucagon release (37).

The tight reciprocal regulation between insulin and glucagon is facilitated by the close communication between their respective cell populations on a vascular, anatomic, and autonomic neuronal level. The α-, β- and δ-cells within the islet have been described as functional syncytia (38). α-Cells are situated in the area of venous drainage of β-cells, the close anatomical relationship allows the diffusion of paracrine active substances between cell types (37), and both vagal and sympathetic nerve fibres densely innervate the islets (39).

1.2.4 Tissue-specific regulation of energy metabolism

The liver performs a wide range of key enzymatic steps of energy metabolism and therefore holds a central function in substrate flux and the conversion of substrates between tissue compartments. In comparison, the metabolic capacities of skeletal muscle and adipose tissue are limited to meet their specific function and where similar pathways are present, some reactions are regulated differently.

1.2.4.1 Liver

In the postprandial state, glucose is readily available for energy metabolism and the excess is used for storage. The first intracellular modification of alimentary glucose is its phosphorylation. Whereas in most tissues this reaction is catalysed by hexokinase (K_m 0.1mM), glucokinase (Gck) performs this task in the liver under control by the Gck regulatory protein (40). Gck is more substrate specific, cannot be saturated under physiological conditions even by the higher portal glucose concentrations (K_m 15mM), is not inhibited by its product glucose 6-phosphate, and the enzyme is induced by insulin (41). Following further intermediary reactions the 'committed step' towards

glycolysis is catalysed by liver phosphofructokinase (Pfkfb1). Through the increase of an intermediate substrate, fructose 2,6-biphosphate, insulin functionally raises Pfkfb1 activity whilst at the same time increasing overall enzyme levels. Glucagon, on the other hand, reduces Pfkfb1 activity by a similar, indirect mechanism (35). The last cytosolic step of glycolysis, the conversion of phospho*enol*pyruvate to pyruvate, is catalysed by the liver isoform of pyruvate kinase (Pklr). Insulin induces *Pklr* mRNA levels, whereas glucagon inhibits the enzymatic activity of the hepatic isoform by phosphorylation. Whilst the regulatory effects of insulin are well recognised (42), glucose itself influences *Pklr* expression in an insulin-independent manner through the carbohydrate response element-binding protein (ChREBP), a transcription factor recently discovered in hepatocytes (43).

Glucose surplus to immediate energy requirements is directed either towards polymerisation and storage as glycogen, or, following glycolysis to acetyl co-enzyme A (acetyl-CoA), is channelled into lipogenesis. In glycogenesis, the activity of the liver isoform of glycogen synthase (Gys2) is increased by a rise in glucose 6-phosphate and by insulin (44). This process is mediated by the activation of protein kinase B (PKB; also known as Akt) and subsequent inhibition of glycogen synthase kinase-3 (Gsk3) (45, 46). Lipogenesis is initiated by acetyl-CoA carboxylase (Acc) as the rate-limiting step towards committed fatty acid synthesis. Subsequent elongation of the acyl chain is catalysed by the multi-domain enzyme fatty acid synthase (Fasn). Insulin induces both Acc and Fasn expression and in addition increases Acc activity by reducing its phosphorylation status (47, 48). In addition, insulin-independent regulation by glucose through ChREBP leads to upregulation of *Acc* and *Fasn* (49).

In the fasted state, glucose is synthesised *de novo* and also released from glycogen stores. One of the earliest steps in the process of gluconeogenesis involves the synthesis of phospho*enol*pyruvate from oxaloacetate, which is catalysed by phospho*enol*pyruvate carboxykinase (Pck1). This enzyme is

activated by glucagon and its expression reduced by insulin (50). The next regulated step is catalysed by fructose biphosphatase, representing the reversed function of the bi-directional enzyme Pfkfb1. This catalytic action is reflected in its control: Glucagon enhances this reaction whilst insulin reduces Pfkfb1 activity (35, 51). The last step prior to the release of glucose into the circulation is catalysed by glucose 6-phosphatase (G6pc), a reaction energetically more favourable than the reversal of Gck activity. G6pc activity is increased by glucagon and expression is reduced by insulin (52, 53).

The release of glucose monomers from glycogen is mediated by liver glycogen phosphorylase following activation through a cascade of kinases. This process is initiated by glucagon and by an adrenaline-mediated stress response through cAMP-dependent protein kinase (PKA), with glucose and insulin having an opposite effect (54). As occurs during gluconeogenesis, G6pc subsequently mediates the final step of glucose release from the hepatocyte whereby the enzyme is regulated by insulin as described above.

To avoid directing glucose towards fatty acid synthesis during fasting, glucagon increases PKA activity, which leads to enhanced phosphorylation and thus inhibition of Acc (47).

1.2.4.2 Skeletal muscle

The energy requirements of skeletal muscle vary widely according to the degree of physical activity and may be considerable for prolonged periods. During the resorptive phase, the myocytes' capacity for glucose uptake is greatly enhanced under the influence of insulin. This is mediated by the reversible translocation of Glut4 molecules into the cell membrane and accounts for more than 80% of the body's glucose disposal. Both insulin and exercise induce this translocation (55). Intracellular glucose either enters

glycolysis immediately or is stored as glycogen similar to hepatic mechanisms. Small amounts of triglycerides are stored within myocytes but largely reflect lipid uptake rather than lipogenesis from glucose (56).

In the fasted state at rest, glycogenolysis is regulated primarily by substrate related allosteric mechanisms. During exercise, muscle glycogen phosphorylase activity is predominantly stimulated by the Ca^{2+} influx occurring with motor activity and by adrenaline, but not by glucagon (57). Similarly, glucose uptake during prolonged exercise is mainly dependent on Ca^{2+} and not on insulin, although both have additive effects (58). As skeletal muscle tissue lacks G6pc, the glucose liberated from glycogen cannot be released into the circulation to supply other tissues but is used solely for muscle energy requirements.

1.2.4.3 Adipose tissue

The primary role of adipose tissue in energy metabolism is to store surplus substrate in the form of triglycerides, but it also has an important role as a source of intermediary metabolites and of hormones that regulate long-term energy homeostasis and thus influence insulin resistance.

In the postprandial state, *de novo* lipogenesis occurs in adipose tissue directly from acetyl-CoA. As in the liver, the pathway of fatty acid synthesis via Acc and Fasn is activated by insulin. Glucose is the main source for glycerol synthesis required for triglyceride (TG) formation. The reverse reaction, the hydrolysis of TG, is catalysed by the multi-enzyme complex hormone-sensitive lipase. This enzyme's activity is inhibited by insulin with a consequent reduction of non-esterified fatty acid (NEFA) release into the circulation (59). Pre-formed fatty acids, which constitute part of chylomicrons or lipoproteins, can be taken up directly by adipocytes following their hydrolysis by lipoprotein lipase. This enzyme is induced as well as activated by insulin (60).

In the fasted state, the release of glucagon inhibits Acc and Fasn, whilst catecholamines initiate lipolysis by activating hormone-sensitive lipase through PKA (61). Glycerol and NEFA are thus released into the circulation and NEFA subsequently enter fatty acid oxidation in the liver and lead to the formation of ketone bodies.

1.2.5 Metabolic effects of insulin resistance

The metabolic control exerted by insulin is impaired in the insulin resistant state which affects both postprandial and fasted energy substrate flows. Even the presence of hyperinsulinaemia cannot completely normalise the metabolic defects, as a reduced inhibition of glucagon release contributes to the ongoing counterregulatory responses in the face of already impaired glucose handling.

In the liver, the metabolic balance is shifted in favour of glycogenolysis and gluconeogenesis, both contributing to unsuppressed hepatic glucose output. In skeletal muscle, glucose disposal as well as glycogen formation is impaired, and the release of gluconeogenic amino acid precursors increases. In adipose tissue, glucose uptake and triglyceride synthesis are reduced, and persistent lipolysis in adipocytes increases circulating levels of both glycerol and NEFA. Whilst glycerol increases the substrate availability for gluconeogenesis, NEFA further aggravate hepatic insulin resistance, induce hepatic glucose production, and also impair β-cell function (62, 63).

1.2.6 Direct and indirect effects of insulin on the liver

Persistent hepatic glucose production is the main contributor to the fasting hyperglycaemia observed in type 2 diabetes, primarily due to uncontrolled gluconeogenesis rather than glycogenolysis (64). This dysregulation was

assumed to be a consequence of impaired direct, insulin receptor-mediated signalling in the liver. However, in insulin resistant humans the reduction of hepatic glucose output by insulin was shown in clamp studies to be mainly via an indirect effect (65). There are several indirect mechanisms by which insulin influences hepatic glucose output. Insulin inhibits the secretion of glucagon from pancreatic α-cells, which subsequently reduces hepatic glucose output (66). Furthermore, insulin limits substrate availability from intermediary metabolism by regulating the release of gluconeogenic amino acid precursors from skeletal muscle and of glycerol from adipose tissue. The insulin-mediated suppression of lipolysis also reduces NEFA availability and thus ameliorates their effect on the liver and β-cells. Much effort has since been made to establish the relative importance of direct and indirect insulin action on the liver and the effects on glucose metabolism (67).

The question has been addressed in studies in dogs, in which either pancreatectomy or a somatostatin clamp controlled the endocrine pancreatic function, whilst glucagon concentrations were maintained at basal levels by infusion. Insulin concentrations in the peripheral circulation and/or in the portal vein were then selectively changed (27). A rapid decline in glucose production was seen when portal insulin concentrations were raised in isolation, mainly due to the inhibition of glycogenolysis. A selective increase of peripheral insulin concentrations led to a similar or even more pronounced fall in hepatic glucose output, albeit at a slower rate than the portal vein infusion. This was associated with reduced uptake of intermediary substrates, in particular of NEFA (68-70). The associated fall in circulating NEFA levels was subsequently shown to be responsible for more than half of the peripheral effect of insulin on hepatic glucose output, by reducing the hepatic uptake of gluconeogenic substrate (71).

To further delineate the direct and indirect insulin effects on the liver, the uptake of glucose was also studied in a canine model as described above (72).

Half of the insulin-induced increase in hepatic glucose uptake was attributed to indirect effects, which were associated with increased glycolysis. The directly mediated effects, seen with high insulin levels within the hepatic sinusoids, were accompanied by a rise in glycogen synthesis. Thus, it appears that the direct insulin effects on the liver are predominantly attributable to alterations in glycogen metabolism whilst indirect effects simultaneously direct substrate flux away from gluconeogenesis.

In addition to this indirect metabolic regulation, insulin exerts an influence on liver carbohydrate metabolism through neuronal circuits. A CNS-mediated indirect insulin effect was demonstrated by studies that reduced insulin receptor expression in the medial arcuate nucleus of the hypothalamus by intracerebro-ventricular administration of antisense oligonucleotide to *Insr*. This resulted in the impaired suppression of hepatic glucose output by insulin (73, 74). The effect was mediated by insulin-sensitive K_{ATP} channels, activation of which required intact neuronal signalling to the liver via the hepatic branch of the vagus nerve (75-77). Therefore insulin indirectly controls hepatic glucose production by a dedicated signalling network in the hypothalamus.

1.3 The insulin signalling cascade

Direct effects of insulin on the liver are mediated through an intricate network of intracellular pathways downstream of its receptor (**Figure 1.3**). Its pleiotropic effects occur along different pathways that diverge but potentially cross talk at some stages, whilst providing redundancy and positive/negative regulation at others. The multitude of protein isoforms at several stages of the insulin signalling cascade provides further possibilities for fine-tuning and the integration of cellular functions (78).

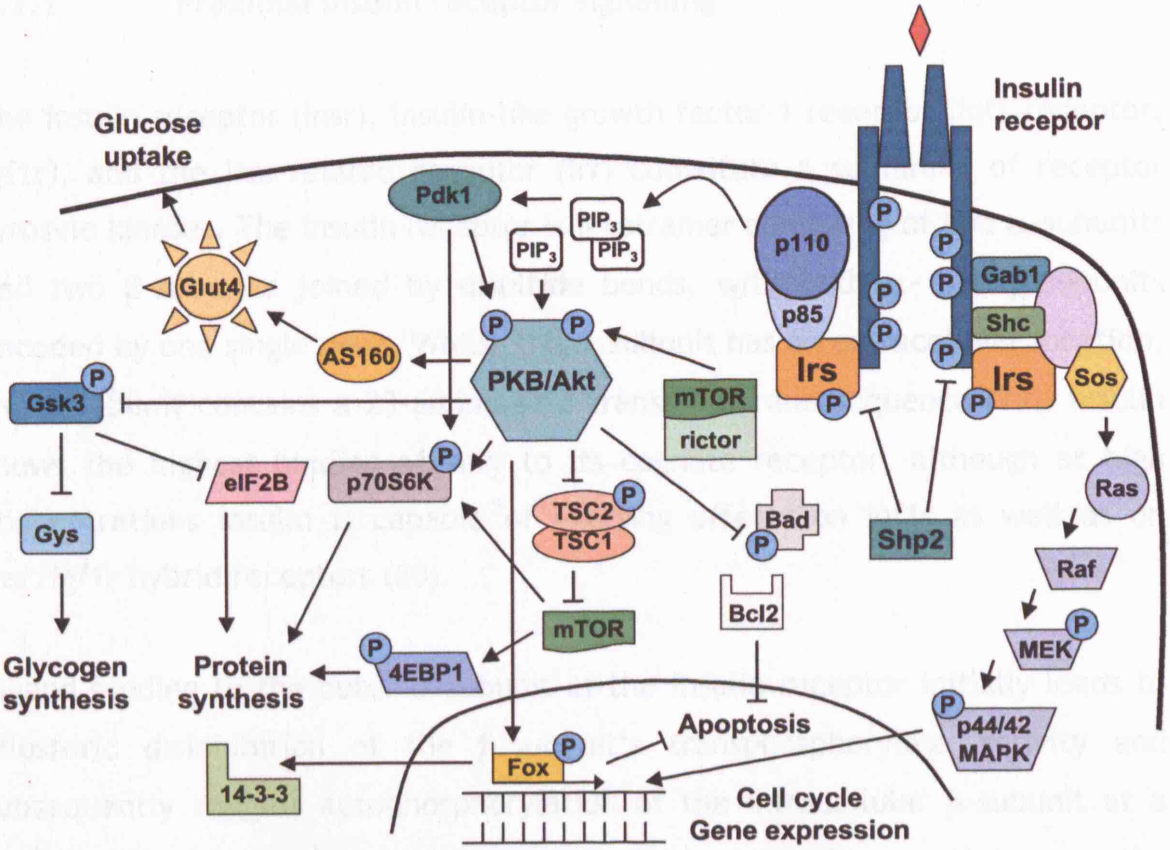

Figure 1.3 Simplified diagram of the insulin signalling cascade

Following ligand binding, the activated insulin receptor recruits insulin receptor substrate (Irs) and other molecules (Grb2, Gab1, Shc). These scaffold proteins initiate a signalling cascade via Sos-Ras-Raf-MEK to activate p44/42 MAPK, which regulates gene transcription related to cell proliferation and apoptosis.

p110 recruitment to Irs-bound p85 activates PI3K and generates PIP_3 molecules. This leads to Pdk1-mediated PKB/Akt activation, which diversifies the insulin signal. Glucose transport is enhanced by AS160-mediated Glut4 translocation, and glycogen synthesis is stimulated by Gsk3 inhibition. PKB/Akt increases protein synthesis directly by activating p70S6 kinase and indirectly through TSC1:TSC2 complex phosphorylation, the mTOR-4EBP1 pathway, and the Gsk3-associated de-repression of eIF2B.

PKB/Akt phosphorylates nuclear Fox transcription factors, leading to their exclusion from the nucleus. Fox proteins control gene expression, elements of the cell cycle and influence apoptosis. PKB/Akt also regulates apoptosis through Bcl2-related proteins.

The abbreviations used are given on page 13.

1.3.1 Proximal insulin receptor signalling

The insulin receptor (Insr), insulin-like growth factor-1 receptor (Igf1 receptor, Igf1r), and the Insr-related receptor (Irr) constitute a subfamily of receptor tyrosine kinases. The insulin receptor is a tetramer consisting of two α-subunits and two β-subunits joined by disulfide bonds, with both α- and β-subunits encoded by one single gene. Whilst the α-subunit has an extracellular location, the β-subunit contains a 23-amino acid transmembrane sequence (79). Insulin shows the highest binding affinity to its cognate receptor, although at high concentrations insulin is capable of exerting effects on Igf1r as well as on Insr/Igf1r hybrid receptors (80).

Ligand binding to the outer α-subunit of the insulin receptor initially leads to allosteric disinhibition of the β-subunit's transphosphorylase activity and subsequently triggers autophosphorylation of the intracellular β-subunit at a number of tyrosine residues. Conformational changes subsequently expose the catalytic domain of the intrinsic receptor kinase that results in tyrosine phosphorylation of a range of cytosolic proteins. These comprise the insulin receptor substrate proteins (Irs) as well as further scaffold proteins such as Src homology-2 containing protein (Shc), Grb2-associated binder-1 (Gab1), and others (81). Shc and Gab1 initiate the p44/42 mitogen-activated protein kinase (MAPK) pathway that predominantly mediates growth and differentiation events, which differs from the mainly metabolic actions of the other branches of the signalling cascade.

1.3.2 Insulin receptor substrate proteins

Tyrosine-phosphorylated Irs molecules act as an interface between the activated insulin receptor (as well as the Igf1r and certain cytokine receptors) and downstream signal-transducing proteins. When bound to the activated insulin receptor, their phosphotyrosine residues allow the docking of various Src homology-2 (SH2) domain-containing molecules (82, 83). The diversity of these proteins can in part explain the multitude of insulin actions.

Four Irs proteins have so far been described in the mouse, with homologous proteins in humans known except for Irs3 (84). They are structurally closely related (**Figure 1.4**) with a molecular weight of between 165-185kDa for Irs1, Irs2, and Irs4. Irs3 has a molecular weight of 60kDa. A conserved pleckstrin homology (PH) domain is located at the NH_2 terminus, which facilitates interaction with membrane phosphoinositides and acidic protein motifs. An adjacent phosphotyrosine-binding domain (PTB) can associate with Insr and Igf1r regions close to the cellular membrane via an NPxY sequence. The C-terminus is less conserved and of variable length depending on the isoform, with numerous tyrosine residues in this region allowing SH2 domain binding. Irs proteins interact with adapter molecules and enzymes through YMxM and YxxM motifs (85). Irs1 and Irs2 are associated with the low-density microsome fraction of intracellular structures (86), and Irs3 and Irs4 with the plasma membrane (87). Irs1, Irs2 and Irs4 are encoded as a single exon, whereas Irs3 consists of two exons (88).

Irs1 was the first intracellular substrate of the activated insulin receptor to be discovered (89, 90). Irs2 was described subsequently and it contains a unique sequence (amino acids 591-786) that interacts with the kinase regulatory loop of the Insr β-subunit (91-93). Irs1 and Irs2 are widely expressed and functionally the most important proteins for insulin signal transduction, but not interchangeable in their action (94). Irs1 plays a major role in growth

signalling, as it is the predominant Irs associated with the Igf1r, whereas insulin receptor-mediated metabolic signals are mostly transduced via Irs2. Murine Irs3 has a shorter C-terminal region than Irs1 and Irs2 and is highly expressed in early embryonic life (88, 95). The Irs4 protein was first detected in 1995 but identified and characterised later (96, 97). It is of very low abundance in the mouse (98), but gene transcripts have been detected in most tissues and predominantly in the hypothalamus (99). Both Irs3 and Irs4 are thought to play a more limited role in growth and metabolic regulation (100, 101).

Whilst tyrosine phosphorylation of Irs molecules activates their docking sites and thus downstream signalling potential, the phosphorylation of serine or threonine residues of Irs proteins reduces their capacity of signal transduction, in particular if the region proximal to the phosphotyrosine binding domain is involved (102).

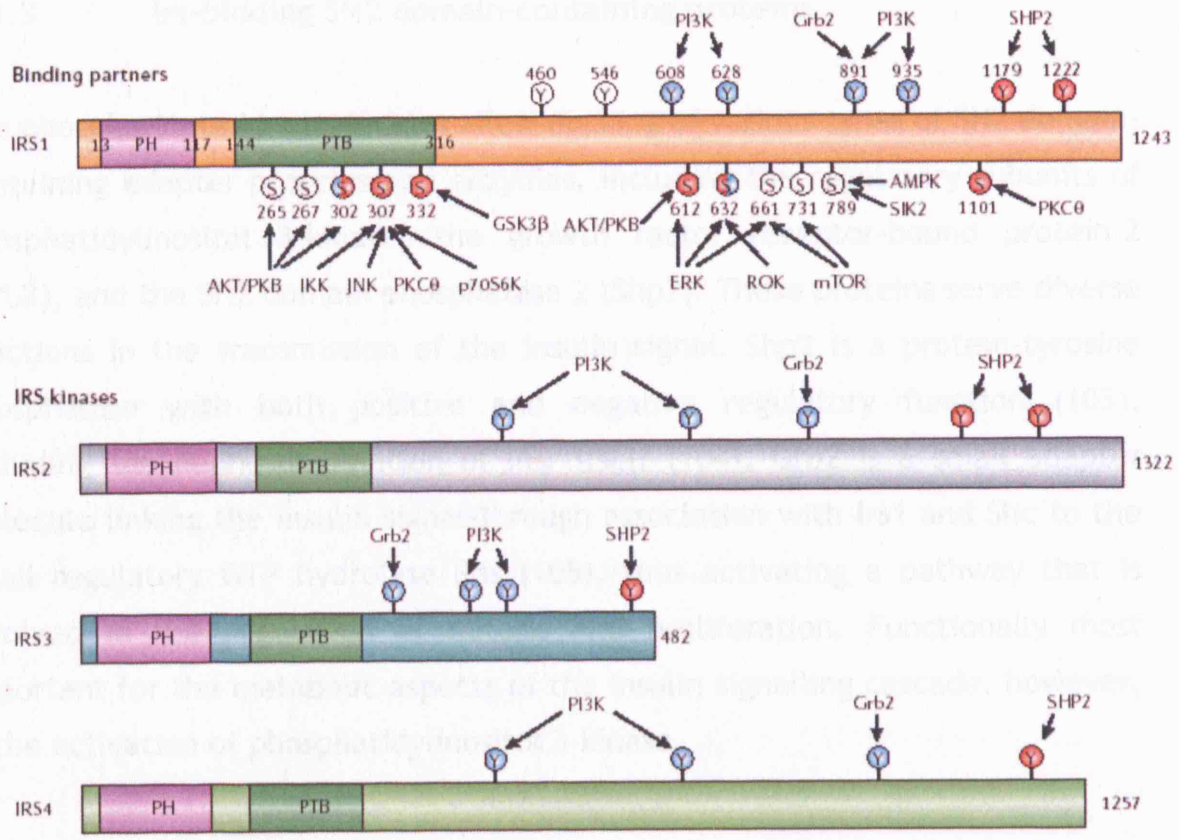

From (78)

Figure 1.4 Structural alignment of Irs proteins

The N-terminal pleckstrin-homology (PH) domain is followed by the phosphotyrosine-binding domain (PTB). Insr-mediated tyrosine phosphorylation sites are shown by Y and serine residues by S. Blue circles indicate positive, red circles negative, and white circles as yet unknown regulatory function (78).

Protein binding partners and kinases shown in this graph are phosphatidylinositol 3-kinase (PI3K), growth-factor-receptor-bound protein-2 (Grb2), Src-homology-2 domain-containing tyrosine phosphatase-2 (SHP2), Akt or protein kinase B (AKT/PKB), IκB kinase (IKK), c-Jun-N-terminal kinase (JNK), protein kinase C θ (PKCθ), protein 70 S6 kinase (p70S6K), glycogen synthase kinase-3 β (GSK3β), extracellular signal-regulated kinase (ERK), Rho kinase (ROK), mammalian target of rapamycin (mTOR), AMP-activated protein kinase (AMPK), and salt-inducible kinase-2 (SIK2).

1.3.3 Irs-binding SH2 domain-containing proteins

The phosphorylated Irs molecules allow docking of various types of SH2 domain-containing adapter proteins and enzymes, including the regulatory subunits of phosphatidylinositol 3-kinase, the growth factor receptor-bound protein-2 (Grb2), and the SH2 domain phosphatase 2 (Shp2). These proteins serve diverse functions in the transmission of the insulin signal. Shp2 is a protein-tyrosine phosphatase with both positive and negative regulatory function (103), including the dephosphorylation of Insr itself (104). Grb2 is a small adapter molecule linking the insulin signal through association with Irs1 and Shc to the small regulatory GTP hydrolase Ras (105), thus activating a pathway that is involved in the regulation of mitosis and proliferation. Functionally most important for the metabolic aspects of the insulin signalling cascade, however, is the activation of phosphatidylinositol 3-kinase.

1.3.4 Phosphatidylinositol 3-kinase

A range of isoforms exists of the enzyme generating 3-phosphorylated inositides from substrates in the cell membrane, termed phosphatidylinositol 3-kinase (PI3K). Four structurally homologous regions are recognised within these proteins, with the catalytic domain being the most conserved. According to their regulation and substrate specificity, the isoforms are subdivided into classes I, II, and III. Class I comprises the main forms of PI3K involved in insulin signalling. They consist of a 110kDa catalytic subunit and a regulatory adapter subunit (106). Four isoforms of the p110 catalytic protein exist, of which the α, β, and δ subtypes are grouped together as class IA. They form heterodimers with the regulatory subunit of 85kDa, whereby splice variants with a molecular weight of 50kDa and 55kDa occur (107, 108). Several isoforms of the regulatory p85 protein exist, too, with p85α accounting for approximately 75% and p85β for 20% of this subunit (78). In contrast, the only member of class IB, the p110γ isoform, is regulated differently by G-proteins.

Each of the phosphorylated Irs proteins can associate with the p85 adapter subunit through its SH2 domains, thereby recruiting the p110 subunit to the plasma membrane, where activated PI3K phosphorylates its phospholipid substrates at the 3' position of the inositol ring. Phosphatidylinositol (3,4,5) triphosphate (PIP_3) is the main product transducing the insulin signal further to several members of the AGC kinase family through binding to their PH domain (106). These serine/threonine kinases include PKB/Akt, ribosomal p70 S6 kinase (p70S6K), and several isoforms of protein kinase C (PKC) (109). They play a central role in the insulin signal diversification to downstream pathways relating to carbohydrate metabolism and lipolysis, as well as to gene expression, transcription and protein turnover (110).

The importance of functional PI3K signalling was demonstrated by the finding that the ablation of either p110α or p110β in mice was embryonic lethal but heterozygosity did not lead to a metabolic or growth phenotype (111-113). An animal model with heterozygosity for a kinase-dead p110α showed a severe reduction in Irs-associated signalling, leading to glucose intolerance and hyperinsulinaemia, as well as hyperphagia and adiposity, in the context of significant generalised growth reduction (114). Functional comparison of p110α and p110β during overexpression in 3T3 L1 adipocytes showed that insulin-mediated glucose uptake was predominantly associated with the p110β isoform (115). Animal studies of the regulatory subunit showed that the absence of p85α and both its shorter splice variants led to liver necrosis, hypoglycaemia, and perinatal death (116). In mice lacking only full-length p85α, increased insulin sensitivity due to enhanced glucose transport into skeletal muscle and adipose tissue was noted (107), and similar observations were made in mice with an isolated deletion of the p85β isoform (117).

1.3.5 Pdk1 and PKB/Akt activation

PIP_3 molecules generated by PI3K mediate the next steps in insulin signalling by binding to the PH domain of several target molecules, an event that leads to their translocation to the cytosolic cell membrane (118). The serine/threonine kinase PKB/Akt is activated in this manner (119), but also requires phosphorylation by phosphoinositide-dependent kinase-1 (Pdk1), a 63kDa monomeric enzyme (120, 121). PIP_3 alters the conformation of PKB/Akt and facilitates its phosphorylation. It binds to Pdk1 directly, too, thus increasing the rate of PKB/Akt activation (122). Pdk1 is constitutively associated with the cell membrane but is also present in the cytosol (108), and controversy remains as to whether further translocation occurs upon insulin stimulation (123).

Within the catalytic domain, PKB/Akt shares homologies of 40% with other members of the AGC kinase family, all of which require phosphorylation within the T-loop for activation (108). Because p70S6K, atypical PKC isoforms, and several other AGC kinases have been shown in cell culture experiments to undergo a PIP_3-associated activation process by Pdk1 similar to PKB/Akt, Pdk1 is considered a 'master regulator' for a wide range of physiological processes (109). These include the role of p70S6K in development and growth, leading to impaired β-cell function in a global knockout model of p70S6K (124, 125), as well as the finding of impaired atypical PKC activation in insulin resistant states (126).

Global absence of *Pdk1* in mice is embryonic lethal due to brain and neural crest abnormalities. Hypomorphic animals expressing 10% of Pdk1 are viable but 40-50% smaller than controls, with a proportionate reduction in cell and organ size (127). Liver-specific *Pdk1* deficiency is associated with impaired glucose tolerance following an intraperitoneal (i.p.) glucose challenge, even though spontaneous glucose and insulin levels remain normal. Hepatic glycogen levels are much reduced and the expression of key gluconeogenic enzymes is not suppressed by feeding. Premature death ensues by 16 weeks of age due to liver failure (128).

The three separately encoded isoforms of PKB/Akt are termed PKBα/Akt1, PKBβ/Akt2, and PKBγ/Akt3. They consist of an N-terminal PH domain and a C-terminal catalytic region and share a greater than 85% sequence homology. Activation of the catalytic domain depends on the phosphorylation of two residues, one located within the catalytic region (Thr308/309/305 for the α/β/γ isoforms, respectively) and one outside within a hydrophobic motif (Ser473/474/472). Whilst Pdk1 phosphorylates the threonine residue of PKB/Akt, the activation of the serine site has been attributed to a complex of the serine/threonine kinase 'mammalian target of rapamycin' (mTOR) and a second protein termed 'rapamycin-insensitive companion of mTOR' (rictor) (129).

Activated PKB/Akt plays a complex role in glucose homeostasis, protein synthesis, and gene transcription, as it has multiple and diverse downstream targets.

1.3.5.1 PKB/Akt-mediated effects on glucose homeostasis

Isoform-specific studies of PKB/Akt show that the deletion of PKBβ/Akt2 in mice leads to normal growth but insulin resistance and hyperglycaemia (130). PKBβ/Akt2 mediates the insulin-dependent translocation of Glut4 molecules from intracellular storage vesicles into the plasma membrane through the 'Akt substrate of 160kDa' (AS160) (131, 132), thus facilitating glucose influx into the cell and lowering plasma glucose levels. Conversely, the absence of PKBα/Akt1 causes increased apoptosis and a reduction in body size, but no abnormalities in glucose homeostasis (133, 134). PKBγ/Akt3 deletion interferes with brain development, but has no effect on either glucose homeostasis or postnatal growth (135).

The relevance of PKB/Akt signalling for human disease was demonstrated in a family with autosomal dominant inheritance of severe insulin resistance and diabetes, which was found to be due to a mutation in PKBβ/Akt2 (136).

PKB/Akt phosphorylates Gsk3, a serine kinase that exists in two isoforms, Gsk3α (51kDa) and Gsk3β (47kDa). They share 85% sequence homology overall and 97% of their catalytic domain (137). Phosphorylation of the N-terminal residues Ser21 (Gsk3α) or Ser9 (Gsk3β) inhibits its enzymatic activity, which allows the dephosphorylation and activation of glycogen synthase, its metabolic target enzyme. This leads to glycogen formation and storage in liver and skeletal muscle (45, 138). A small molecule inhibitor of Gsk3 was effective in improving oral glucose tolerance in diabetic mice by selectively increasing hepatic glycogen synthesis (139). In transgenic mice expressing a mutated variant of Gsk3 that lacked the serine residues required for PKB/Akt-mediated regulation, insulin failed to stimulate hepatic glycogen synthase activity in fasting mice (140).

1.3.5.2 PKB/Akt-mediated effects on protein synthesis

Apart from glycogen metabolism, Gsk3 has other functions within the insulin signalling network. Active, i.e. non-phosphorylated Gsk3 inhibits the function of the eukaryotic initiation factor 2 B (eIF2B) by phosphorylation at several serine residues (141). This guanine nucleotide exchange factor initiates mRNA translation and protein synthesis. Thus PKB/Akt, through Gsk3 inhibition, promotes eIF2B dephosphorylation and activation, and consequently protein synthesis (142).

PKB/Akt also inhibits tuberous sclerosis complex 2 (TSC2; also known as tuberin) through phosphorylation (143). In the basal state, this protein acts as a complex jointly with TSC1 (hamartin) to suppress the activity of mTOR (144,

145). mTOR phosphorylates p70S6K and elongation factor 4E-binding protein-1 (4EBP1), both of which regulate the translation of certain mRNA subclasses that encode proteins of the translational apparatus itself, such as ribosomal proteins (146, 147). PKB/Akt thus relieves the TSC1:TSC2 inhibition of mTOR and enhances protein synthesis (148).

1.3.5.3.1 PKB/Akt-mediated effects on gene expression: Forkhead transcription factors

The winged helix/forkhead box-containing nuclear transcription factors are direct targets for PKB/Akt (149, 150). Forkhead box (Fox) proteins are characterised by their 100 amino acid monomeric DNA binding domain (151), and following phosphorylation they are excluded from the nucleus and associate with 14-3-3 proteins within the cytoplasm (152). Several forkhead transcription factors are important for metabolism, as they regulate the expression of gluconeogenic and lipogenic enzymes.

Foxo1 is required for the activation of hepatic gluconeogenic gene transcription, whereby it interacts with the α-isoform of the peroxisome proliferator-activated receptor-γ coactivator-1 (Pgc1) (153). Foxo1 inhibition improved fasting glycaemia in mice and was associated with reduced expression of *Pck1* and *G6pc* (154). Conversely, hepatic overexpression of Foxo1 increased fasting glucose levels and led to impaired glucose tolerance, whereas glycolytic and lipogenic gene expression was reduced (155).

The permanent exclusion of Foxa2 from the nucleus observed in three insulin resistant, hyperinsulinaemic mouse models was associated with hepatic lipid accumulation and hypertriglyceridaemia (156). Vector expression of constitutively active Foxa2 reversed these effects and also increased the transcription of glycolytic, β-oxidative, and ketogenic genes. Recently, Pgc1β

was shown to coactivate Foxa2. This lowered hepatic TG content as well as increased plasma triglyceride concentrations. In addition, the secretion of very low density lipoproteins (VLDL) from the liver was enhanced by the combined Foxa2 and Pgc1β activation. Insulin was shown to reverse the VLDL hypersecretion (157).

1.3.5.3.2 PKB/Akt-mediated effects on gene expression: Srebp transcription factors

PKB/Akt has a direct effect on another class of transcription factors, the sterol regulatory element-binding proteins (Srebp; also known as factor, Srebf). They regulate lipid metabolism and belong to the family of basic helix-loop-helix leucine-zipper transcription factors. Srebp1a and Srebp1c are derived from different promoters of the same gene, whereas Srebp2 is encoded separately. Srebp1a activates the full range of genes responsible for uptake and synthesis of fatty acids, triglycerides, cholesterol, and phospholipids. In contrast, Srebp1c more selectively induces transcription of genes for fatty acid synthesis and Srebp2 preferentially regulates genes for cholesterol synthesis (158). Srebp1c is the predominant isoform in the liver (159).

Induction of PKB/Akt activity in hepatocyte culture increased *Srebf1* mRNA levels (160), PKB/Akt inhibition resulted in reduced *Srebf1* transcription, and a constitutively active PKB/Akt fusion protein mimicked insulin-stimulated Srebp1 induction (161). In a cell culture experiment using DNA microarray analysis following Tamoxifen-induced PKB/Akt fusion protein activation, several target genes involved in fatty acid and cholesterol synthesis were upregulated that are known to be controlled by Srebp. At the same time, PKB/Akt induced Srebp1 and Srebp2, as well as Fasn, at protein level (162).

Insulin increased hepatic *Srebf1c* mRNA levels in streptozotocin-treated rats, which paralleled changes in protein expression (163). The activation of liver X receptor-α was also necessary to exert this effect, a nuclear transcription factor that induced the production of the Srebp1c precursor protein (164). Insulin induced the subsequent maturation to transcriptionally active Srebp1c (164, 165).

1.3.6 Insulin effects on growth and survival

In addition to insulin's wide-ranging regulation of metabolism, it plays a significant role in regulating cell growth, mitosis, differentiation, and apoptosis (108, 110). The majority of these effects are transmitted through a pathway that initially depends on phosphorylated Irs proteins but then diverges from the PI3K-mediated branch and leads to p44/42 MAPK, whilst PKB/Akt-associated signalling is also involved in mediating some of these functions.

1.3.6.1 The mitogen-activated protein kinase pathway

The intracellular insulin signal regulates effector molecules for growth and differentiation predominantly through a cascade leading to a subgroup of MAPK that is characterised by its activation through receptor tyrosine kinases. The two isoforms of 44kDa and 42kDa are also known as extracellular signal-regulated kinases (ERK1, ERK2).

This p44/42 MAPK branch of insulin signalling is initiated by the adapter protein Grb2 that forms a complex with the son of sevenless (Sos) guanine nucleotide exchange factor, whilst Grb2 is associated through the SH2 domain with an Irs protein. Sos is thus recruited from the cytoplasm and activates the membrane-bound G-protein Ras by exchanging GDP for GTP. Active Ras subsequently binds

and phosphorylates the serine/threonine kinase Raf, which activates a downstream cascade of intermediary MAPK and ERK-related kinases (MEK). MEK1 and MEK2 in turn phosphorylate ERK1 and ERK2, which translocate to the nucleus and regulate the transcription of a wide range of target genes controlling cell proliferation, development, stress response and apoptosis (166, 167).

1.3.6.2 PKB/Akt-mediated effects on apoptosis and survival

Signals derived from the PI3K pathway regulate cellular survival by several mechanisms (168).

Forkhead transcription factors under PKB/Akt control are, in addition to their metabolic signalling potential, important regulators of survival and of the cell cycle (152, 169). Several transcriptional targets of Foxo have been identified to regulate the apoptotic process, repair of DNA damage, protection from oxidative stress, and cell cycle progression (170). PKB/Akt induces the expression of the pro-apoptotic ligand to the Fas receptor (a member of the tumour necrosis factor receptor family) through Foxo phosphorylation (152), which initiates an intracellular cascade leading to cystein aspartate protease (caspase) activation and cell death (171).

On the other hand, PKB/Akt phosphorylates the B-cell lymphoma-associated protein-2 (Bcl2) associated death agonist (Bad) at Ser136, which inhibits its interaction with the anti-apoptotic Bcl2 or Bcl-X_L proteins that consequently delays cell death (172). The phenotype of a transgenic mouse incapable of any serine phosphorylation of Bad resembled that of PKBα/Akt1 knockout mice (133, 134, 173).

PKB/Akt also exerts an anti-apoptotic effect through a delay in p53-mediated apoptosis. This transcription factor acts as a tumour suppressor protein by inducing cell cycle arrest or apoptosis in response to DNA damage. In cells where apoptosis was solely dependent on p53 function, constitutive overexpression of PKB/Akt led to reduced apoptosis (174), possibly by increasing p53 degradation (175).

Although the PI3K pathway is largely distinct from the p44/42 MAPK signalling branch, there is cellular communication between both. Cross-talking signal transduction occurs at the level of PI3K and during the regulation of effector molecules, such as cyclin D1 transcription or p53-dependent apoptosis (176-178).

1.4 Animal models and cell culture experiments

The study of murine models with alterations of specific elements of the insulin-signalling cascade has significantly advanced the understanding of insulin action at organismal and molecular level. The *in vivo* analysis of whole animal physiology has complemented the insights gained from the *in vitro* study of isolated cell lines (179, 180). Using gene-targeting techniques, the expression of a wide range of insulin signalling molecules has been modified to determine their individual contribution within the complex network described above (**Figure 1.3**). In addition to global gene ablation in the mouse, more defined genetic manipulations have become possible *in vivo* with the development of the Cre/*loxP* recombinase system. This strategy is designed to achieve tissue-specific gene deletion and, furthermore, with inducible systems a gene can be removed at a particular time during development (181).

1.4.1 Global insulin receptor null mice

Experiments of the global ablation of the insulin receptor gene (*Insr*) in mice (insulin receptor knockout or 'IRKO' animals) abolished the majority of insulin-mediated signalling. Hyperglycaemia developed almost immediately after birth, ketonaemia ensued and the animals died from ketoacidosis within 48-72 hours (182). Mice generated by another group were viable for 7 days and showed a twelve-fold increase in plasma insulin and a six-fold rise in plasma triglyceride levels, and there was fatty infiltration of the liver but a marked lack of glycogen stores (183). These findings indicate a lack of compensatory signalling by other mechanisms, which contrasts with the situation in humans. In Rabson-Mendenhall and Donohue's syndrome (Leprechaunism), survival of the complete absence of insulin receptors is possible as Igf1 signalling provides an alternative pathway (184).

In IRKO mice, transgenic re-expression of the insulin receptor in the brain, liver and β-cells prevented neonatal death, the development of diabetes in 65%, and normalised fat mass and reproductive function (185). Thus, surprisingly, the restoration of insulin signalling in non-classical target tissues reversed the diabetic phenotype.

1.4.2 Tissue-specific insulin receptor null mice

Because detailed metabolic studies were impossible in animals with global insulin receptor ablation, subsequent experiments investigated the effects of insulin signalling in individual tissues. In these studies the *Insr* deletion was limited to the classic target tissues of insulin signalling, and also to areas of the CNS where the insulin receptor is expressed and known to be involved in glucose homeostasis.

1.4.2.1 Liver-specific IRKO mice

Liver *Insr* knockout (LIRKO) animals developed severe insulin resistance with hyperglycaemia in the fed and fasted state, and glucose intolerance during an i.p. glucose tolerance test (GTT) (186). Insulin levels were elevated 20-fold due to a combination of reduced hepatic insulin clearance in the absence of Insr and a compensatory increase in β-cell mass in the presence of insulin resistance. TG and NEFA levels were reduced by almost 50%. Whilst the lack of Insr and associated signalling events were confirmed in the liver, a reduction of Insr expression by up to 20% was also found in skeletal muscle and considered to be a consequence of compensatory receptor downregulation in hyperinsulinaemia (187). Despite a parallel reduction in Insr-associated signalling events of 20% in LIRKO mice compared to controls, overall glucose transport into skeletal muscle did not reveal any differences at functional

level. Basal Irs1 levels remained unchanged but there was a five-fold increase of Irs2 expression in LIRKO mice. Increased expression of *Pck1* and *G6pc* with a decrease of *Gck* and *Pklr* was seen despite the presence of severe hyperinsulinaemia, a transcription pattern characteristically associated with the fasted state. This was reflected in hyperinsulinaemic-euglycaemic clamp studies (2.5mU/kg/min) where a normal basal hepatic glucose production (HGP) in LIRKO mice failed to suppress during insulin stimulation. High-dose clamp studies (20mU/kg/min) that aimed to fully stimulate insulin-sensitive tissues, even in the presence of insulin receptor down-regulation, still failed to induce HGP suppression in LIRKO mice, indicating severe hepatic insulin resistance (188). In young LIRKO animals the hepatic morphology appeared normal except for reduced glycogen content, but with advancing age the liver architecture was disrupted by the development of dysplastic nodules. This led to progressive hepatic dysfunction and an eventual amelioration of the diabetic phenotype, as the unsuppressed HGP became less severe with the deterioration of synthetic capacity of the liver.

These findings suggested the central role of hepatic insulin signalling in the maintenance of glucose homeostasis and normal liver function, favouring direct over indirect insulin effects to suppress HGP and to store glycogen. Intact hepatic insulin signal transduction was shown to be required for both the direct and indirect effects of insulin.

1.4.2.2 Skeletal muscle-specific IRKO mice

Mice with a disruption of *Insr* in skeletal muscle tissue (MIRKO) exhibited normal blood glucose and insulin levels, as well as normal glucose tolerance, but had increased fat mass and circulating levels of TG and NEFA (189). Hyperinsulinaemic-euglycaemic clamp studies demonstrated an 80% reduction in muscle glucose transport and glycogen synthesis, with a simultaneous three-

fold increase of glucose uptake into adipose tissue (190). Glut4 contents of skeletal muscle and of adipose tissue were unchanged, suggesting that Glut4 translocation activity is predominantly affected. These findings also indicated that muscle insulin resistance leads to substrate redistribution from muscle to adipose tissue and to abnormalities in lipid metabolism.

1.4.2.3 Adipose tissue-specific IRKO mice

In contrast, fat-specific *Insr* knockout mice (FIRKO) had a lower fat mass and were resistant to age-related, hypothalamic-lesion-induced, or diet-related obesity (191). Although in isolated adipocytes insulin resistance was demonstrated, whole body glucose tolerance was maintained and the animals had an increased lifespan (192). In keeping with improved insulin sensitivity, fasting insulin levels were lower in FIRKO animals at comparable glucose values and triglyceride levels were also reduced. A bimodal size distribution of adipose cells was found, with the 45% small adipocytes showing a relative reduction of Fasn and Srepb1 protein levels, as well as being resistant to triglyceride storage. These results showed that absent insulin signalling in adipose tissue does not induce insulin resistance in other tissue compartments, but rather improves insulin sensitivity by reducing the susceptibility to diet-induced obesity.

1.4.2.4 Neuron-specific IRKO mice

The disruption of *Insr* selectively in neurons (NIRKO) did not disturb brain development or alter neuronal survival (193). Female mice exhibited hyperphagia and both sexes developed diet-induced obesity with increased adipose tissue mass, hypertriglyceridaemia and elevated levels of insulin and leptin. Glucose tolerance remained normal but the response to an

intraperitoneal insulin challenge was blunted. A reduction in fertility was due to hypothalamic dysregulation of luteinising hormone secretion, which led to impaired follicular maturation and spermatogenesis. These results demonstrated that insulin signalling in the brain is important in the regulation of energy metabolism and reproduction. More recently, impaired neuronal insulin receptor signalling has been found to predispose to neurodegenerative disorders associated with τ-hyperphosphorylation, such as Alzheimer's disease, independent from alterations in fuel homeostasis (194).

1.4.3 Combined Insr reduction in muscle and adipose tissue

Employing a transgenic technique rather than gene ablation, a mouse model with dominant negative insulin receptor function in both muscle and adipose tissue was generated to study the combined effects (195). Animals demonstrated a reduction of insulin-stimulated receptor tyrosine phosphorylation by 90% in skeletal muscle and by 80% in adipose tissue, whereas hepatic insulin receptor function was normal. The animals showed insulin resistance and impaired glucose tolerance, as well as increased NEFA levels, but did not develop diabetes. In the liver, glycogen synthesis and *Pck2* expression was unaltered compared to controls. This suggested that insulin resistance in the liver develops independently from insulin resistance in the classic insulin target tissues and therefore is an independent prerequisite for the development of diabetes.

1.4.4 Insulin receptor substrate knockout animal models

To improve the understanding of the mechanisms of insulin signal diversification downstream of the receptor, the Irs molecules have been studied in gene targeting experiments selectively deleting individual proteins.

1.4.4.1 *Irs1* null mice

Global deletion of *Irs1* led to insulin resistance predominantly in skeletal muscle, but not to overt diabetes. A marked and sustained β-cell expansion occurred, leading to hyperinsulinaemia and the maintenance of overall glucose homeostasis (196, 197). Adenoviral reintroduction of *Irs1* into the liver of $Irs1^{-/-}$ mice led to the near-normalisation of insulin sensitivity (198).

In the absence of major metabolic disturbances, *Irs1* null mice showed a 50% intrauterine and postnatal growth retardation. Irs1 accounted for 75% of Igf1-mediated cell growth, and in particular for cell cycle progression (199). These results suggested that Irs1 preferentially mediates mitogenic rather than metabolic signals.

1.4.4.2 *Irs2* null mice

In contrast, the global deletion of *Irs2* led to the rapid onset of diabetes with near normal body size (200). *Irs2* null mice developed insulin resistance predominantly in hepatic tissue, whilst glucose disposal into skeletal muscle and adipose tissue was less affected (94). For several weeks after birth adequate compensatory insulin hypersecretion occurred but soon thereafter failed. Relative insulinopenia ensued, led to fasting hyperglycaemia without ketoacidosis and subsequent progression to a terminal catabolic state. The early β-cell failure was due to reduced Irs2-mediated Igf1 signalling causing defects in β-cell development and survival (201). The metabolic phenotype showed marked sexual dimorphism, whereby male animals developed overt diabetes from 8-10 weeks of age and females displayed compensatory hyperinsulinaemia for more than one year. In addition, *Irs2* null mice were found to have an increased food intake, fat mass, and leptin resistance. Female mice displayed defects in their reproductive function at hypothalamic and

pituitary level, similar to those seen in NIRKO animals, as well as at gonadal level with small ovaries and reduced follicle numbers (202). Thus Irs2 predominantly transduces metabolic rather than mitogenic signals, is important for normal β-cell function, and integrates nutritional and reproductive function at hypothalamic level. Transplants of islets with β-cell specific transgenic Irs2 expression were able to prevent obesity- and age-related diabetes (203), emphasising its importance for normal β-cell function.

Reduced levels of hepatic *Irs2* mRNA were found in two models of hyperinsulinaemia associated with insulin resistance (204), mediated through a specific response element for negatively regulated insulin-responsive genes (205). These latter findings suggested Irs2 downregulation to be an effect rather than cause, although a true inverse relationship could not be excluded. The importance of Irs2 in the liver for glucose homeostasis was shown in experiments restoring hepatic Irs2 in global *Irs2* null mice by adenoviral infection (206). The endogenous glucose production rate normalised, even though glucose utilisation remained impaired.

1.4.4.3 Compound heterozygous *Irs* null mice

Experiments in mice heterozygous for each of the *Irs1* and *Irs2* null alleles confirmed that both proteins are vital for embryonic and postnatal development, with Irs1 playing the principal role in somatic growth (201). Irs2 deficiency was found to determine the early development of diabetes, a consequence of its dual effect on peripheral energy metabolism and β-cell function.

The contribution of Irs1-mediated signalling to glucose homeostasis has been elucidated in animals double heterozygous for the insulin receptor and *Irs1* null alleles (207). A synergistic effect of both deletions on insulin resistance was

evident, but still allowed for appropriate β-cell expansion. With increasing age, 40% of animals developed diabetes, indicating that in presence of other predisposing genetic abnormalities Irs1 function is important also for metabolic signalling.

In a further study, mice heterozygous for the null alleles of *Insr* and either *Irs1* or *Irs2* developed diabetes with a frequency of around 20% in each group (208). Animals with *Insr*::*Irs1* double heterozygosity developed β-cell hyperplasia in the face of severe insulin resistance in skeletal muscle and in liver. *Insr*::*Irs2* compound heterozygous mice exhibited severe insulin resistance in liver, mild insulin resistance in skeletal muscle, and only modest concomitant β-cell hyperplasia. These metabolic differences suggested that Irs1 predominantly mediates insulin action in skeletal muscle whereas Irs2 acts in the liver.

1.4.4.4 *Irs3* and *Irs4* null mice

In a global knockout model, *Irs3* was found to be dispensable for normal growth and glucose homeostasis (100), and *Irs4* null mice showed only minor alterations in growth, glucose homeostasis and reproduction (101). These Irs molecules thus appear to serve only a minor or redundant role compared to Irs1 and Irs2 in metabolic and mitogenic insulin signalling.

1.4.5 Cell culture experiments on hepatocytes from knockout mice

The effects on the liver by impaired insulin signal transduction in global knockout models have been investigated further in cell culture experiments. The study of isolated hepatocytes has allowed the assessment of intrinsic metabolic and signalling changes associated without the interference of indirect metabolic or neuronal effects that are seen *in vivo*.

1.4.5.1 IRKO hepatocytes

The role of liver Irs proteins following insulin stimulation was examined in immortalised hepatocyte culture derived from IRKO mice (85). Insulin phosphorylated Irs1 through Igf1 receptors and led to Irs1 association with PI3K, whereas Irs2 phosphorylation and PI3K binding were markedly reduced. The most abundant tyrosine-phosphorylated proteins coprecipitating with p85 were Irs2, and to a lesser extent Irs1, thus no significant compensation by Irs3 or Irs4 occurred. The reduced Irs2 association with PI3K correlated with the failure of insulin to stimulate glycogen synthesis and to suppress HGP. Growth rates of IRKO and wild type hepatocytes were similar when stimulated with Igf1, whereas IRKO cells grew only half as much as controls when stimulated with insulin. These findings supported studies that suggested that growth was mediated by Igf1 mainly via Irs1, and by insulin through the insulin receptor via Irs2. In conclusion, Irs2 was found to be main mediator of insulin action in the liver for both its metabolic and, to a lesser extent, mitogenic effects.

1.4.5.2 *Irs2* null hepatocytes

Another study assessed insulin signalling in hepatocytes derived from *Irs2* null animals (209). PI3K activity was reduced by 50% in the absence of Irs2, without compensatory Irs1 upregulation, phosphorylation, or Irs1-associated PI3K activity. This was reflected in reduced downstream signalling with reduced phosphorylation of PKB/Akt, Gsk3, Foxo1, and PKC ζ/λ. Adenovirus-mediated reintroduction of *Irs2* was able to normalise these defects. Insulin failed to induce glycogen synthase activity and was unable to suppress the expression of the gluconeogenic genes *Pck1* and *G6pc* in the absence of Irs2. These responses reverted to normal following the reconstitution of Irs2 signalling. p70S6K activation was unaffected by Irs2 deficiency, indicating a signalling pathway independent from PI3K that regulates protein synthesis. These experiments again suggested the dominant role of Irs2 in hepatic glucose homeostasis.

1.4.6 Acute knockdown of insulin signalling proteins in adult mice

Conventional gene targeting takes effect from the time of first gene expression so that the genetic absence during intrauterine development may contribute to the adult phenotype. Techniques such as RNA interference (RNAi) or antisense oligonucleotide administration have therefore been used to study the effect of a short-term reduction (knockdown) of insulin signalling molecule expression on hepatic metabolism and signalling events in adult mice. The observed effects in such experiments are usually short-lived and thus can provide information on the acute regulation of signal transduction.

1.4.6.1 Insulin receptor knockdown

Insulin receptor expression was experimentally reduced in wild type mice by administration of sequence-specific antisense oligonucleotides over the period of a week (210). Insulin receptor levels were reduced by 95% in the liver and in adipose tissue by 65%, whilst skeletal muscle and hypothalamus remained unaffected. Insulin-mediated PKB/Akt activation was reduced in the liver, but not in adipose tissue and the hepatic glycogen content was reduced. Hyperinsulinaemic-euglycaemic clamp studies in conscious animals, however, failed to detect any changes in insulin sensitivity, glucose uptake, or glucose production. These results indicated that an acute impairment of direct insulin signalling in hepatocytes is insufficient to induce insulin resistance. This contrasted with the chronic situation of LIRKO mice, where severe metabolic changes occur.

1.4.6.2 Irs knockdown

In another study, hepatic *Irs1* and *Irs2* transcription was reduced in wild-type animals by adenovirus-mediated short hairpin RNAi. Five days after treatment, protein levels of Irs1, Irs2, or both, were reduced by 70-80% (211). Irs1 knockdown was associated with an increased expression of enzymes of gluconeogenesis, in particular *Pck1* and *G6pc*, as well as of the transcription factor *Hnf4a*, whilst *Gck* expression was reduced. Irs2 reduction resulted in an increased expression of the lipogenic transcription factor *Srebf1c* and of *Fasn* mRNA, and also in increased hepatic triglyceride content. In both conditions a non-significant rise in fasting blood glucose levels was observed, but when both *Irs1* and *Irs2* RNAi were combined, significant insulin resistance, glucose intolerance and liver steatosis developed. With simultaneous knockdown, defects in PI3K and PKB/Akt activation were observed, as well as reduced Foxo1 phosphorylation. These findings suggested Irs1 function predominantly to be linked to glucose homeostasis and Irs2 to lipid metabolism.

1.5 Summary

Insulin resistance precedes the development of type 2 diabetes and is associated with increased cardiovascular risk. Insulin resistance in skeletal muscle is one of the earliest detectable metabolic abnormalities in diabetes, but it is apparently the impaired hepatic response to insulin that leads to the characteristic fasting hyperglycaemia. The individual contribution of insulin resistance in specific tissue compartments to the overall diabetic phenotype remains a complex issue.

The liver is central for the integration of hormonal and neuronal signals with nutrient availability and requirements in order to maintain energy homeostasis. Insulin plays a critical role in the regulation of hepatic glucose and lipid metabolism, exerting direct and indirect effects. Direct receptor signalling on hepatocytes is complemented by indirect mechanisms controlling gluconeogenic precursor availability from peripheral tissues, by feedback on glucagon release, and by neuronal circuits involving the medial hypothalamus and the autonomic nervous system. The relative contribution of direct and indirect insulin effects on hepatic fuel metabolism, however, is subject to ongoing debate.

LIRKO mouse studies confirmed the requirement of intact hepatic insulin signalling for both the direct and indirect effects of insulin on HGP. In contrast, experiments of short-term near-ablation of the liver insulin receptor found direct insulin signalling in the liver to be dispensable for whole body glucose homeostasis.

Irs2 has been found to be the main mediator of insulin signalling in the liver. It is predominantly associated with the metabolic effects of insulin and possibly preferentially involved in lipid homeostasis. Global deletion of *Irs2* in mice caused marked liver insulin resistance; however, a major contributing factor for the rapid onset of diabetes in these animals was the concomitant deleterious effect on β-cell development and survival, as well as perhaps the loss of Irs2-associated signalling in the CNS.

1.6 Hypothesis and aims of the project

I therefore chose a tissue-specific gene targeting approach in the presented work to eliminate the interference by other tissue compartments and thus to investigate the relative contribution of the liver to the global *Irs2* null phenotype.

The characterisation of liver-specific *Irs2* knockout mice would therefore help to resolve uncertainties about the

- Role of Irs2 in hepatic insulin signalling
- Importance of hepatic insulin resistance in type 2 diabetes
- Direct *versus* indirect effects of insulin on hepatic metabolism

I hypothesised that in mice the selective deletion of *Irs2* in the liver would

- Impair hepatic insulin signalling events
- Induce significant liver and whole-body insulin resistance
- Lead to impaired insulin-mediated regulation of hepatic carbohydrate and lipid metabolism
- Leave β-cell function intact and therefore lead to the development of compensatory hyperinsulinaemia

I have conducted the following experiments to test these hypotheses

- Generation of *LivIrs2KO* animals
- Assessment of fertility and growth
- Analysis of hepatic insulin signalling events
- Study of whole-animal carbohydrate metabolism
- Measurement of parameters of lipid metabolism
- Repeat metabolic assessment following exposure to high fat diet
- Gene expression analysis in the fasted state and following refeeding
- Measurement of liver function parameters

Chapter 2 MATERIALS & METHODS

2.1 Animals

All animal procedures were approved under the British Home Office Animals Scientific Procedures Act 1986 (Project Licences No. 70/5179 and 70/6290).

Animals were housed in specific pathogen-free barrier facilities and maintained in a controlled environment (temperature 21-23°C, 12-hour light/dark cycle, lights on at 07:00h) with *ad libitum* access to water and food. Standard rodent chow (RM1; Special Diet Services, Witham, Essex, UK) consisted of 4.3g fat, 44.3g carbohydrates, and 19g protein per 100g, providing 13.25MJ/kg of metabolic energy. High fat chow was prepared to order with a caloric density of 18.96MJ/kg, which derived from fat 45%, from carbohydrate 35%, and from protein 20% (Diet code 829161; Special Diet Services).

2.1.1 *Irs2lox* strain

Mice harbouring alleles of the *Irs2* gene flanked by *loxP*-target sites for the Cre recombinase (*Irs2lox*$^{+/+}$) were generated in Professor Withers' laboratory using standard gene targeting techniques (212). These animals were indistinguishable from their wild type littermates.

2.1.2 *AlbCre* strain

Animals expressing Cre recombinase in hepatocytes under the control of the albumin promoter (*AlbCre*) were obtained from The Jackson Laboratory (Bar Harbor, ME, USA). They are estimated to contain 7 copies of the transgene and details of their generation have been described previously (213). *AlbCre*-

mediated gene deletion is efficient and reported to be complete by 6 weeks of age (214). *AlbCre* transgenic animals showed no phenotypical differences compared to wild type animals.

2.1.3 Generation of mice with liver-specific deletion of *Irs2*

Irs2lox and *AlbCre* colonies were maintained on a mixed 129Sv/C57BL/6J genetic background to reduce influences caused by biological strain diversity. Initially, *Irs2lox*$^{+/-}$ mice were crossbred with *AlbCre*$^{+}$ animals to obtain *Irs2lox*$^{+/-}$::*AlbCre*$^{+}$ mice. Male and female animals of these genotypes were subsequently intercrossed to obtain *Irs2lox*$^{+/+}$::*AlbCre*$^{+}$ mice. These animals were designated *LivIrs2KO* to reflect the absence of both alleles of *Irs2* in hepatocytes.

2.1.4 Mouse identification and tail tissue sampling

Animals were earmarked and tail tipped (< 5mm of tail) at the age of 14-21 days. Ethyl chloride spray was applied to the tails for local anaesthesia. The tissue was subsequently used for DNA extraction and for genotyping by polymerase chain reaction (PCR).

2.2 DNA extraction from tissues

For DNA extraction from tail tissue the proteinase K method was initially employed but subsequently replaced by the simpler method of alkaline hydrolysis. DNA was obtained from hepatic tissue by chloroform-isoamyl alcohol extraction.

2.2.1 Proteinase K method

The tail biopsy was placed in a 1.5mL reaction tube, 100µL of tail lysis buffer added [6.7mM Tris pH 8.8, 1.66mM $(NH_4)_2SO_4$, 0.67mM $MgCl_2$, 0.5% Triton X-100, with 1% β-mercaptoethanol added freshly], and the sample heated to 95°C for 10 minutes in a heat block. Following cooling to room temperature, proteinase K was added to a final concentration of 1mg/mL and the tissue incubated at 55°C for 2 hours. Heating to 95°C for 10 minutes subsequently inactivated proteinase K. The digested tissue was centrifuged with 15,600 x g for 5 minutes and the supernatant used as template for PCR amplification.

2.2.2 Alkaline hydrolysis method

The tail biopsy was placed in a 1.5mL reaction tube, 600µL of 50mM NaOH added, and heated to 100°C for 10 minutes in a heat block. Following cooling to room temperature, 100µL of 1M Tris pH 8.0 was added, the sample briefly vortexed and centrifuged with 15,600 x g for 5 minutes. The supernatant was used as template for PCR amplification.

2.2.3 Chloroform-isoamyl alcohol method

100mg of snap frozen liver tissue was placed in a 1.5mL reaction tube, 525µL of extraction buffer [50mM Tris pH 8.0, 100mM EDTA, 100mM NaCl, 1% SDS, proteinase K 0.65mg/mL] was added and the sample incubated at 55°C for 12 hours. To disperse the tissue, the specimen was briefly vortexed, 2µL of RNAse-A (0.2mg/mL) added, and at 37°C incubated for 1 hour. 200µL of 5M NaCl was added and the sample gently mixed by inversion. 700µL of chloroform-isoamyl alcohol (24:1 vol/vol) was added and the specimen incubated at room

temperature for 2 hours on a rocking platform. Following centrifugation with 15,600 x g for 10 minutes, 500μL of the upper aqueous layer was transferred into a new reaction tube, 500μL of isopropanol added, and gently mixed by inversion. Following centrifugation with 15,600 x g for 10 minutes, the supernatant was discarded, 300μL of 70% ethanol was added, and the sample incubated at 4°C for 1 hour. The supernatant was discarded, the pellet resuspended in 20μL of TE buffer [10mM Tris pH 8.0, 1mM EDTA], and used as template for PCR amplification.

2.3 PCR amplification

PCR amplification of genomic DNA extracted from tissue was performed to determine the genotypic status of the animals and also to confirm the Cre-mediated *Irs2* deletion event in the liver. 1μL of the DNA extracts was used as template, the final primer concentrations were 0.4μM in a commercial PCR reagent mixture (ReddyMix; ABgene, Epsom, UK), and the reactions were carried out in a 25μL volume in a thermocycler (MJ Research, Waltham, MA, USA). The PCR products were separated by electrophoresis in a 2% agarose gel prepared with TAE buffer [40mM Tris acetate pH 8.3, 1mM EDTA] and 0.02% ethidium bromide, and were subsequently imaged in ultraviolet light.

2.3.1 PCR strategy for *Irs2lox* detection

Primers flanking the 3' *loxP* site (loxP-Forward: 5'-ACT TGA AGG AAG CCA CAG TCG-3'; loxP-Reverse: 5'-AGT CCA CTT TCC TGA CAA GC-3') were used to detect the presence of a floxed allele of *Irs2*. PCR amplification from a wild-type allele yielded a 200bp product, whilst the presence of the *loxP* region and an adjacent short linker sequence increased this size to 250bp. Cycling

conditions were 94°C for 1min, followed by 30 cycles of 94°C for 30sec, 65°C for 30sec, and 72°C for 1:30min, and finally 72°C for 10min.

2.3.2 PCR strategy to detect *Irs2* deletion

To confirm deletion of *Irs2*, a primer binding 1.1kb upstream of the 5' *loxP* site (loxP-Deletion-Forward: 5'-GGG AAC CTG ACA AGT GAA TG-3') was used instead of the loxP-Forward primer. Thus, if Cre-mediated recombination had occurred, a 1.3kb fragment was amplified. The length of the intervening *Irs2* gene prohibited a successful PCR reaction otherwise. Cycling conditions were 95°C for 3min, followed by 30 cycles of 95°C for 1min, 52°C for 1min, and 72°C for 1min, and finally 72°C for 7min.

2.3.3 PCR strategy for *AlbCre* transgene presence

Presence of the *AlbCre* transgene was confirmed by the amplification of a 565bp fragment from within the rat albumin enhancer/promoter region. The Cre 102 primer sequence was 5'-CGC CGC ATA ACC AGT GAA AC-3' and that of the Alb-3' primer was 5'-ATG AAA TGC GAG GTA AGT ATG G-3'. A 324bp fragment from the *interleukin-2* gene in genomic DNA served as internal control and was obtained with a second primer pair (IL2-Forward: 5'-CTA GGC CAC AGA ATT GAA AGA TCT-3'; and IL2-Reverse: 5'-GTA GGT GGA AAT TCT AGC ATC ATC C -3') (215). Cycling conditions were 94°C for 6min, followed by 40 cycles of 94°C for 1min, 60°C for 30sec, and 72°C for 30sec, and finally 72°C for 7min.

2.4 *In vivo* physiology

All *in vivo* experiments were performed within the animal facility. Mice were allowed to recover for at least 5 days between experiments involving an overnight fast and/or recurrent tail blood collection.

2.4.1 Body weight

Animals were weighed with a MasterPro LA electronic balance (Sartorius, Epsom, UK) between 08:00h and 11:00h, except when animals were sacrificed in the fed state and readings immediately prior were taken. Mice placed on high fat chow were weighed weekly during that period and other cohorts at the ages specified.

2.4.2 Blood glucose

Blood glucose levels were determined in whole blood with an Elite glucometer (now Ascensia; Bayer, Newbury, UK) from a tail bleed after topical application of ethyl chloride as a local anaesthetic.

Fasted blood glucose (FBG) levels were obtained after an overnight fast of 14 hours during the early light phase between 08:00h and 10:00h. Fed blood glucose levels were determined during the dark phase between 23:00h and 01:00h, i.e. at least 4 hours after lights off, in animals with free access to food.

2.4.3 Intraperitoneal glucose tolerance test

Animals were weighed, fasted for 14 hours overnight, and FBG levels obtained as above. Subsequently an intraperitoneal injection of 20% glucose at a dose of 2g glucose kg^{-1} body weight was administered. Tail vein whole blood glucose levels were measured 15, 30, 60, and 120 minutes post-injection.

2.4.4 Intraperitoneal insulin tolerance test

Animals had free access to food during the preceding dark phase and until food was withdrawn at 12:00h. Following a 3-hour fast, blood glucose levels were obtained as above. Subsequently an intraperitoneal injection of soluble insulin at a dose of 0.75IU kg^{-1} body weight was administered at a concentration of 0.1IU/mL (100IU/mL and proprietary diluent solution; NovoNordisk, Crawley, UK). Tail vein whole blood glucose levels were measured 15, 30, and 60 minutes post-injection.

2.5 Hyperinsulinaemic-euglycaemic clamp

Metabolic studies under hyperinsulinaemic-euglycaemic clamp conditions were performed in collaboration with Professor Remy Burcelin, Centre Hospitalier Universitaire Rangueil, Toulouse, France (216). Animals were bred and genotyped at University College London (UCL) and subsequently transferred to France, where they were maintained according to local animal welfare requirements. Members of Professor Burcelin's team performed the surgery and supervised the clamp studies jointly with myself. The analytical assays were performed by myself on site, as were the initial statistical analyses. Professor Burcelin reviewed all results for a final interpretation.

2.5.1 Surgery

Animals were kept in a reverse light/dark cycle for at least 5 days prior to surgery to optimise post-operative recovery. Anaesthesia was induced by intraperitoneal injection of a mixture of ketamine 100mg/mL, xylazine 100mg/mL and water for injection (10:1:89 vol/vol/vol) at a dose of 10mL kg^{-1} body weight. Aided by a stereo dissection microscope (Zeiss, Le Pecq, France), a silicone rubber catheter (0.305/0.635mm inner/outer diameter) was placed in the left femoral vein. In addition to a securing ligature, cyanacrylate tissue glue (VetBond; 3M, Cergy-Pontoise, France) was applied to the adjacent tissue with a heparinised glass capillary. The distal end of the catheter was tunnelled subcutaneously towards the back of the animal and externalised via a polyethylene catheter port in the interscapular region. Ligatures and tissue glue secured the port, and the skin incisions were closed with surgical clips (Autoclip; Becton Dickinson, Le Pont de Claix, France). Animals were allowed to recover for at least five days and reverted to a standard light/dark cycle prior to study.

2.5.2 Clamp study

Animals were fasted for 6 hours on the day of the experiment and weighed. An infusion of soluble insulin (100IU/mL; Lilly, Suresnes, France) and D-[3-^{3}H]-glucose (370-740GBq/mmol; Perkin Elmer NEN, Courtaboeuf, France) was administered at constant rates of 18mU kg^{-1} min^{-1} and of 1.1MBq kg^{-1} min^{-1}, respectively. A variable infusion of 15% glucose was given simultaneously. Blood glucose levels were determined in whole blood from a tail bleed with an Accu-Chek Active glucometer (Roche Diagnostics, Meylan, France) every 10 minutes throughout the study (**Figure 2.1**). Euglycaemia (5-7mM) was maintained by rate adjustment of the 15% glucose infusion and achieved steady state after 2 hours. During the last hour an additional 5µL of whole blood was collected at each time point for subsequent analysis of ^{3}H-glucose enrichment (**Figure 2.2**).

The samples were precipitated in a 96-well plate with 125µL of 0.1M $ZnSO_4$ and 125µL of 0.1M $Ba(OH)_2$. 5µL of the insulin:D-[3-^{3}H]-glucose infusate was precipitated in quintuplicate and the plate was stored at -20°C until analysis.

At the end of the study period, blood was collected by the retro-orbital approach, allowed to clot, and centrifuged at 4°C with 6,900 x g for 10 minutes. Serum was separated immediately and stored at -80°C. Insulin-responsive tissues (liver, muscle, and adipose tissue) were collected, snap frozen in liquid nitrogen and stored at -80°C until analysis.

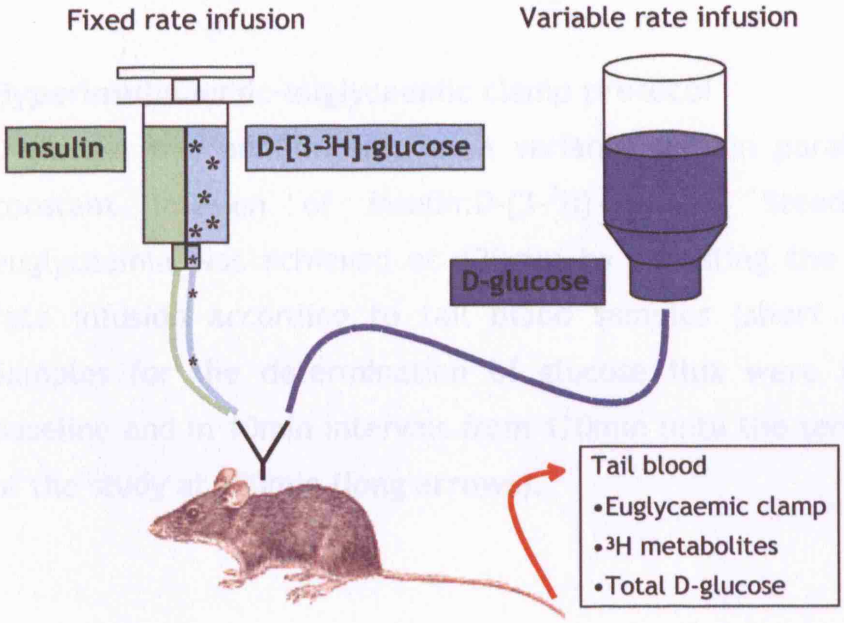

Figure 2.1 Setup of hyperinsulinaemic-euglycaemic clamp experiment
A fixed ratio insulin:D-[3-^{3}H]-glucose infusion was administered into a central vein at a constant rate, whilst in parallel D-glucose was infused at a variable rate. Tail blood samples guided the adjustment of the D-glucose flow rate that aimed to maintain euglycaemia. In steady state conditions, further samples were collected for the determination of parameters of glucose metabolism.

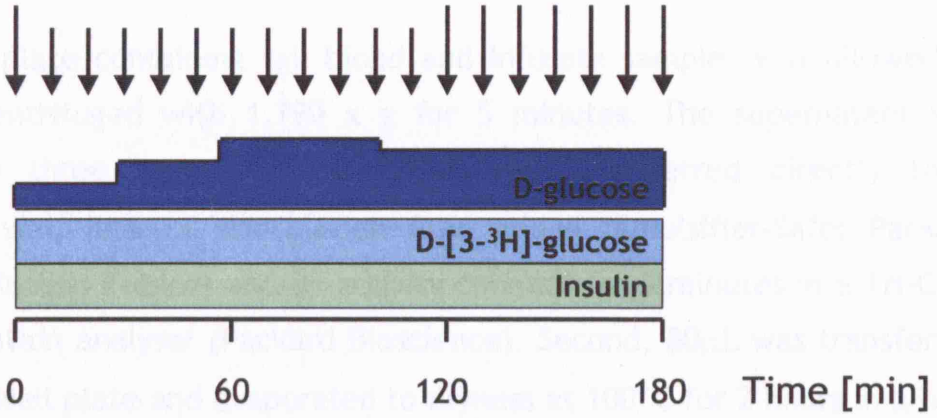

Figure 2.2 Hyperinsulinaemic-euglycaemic clamp protocol
D-glucose was administered at a variable rate in parallel to a constant infusion of insulin:D-[3-^{3}H]-glucose. Steady state euglycaemia was achieved at 120min by adjusting the variable rate infusion according to tail blood samples (**short arrows**). Samples for the determination of glucose flux were taken at baseline and in 10min intervals from 120min until the termination of the study at 180min (**long arrows**).

2.5.3 Analysis of tritiated metabolites and of glucose

The deproteinised tail blood samples were analysed threefold: First, for total ^{3}H activity, comprising D-[3-^{3}H]-glucose and ^3H_2O derived from tracer glycolysis. Second, for D-[3-^{3}H]-glucose alone, following the evaporation of ^3H_2O. Third, for total glucose, using a colorimetric glucose oxidase method (Glucose RTU; BioMérieux, Marcy l'Etoile, France). For the latter, a serial dilution of glucose was prepared with dH_20 at concentrations of 0.0, 0.5, 1.0, and 2.0mg/mL to be used for the generation of a standard curve. 5µL of the

standards were in duplicate treated with $ZnSO_4/Ba(OH)_2$ in 1.5mL reaction tubes and centrifuged with 1,480 x g for 5 minutes.

The 96-well plate containing tail blood and infusate samples was allowed to thaw and centrifuged with 1,790 x g for 5 minutes. The supernatant was divided into three samples: First, 20µL was transferred directly to a scintillation vial, 5mL of scintillation fluid added (Emulsifier-Safe; Packard Bioscience, Rungis, France) and ^3H-activity counted for 3 minutes in a Tri-Carb 1500 scintillation analyser (Packard Bioscience). Second, 80µL was transferred to a new 96-well plate and evaporated to dryness at 100°C for 2 hours in a heat block. After cooling to room temperature, the precipitate was resuspended in 200µL of dH_2O. 180µL thereof was transferred to a scintillation vial and ^3H-activity measured as above. Third, 60µL was transferred to a new 96-well plate, as was 60µL of the standard supernatants. 200µL of Glucose RTU reagent was added, incubated for 15 minutes, and the absorbance read at a wavelength of 505nm.

2.5.4 Data derivation

Animal body weight, concentration and rate of infused solutions, scintillation counts, and results from the glucose oxidase assay were used to calculate secondary data on mean glucose infusion rate, glucose turnover and clearance, glycolysis and glycogen production. Mice showing variations in specific activity of over 15% were excluded from the study (217).

2.6 Terminal procedures

Animals were terminally anaesthetised by intraperitoneal injection to allow open cardiac puncture or intravenous insulin stimulation. Sodium

pentobarbitone (Euthatal; Rhône Mérieux, Harlow, UK) was used for anaesthesia at a dose of 500mg kg^{-1} body weight for gene expression studies requiring rapid dissection. A mixture of midazolam 5mg/mL, fentanyl citrate/fluanisone 10.315mg/mL (Hypnorm; Janssen, High Wycombe, UK) and water for injection (1:1:2 vol/vol/vol) was administered at a dose of 10mL kg^{-1} body weight for insulin stimulation experiments requiring an incubation period.

Following either procedure the insulin-responsive tissues were collected (in the sequence of liver, quadriceps muscle, and epididymal adipose tissue), snap frozen in liquid nitrogen, and stored at -80°C until analysis. Non-stimulated fasted or fed tissues were obtained immediately after cardiac puncture. Following stimulation with insulin, animals were dissected at a defined time point.

2.6.1 Cardiac puncture

Mice were anaesthetised as above. A midline and a central transverse abdominal incision were made, carefully avoiding the infracostal vessels to reduce blood loss from the wound. The diaphragm was incised behind the sternum to cause collapse of the lungs for ease of cardiac puncture. The heart was exposed through an extension of the diaphragmatic incision to the left. A 1mL insulin syringe with a 12mm fixed 30G needle (Becton Dickinson, Oxford, UK) was used to gently puncture the right ventricle. Blood was both aspirated and expelled slowly into a 1.5mL reaction tube to prevent haemolysis. The sample was allowed to clot and then placed on ice until centrifugation at 4°C with 15,600 x g for 10 minutes. Serum was immediately separated and stored at -80°C until analysis.

2.6.2 Insulin stimulation of tissues

Mice were fasted for 14 hours overnight and anaesthetised as above during the early light phase (08:00h - 11:00h). A midline abdominal incision was extended to the right to expose the liver and inferior vena cava (IVC). A 0.5mL insulin syringe with a 12mm fixed 30G needle (Becton Dickinson) was used to cannulate the IVC and to inject 5IU of human soluble insulin (100IU/mL; NovoNordisk). 50μL of 0.9% saline was administered to control animals. The needle was kept *in situ* for 75 seconds after injection to reduce bleeding from the IVC following its subsequent withdrawal. 5 minutes after injection, the tissues were rapidly dissected as described above.

2.7 Assays

Serum specimens were collected by open cardiac puncture as described above or from a prolonged tail bleed obtained with the aid of a pipette. The latter samples were transferred into 0.5mL reaction tubes, allowed to clot and placed on ice until centrifugation at 4°C with 15,600 x g for 10 min. Serum was immediately separated and stored at -80°C until analysis.

2.7.1 Insulin

Insulin levels were measured according to the manufacturer's instructions of a commercially available rat insulin ELISA kit (Crystal Chem, Downers Grove, IL, USA), using a mouse insulin standard. In brief, 100μL of diluted mouse serum was incubated in a guinea pig anti-rat insulin antibody coated microtitre well for 2 hours. Following a series of washes, 100μL of horseradish peroxidase (HPO)-conjugated anti-insulin antibody was added and incubated for 30min. After further washes, 100μL of a TMB substrate solution was added, incubated

for 40min, the reaction terminated with 100μL of 0.5M sulfuric acid, and the absorbance at 450nm measured. The lyophilised mouse standard was reconstituted to concentrations of 0.0, 0.1, 0.2, 0.4, 0.8, 1.6, 3.2, and 6.4ng/mL. All samples were assayed in duplicate and in one assay to avoid inter-assay variation.

2.7.2 Leptin

Leptin levels were measured in a similar way, but both a rabbit anti-mouse leptin antibody bound to the microtitre plate as well as a soluble guinea pig anti-mouse leptin IgG were used in the first reaction step. The secondary antibody consisted of an anti-guinea pig IgG antibody conjugated to HPO. Otherwise the protocol was followed as described for insulin and a mouse leptin standard was used.

2.7.3 Liver function tests

All liver function parameters were measured in serum at 37°C on a Dimension RXL multi-channel analyser (Dade-Behring, Milton Keynes, UK). The samples were processed at the 'Mouse Biochemistry Laboratory' within the Department of Clinical Biochemistry, Addenbrooke's Hospital, Cambridge, UK. The laboratory participates in the National External Quality Assessment Service scheme and assays were performed in accordance with protocols agreed by the International Federation of Clinical Chemistry (IFCC) (**Table 2.1**).

Table 2.1 Biochemical assays for the determination of liver function

Parameter	Method / Chromogen	Inter-assay variation / Sample concentration	Reference
• Albumin	Dye binding / Bromocresol purple	4.3% / 23g/L 2.6% / 38g/L	(218)
• Alanine trans-aminase (ALT)	2-step enzymatic / NAD^+	9.7% / 42U/L 2.2% / 180U/L	(219)
• Aspartate trans-aminase (AST)	2-step enzymatic / NAD^+	10.0% / 42U/L 4.3% / 260U/L	(220)
• Alkaline phosphatase	Hydrolysis / Nitrophenolate	12.9% / 45U/L 4.8% / 272U/L	(221)
• Bilirubin	Diazotisation / Diazobilirubin	13.6% / 11μM 2.9% / 119μM	(222)
• Non-esterified fatty acids	3-step enzymatic / TBHB + 4-AA	6.2% / 349μM 4.1% / 954μM	(223)

2.8 Signalling studies

All protein analyses were performed on tissue snap frozen at the time of dissection. Tissue lysates used for immunoprecipitation were prepared fresh on the day of study; those used for immunoblotting were stored at -80°C between experiments. Details of the antibodies used are provided at the end of this section (**Table 2.2**).

2.8.1 Tissue homogenisation

Protein lysis buffer [10mM Tris, 5mM EDTA, 50mM NaCl, 30mM $Na_2H_2P_2O_7$, 1% Triton X-100, 50mM NaF, 0.1mM Na_3VO_4, adjusted to pH 7.6] was freshly prepared by dissolving a protease inhibitor mixture tablet (MiniComplete;

Roche Diagnostics, Lewes, UK) per 10mL of buffer, and by adding PMSF to a final concentration of 1mM immediately prior to use. 300-500mg of tissue was homogenised on ice in 1mL of lysis buffer in a 5mL flat-bottom universal container at 12,000rpm with a Turrax T25 rotor-stator dispersing tool (IKA, Staufen, Germany). The lysate was incubated on ice for 30 minutes to increase protein solubilisation and transferred to a 1.5mL reaction tube. Following centrifugation with 15,600 x g for 20 minutes at 4°C, the clear phase between the lipid-containing upper phase and the sedimented insoluble tissue components was transferred to a new reaction tube. Protein concentration was determined by a Bradford reaction assay (BioRad, Hemel Hempstead, UK).

2.8.2 Immunoprecipitation of Irs1 and Irs2

2mg of protein lysate was incubated with 10µL of antibody in a total volume of 1mL at 4°C for 12 hours on a rotary mixer. 50µL of packed protein-A agarose beads (Roche Diagnostics) was suspended in 50µL of freshly prepared lysis buffer, sedimented with 15,600 x g for 1 minute and the supernatant aspirated by water suction pump. The beads were washed twice more and finally resuspended in 50µL of buffer. Using a wide orifice tip, the 100µL of 1:1 slurry was added to the 1mL immunoprecipitate and incubated at 4°C for 120 minutes on a rotary mixer. Following sedimentation as above, the beads were washed twice with lysis buffer and the supernatant aspirated to near-dryness. 20µL of 2x sample buffer [125mM Tris pH 6.8, 20% glycerol (vol/vol), 4% SDS, 1% bromophenol blue, 200mM β-mercaptoethanol] was added and the sample heated to 100°C for 5 minutes in a heat block. Following centrifugation with 15,600 x g for 2 minutes, the supernatant was used for SDS-polyacrylamide gel electrophoresis.

2.8.3 Immunoblotting

Polyacrylamide gel electrophoresis was performed using the Mini-Protean electrophoresis system (BioRad). Gels with 10% polyacrylamide content were used for proteins of a molecular weight between 40-80kDa; Irs proteins (160-180kDa) were resolved on 6% or 7.5% polyacrylamide gels.

Gels were prepared according to standard procedures (224) and immersed in running buffer [25mM Tris, 192mM glycine, 0.1% SDS]. 20μL of recovered immunoprecipitate or 50μg of protein lysate was loaded per lane of gel after heating to 100°C for 5 minutes. 10μL of a coloured molecular weight marker was used to indicate protein size (Rainbow; Amersham, Little Chalfont, UK). Electrophoresis was performed at 100V for 60-90 minutes.

Proteins were transferred from the gel to a polyvinylidene-difluoride membrane (Amersham) in transfer buffer [25mM Tris, 192mM glycine, 20% methanol (vol/vol)] at 100V for 90-120 minutes. The membrane was incubated in blocking solution (5% non-fat dried milk in TNT buffer [50mM Tris pH 8.0, 150mM NaCl, 0.1% Tween 20]) at room temperature for 60 minutes to reduce non-specific binding of antibody.

Primary antibody was diluted to a concentration of 1:1,000 with blocking solution, in which the blot was incubated at 4°C for 12 hours. The antibody solution was recovered and sodium azide added to a final concentration of 0.02%. The membrane was washed thrice in TNT buffer for 5 minutes and incubated at room temperature for one hour in a HPO-conjugated secondary antibody preparation (1:10,000 dilution in blocking solution).

Following a further series of three washes in TNT buffer for 5 minutes, the blot was analysed by application of a chemiluminescence detection kit (ECL Plus; Amersham) and autoradiography (Hyperfilm ECL; Amersham).

Exposed films were quantified with a self-calibrating GS 800 densitometer and proprietary software (Quantity One 4.5; BioRad).

Table 2.2 Antibodies for immunoprecipitation and immunoblotting

Primary antibodies

Protein recognised	Supplier	Cat. #	Species	Size of protein
Insrβ (29B4)	Santa Cruz	sc-09	Mouse	95kDa
Irs1	Withers lab	N/A	Sheep	160-180kDa
Irs2	Withers lab	N/A	Sheep	160-180kDa
Irs1	Upstate	06-248	Rabbit	160-180kDa
Irs2	Upstate	06-506	Rabbit	160-180kDa
Total p85	Upstate	06-195	Rabbit	85kDa
P-Pdk1^{Ser241}	Cell Signaling	3061	Rabbit	58, 63, 68kDa
Total PKB/Akt	Cell Signaling	9272	Rabbit	60kDa
P-PKB/Akt^{Ser473}	Cell Signaling	9271	Rabbit	60kDa
Total p70S6K	Santa Cruz	sc-230	Rabbit	70kDa, 85kDa
Total Gsk3α/β	Cell Signaling	9332	Rabbit	47kDa
P-Gsk3α/β$^{Ser9/21}$	Cell Signaling	9331	Rabbit	47kDa, 51kDa
Total MAPK	Cell Signaling	9102	Rabbit	42kDa, 44kDa
P-MAPK$^{Thr202/Tyr204}$	Cell Signaling	9101	Rabbit	42kDa, 44kDa

Antibodies were of polyclonal origin, except for Insrβ.

Secondary antibodies

HPO-conjugated polyclonal goat anti-rabbit antibody (Dako, P 0448)
HPO-conjugated polyclonal sheep anti-mouse antibody (Amersham, NA 931)

Supplier details

Amersham, Little Chalfont, UK
Dako, Ely, UK
Santa Cruz Biotechnology, through: Insight Biotechnology, Wembley, UK
Cell Signaling Technology, through: New England Biolabs, Hitchin, UK
Upstate Biotechnology, Dundee, UK

2.9 Gene expression

Gene expression studies were performed in Dr Antonio Vidal-Puig's laboratory, Department of Clinical Biochemistry, Addenbrooke's Hospital, Cambridge. RNA was extracted at UCL from tissue snap frozen at the time of dissection. Real-time PCR was performed and analysed in Cambridge under guidance of a member of Dr Vidal-Puig's team, as was the design of primers and probes for glucose 6-phosphatase, glucokinase, and liver pyruvate kinase.

Sequences of the primers and probes used in these experiments are listed at the end of this section (**Table 2.3**), with the exception of *Gys2* and *Igfbp1* (Applied Biosystems), which were unobtainable for reasons of commercial confidentiality.

2.9.1 RNA extraction

Throughout handling of tissue and the extraction process, standard precautions were taken to reduce the risk of RNAse contamination. Bench surfaces, tools, and pipettes were treated with RNAse inhibitor spray (RNase*Zap*; Ambion, Huntingdon, UK), filtered pipette tips used, and gloves frequently changed.

100mg of tissue was homogenised on ice in a 5mL flat-bottom universal container at 12,000rpm with a Turrax T25 dispersing tool in 1mL of a phenol/guanidine isothiocyanate solution according to the manufacturer's instructions (TRIZOL; Invitrogen, Paisley, UK). The precipitated RNA was resuspended in 60μL of nuclease-free H_2O (Promega, Southampton, UK), placed at 65°C in a switched-off heat block and allowed to cool to room temperature over 2-3 hours to facilitate dissolution. RNA content and purity were determined by measuring the absorbances at 260nm and 280nm in a CE 2041 spectrometer (Cecil Instruments, Cambridge, UK). RNA concentration was adjusted to 100ng/μL with nuclease-free H_2O and an aliquot visualised by 2% TAE agarose gel electrophoresis.

2.9.2 Reverse transcription

Complementary DNA (cDNA) template for real-time PCR quantification was generated by reverse transcription of RNA. The RNA samples were heated to 65°C for 5 minutes and 125ng used as template. The reaction mix contained 5ng of random hexamer primers (Promega), and 400U of MMLV reverse transcriptase, 5U RNAse inhibitor protein, 2mM dNTP, and 2.5mM $MgCl_2$ (all Invitrogen). Reverse transcription was carried out in a 30µL volume in single 0.2mL reaction tubes in a thermocycler (BioRad). The reaction mix was incubated at 37°C for 60 min, the reverse transcriptase subsequently inactivated by heating the samples to 95°C for 5min, and the generated cDNA stored at -20°C until PCR analysis.

2.9.3 Target gene primer design and evaluation

Primer and probes for *G6pc*, *Gck*, and *Pklr* were specifically designed for this project, using proprietary software (Primer Express 2.0; Applied Biosystems, Warrington, UK). Suitable sequences across intron/exon boundaries were identified and oligonucleotides commercially synthesised (Sigma-Genosys, Haverhill, UK). The primer pairs were used in a PCR reaction in the presence of SYBR Green (Applied Biosystems), a fluorescent dye emitting intense light only when bound to double-stranded DNA. During a subsequent temperature ramp step the automated fluorescence detection system generated a fluorescence/temperature graph. This melting curve allowed the detection of primer-dimers and mispriming prior to the routine use of a probe and primer pair. In addition, the PCR products were visualised by 3% TAE agarose gel electrophoresis.

Primers were evaluated at final concentrations of 3µM, 1.5µM, and 0.3µM in the supplied SYBR Green reaction mix. The reactions were carried out in a 25µL reaction volume in an ABI Prism 7900 HT thermocycler (Applied Biosystems).

The manufacturer's recommended cycling conditions were employed, which for PCR consisted of 50°C for 2min and subsequent 95°C for 10min, followed by 40 cycles of 95°C for 15sec and 60°C for 1min, with all temperature changes occurring at maximum ramp speed. For the melting curve, two subsequent steps of 95°C for 15sec and 60°C for 15sec also occurred at maximum ramp speed and were followed by a slow 2% temperature ramp step to 95°C. The integrated 488nm Argon laser excitation/detection system used SDS 2.1 software (Applied Biosystems).

2.9.4 Real-time polymerase chain reaction

Quantitative PCR was performed with the TaqMan system (Applied Biosystems) (**Figure 2.3**). All target gene probes (Sigma-Genosys) were 5'-labelled with FAM as reporter dye and 3'-labelled with TAMRA as quencher dye. *Gys2* and *Igfbp1* probes contained a proprietary, non-fluorescent quencher dye.

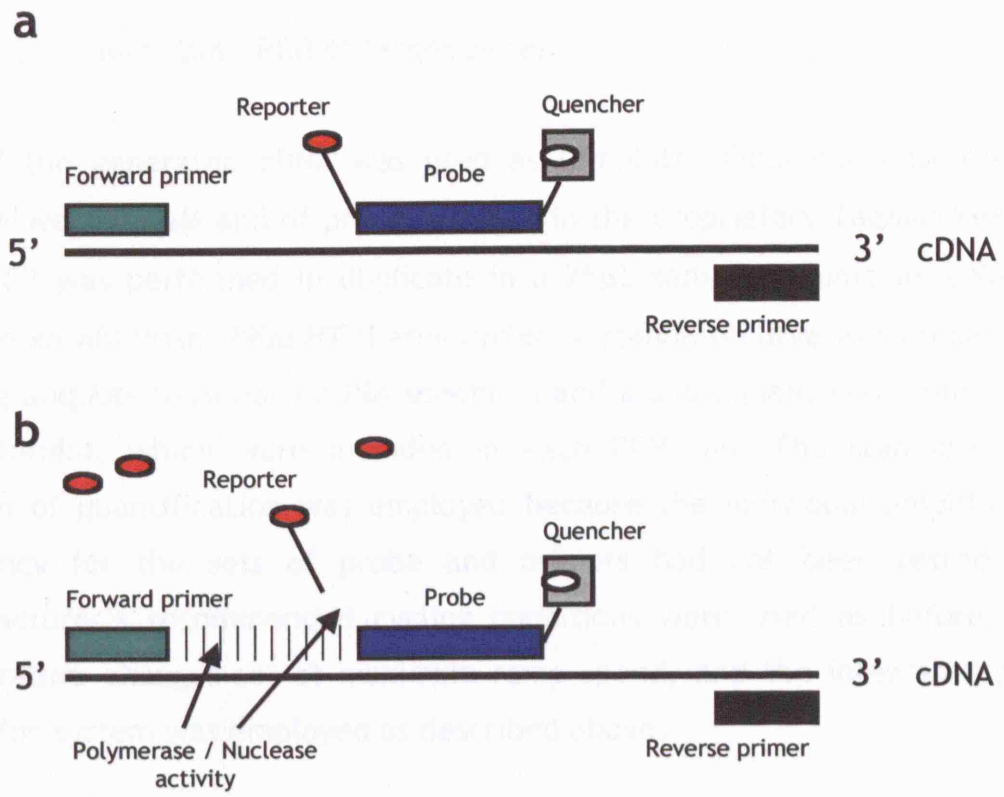

Figure 2.3 Diagram of the TaqMan real-time polymerase chain reaction
Three oligonucleotides are employed, a primer pair and a probe that is dual fluorescence-labelled with a reporter dye at the 5' end and a quencher dye at the 3' end. Any fluorescence emitted by the reporter dye following laser excitation is absorbed by the quencher dye due to their proximity (**a**). The polymerase used also possesses 5'→ 3' nuclease activity and upon reaching the probe liberates the reporter dye (**b**).

With each amplification cycle the availability of free, non-quenched reporter dye increases. During the exponential phase, the fluorescence detected is proportional to the number of DNA molecules generated. The number of cycles (C_t value) required to reach an arbitrary threshold of fluorescence is logarithmically proportional to the amount of cDNA template. From this the amount of mRNA and hence gene expression can be deducted.

2.9.5 Real-time PCR of target genes

2μL of the generated cDNA was used as template. Final concentrations of primers were 0.3μM and of probes 0.15μM in the proprietary TaqMan reaction mix. PCR was performed in duplicate in a 25μL sample volume in a 96-well plate in an ABI Prism 7900 HT thermocycler. A standard curve was prepared by pooling aliquots from each cDNA specimen and a subsequent serial dilution of 1:4:4:4:4:4:4, which were included in each PCR run. The standard curve method of quantification was employed because the individual amplification efficiency for the sets of probe and primers had not been tested. The manufacturer's recommended cycling conditions were used as before, with temperature changes set at maximum ramp speed, and the integrated signal detection system was employed as described above.

2.9.5 Real-time PCR of internal standard

cDNA generated from 18S ribosomal RNA was used as an internal standard to allow normalisation of the target gene results. Due to their abundance, 18S RNA required a dilution of 1:30 of both standard curve and specimens. The proprietary 18S probe (Applied Biosystems) was 5'-labelled with VIC as reporter dye and 3'-labelled with TAMRA as quencher dye.

2μL of the diluted samples was used as template. Final primer concentrations were 50nM and that of the probe 200nM in the supplied TaqMan reaction mix. PCR was performed as described above.

2.9.6 Data derivation

Target gene C_t values were read off the generated standard curve and converted to arbitrary units by inverse logarithm. This mathematical approach was also applied to 18S C_t values and the target gene/18S ratio calculated. Corrected values were expressed as relative difference in gene expression.

Table 2.3 Primer and probe sequences for quantitative PCR studies

Acox1	F	AAT TGG CAC CTA CGC CCA G
	R	AGT GGT TTC CAA GCC TCG AA
	Probe	FAM-6-CGG AGA TGG GCC ACG GAA CTC AT-TAMRA
Cpt1a	F	GCG TGC CAG CCA CAA TTC
	R	TCC ATG CGG TAA TAT GCT TCA T
	Probe	FAM-6-CCG GTA CTT GGA TTC TGT GCG GCC-TAMRA
Fasn	F	GCC CAG ACA GAG AAG AGG CA
	R	CTG ACT CGG GCA ACT TCC C
	Probe	FAM-6-GGA GGA GGT GGT GAT AGC CGG TAT GTC-TAMRA
G6pc	F	ACT CTT GCT ATC TTT CGA GGA AAG A
	R	CCA ACC ACA AGA TGA CGT TCA
	Probe	FAM-6-AAA GCC AAC GTA TGG ATT CCG GTG T-TAMRA
Gck	F	GGT GCT TTT GAG ACC CGT TTT
	R	GAG TGC TCA GGA TGT TAA GGA TCT G
	Probe	FAM-6-TGT CGC AGG TGG AGA GCG ACT CTG-TAMRA
Gys2	Celera ID	mCT5582
	Context sequence	TAC ACA CCA GCT GAA TGC ACA GTG A
Igfbp1	Celera IDs	mCT169748, mCT19350
	Context sequence	CTC AAG AAA TGG AAG GAG CCC TGC C

Table 2.3 Continued

Pck1	F	TGT GGG CGA TGA CAT TGC
	R	TGG CAT TTG GAT TTG TCT TCA C
	Probe	FAM-6-TAT CCA CCC AGA AAA CGG GTT TTT TG-TAMRA
Ppara	F	CCT CAG GGT ACC ACT AGG GAG T
	R	GCC GAA TAG TTC GCC GAA A
	Probe	FAM-6-CAC GCA TGT GAA GGC TGT AAG GGC TT-TAMRA
Pparg	F	TTT AAA AAC AAG ACT ACC CTT TAC TGA AAT T
	R	AGA GGT CCA CAG AGC TGA TTC C
	Probe	FAM-6-AGA GAT GCC ATT CTG GCC CAC CAA CTT-TAMRA
Pgc1b	F	GGC CTT GTG TCA AGG TGG AT
	R	GGT GCT TAT GCA GTT CCG TAC A
	Probe	FAM-6-AGA CCC CCA CAC TGC GGG CTC-TAMRA
Pklr	F	CGA CGG GCT CAT CTC CTT AG
	R	GAA ACC ACC GTG TTC CAC TTC
	Probe	FAM-6-CGG AAA ATT GGC CCA GAG GGA CTG-TAMRA
Srebf1c	F	GCC ATG GAT TGC ACA TTT GA
	R	GGC CCG GGA AGT CAC TG
	Probe	FAM-6-GAC ATG CTC CAG CTC ATC AAC AAC CAA G-TAMRA

2.10 Data analysis and presentation

Raw data was first collected and manipulated using Excel spreadsheets (Microsoft, Redmond, WA, USA), which were also used for the standardisation of the gene analysis results. Subsequent calculations, statistical analyses, and graph generation were carried out with Prism 4 software (GraphPad Software, San Diego, CA, USA). Differences between groups were compared by paired or unpaired two-tailed Student's t-test. A p-value <0.05 was considered significant and is indicated by an asterisk (*); a p-value <0.01 is indicated by (**). Results are representative of at least five animals per group, unless stated otherwise, and are expressed as the mean ± standard error of the mean (SEM).

2.11 Suppliers

General laboratory chemicals were purchased from Sigma-Aldrich, Gillingham, UK, except where stated otherwise.

Chapter 3 RESULTS: ANIMALS

3.1 Breeding and fertility

More than 800 animals were bred over the course of this project, and the *LivIrs2KO* mice were indistinguishable from their littermates. Over a six month period, ten female mice gave birth to 31 litters, 26 of which survived to weaning. Average litter size was 8.9 pups (range 4-13) with a male:female ratio of 56.6 to 43.4. Of the 233 animals born to these mothers, only 27 (11.6%) were negative for the *AlbCre* transgene, indicating that most parental animals were homozygous for this genotype. The offspring (n=105) of three female *Irs2lox*$^{+/+}$::*AlbCre*$^{+}$ mice, which had been selected for higher-density *LivIrs2KO* breeding, demonstrated in 60.9% homozygosity for the floxed allele of *Irs2* (expected 75%) and in 39.1% heterozygosity (expected 25%). In other offspring the expected Mendelian frequencies were obtained, with 25.2% of *Irs2lox*$^{+/+}$, 48.5% of *Irs2lox*$^{+/-}$, and 26.3% of *Irs2lox*$^{-/-}$ animals.

3.2 Determination of genotype

The genotype of the animals was assessed by PCR of genomic DNA from tail tissue, with the detection of characteristic bands by subsequent agarose gel electrophoresis of the amplification products.

3.2.1 *Irs2lox*

Amplification of the wild type allele yielded a 200bp fragment, whereas the floxed allele gave a 250bp product (**Figure 3.1**).

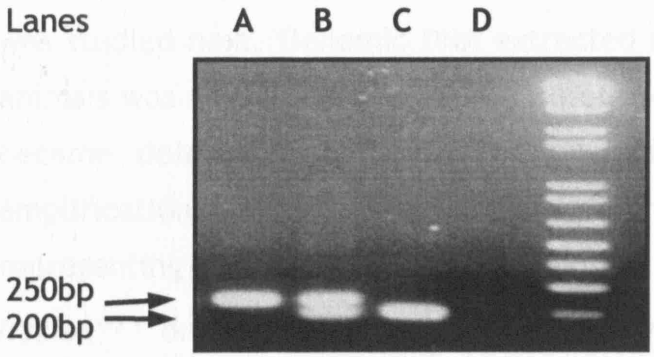

Figure 3.1 ***Irs2lox*** **PCR products**

Genomic DNA extracted from a tail biopsy was amplified by PCR and separated by electrophoresis.

3.2.2 *AlbCre* transgene

The transgene was detected by the presence of a 565bp product. The internal control primers amplified a 324bp fragment from the *interleukin-2* locus (**Figure 3.2**).

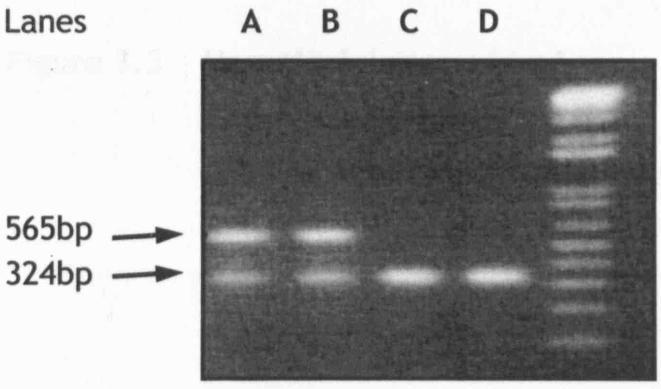

Figure 3.2 ***AlbCre*** **PCR products**

Genomic DNA extracted from a tail biopsy was amplified by PCR and separated by electrophoresis

3.3 Confirmation of *Irs2* deletion

The correlation between the assigned genotype and the AlbCre-mediated recombination event, the deletion of the *loxP*-flanked *Irs2* gene in the liver, was studied next. Genomic DNA extracted from hepatic tissue of 4 month-old animals was amplified by PCR. In case of successful deletion, a 1.3kb fragment became detectable, whereas the presence of full-length *Irs2* made PCR amplification impossible. Therefore 16 mice were chosen for analysis, representing the 4 allelic combinations of *AlbCre* presence or absence, and $Irs2lox^{+/+}$ or $Irs2lox^{-/-}$. The recombination event was appropriately detected or found to be absent in 16/16 samples (**Figure 3.3**).

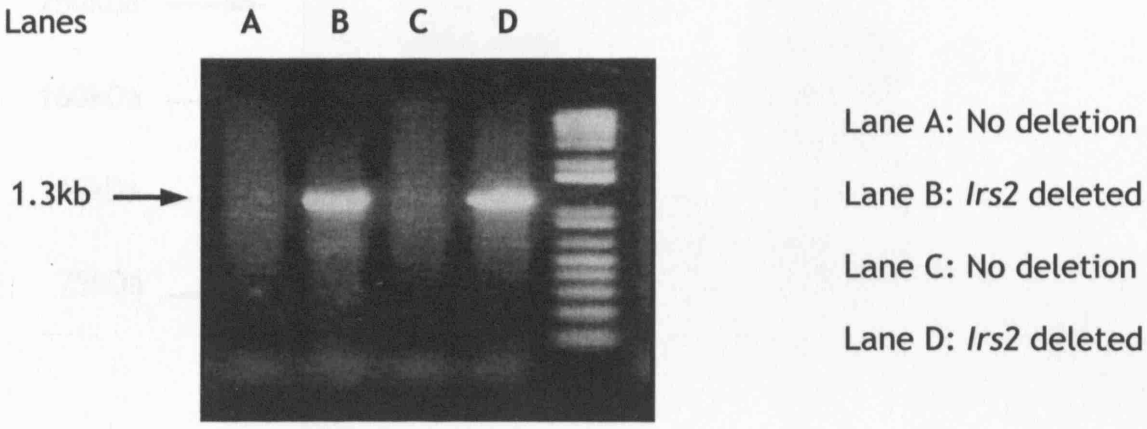

Figure 3.3 Hepatic deletion of *Irs2*

Genomic DNA extracted from liver tissue was amplified by PCR and separated by electrophoresis.

3.4 Confirmation of absence of liver Irs2 expression

To investigate whether the genetic recombination event detected by PCR translated into changes in hepatic Irs2 protein production, immunoprecipitates of Irs2 were analysed by immunoblotting. A cohort of 3 month-old animals was studied, as the Cre-mediated excision is known to be complete at 6 weeks (214). Results showed that Irs2 was absent in all 4 *LivIrs2KO* animals (**Figure 3.4**).

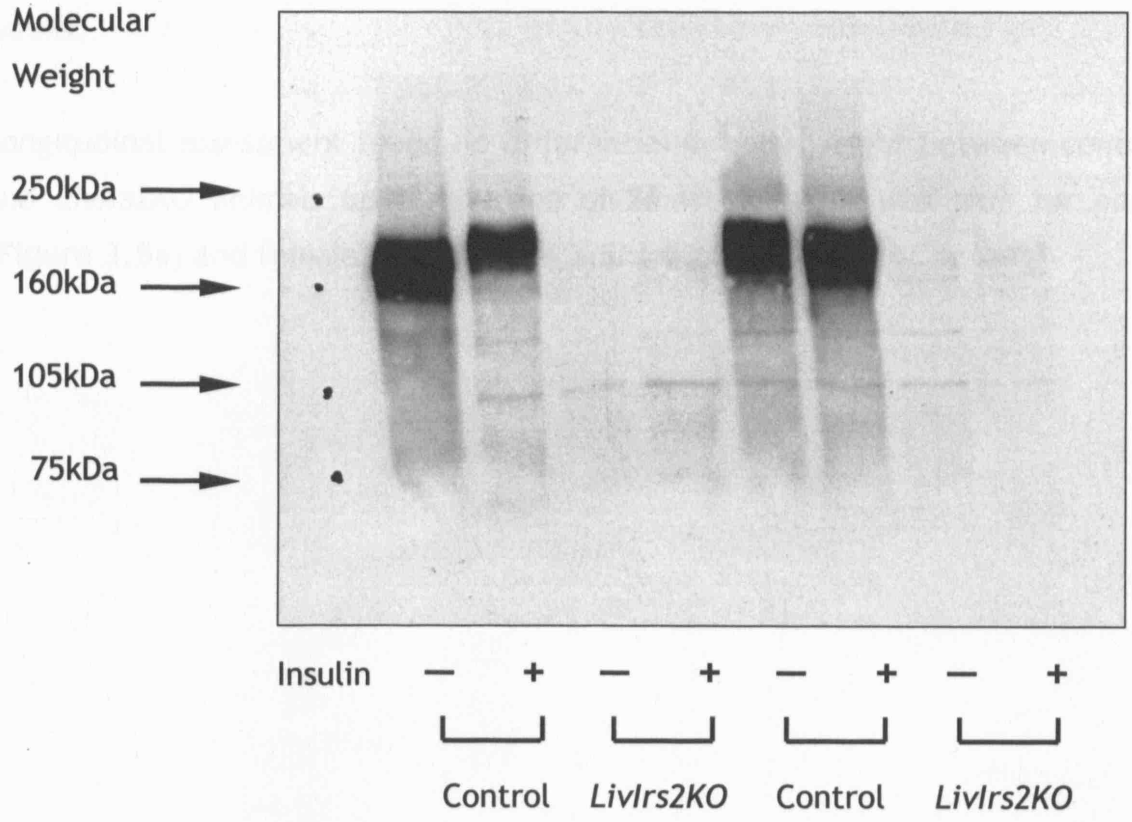

Figure 3.4 Absence of Irs2 protein in the liver

Saline (—) and insulin-stimulated liver lysates (+) from control and *LivIrs2KO* mice were subjected to Irs2 immunoprecipitation and subsequent Irs2 immunoblotting. Results represent three independent experiments. A band shift effect due to insulin-mediated phosphorylation of Irs2 is visible in the first two lanes.

3.5 Body weight and growth pattern

There were no obvious differences in early postnatal development and pre-weaning growth between *LivIrs2KO* animals and their littermates. Global *Irs2* null mice are approximately 10% smaller than wild type animals and male mice develop diabetes at around the age of 10 weeks (200). This coincides with a peak body weight of approx. 25g (unpublished data); progressive weight loss occurs thereafter due to the associated catabolic state. To detect growth abnormalities in adulthood, animal weight was measured up to the age of 26 weeks.

Longitudinal assessment found no differences in body weight between control and *LivIrs2KO* animals up to the age of 26 weeks. This was true for male (**Figure 3.5a**) and female mice (**Figure 3.5b**).

a

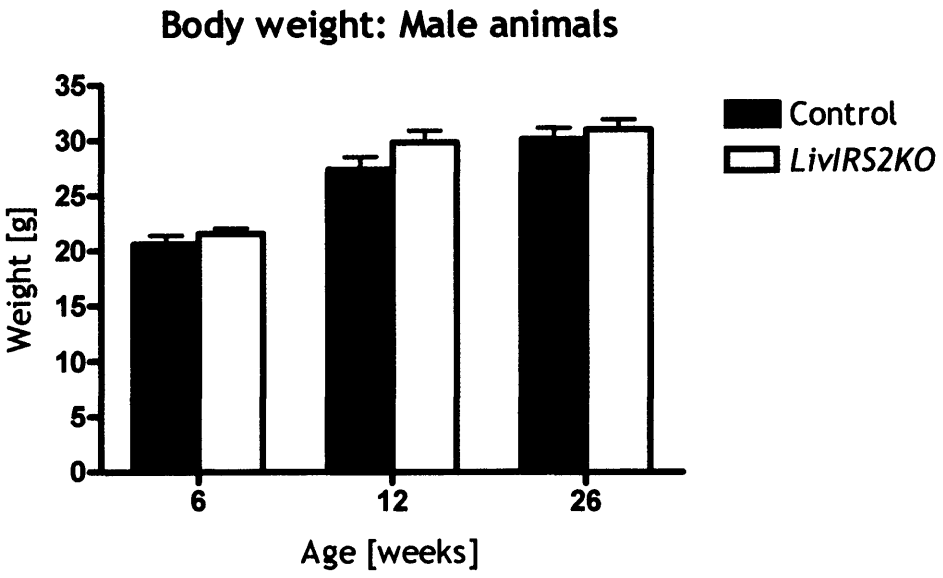

b

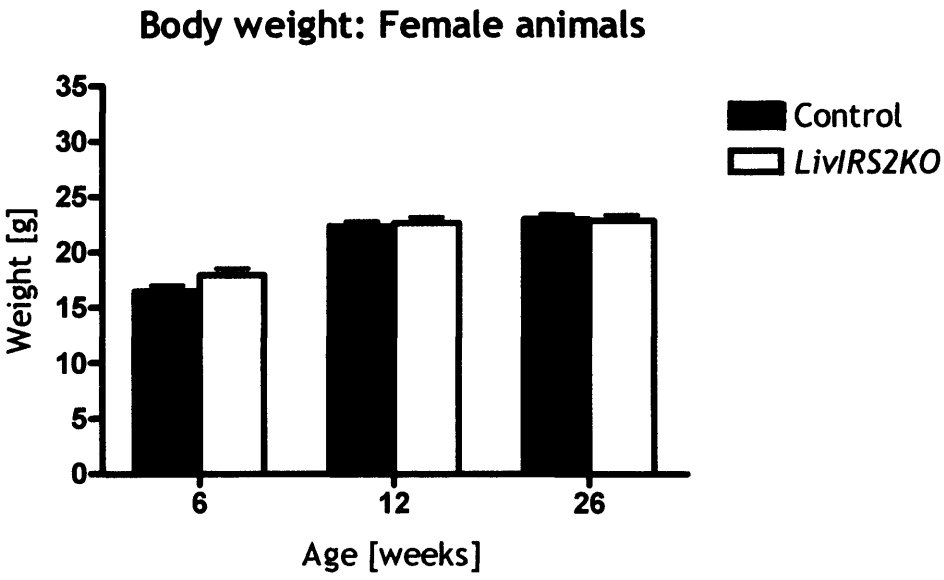

Figure 3.5 Body weights at 6, 12, and 26 weeks

Control and *LivIrs2KO* mice on regular chow were weighed at indicated ages. Data represent the mean ± SEM for 5-18 male (**a**) and 7-22 female animals (**b**).

Chapter 4 RESULTS: INSULIN SIGNALLING EVENTS

The deletion of a key molecule of the insulin signalling cascade, such as Irs2, has the potential to alter signalling events in several ways. Compensatory upregulation of redundant pathways, reduction of downstream signalling, or complex effects across usually independent cascades could occur.

In global *Irs2* null mice, the absence of Irs2 resulted in dysregulated Irs1-associated PI3K activation and in hepatic insulin resistance (200, 225). Hepatic expression of the insulin receptor was unchanged, although receptor downregulation in response to severe hyperinsulinaemia is associated with insulin resistance (226).

Furthermore, both Irs1 and Irs2 are expressed in the liver and there is overlap in the function of both docking molecules. Whilst in the global *Irs2*$^{-/-}$ model no differences in Irs1 expression were observed, compensatory upregulation of Irs2 expression was demonstrated in the liver of mice lacking *Irs1* in all tissues (227).

Thus, the expression and phosphorylation status of key insulin signalling molecules were studied in hepatic tissue of terminally anaesthetised 12 week-old male mice, five minutes after the intravenous administration of 5IU of insulin.

4.1 Proximal insulin signalling

The proximal part of the insulin signalling cascade was assessed by analysis of hepatic Insrβ expression in control and *LivIrs2KO* animals. Irs1 levels were examined to determine any compensatory change that may occur as a consequence of the tissue-specific absence of Irs2.

The results showed no differences in Insrβ expression; either between control and *LivIrs2KO* animals, or between the insulin-stimulated and control groups (**Figures 4.1a, b**). Irs1 expression was also found to be similar in control and *LivIrs2KO* mice (**Figures 4.1c, d**).

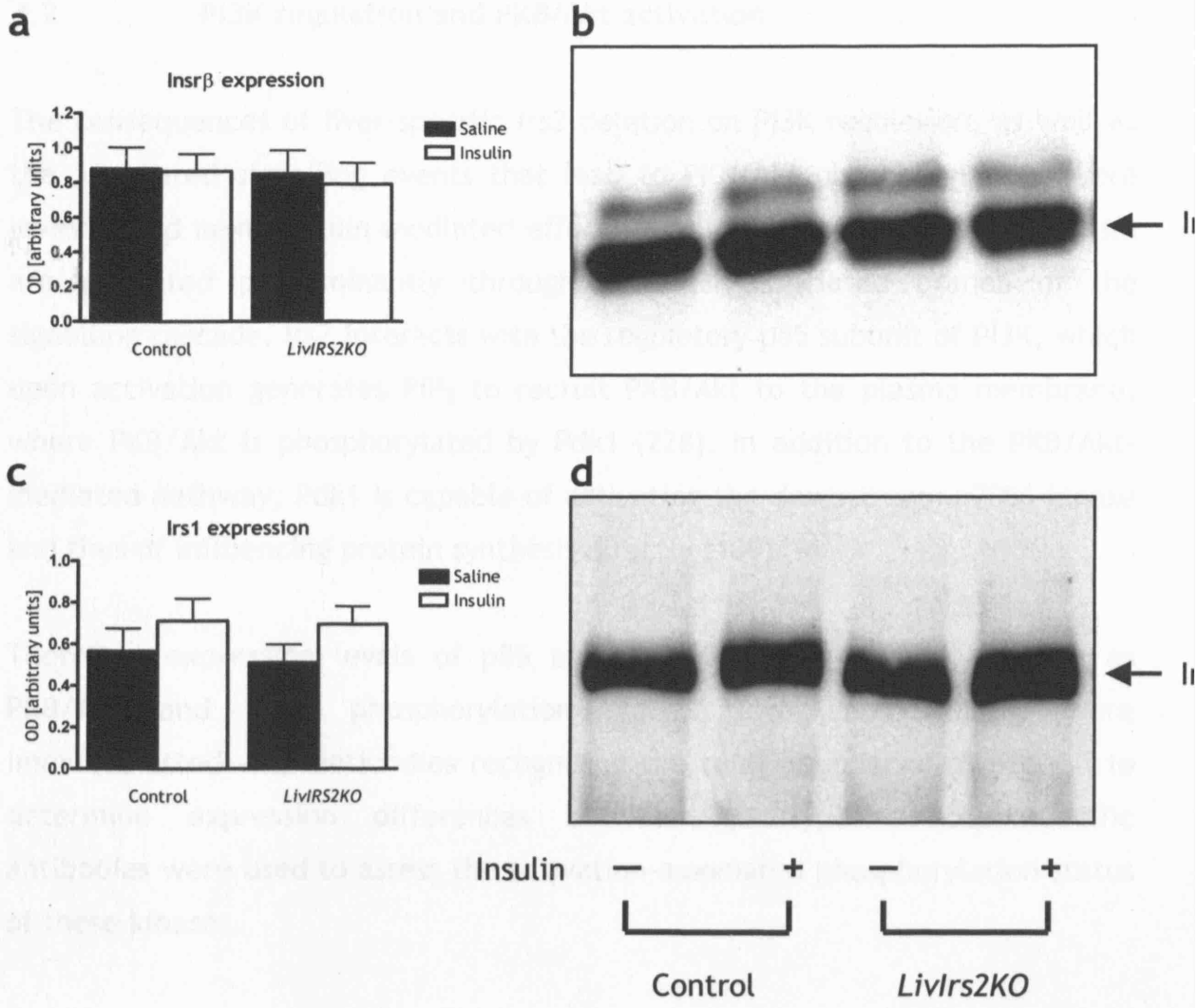

Figure 4.1 Proximal insulin signalling

Liver homogenates from saline (–) and insulin-stimulated (+) control and *LivIrs2KO* mice were immunoprecipitated with Insrβ (**a, b**) and Irs1 (**c, d**) and subsequently immunoblotted with anti-Insrβ and anti-Irs1 antibody, respectively. Results are presented as paired graphs and blots. Relative image densities obtained by blot quantification are given on the left and a corresponding example blot is shown on the right. Results represent 4 animals of each genotype and quantification graphs are expressed as the mean ± SEM.

4.2 PI3K regulation and PKB/Akt activation

The consequences of liver-specific *Irs2* deletion on PI3K regulation, as well as the associated signalling events that lead to PKB/Akt phosphorylation, were investigated next. Insulin-mediated effects on glucose and protein metabolism are mediated predominantly through the PI3K-associated branch of the signalling cascade. Irs2 interacts with the regulatory p85 subunit of PI3K, which upon activation generates PIP_3 to recruit PKB/Akt to the plasma membrane, where PKB/Akt is phosphorylated by Pdk1 (228). In addition to the PKB/Akt-mediated pathway, Pdk1 is capable of activating the downstream p70S6 kinase and thus of influencing protein synthesis directly (109).

Therefore expression levels of p85 and PKB/Akt were studied, as well as PKB/Akt and Pdk1 phosphorylation status. Liver homogenates were immunoblotted with antibodies recognising the total abundance of protein to determine expression differences between genotypes. Phosphospecific antibodies were used to assess the activation-associated phosphorylation status of these kinases.

The experiments did not reveal any differences in expression levels of p85 (**Figures 4.2a, b**) or in Pdk1 phosphorylation (**Figures 4.2c, d**) between control and *LivIrs2KO* animals, either in the basal state or following insulin stimulation. Whilst overall PKB/Akt expression did not differ by genotype or insulin stimulation status (**Figures 4.3a, b**), basal PKB/Akt phosphorylation appeared to be non-significantly increased in *LivIrs2KO* animals compared to controls (**Figures 4.3c, d**). Upon administration of insulin, both genotypes reached similar levels of PKB/Akt phosphorylation.

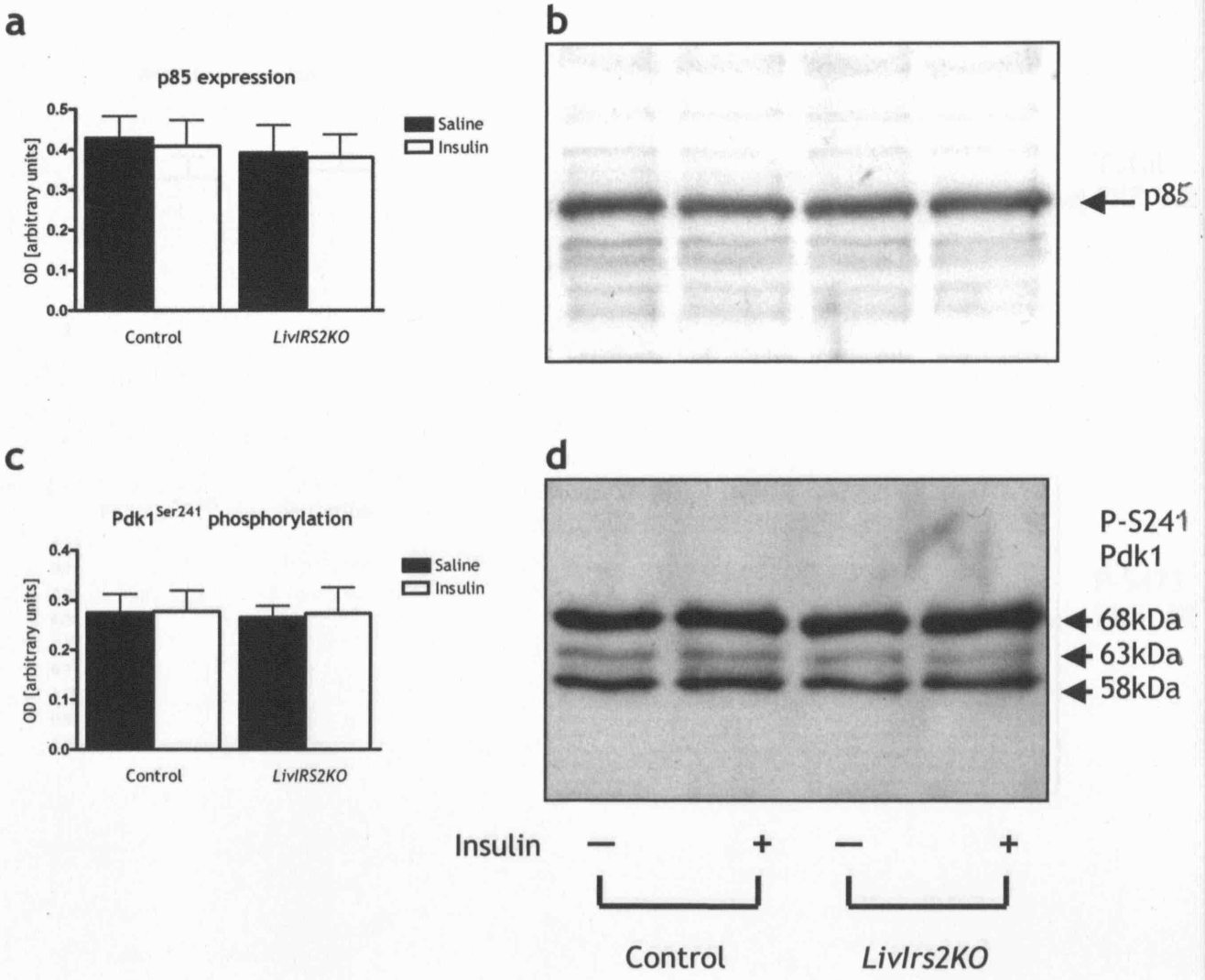

Figure 4.2 PI3K-associated signalling

Liver lysates from saline (—) and insulin-stimulated (+) control and *Livlrs2KO* mice were immunoblotted with anti-p85 (**a, b**) and anti-phospho-Pdk1^{Ser241} antibody (**c, d**). The anti-phospho-Pdk1^{Ser241} antibody recognises three protein isoforms (58kDa, 63kDa, and 68kDa). Results are presented as paired graphs and blots. Relative image densities obtained by blot quantification are given on the left and a corresponding example blot is shown on the right. Results represent 4 animals of each genotype and quantification graphs are expressed as the mean ± SEM.

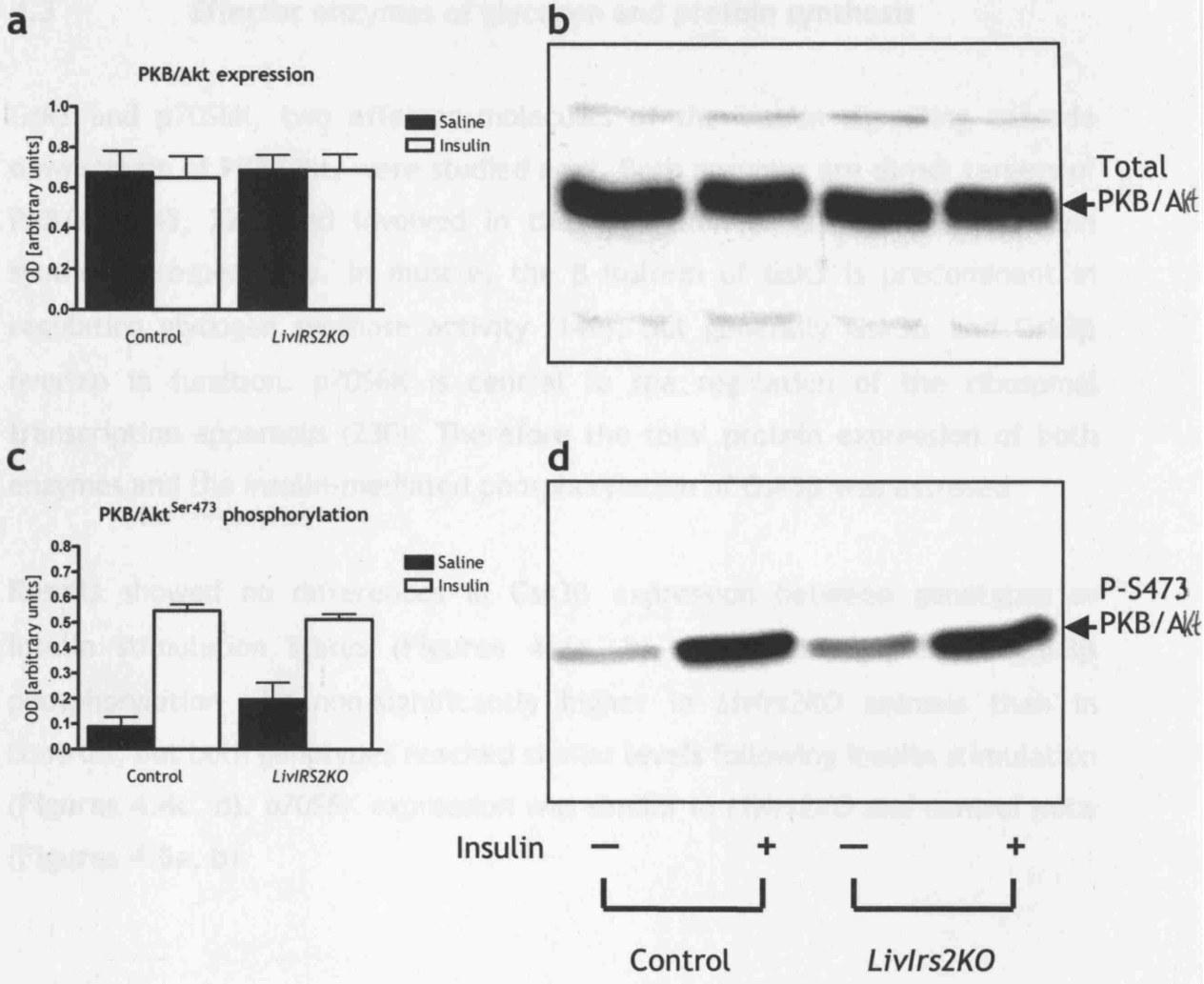

Figure 4.3 PKB/Akt activation

Liver lysates from saline (—) and insulin-stimulated (+) control and *LivIrs2KO* mice were immunoblotted with anti-PKB/Akt (**a, b**), and anti-phospho-PKB/Akt^{Ser473} antibody (**c, d**). Results are presented as paired graphs and blots. Relative image densities obtained by blot quantification are given on the left and a corresponding example blot is shown on the right. Results represent 4 animals of each genotype and quantification graphs are expressed as the mean ± SEM.

4.3 Effector enzymes of glycogen and protein synthesis

Gsk3 and p70S6K, two effector molecules of the insulin signalling cascade downstream of PKB/Akt, were studied next. Both enzymes are direct targets of PKB/Akt (45, 229) and involved in the regulation of glycogen and protein synthesis, respectively. In muscle, the β-isoform of Gsk3 is predominant in regulating glycogen synthase activity (140), but generally Gsk3α and Gsk3β overlap in function. p70S6K is central to the regulation of the ribosomal transcription apparatus (230). Therefore the total protein expression of both enzymes and the insulin-mediated phosphorylation of Gsk3β was assessed.

Results showed no differences in Gsk3β expression between genotypes or insulin stimulation status (**Figures 4.4a, b**). The basal degree of Gsk3β phosphorylation was non-significantly higher in *LivIrs2KO* animals than in controls, but both genotypes reached similar levels following insulin stimulation (**Figures 4.4c, d**). p70S6K expression was similar in *LivIrs2KO* and control mice (**Figures 4.5a, b**).

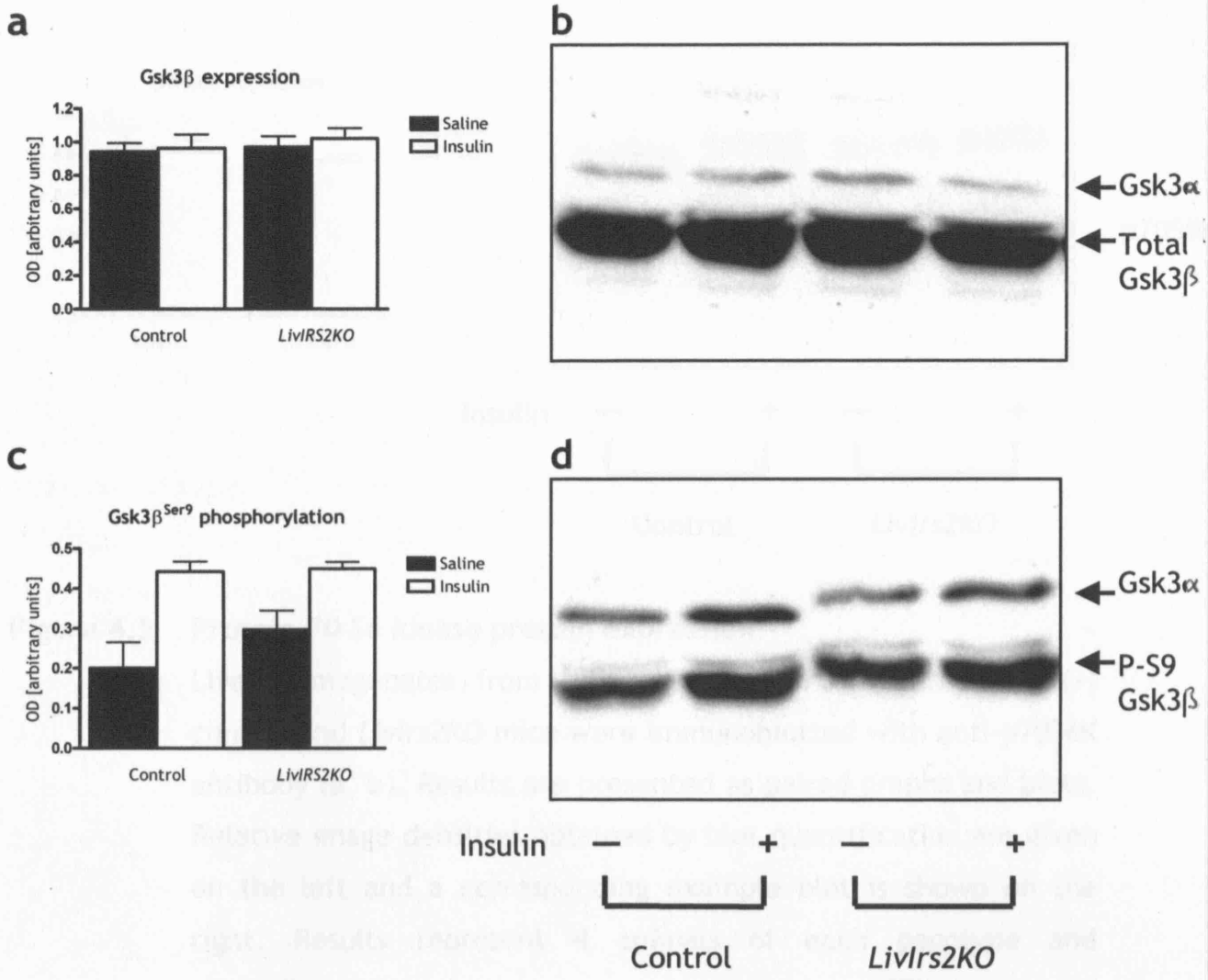

Figure 4.4 Glycogen synthase kinase-3 phosphorylation

Liver homogenates from saline (–) and insulin-stimulated (+) control and *LivIrs2KO* mice were immunoblotted with anti-Gsk3 (**a, b**) and anti-phospho-Gsk3$\alpha/\beta^{Ser9/21}$ antibody (**c, d**). The anti-Gsk3 antibodies detect both α- and β-isoforms (47kDa and 51kDa, respectively), and the β-isoform was quantified. Results are presented as paired graphs and blots. Relative image densities are given on the left and an example blot is shown on the right. Results represent 4 animals of each genotype and graphs are expressed as the mean ± SEM.

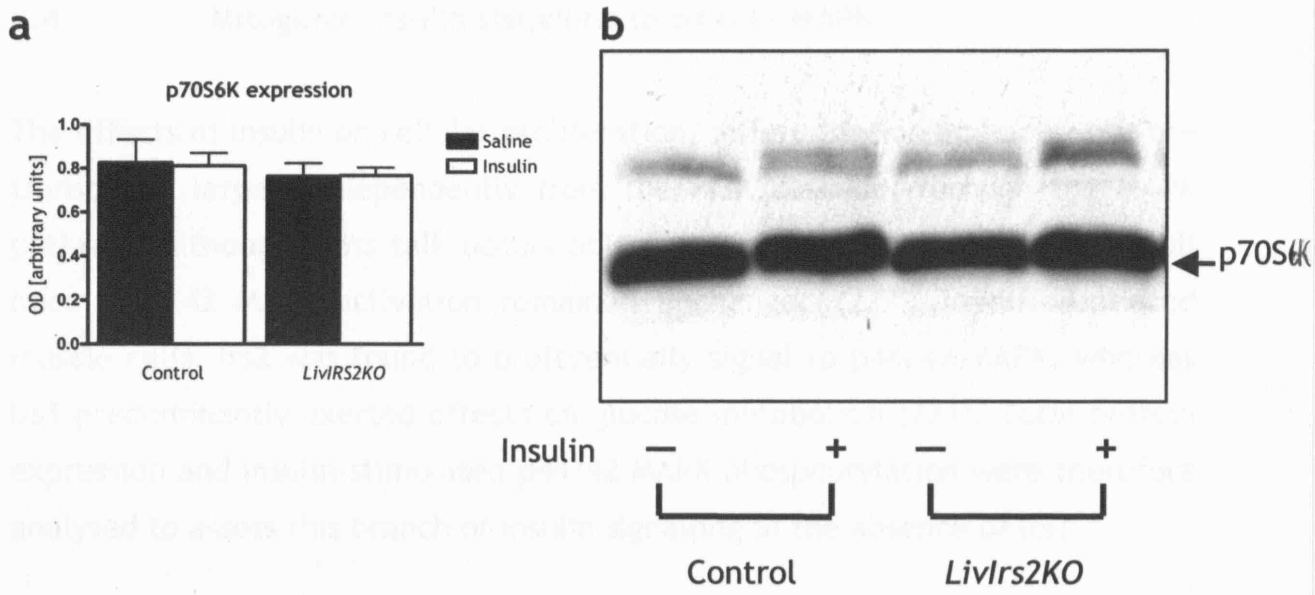

Figure 4.5 Protein-70 S6 kinase protein expression

Liver homogenates from saline (–) and insulin-stimulated (+) control and *LivIrs2KO* mice were immunoblotted with anti-p70S6K antibody (**a, b**). Results are presented as paired graphs and blots. Relative image densities obtained by blot quantification are given on the left and a corresponding example blot is shown on the right. Results represent 4 animals of each genotype and quantification graphs are expressed as the mean ± SEM.

4.4 Mitogenic insulin signalling to p44/42 MAPK

The effects of insulin on cellular proliferation, differentiation and apoptosis are transduced largely independently from the PI3K cascade, through the MAPK pathway, although cross talk occurs at several levels. In the liver of *Irs1* null mice, p44/42 MAPK activation remained unchanged (227). In differentiated muscle cells, Irs2 was found to preferentially signal to p44/42 MAPK, whereas Irs1 predominantly exerted effects on glucose metabolism (231). Total protein expression and insulin-stimulated p44/42 MAPK phosphorylation were therefore analysed to assess this branch of insulin signalling in the absence of Irs2.

The results demonstrated similar basal p44/42 MAPK expression in all groups (**Figures 4.6a, b**), and a comparable insulin-stimulated response of p44/42 MAPK phosphorylation between control and *LivIrs2KO* animals (**Figures 4.6c, d**).

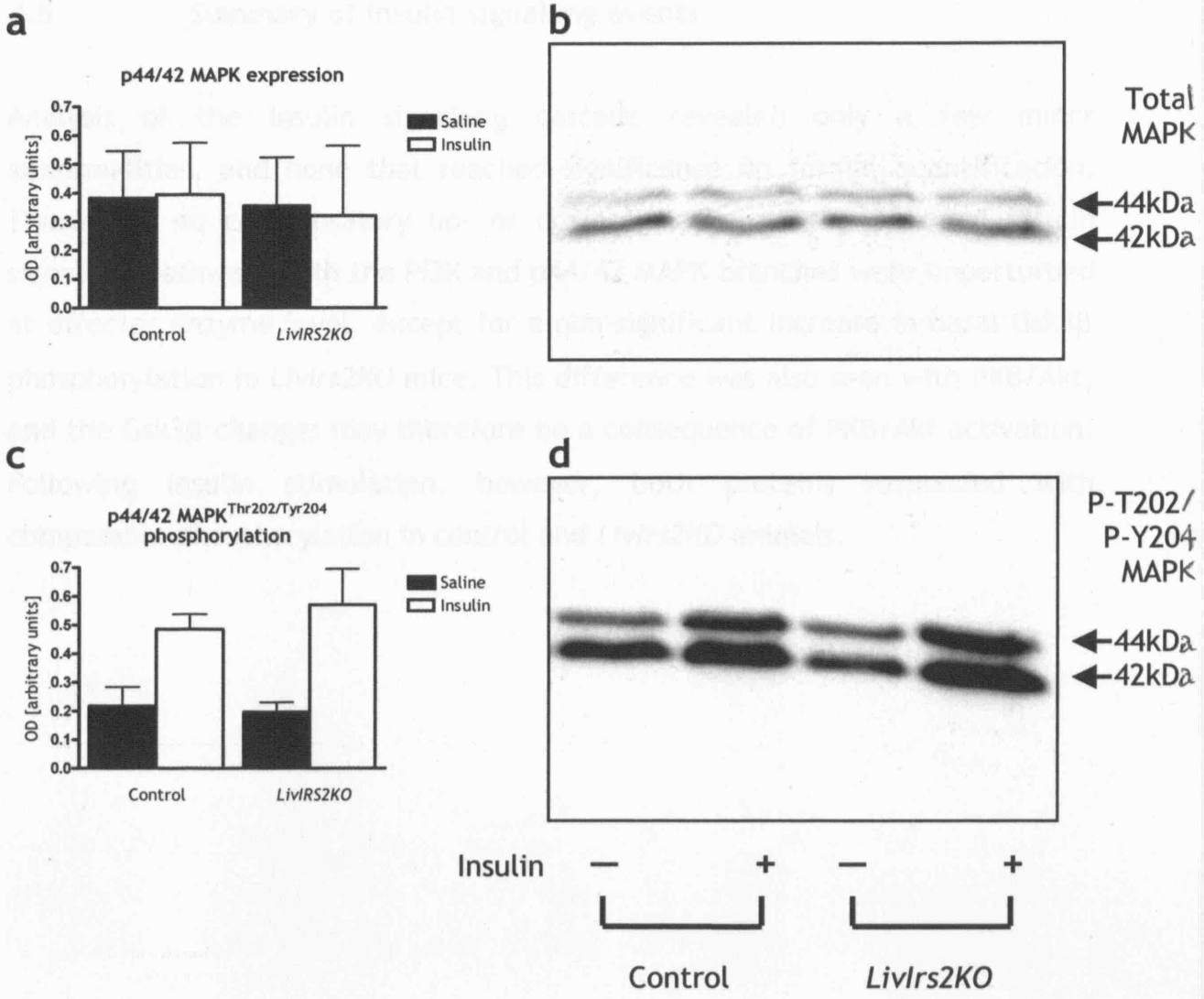

Figure 4.6 Mitogenic insulin signalling

Liver lysates from saline (—) and insulin-stimulated (+) control and *LivIrs2KO* mice were immunoblotted with anti-p44/42 MAPK (**a, b**) and anti-phospho-p44/42 MAPK$^{Thr202/Tyr204}$ antibody (**c, d**). Results are presented as paired graphs and blots. Relative image densities obtained by blot quantification are given on the left and a corresponding example blot is shown on the right. Results represent 4 animals of each genotype and quantification graphs are expressed as the mean ± SEM.

4.5 Summary of insulin signalling events

Analysis of the insulin signalling cascade revealed only a few minor abnormalities, and none that reached significance on formal quantification. There was no compensatory up- or downregulation of the proximal insulin signalling pathway. Both the PI3K and p44/42 MAPK branches were unperturbed at effector enzyme level, except for a non-significant increase in basal Gsk3β phosphorylation in *LivIrs2KO* mice. This difference was also seen with PKB/Akt, and the Gsk3β changes may therefore be a consequence of PKB/Akt activation. Following insulin stimulation, however, both proteins responded with comparable phosphorylation in control and *LivIrs2KO* animals.

Chapter 5 RESULTS: GLUCOSE METABOLISM

The analysis of key insulin signalling molecules in the liver unexpectedly revealed no significant alterations caused by the absence of *Irs2*. Therefore *in vivo* experiments were carried out to determine a possible effect on whole-body glucose homeostasis.

5.1 Glucose metabolism on regular chow

Glucose homeostasis was first assessed in male animals whose diet consisted of a standard rodent chow, with carbohydrates providing 50% of caloric content.

5.1.1 Blood glucose levels

Fasted blood glucose levels were measured in 3 month-old male mice (**Figure 5.1a, left panel**). No difference between control and *LivIrs2KO* animals was found, and the results were within the normal range.

As disturbances in glucose metabolism become more overt with age and in the postprandial state, blood glucose levels were determined in fed 6 month-old male mice (**Figure 5.1a, right panel**). Again, the findings showed no significant differences between the genotypes.

5.1.2 Insulin levels

Serum insulin levels are a marker of insulin resistance and also provide information on pancreatic β-cell function. Insulin resistance increases with age, which leads to adaptive β-cell expansion and increased insulin secretion. In

global *Irs2* null mice this compensatory response was impaired (200). Fasted insulin levels were therefore studied in 3 and 6 month-old male mice.

Results showed no difference in serum insulin in *LivIrs2KO* mice compared to controls at either age (**Figure 5.1b**).

5.1.3 Glucose tolerance

Since subtle changes in carbohydrate metabolism may become evident following a challenge with a defined glucose load, an i.p. GTT was performed in 3 month-old male animals.

The results showed a similar appearance of the glucose excursion graphs in both genotypes (**Figure 5.2a**). Formal analysis of the glucose area-under-the-curve (AUC) excluded any significant difference between the groups (**Figure 5.2b**).

5.1.4 Insulin tolerance

The response of glucose levels to the administration of insulin is an indicator of insulin sensitivity. Thus an i.p. insulin tolerance test (ITT) was performed in 3 month-old male mice and glucose levels relative to baseline values measured.

No difference was found between control and *LivIrs2KO* animals (**Figure 5.3**).

a

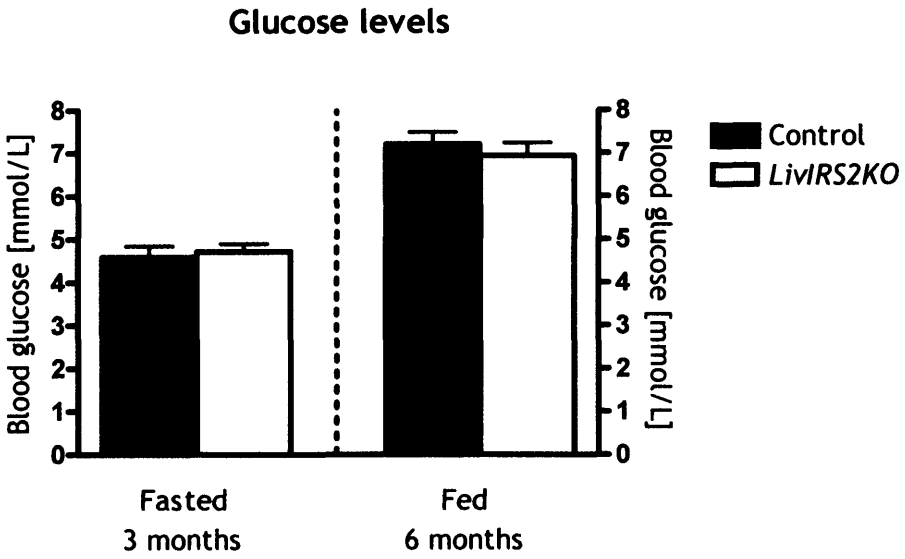

b

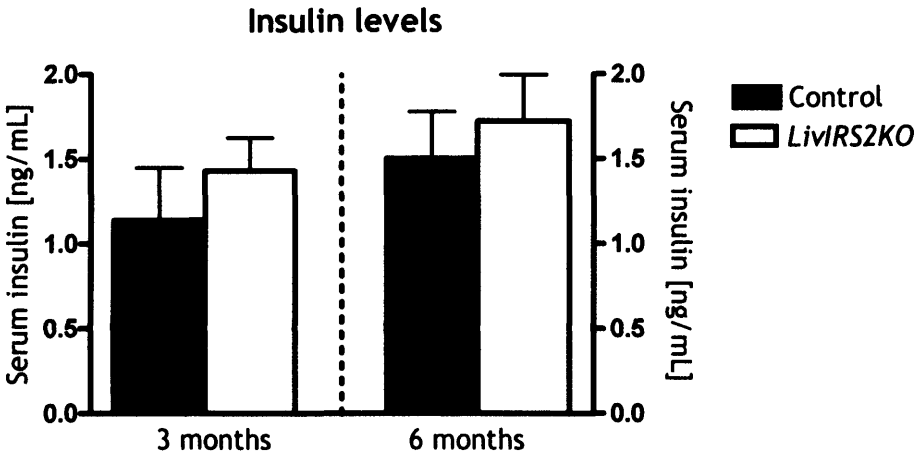

Figure 5.1 Blood glucose and fasted insulin levels

Fasted (**a, left panel**) and fed glucose levels (**a, right panel**) were determined on 3 and 6 months-old male control and *LivIrs2KO* animals, respectively. Data represent the mean ± SEM of 8-12 mice per group. Fasted serum insulin levels were measured on 3 month-old (**b, left panel**) and 6 month-old mice (**b, right panel**). Data represent the mean ± SEM of 3-8 animals per group.

a

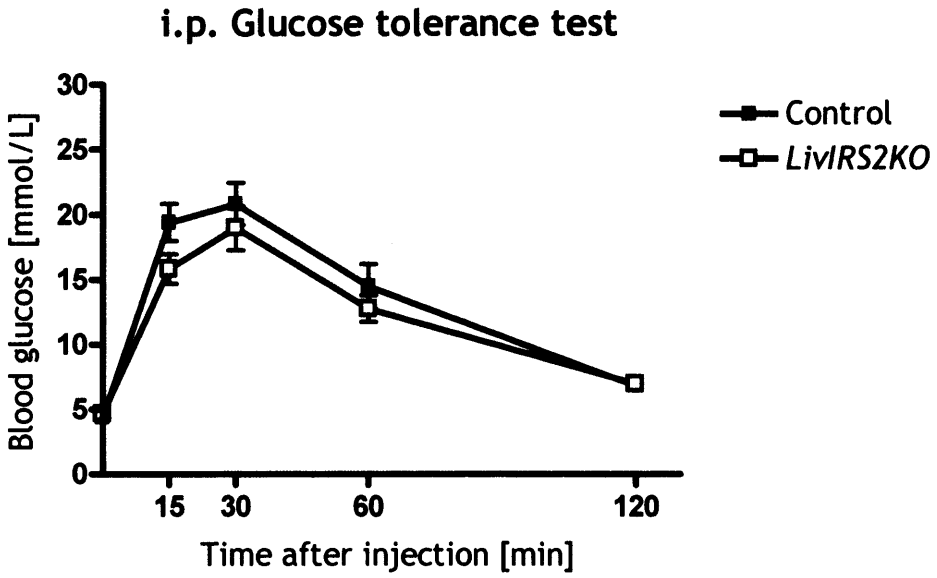

b

Figure 5.2 Glucose tolerance test on 3 month-old animals

2g kg^{-1} of glucose was administered i.p. to male control (*closed squares*) and *LivIrs2KO* animals (*open squares*) (**a**). The areas-under-the-curve for glucose were derived from the same data (**b**). Data represent the mean ± SEM of 6-8 animals of each genotype.

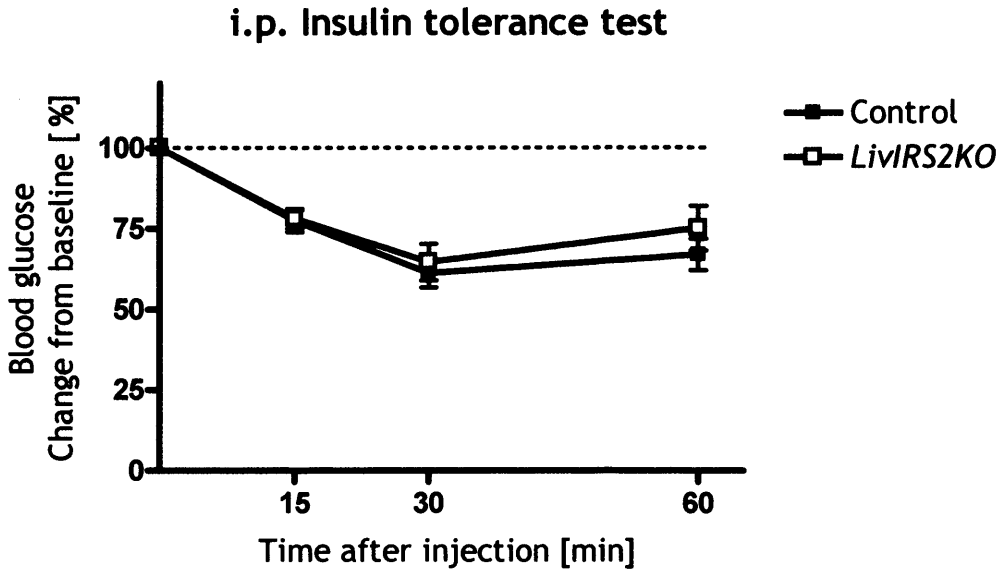

Figure 5.3 Insulin tolerance test on 3 month-old animals

0.75IU kg^{-1} of insulin was administered i.p. to male control (*closed squares*) and *LivIrs2KO* mice (*open squares*). Glucose levels are presented as relative change from baseline and data represent the mean ± SEM for 8 animals.

5.2 Glucose metabolism on high-fat diet

On regular chow, no significant changes in glucose homeostasis were detected in *LivIrs2KO* animals compared to controls. Abnormalities of glucose and lipid metabolism are commonly exacerbated by a high calorie, high fat content diet (232), which in particular leads to a rise in hepatic glucose output (233). Therefore a cohort of 3 month-old male mice was placed on a high fat-containing chow for a period of 3 months (lipids providing 45% of caloric content). Parameters of glucose metabolism were subsequently studied.

5.2.1 Weight gain

The animals were weighed weekly and had *ad libitum* access to water and chow.

As expected, animals gained more weight on high fat diet (HFD) than on regular chow (**Figure 5.4**). Over the study period of three months, control animals gained an average of 7.7 ± 1.7g (high fat) and 3.8 ± 0.7g (regular diet), whereas *LivIrs2KO* mice gained 8.3 ± 1.4g and 4.2 ± 0.5g, respectively. The differences in weight gain between diets were statistically significant (controls, p=0.031; *LivIrs2KO*, p=0.019), but those between genotypes within the dietary cohorts were not.

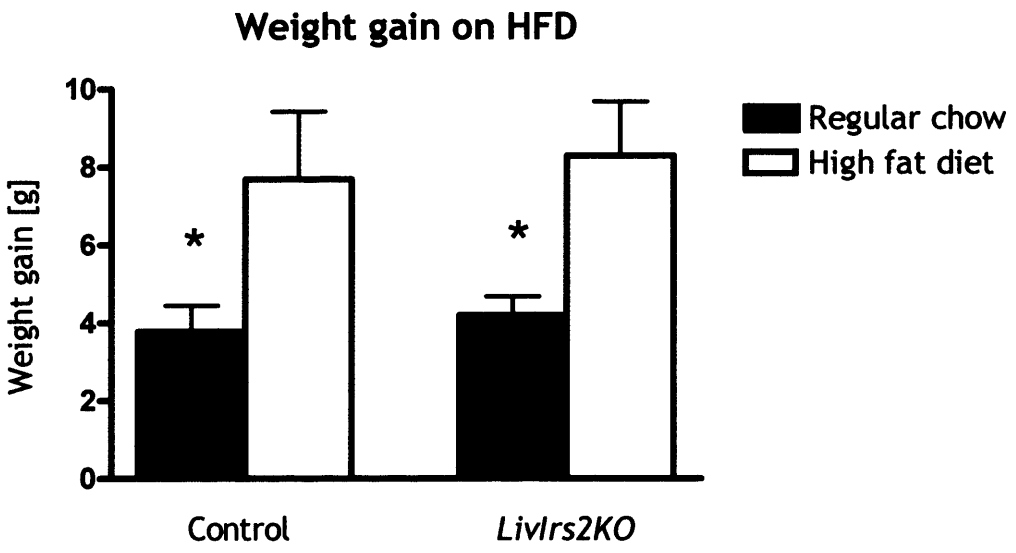

Figure 5.4 Weight gain on high fat diet

3 month-old male control and *LivIrs2KO* mice were offered high fat chow for 3 months. Weight gain of 6 month-old animals was measured at the end of the study period. Data represent the mean ± SEM of 5-8 animals. * $p<0.05$.

5.2.2 Blood glucose levels

Fasted blood glucose levels were measured after 3 months on HFD in 6 month-old mice. On regular diet, fasted blood glucose levels remained within the non-diabetic range in both control and *LivIrs2KO* animals (**Figure 5.5a**). In the HFD group, glucose concentrations of control animals were at the threshold for the diagnostic criterion for diabetes (7.0 ± 0.36 mmol/L) and they were significantly elevated in *LivIrs2KO* mice (8.2 ± 0.19 mmol/L; $p=0.024$).

To examine whether this disturbance in fasted glucose metabolism became more pronounced in the postprandial state, fed blood glucose levels were

determined. The results showed no differences between the diets or between genotypes (**Figure 5.5b**). Unexpectedly, the elevation in blood glucose of fasted *LivIrs2KO* mice was no longer apparent in the fed state.

5.2.3 Glucose tolerance

After 10 weeks of dietary intervention an i.p. GTT was performed.

The results did not reveal any differences between control and *LivIrs2KO* animals on either regular (**Figure 5.6a**) or high fat diet (**Figure 5.6b**).

The analysis of the AUC for glucose showed no differences in glucose disposal in control compared to *LivIrs2KO* animals, regardless of the type of diet (**Figure 5.7**).

5.2.4 Insulin tolerance

The glucose response to insulin was studied during an i.p. ITT following 12 weeks of dietary intervention.

No difference was found between control and *LivIrs2KO* animals on regular diet (**Figure 5.8a**). In the HFD cohort, *LivIrs2KO* mice appeared to show a more pronounced fall in glucose levels than controls, with the largest difference observed at 30min (**Figure 5.8b**). Even at this time point, however, the difference remained non-significant (p=0.195).

At 60min, control animals displayed significantly higher glucose values on HFD when compared to regular diet (p=0.009) (**Figure 5.9**).

a

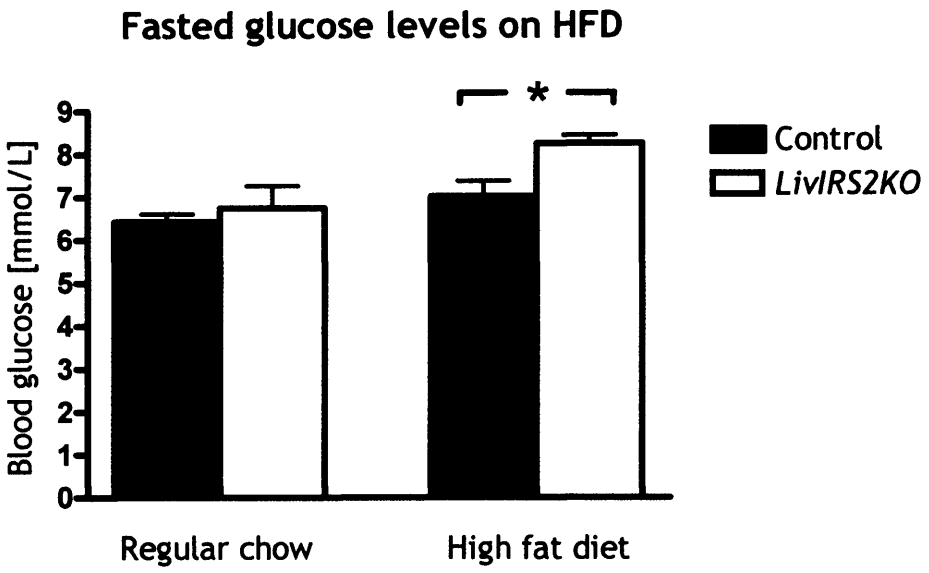

b

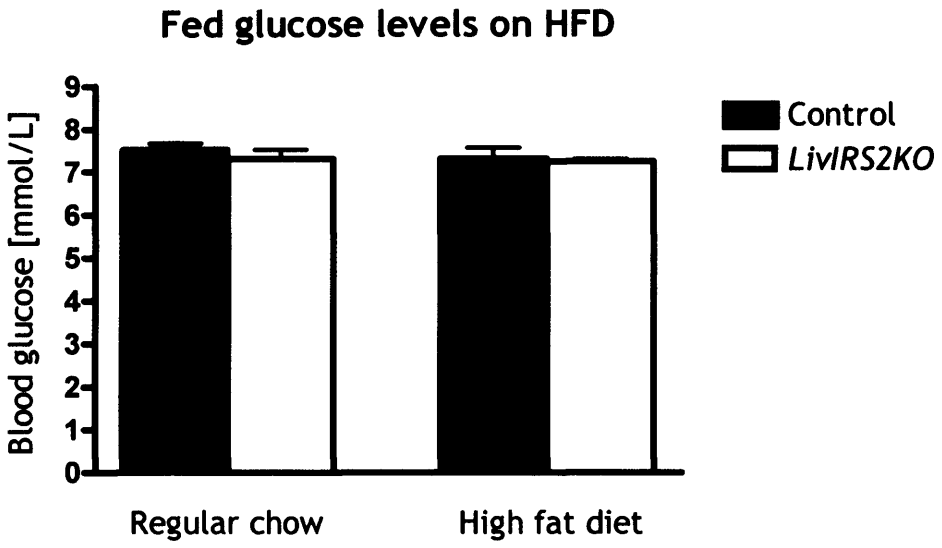

Figure 5.5 Blood glucose levels on high fat diet

Fasted (a) and fed glucose levels (b) were measured on 6 month-old male control and *LivIrs2KO* animals after 3 months on high fat diet. Data represent the mean ± SEM of 4-8 animals per group.

* $p<0.05$.

a

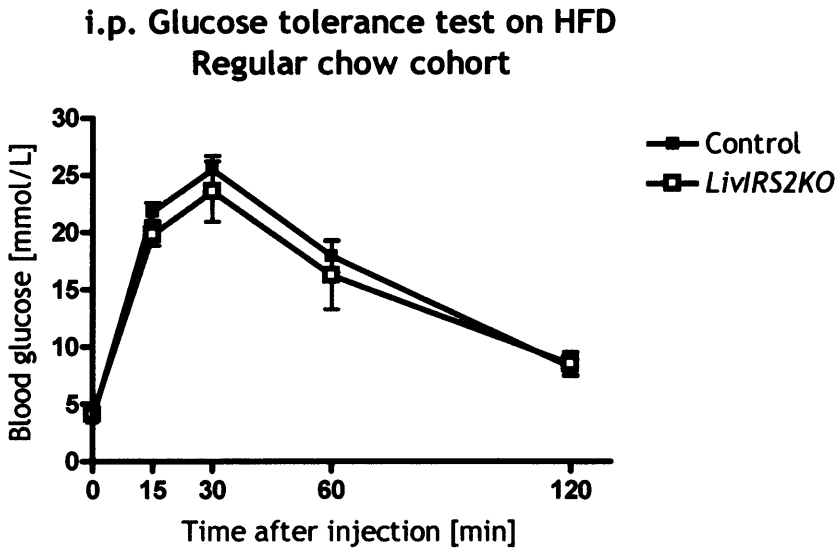

b

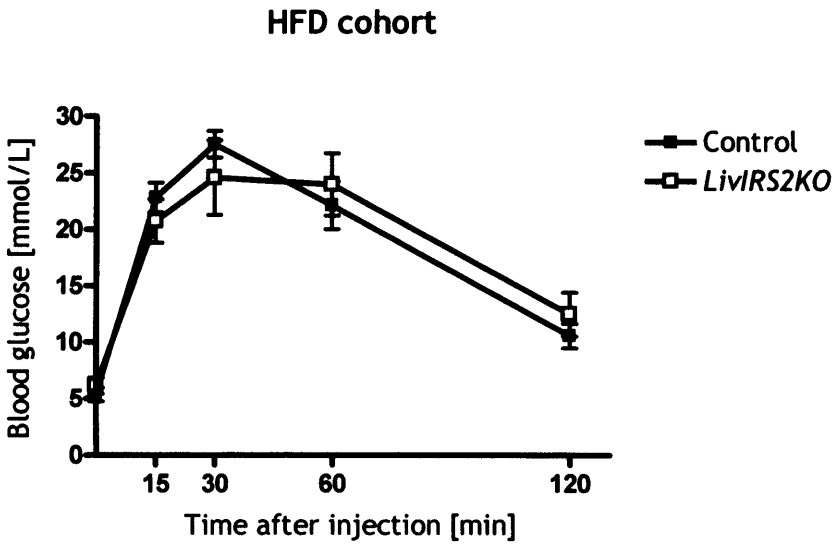

Figure 5.6 Glucose tolerance test on high fat diet

2g kg^{-1} of glucose was administered i.p. to 5 month-old male control (*closed squares*) and *LivIrs2KO* mice (*open squares*) after 10 weeks on regular (**a**) and high fat chow (**b**). Data represent the mean ± SEM of 5-8 animals per group.

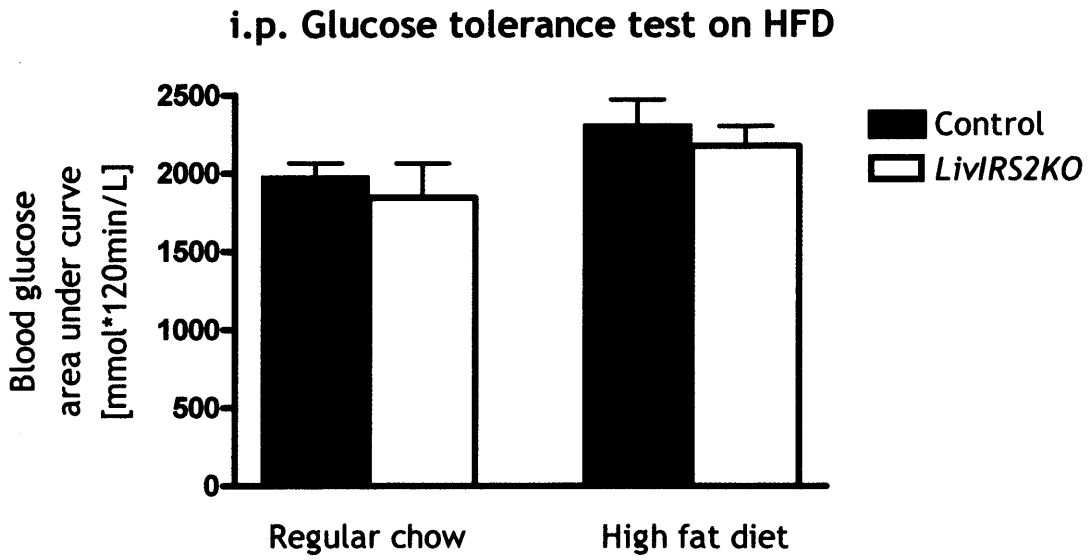

Figure 5.7 Areas-under-the-curve for glucose during a GTT on HFD
The data shown are derived from those shown in Figure 5.6.

a

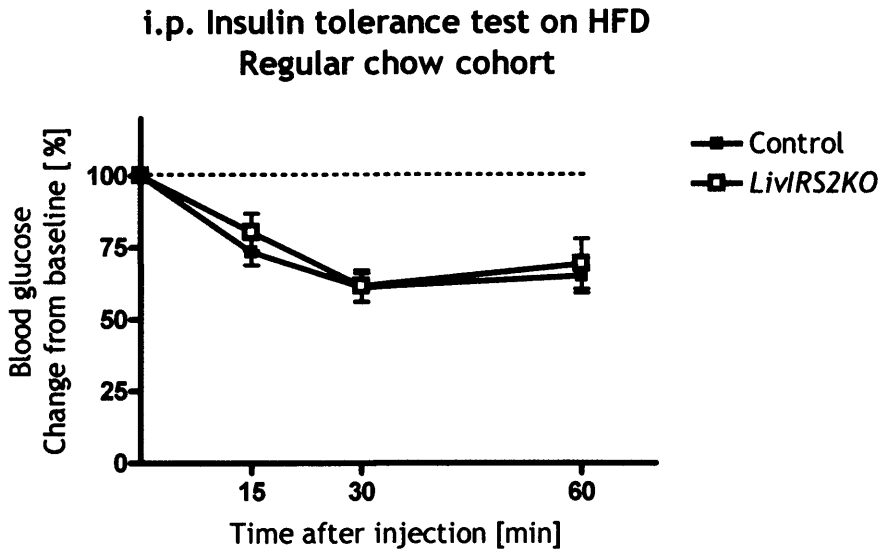

b

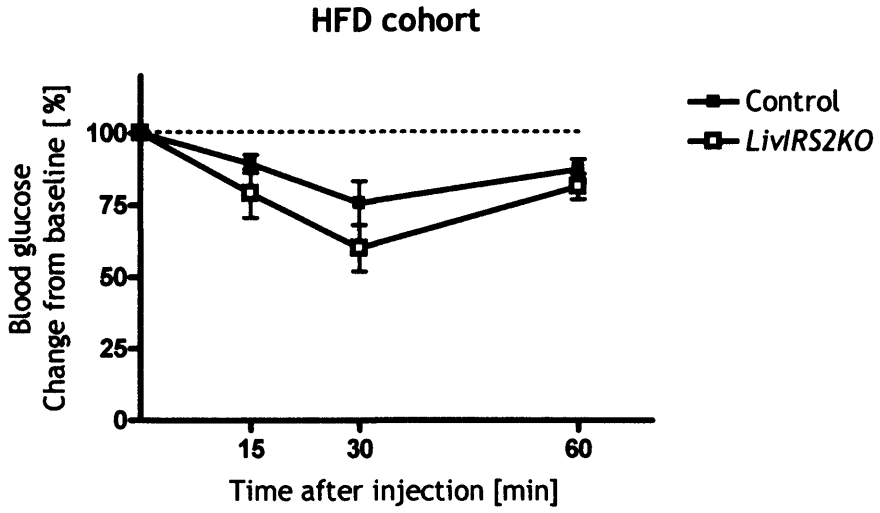

Figure 5.8 Insulin tolerance test on high fat diet

0.75IU kg^{-1} of insulin was administered i.p. to 6 month-old male control (*closed squares*) and *LivIrs2KO* mice (*open squares*) after 12 weeks on regular chow (**a**) and high fat diet (**b**). Glucose levels are presented as relative change from baseline and data represent the mean ± SEM for 5-8 animals per group.

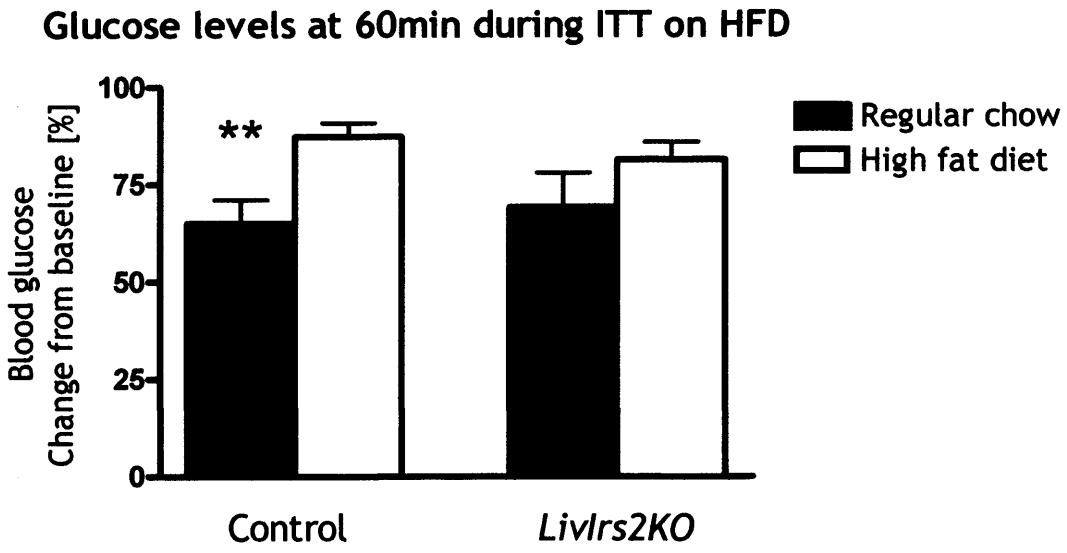

Figure 5.9 Glucose levels at the end of an ITT on HFD

Glucose responses at the 60min time point are presented as relative change from baseline. The data shown are derived from those plotted in Figure 5.8. ** $p<0.01$.

5.3 Summary of the assessment of glucose metabolism

LivIrs2KO animals did not display a significant abnormality in whole-body glucose homeostasis. Insulin levels were comparable in *LivIrs2KO* mice and controls. During the exposure to a high-fat chow, all animals gained significantly more weight, but without an additional effect by hepatic *Irs2* deficiency. Whilst *LivIrs2KO* mice showed a mild elevation of fasted glucose levels following a 3 month exposure to HFD, fed glucose levels and the response to an i.p. GTT did not support the notion of a significant disturbance of glucose disposal on either diet. During an i.p. ITT, glucose levels fell to a similar degree in control and *LivIrs2KO* animals, although HFD adversely affected the 60min response of control animals.

Chapter 6 RESULTS: LIPID METABOLISM

Insulin regulates lipolysis in adipose tissue and an elevation of NEFA levels is both a result of insulin resistance and further aggravates the insulin resistant state (234). Furthermore, the dyslipidaemia seen with insulin resistance and in type 2 diabetes characteristically shows elevated levels of TG, resulting from hepatic *de novo* lipogenesis derived from glucose, chylomicron remnant uptake, and NEFA availability (235). This is compounded by reduced postprandial clearance from the circulation by insulin-sensitive lipoprotein lipase (236). In chronic insulin resistance and diabetes, triglycerides accumulate in hepatic tissue and lead to steatosis (237).

Global *Irs2* null mice showed marked adipose tissue insulin resistance in hyperinsulinaemic-euglycaemic clamp studies, with reduced suppression of lipolysis and glycerol turnover leading to elevated NEFA levels (94). In two insulin resistant mouse models, ongoing Srepb1c activation led to persistent fatty acid synthesis despite a concomitant downregulation of Irs2 (204).

Irs2$^{-/-}$ animals also displayed hyperphagia and developed obesity (202), as well as hyperleptinaemia and hypothalamic leptin resistance (206). The adipocyte-derived cytokine leptin furthermore influences insulin resistance not only through its regulatory effect on caloric intake and fat mass, but can also directly enhance insulin-mediated inhibition of HGP and alter hepatic gene expression (238). The effect of leptin on HGP is at least in part mediated by Irs2 (239).

Therefore the effects of hepatic *Irs2* deficiency on acute insulin-regulated lipid homeostasis and leptin levels were investigated.

6.1 Serum non-esterified fatty acid and triglyceride levels

NEFA and TG levels were measured in 12 week-old male mice following an overnight fast and a subsequent 2-hour refeeding period.

Results showed a marked reduction of NEFA levels by refeeding, but no significant differences were observed between control and *LivIrs2KO* animals within each group (**Figure 6.1a**).

Refeeding did not significantly increase TG levels (**Figure 6.1b**). There were no differences between *LivIrs2KO* animals and controls in both the fasted state and after refeeding.

6.2 Leptin levels

Fasted leptin levels were studied in 6 month-old male mice.

No difference between control and *LivIrs2KO* mice was found (**Figure 6.2**).

a

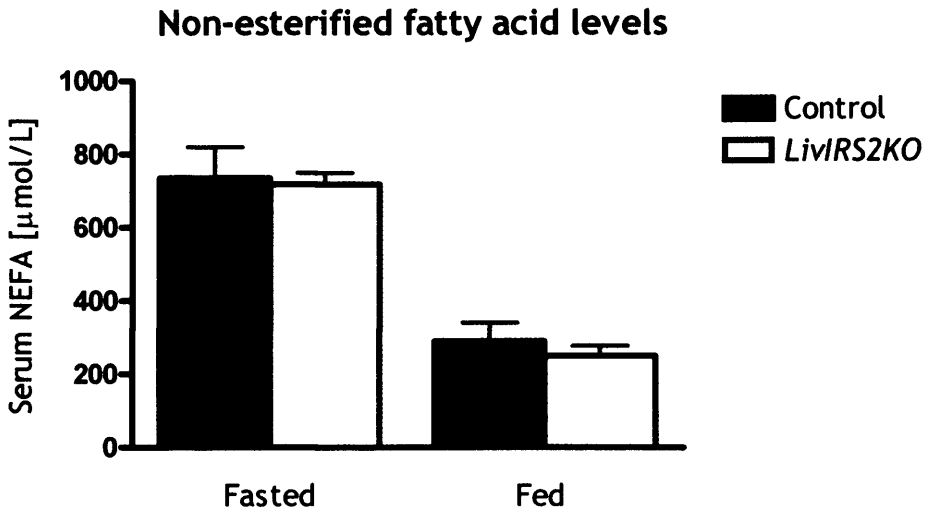

b

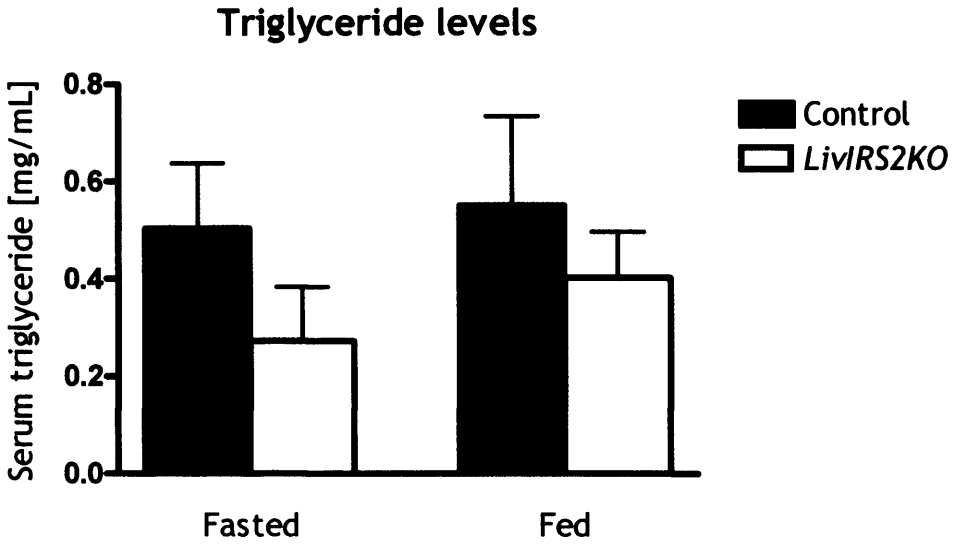

Figure 6.1 Parameters of lipid metabolism

Fasted and fed serum levels of NEFA (**a**) and triglycerides (**b**) were measured after an overnight fast and a subsequent 2-hour refeeding period in 12 week-old control and *LivIrs2KO* mice. Data represent the mean ± SEM for 5 animals of each genotype.

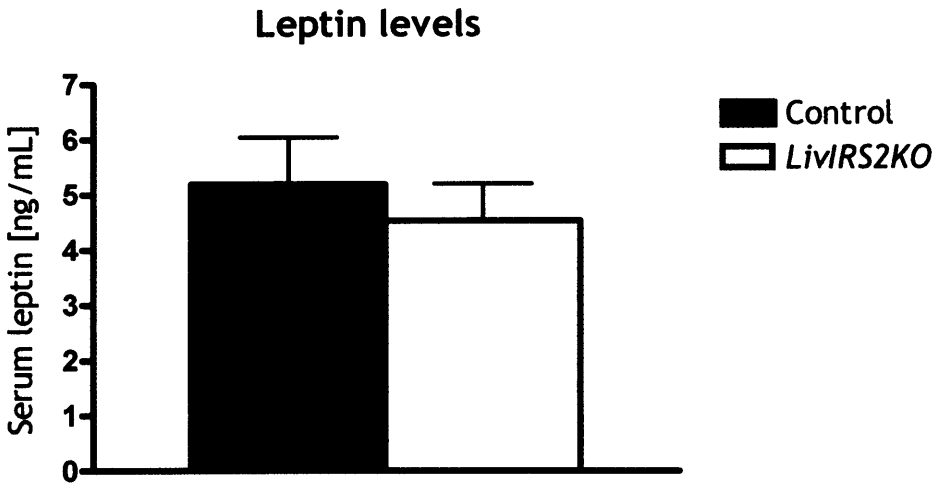

Figure 6.2 Serum leptin levels

Fasted serum concentrations of leptin were determined on 6 month-old male control and *LivIrs2KO* mice. Data represent the mean ± SEM for 5 animals of each genotype.

6.3 Summary of the assessment of lipid metabolism

No abnormality in lipid metabolism was detected in *LivIrs2KO* animals. Refeeding appropriately suppressed NEFA levels but did not alter TG levels. There were no differences between control and *LivIrs2KO* mice in any subgroup. Fasted leptin levels were similar in both genotypes.

Chapter 7 RESULTS: CLAMP EXPERIMENTS

The *in vivo* physiology experiments to assess glucose homeostasis did not reveal major abnormalities in the absence of hepatic *Irs2*. Changes in glucose metabolism, however, may be offset by compensatory mechanisms between different tissue compartments or may be too subtle to be detected by approaches such as GTT or ITT (240).

Hyperinsulinaemic-euglycaemic clamp studies with ^{3}H-labelled glucose were thus performed on conscious 3 month-old mice after a 6-hour fast for a more detailed analysis of glucose homeostasis. This tracer method allowed the assessment of additional metabolic parameters relating to the whole animal. Results were derived from multiple samples obtained during the steady-state period.

7.1 Endogenous glucose production and glycolysis

The balance between endogenous glucose production and the rate of glycolysis is an important factor in the maintenance of glucose homeostasis (241). Insulin plays a major role the regulation of these processes by shifting the balance in favour of glycolysis under feeding conditions, whilst gluconeogenesis remains tightly controlled during fasting. Endogenous glucose production and glycolysis rate were thus measured to assess the effect of absent hepatic Irs2 on the insulin-mediated regulation of these parameters.

There was no difference in endogenous glucose production between control and *LivIrs2KO* animals (**Figure 7.1a**). Glycolytic rates were also comparable between genotypes (**Figure 7.1b**).

7.2 Glucose turnover and glycogen synthesis

Whole-body glucose utilisation (also described as glucose turnover) consists of glycolysis, glycogen synthesis, and the synthesis of intermediary metabolites such as glycerol and other sugars (241). Insulin enhances the activity of all three pathways, and therefore whole-body glucose turnover and glycogen synthesis were measured during the clamp studies. The results showed a small, but significant reduction of glucose turnover in *LivIrs2KO* animals compared to controls (p=0.044) (**Figure 7.2a**).

Since the rates of glycolysis were similar in both genotypes, glycogen synthesis was studied to identify the underlying metabolic defect causing a reduction in glucose turnover rate. Whole-body glycogen synthesis rates were significantly lower in *LivIrs2KO* mice compared to control animals (p=0.03) (**Figure 7.2b**).

7.3 Glucose infusion rate

The glucose infusion rate that is required to maintain euglycaemia during a steady state condition of hyperinsulinaemia has an inverse relationship to whole-body insulin resistance. The glucose infusion rate was therefore measured. Results showed similar glucose infusion rates in control and *LivIrs2KO* animals (**Figure 7.3**).

a

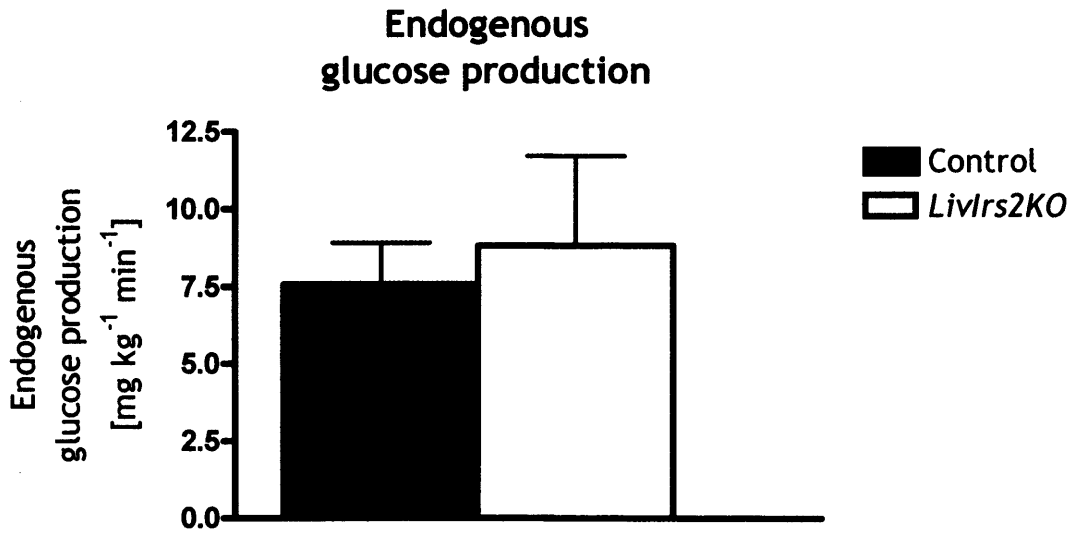

b

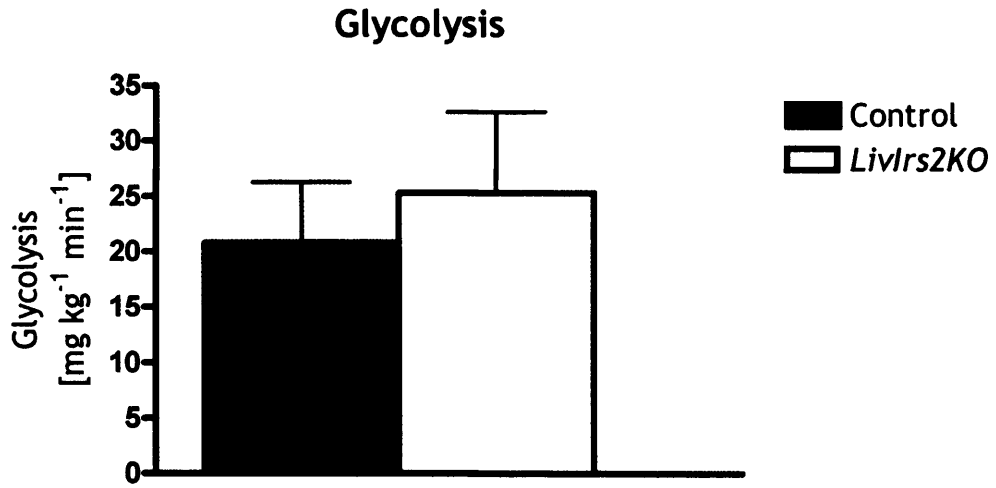

Figure 7.1 Endogenous glucose production and glycolysis

Rates of endogenous glucose production (**a**) and of glycolysis (**b**) were measured on 3 month-old control and *Livlrs2KO* animals. Data represent the mean ± SEM for 8-9 animals of each genotype.

a

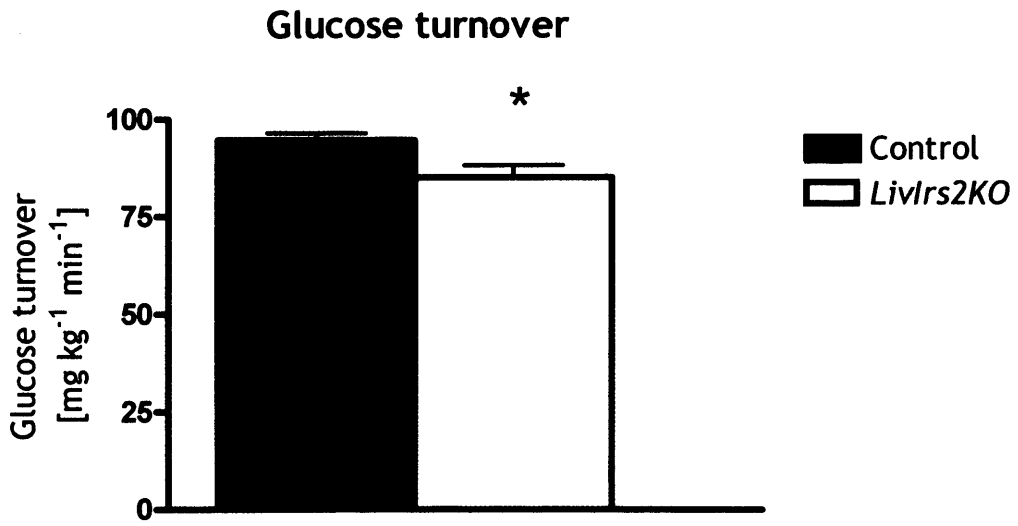

b

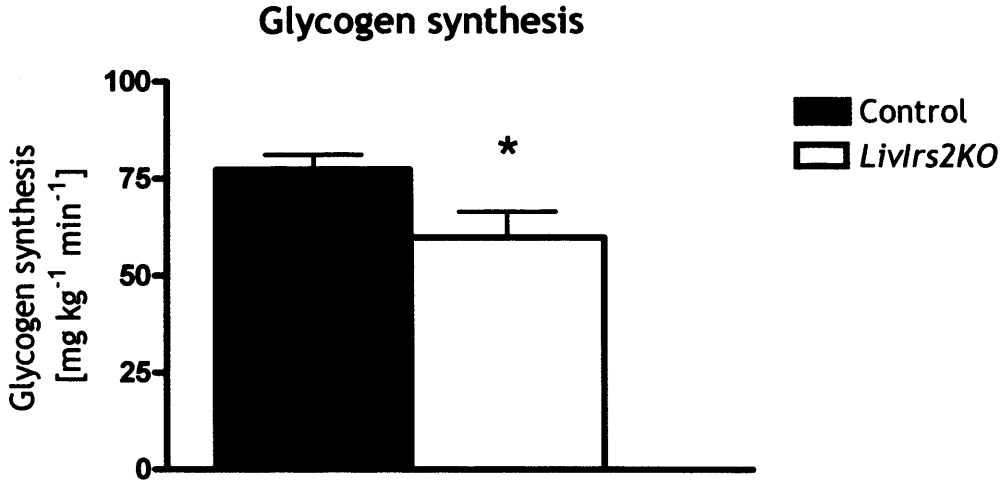

Figure 7.2 Glucose turnover and glycogen synthesis

Rates of glucose turnover (**a**) and of glycogen synthesis (**b**) were measured on 3 month-old control and *Livlrs2KO* animals. Data represent the mean ± SEM for 8-9 animals of each genotype.

* $p<0.05$.

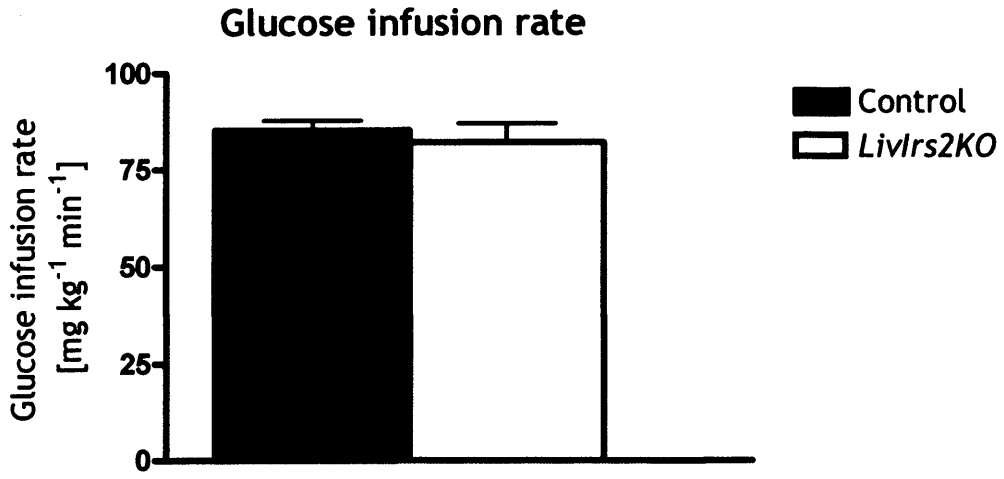

Figure 7.3 Glucose infusion rate

Flow rates of the variable glucose infusion were measured during clamp experiments on 3 month-old control and *LivIrs2KO* animals. Data represent the mean ± SEM for 8-9 animals of each genotype.

7.4 Summary of hyperinsulinaemic-euglycaemic clamp experiments

Detailed clamp studies in conscious animals found few abnormalities in glucose homeostasis in *LivIrs2KO* mice. Rates of glycolysis were comparable between genotypes, and insulin regulated endogenous glucose production appropriately in the absence of hepatic Irs2. The unexpected latter finding suggests additional mechanisms by which gluconeogenesis in the liver is regulated in *LivIrs2KO* mice. *LivIrs2KO* animals demonstrated a lower whole-body glucose utilisation rate than control mice, although this did not affect their glucose infusion requirements to maintain euglycaemia. An explanation for this result was found in the simultaneous reduction in glycogen synthesis in these animals.

Taken together, *LivIrs2KO* mice showed only mild defects in insulin sensitivity, which were related to glycogen metabolism.

Chapter 8 RESULTS: GENE EXPRESSION STUDIES

8.1 Fasted gene expression

Insulin regulates many metabolic changes at transcriptional level through the effects of forkhead transcription factors on specific insulin response elements in the promoter region of key genes of carbohydrate and fatty acid metabolism (242, 243). Abnormalities of fasting glucose homeostasis are characteristic of type 2 diabetes, indicating reduced suppression of hepatic glucose production by insulin. Since a mild but significant rise of fasted glucose levels was observed in *LivIrs2KO* mice on high fat diet, insulin-mediated gene transcription was considered to be dysregulated.

To assess fasted gene expression in hepatic tissue, liver RNA extracts were prepared from 3 month-old male animals following an overnight fast, cDNA generated by reverse transcription, and quantitatively analysed by real-time PCR. The relative mRNA content was calculated after internal standardisation to 18S ribosomal RNA.

8.1.1 Genes regulating gluconeogenesis

Phospho*enol*pyruvate carboxykinase (*Pck1*) and glucose 6-phosphatase (*G6pc*) mRNA was quantified due to their role in the gluconeogenic pathway. The transcription of these genes is controlled by insulin through PKB/Akt-mediated Foxo1 phosphorylation (153, 244).

Results showed no difference in *Pck1* expression between control and *LivIrs2KO* animals (**Figure 8.1a**). *G6pc* expression appeared to be higher in *LivIrs2KO* mice but the difference failed to reach statistical significance (p=0.067) (**Figure 8.1b**).

8.1.2 Genes regulating glycolysis

The expression levels of glucokinase (*Gck*) and liver pyruvate kinase (*Pklr*) were studied, as these two genes are important in hepatic glucose utilisation for energy metabolism. Their expression is regulated by insulin through Foxa2 interaction with their respective promoters (156).

Gck levels were significantly reduced by approximately 75% in *LivIrs2KO* animals compared to controls (p=0.032) (**Figure 8.2a**). The expression of *Pklr* appeared to be higher in *LivIrs2KO* mice (p=0.051) (**Figure 8.2b**).

a

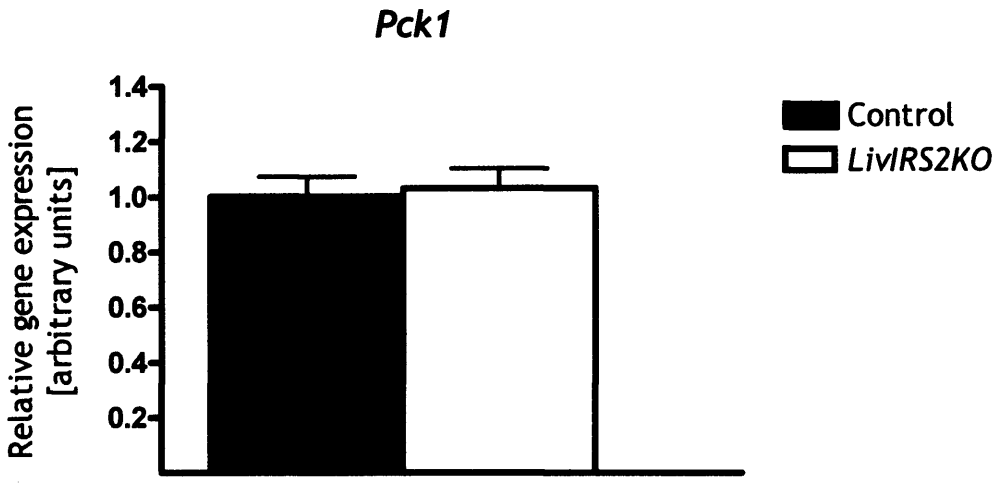

b

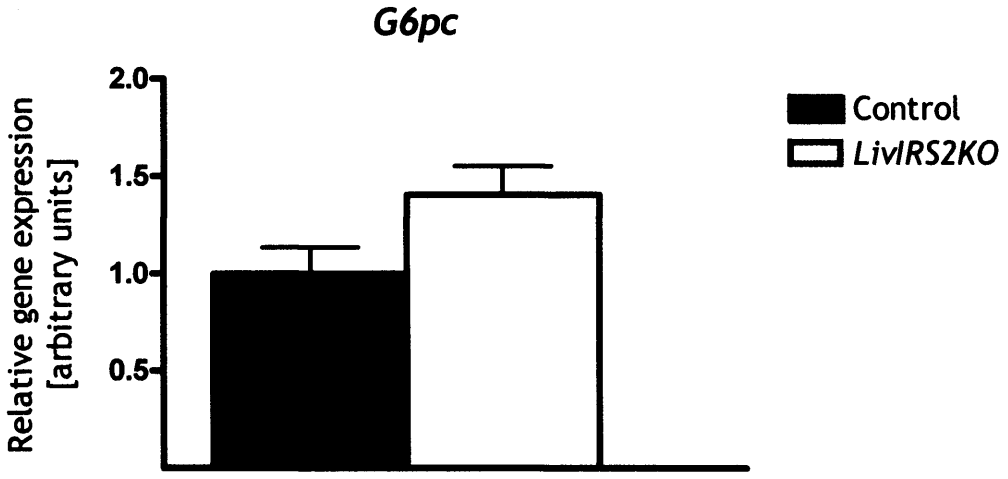

Figure 8.1 Expression of gluconeogenic genes during fasting

Levels of *Pck1* (a) and *G6pc* mRNA (b) were measured in 3 month-old male control and *LivIrs2KO* mice after an overnight fast. Graphic representation was normalised to the level of gene expression in control mice. Data represent the mean ± SEM for 6-8 animals of each genotype.

a

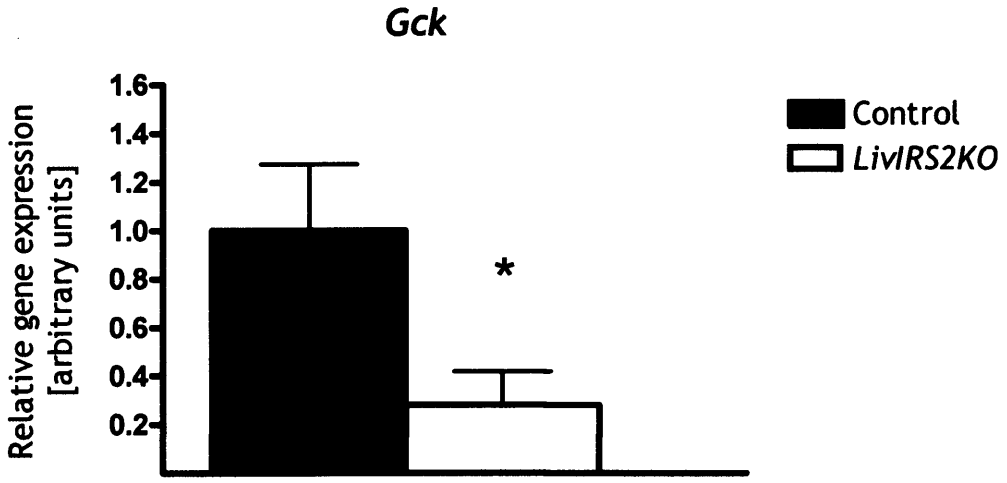

b

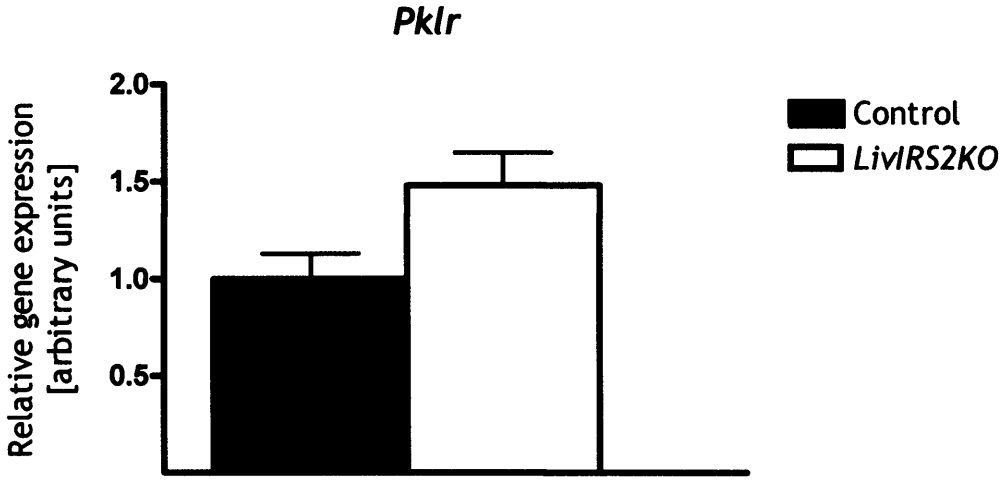

Figure 8.2 Expression of glycolytic genes during fasting

Levels of *Gck* (**a**) and *Pklr* mRNA (**b**) were measured in 3 month-old male control and *LivIrs2KO* mice after an overnight fast. Graphic representation was normalised to the level of gene expression in control mice. Data represent the mean ± SEM for 6-8 animals of each genotype. * $p<0.05$.

8.1.3 Genes regulating fatty acid synthesis

The expression of *Srebf1c* and *Fasn* was analysed to assess the regulation of fatty acid synthesis. Srebp1c is the main hepatic transcript of the *Srebf1c* gene (159), and binding to the enhancer of the fatty acid synthase (*Fasn*) gene induces lipogenesis (245). *Irs2* knockdown in mice resulted in *Srebf1c* upregulation (211).

Results showed no difference in *Srebf1c* mRNA levels between *LivIrs2KO* and control mice (**Figure 8.3a**). *Fasn* expression, too, was similar between the genotypes (**Figure 8.3b**).

8.1.4 Genes regulating fatty acid oxidation

β-oxidation of fatty acids occurs in both the mitochondria and peroxisomes. The acyl-CoA oxidase-1 (*Acox1*) gene encodes a key enzyme of the peroxisomal fatty acid β-oxidation pathway (246). *Acox1* expression is upregulated by peroxisome proliferator-activated receptor (Ppar) through a specific response element (247), and hepatic Ppar-α (*Ppara*) and Ppar-γ (*Pparg*) expression is upregulated in insulin-resistant mice (248). Peroxisome proliferator-activated receptors interact with Pgc1 to adapt hepatic metabolism to fasting conditions, and *Pgc1* mRNA levels rise during fasting (249). Pgc1β is associated with increased fatty acid oxidation, whilst Pgc1α activates gluconeogenesis through interaction with Hnf4α and Foxo1 (250). To assess fasted fatty acid oxidative gene expression in the absence of Irs2, the expression levels of *Acox1*, *Ppara*, *Pparg*, and *Pgc1b* were analysed.

Results showed neither a difference in *Acox1* nor in *Pgc1b* expression between control and *LivIrs2KO* animals (**Figures 8.4a, b**). Similarly, *Ppara* and *Pparg* expression was comparable between both genotypes (**Figures 8.5a, b**).

a

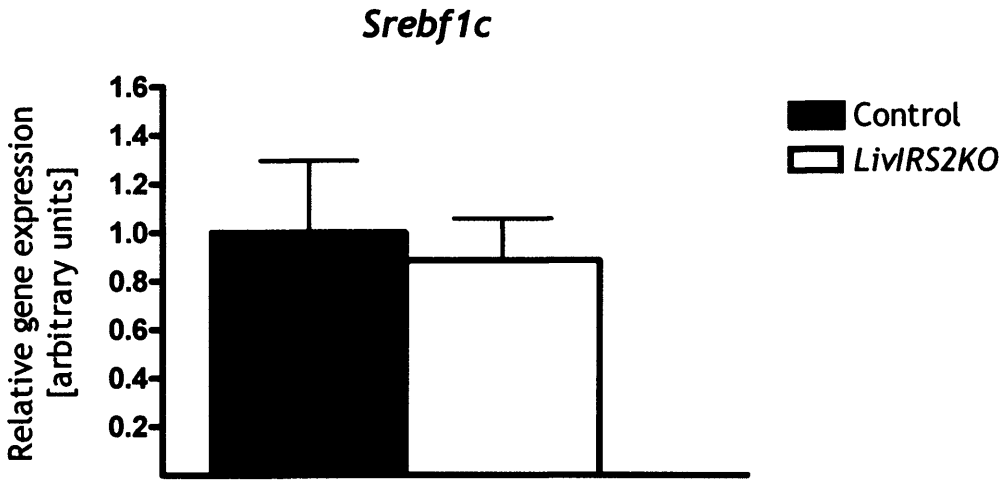

b

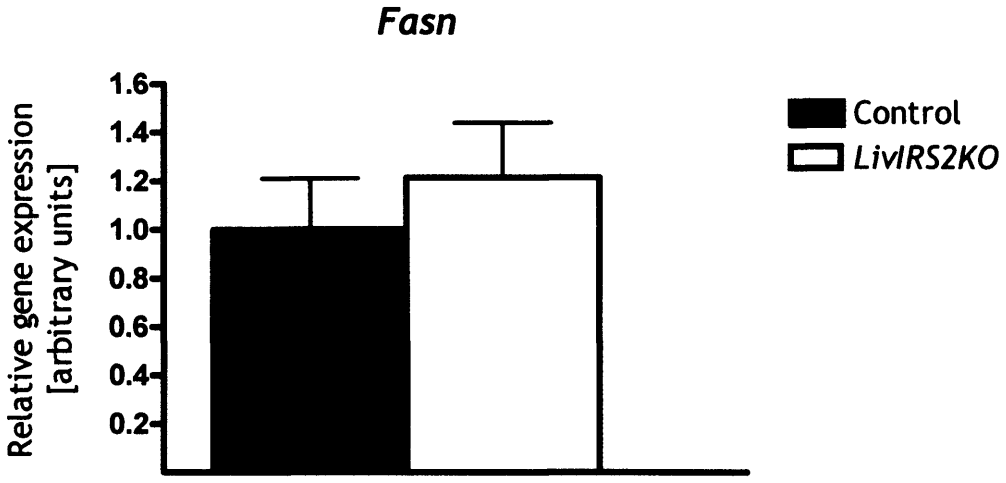

Figure 8.3 Expression of genes of fatty acid synthesis during fasting

Levels of *Srebf1c* (**a**) and *Fasn* mRNA (**b**) were measured in 3 month-old male control and *LivIrs2KO* mice after an overnight fast. Graphic representation was normalised to the level of gene expression in control mice. Data represent the mean ± SEM for 6-8 animals of each genotype.

a

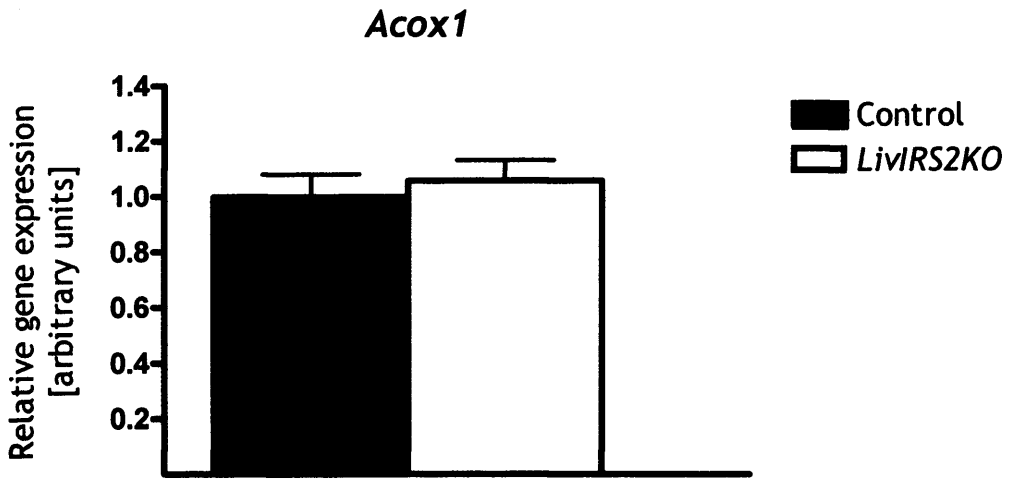

b

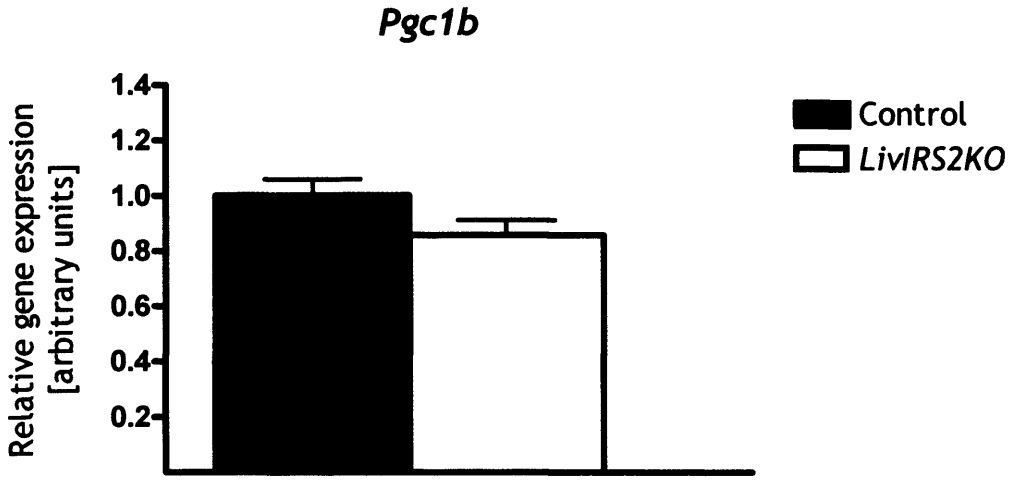

Figure 8.4 Expression of genes of fatty acid oxidation during fasting

Levels of *Acox1* (a) and *Pgc1b* mRNA (b) were measured in 3 month-old male control and *LivIrs2KO* mice after an overnight fast. Graphic representation was normalised to the level of gene expression in control mice. Data represent the mean ± SEM for 6-8 animals of each genotype.

a

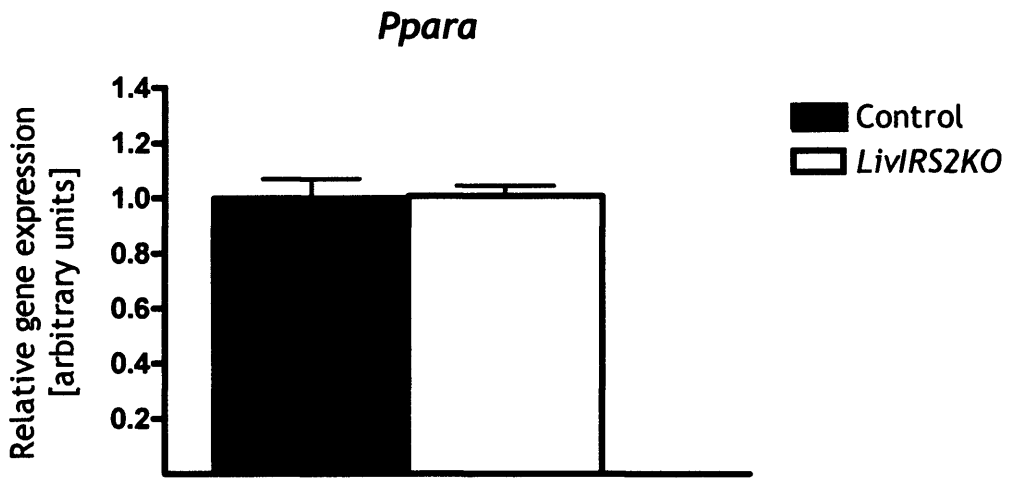

b

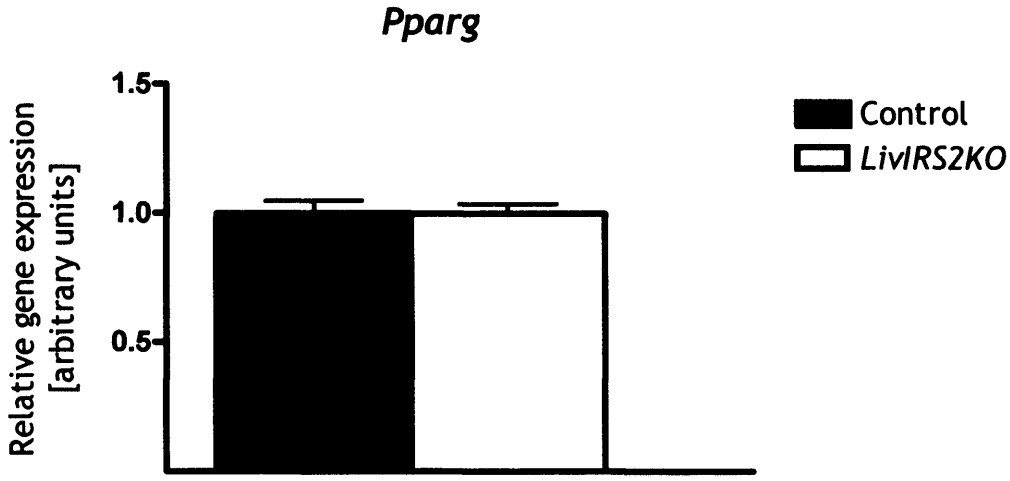

Figure 8.5 Expression of peroxisome proliferator-activated receptor genes during fasting

Levels of *Ppara* (**a**) and *Pparg* mRNA (**b**) were measured in 3 month-old male control and *LivIrs2KO* mice after an overnight fast. Graphic representation was normalised to the level of gene expression in control mice. Data represent the mean ± SEM for 6-8 animals of each genotype.

8.2 Gene expression following refeeding

LivIrs2KO mice were found to have mildly raised fasted blood glucose levels after a three-month period on high fat diet, but glucose concentrations were similar to controls in the fed state. In the fasted state, only *Gck* expression was significantly altered in the absence of Irs2.

However, insulin exerts its main metabolic effects during the postprandial period when it mediates anabolic processes to store surplus energy substrate and inhibit endogenous glucose and lipid production. A major insulin target organ is the liver, where, following the physiological insulin release into the portal vein by feeding, the switch between fasted and postprandial periods is in part regulated at transcriptional level.

These considerations prompted the investigation of gene expression during the switch from the fasted to the fed state. To assess the effect of hepatic *Irs2* deletion on insulin-regulated gene expression during this transition, a cohort of 3 month-old male animals was studied either immediately after an overnight fast or following a subsequent 2-hour refeeding period. Experimental procedures were as described above.

8.2.1 *Igfbp1* as indicator gene

Insulin-like growth factor-binding protein-1 (*Igfbp1*) mRNA levels rapidly declined in hepatoma cells upon insulin administration (251), an effect mediated by Foxo3a (242). To test whether refeeding resulted in a physiologically meaningful degree of insulin release, *Igfbp1* was chosen as an indicator gene and its expression was quantified.

The results demonstrated an 80-90% suppression of *Igfbp1* transcription by refeeding (**Figure 8.6**). There was no difference between control and *LivIrs2KO* animals in either prandial state.

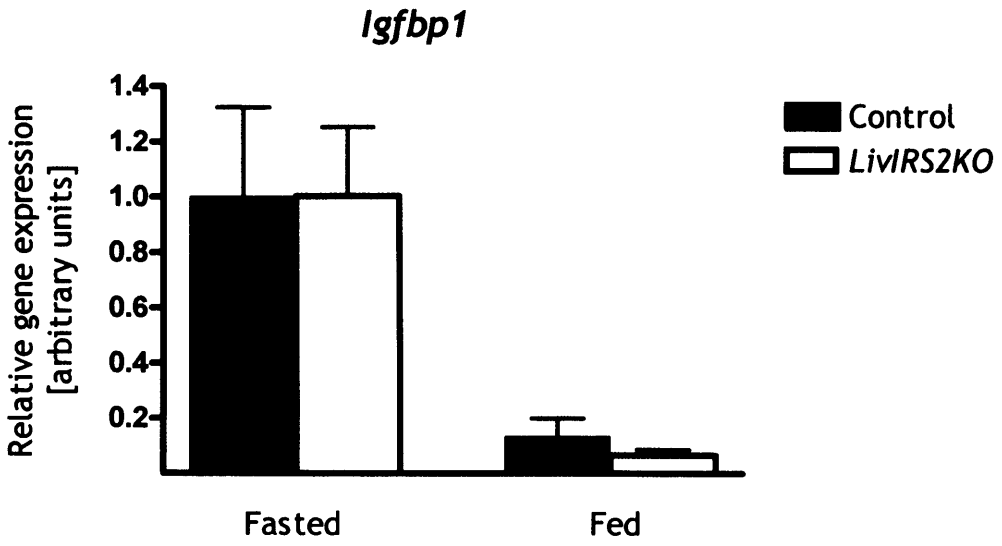

Figure 8.6 Fasted/fed expression of *Igfbp1* gene
Levels of *Igfbp1* mRNA were measured after an overnight fast and a subsequent 2-hour refeeding period in 12 week-old male control and *LivIrs2KO* mice. Graphic representation was normalised to the level of gene expression in fasted control mice. Data represent the mean ± SEM for 5 animals of each genotype.

8.2.2 Genes regulating gluconeogenesis

As before, *Pck1* and *G6pc* expression levels were studied to investigate insulin-regulated gluconeogenesis.

Both genes were downregulated by refeeding as expected. Levels of *Pck1* mRNA did not differ between control and *LivIrs2KO* mice in either prandial state (**Figure 8.7a**). In the fasted state, *G6pc* expression was found to be significantly higher in *LivIrs2KO* animals compared to controls (p=0.011), but following refeeding this difference disappeared (**Figure 8.7b**).

8.2.3 Genes regulating glycolysis

Gck and *Pklr* mRNA levels were, as previously, analysed to assess the control of glycolysis by insulin.

The response of *Gck* expression to refeeding was very pronounced with an increase of more than 50-fold in control animals and 100-fold in *LivIrs2KO* mice (**Figure 8.8a**). Fasted *Gck* expression was lower in *LivIrs2KO* animals (p=0.032), but reached levels comparable to control mice after refeeding. No significant differences in *Pklr* expression were found either between genotypes or prandial state (**Figure 8.8b**).

a

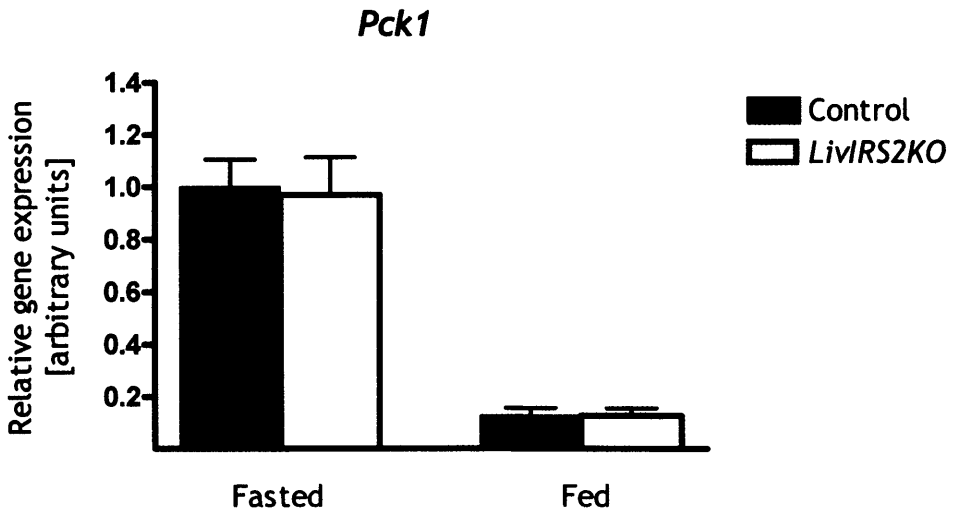

b

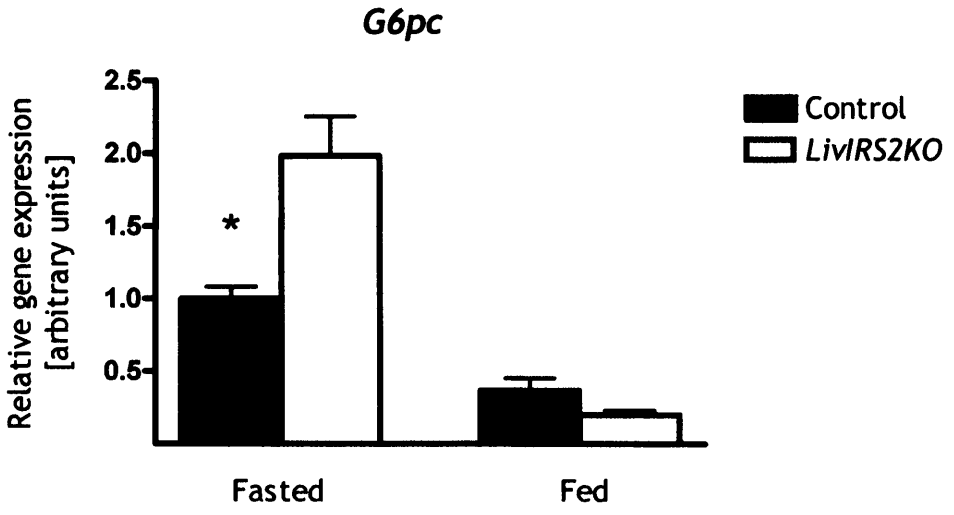

Figure 8.7 Fasted/fed expression of gluconeogenic genes

Pck1 (**a**) and *G6pc* mRNA levels (**b**) were measured after an overnight fast and a 2-hour refeeding period in 12 week-old male control and *LivIrs2KO* mice. The graphic representation was normalised to expression levels in fasted control mice. The mean ± SEM for 5 animals of each genotype is represented. * $p<0.05$.

a

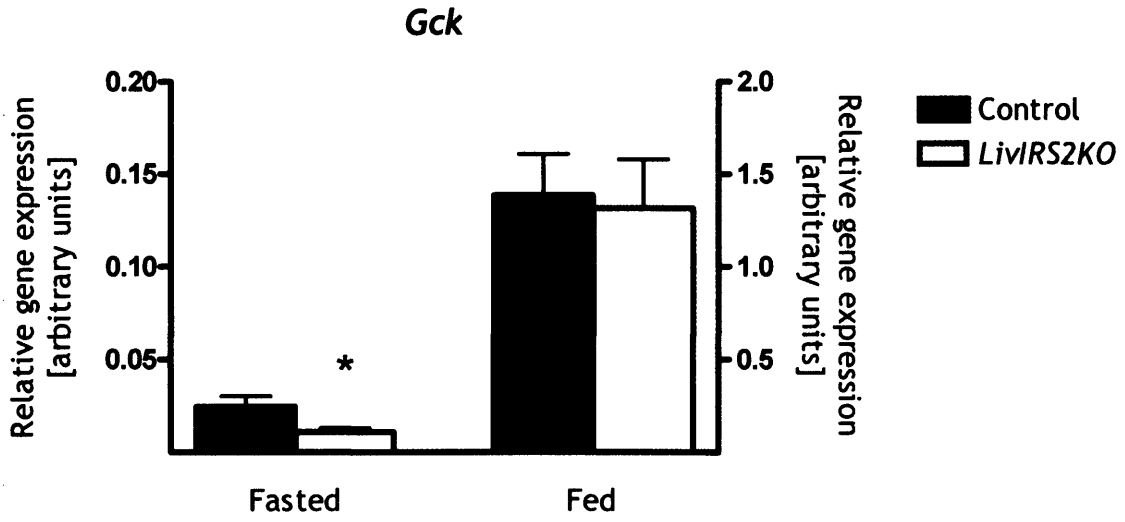

b

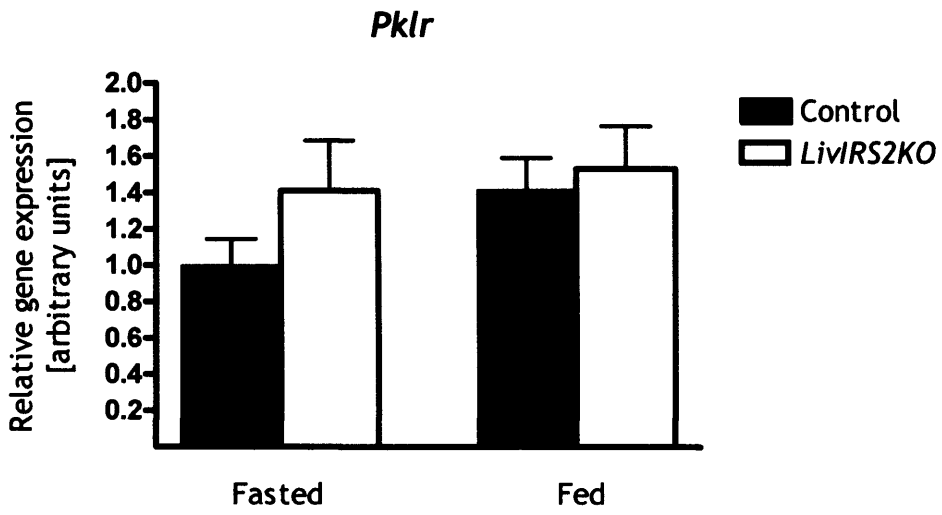

Figure 8.8 Fasted/fed expression of glycolytic genes

Gck (**a**) and *Pklr* mRNA levels (**b**) were measured after an overnight fast and a 2-hour refeeding period in 12 week-old male control and *LivIrs2KO* mice. The graphic representation of *Pklr* was normalised to expression levels in fasted control mice. The mean ± SEM for 5 animals of each genotype is represented.

* $p<0.05$.

8.2.4 Gene regulating glycogen synthesis

Insulin regulated glycogen synthesis at transcriptional level by increasing hepatic glycogen synthase (*Gys2*) mRNA during the fasted/fed transition in both diabetic and non-diabetic rats (252). Chronic hyperinsulinaemia, however, reduced insulin-induced glycogen synthase activity in muscle (253), with glycogen synthesis in muscle found to be quantitatively more important than in liver (254). As *LivIrs2KO* mice showed a mild reduction in glycogen synthesis rate in hyperinsulinaemic-euglycaemic clamp experiments, *Gys2* gene expression was analysed.

Results appeared to show an overall reduction in *Gys2* expression after refeeding (**Figure 8.9**). The fall of approx. 25% showed a similar pattern in each genotype, but was statistically not significant (controls, p=0.357; *LivIrs2KO*, p=0.229). *Gys2* mRNA levels were comparable in control and *LivIrs2KO* animals in both fasted and fed states.

Figure 8.9 Fasted/fed expression of *Gys2* gene

Levels of *Gys2* mRNA were measured after an overnight fast and a subsequent 2-hour refeeding period in 12 week-old male control and *LivIrs2KO* mice. Graphic representation was normalised to the level of gene expression in fasted control mice. Data represent the mean ± SEM for 5 animals of each genotype.

8.2.5 Genes regulating fatty acid synthesis

As before, insulin-regulated fatty acid synthesis was assessed by measuring *Srebf1c* and *Fasn* expression. There were no differences in *Srebf1c* mRNA levels between fasted and fed animals or between genotypes (**Figure 8.10a**). *Fasn* transcription appeared to rise following refeeding in both *LivIrs2KO* and control animals. However, the differences in *Fasn* expression between *LivIrs2KO* and control mice did not reach statistical significance (fasted, p=0.446; fed, p=0.058) (**Figure 8.10b**).

8.2.6 Genes regulating fatty acid oxidation

Acox1 expression was analysed, as previously, to serve as indicator of the regulation of peroxisomal β-oxidation by insulin. Since no differences in the expression of genes related to peroxisomal fatty acid metabolism had been found in the fasted state, carnitine palmitoyl transferase-1a (*Cpt1a*) expression was studied to also investigate fatty acid oxidation in the mitochondria. *Cpt1a* encodes the liver isoform of an enzyme that shuttles fatty acids across the mitochondrial membrane to initiate β-oxidation in this subcellular compartment (255).

Results showed that *Acox1* expression was unaffected by genotype and prandial state (**Figure 8.11a**), and no differences were detected during the analysis of *Cpt1a* mRNA (**Figure 8.11b**).

a

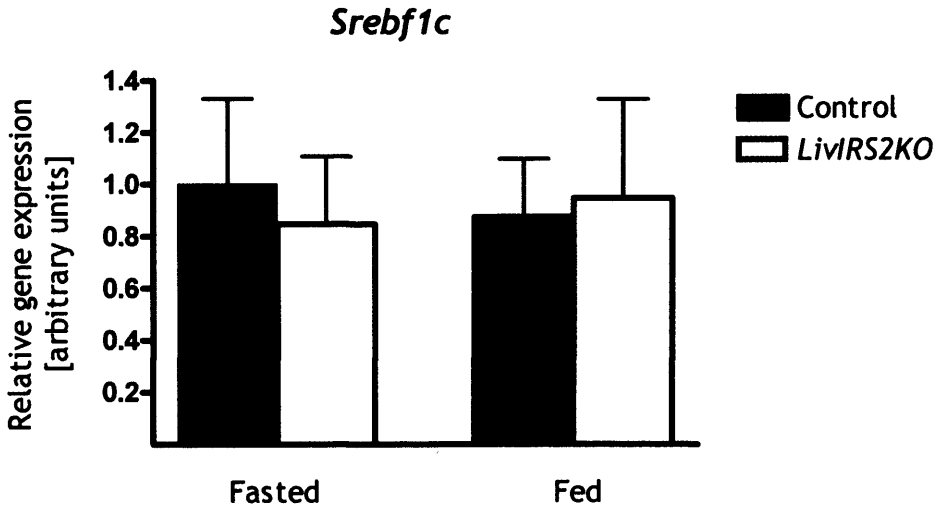

b

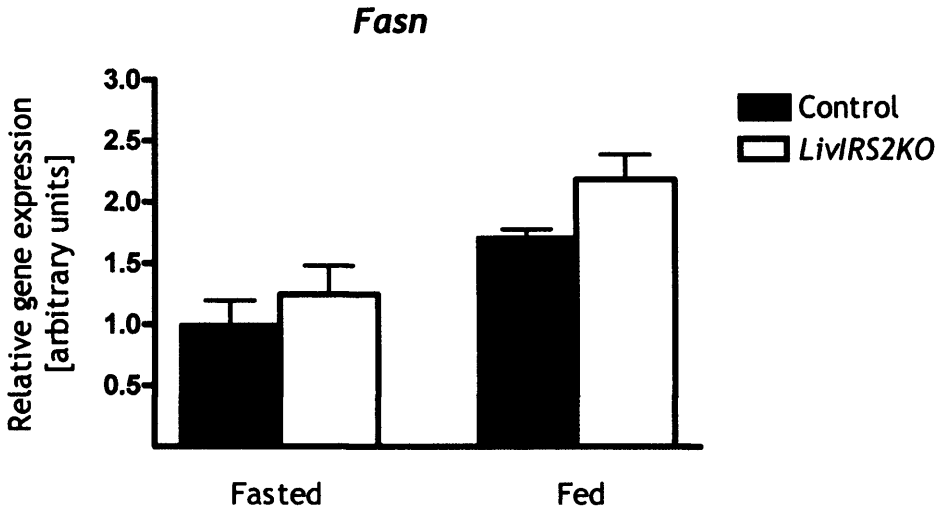

Figure 8.10 Fasted/fed expression of genes of fatty acid synthesis

Srebf1c (**a**) and *Fasn* mRNA levels (**b**) were measured after an overnight fast and a 2-hour refeeding period in 12 week-old male control and *LivIrs2KO* mice. Graphic representation was normalised to gene expression levels in fasted control mice. Data represent the mean ± SEM for 5 animals of each genotype.

a

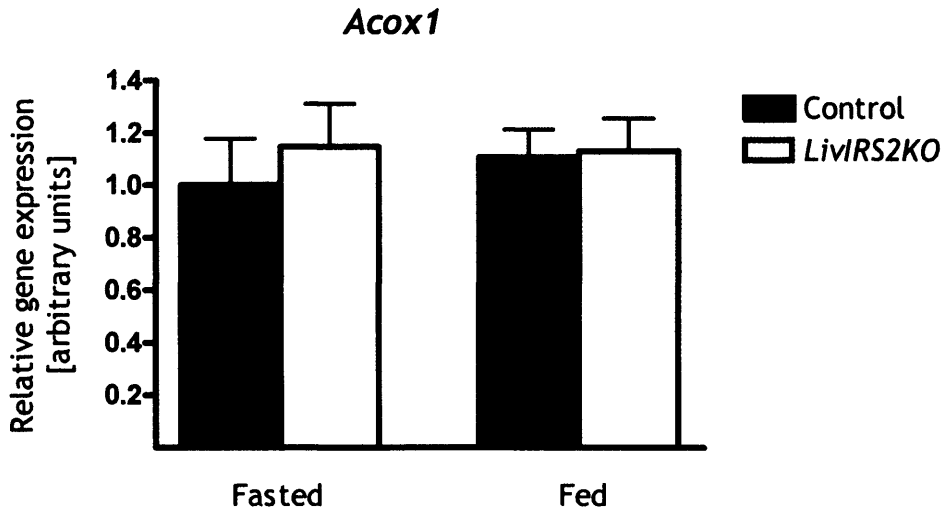

b

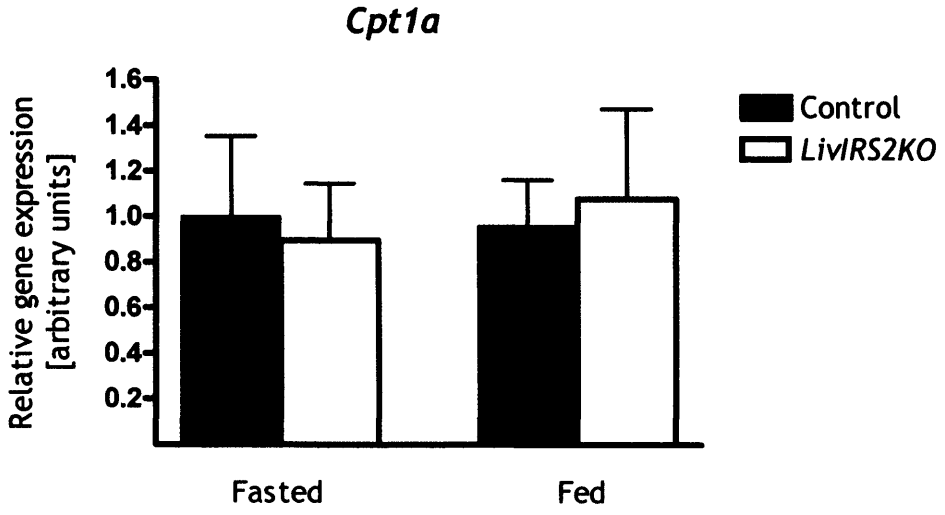

Figure 8.11 Fasted/fed expression of genes of fatty acid oxidation

Acox1 (**a**) and *Cpt1a* mRNA levels (**b**) were measured after an overnight fast and a 2-hour refeeding period in 12 week-old male control and *LivIrs2KO* mice. Graphic representation was normalised to the level of gene expression in fasted control mice. Data represent the mean ± SEM for 5 animals of each genotype.

8.3 Summary of gene expression studies

Following an overnight fast, *G6pc* showed increased expression in *LivIrs2KO* mice, indicating impaired suppression of hepatic gluconeogenesis during a low insulin state. Prandial insulin release, however, reduced *G6pc* mRNA levels in *LivIrs2KO* animals comparable to controls. A reduced transcription of *Gck* was observed in fasted *LivIrs2KO* animals compared to controls. *Gck* expression increased to normal following refeeding, suggesting a reduced induction response of the first key glycolytic enzyme to low insulin concentrations. *Gys2* expression was similar in *LivIrs2KO* mice and in controls in both the fasted and fed state, and levels did not change by refeeding in both genotypes.

No differences were seen in *Srebf1c* transcription and in *Fasn* expression, indicating no impairment of insulin-mediated regulation of fatty acid synthesis. Both *Acox1* and *Cpt1a* mRNA levels were unaffected by prandial state or genotype, indicating normal insulin effects on β-oxidation in both the peroxisomes and the mitochondria. These findings were consistent with the normal results of the previous analysis of the peroxisomal fatty acid oxidation regulatory genes *Ppara*, *Pparg*, and *Pgc1b*.

Chapter 9 RESULTS: LIVER FUNCTION TESTS

In mice lacking the insulin receptor in the liver, hyperglycaemia was observed in young animals that resolved with advancing age as progressive liver failure ensued. Aspartate transaminase (AST) levels rose 2.6-fold and alkaline phosphatase (ALP) was elevated by 50%. Serum albumin levels declined by 50%, indicating significantly reduced synthetic liver function (186). In order to establish whether the deletion of *Irs2* had a detrimental effect on hepatic function, liver enzymes as well as hepatic synthetic and excretory capacity were measured on 3 month-old male animals after an overnight fast.

9.1 Transaminases and alkaline phosphatase

Increased levels of alanine transaminase (ALT) and aspartate transaminase (AST) are indicative of hepatocyte injury, although both the predominantly cytosolic ALT and the mitochondrial AST enzymes are present in other tissues. Although different isoenzymes of alkaline phosphatase exist, in conjunction with other liver function abnormalities elevated levels would suggest damage to the biliary tree (256). Therefore fasted serum ALT, AST, and ALP activities were studied.

Results showed significantly increased ALT and AST levels in *LivIrs2KO* mice compared to controls (**Figure 9.1, left and centre panels**). Concentrations of ALT were 3.4-fold higher ($p=0.028$) and those of AST were elevated 2.7-fold ($p=0.043$). No difference in alkaline phosphatase (ALP) levels was found between both genotypes (**Figure 9.1, right panel**).

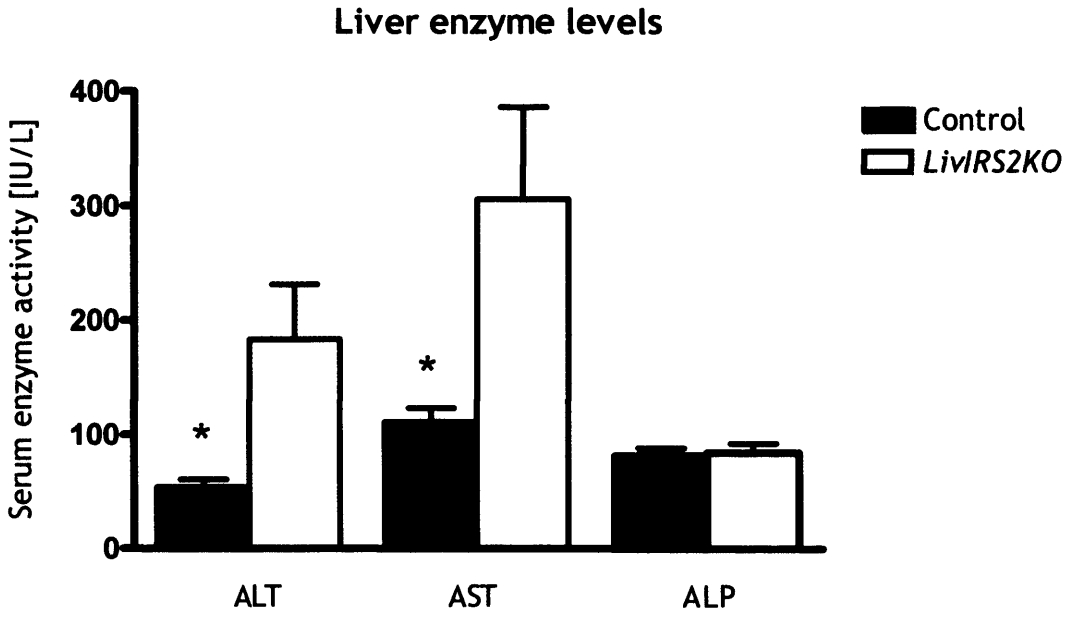

Figure 9.1 Liver enzyme concentrations

Serum alanine transaminase (ALT) (**left panel**), aspartate transaminase (AST) (**centre panel**), and alkaline phosphatase (ALP) levels (**right panel**) were determined in 3 month-old male control and *LivIrs2KO* mice after an overnight fast. Data represent the mean ± SEM for 6 animals of each genotype. * $p<0.05$.

9.2 Albumin and bilirubin

One of the main proteins synthesised in the liver is albumin, and bilirubin is the predominant excretory product (256). To assess these biological functions, serum albumin and bilirubin concentrations were measured.

Results showed similar levels of albumin and bilirubin in control and *LivIrs2KO* mice (**Figure 9.2**).

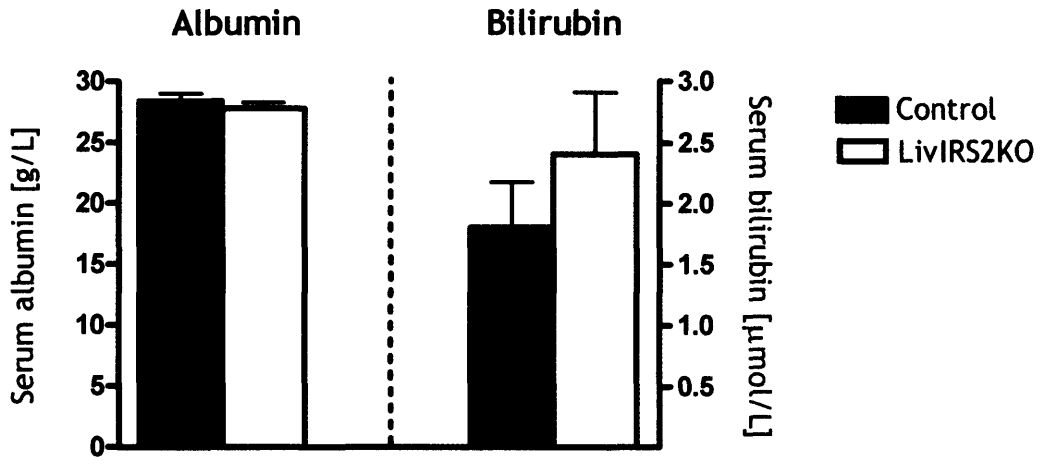

Figure 9.2 Synthetic and excretory liver function

Levels of serum albumin (**left panel**) and bilirubin (**right panel**) were determined in 3 month-old male control and *LivIrs2KO* mice after an overnight fast. Data represent the mean ± SEM for 6 animals of each genotype.

9.3 Summary of liver function tests

At 3 months of age, *LivIrs2KO* animals showed mild biochemical evidence of hepatocellular damage, but not of disturbances within the biliary tree. These abnormalities did not result in a significant impairment of synthetic and excretory function of the liver in *LivIrs2KO* mice.

Chapter 10 DISCUSSION

The liver plays a central role in maintaining glucose and lipid homeostasis. The metabolic pathways regulating these processes are largely controlled by insulin. Their dysregulation and the presence of hepatic insulin resistance plays an important part in the development of type 2 diabetes (15, 257). The mechanism of how insulin exerts its responses on hepatocytes is complex, and both direct and indirect effects have been described. Direct signals are transmitted by its cognate transmembrane receptor, and indirect effects occur either as a consequence of metabolic responses in other tissue compartments or are mediated by central autonomic nervous activation (74). Differences between these direct and indirect mechanisms have been associated with acute or long-term regulatory effects of insulin (67).

Irs2 is a key molecule of the insulin signalling cascade that mediates many of its metabolic effects. Global deletion of *Irs2* in the mouse leads to a phenotype closely resembling human type 2 diabetes with prominent insulin resistance in the liver (200, 225). In order to clarify the role of Irs2 in liver insulin signalling and its contribution to direct, receptor-mediated effects on liver insulin sensitivity, this signalling pathway was specifically disrupted by hepatocyte-specific *Irs2* deletion in a new murine model.

10.1 Phenotype characterisation

The thesis presented here is based on the generation of the *LivIrs2KO* strain and the subsequent characterisation studies undertaken. They involved the analysis of cellular signalling events following insulin stimulation, the detailed assessment of carbohydrate and lipid metabolism, the quantification of key metabolic gene expression, and the measurement of liver function parameters.

10.1.1 Animal growth and development

LivIrs2KO animals bred and developed normally and were shown to have a body mass comparable to control mice. This was in contrast to mice with a global deletion of *Irs2*, which were 10% smaller than their wild-type littermates both at birth and in adulthood (200), and brain size was particularly reduced (258). The normal development seen in the *LivIrs2KO* model thus suggests that *Irs2* in non-hepatic tissues is essential to normal embryonic and postnatal development.

10.1.2 Signalling molecules and events

Analysis of the proximal insulin signalling molecules Insr and Irs1 showed no differences in their hepatic expression in *LivIrs2KO* mice, which is similar to the results obtained in global *Irs2* null mice (200). Thus no significant insulin receptor down- or upregulation occurred as described in other animal models of either significant insulin resistance or insulin sensitivity (259, 260). Neither did the absence of Irs2 lead to a significant compensatory increase of hepatic insulin signalling by Irs1.

Rather unexpectedly, however, the PI3K pathway-related downstream signalling cascade was also found to be unaltered. The regulatory subunit p85 of PI3K was expressed equally in *LivIrs2KO* and control animals, as was total PKB/Akt, and the Pdk1 phosphorylation status did not differ. Whilst basal PKB/Akt phosphorylation was found to be non-significantly higher in *LivIrs2KO* mice compared to controls, a similar degree of activation was detected after insulin stimulation. These results were in keeping with expression studies in animals with global *Irs2* deletion that displayed unchanged levels of p85 (PKB/Akt and Pdk1 data were not reported) (200).

In a hepatocyte cell line derived from *Irs2* null animals immediately after birth, the Irs1-associated PI3K activity was not affected by the absence of Irs2 but overall PI3K activity was reduced by 50%, which suggested that Irs2 contributed significantly to insulin-stimulated PI3K activity (209). In contrast to *LivIrs2KO* animals, in this cell culture model the dose-dependent insulin-mediated PKB/Akt phosphorylation was impaired by the absence of Irs2, with basal PKB/Akt expression comparable to wild-type cells. Whilst Pdk1 data was not presented, insulin-mediated Gsk3 phosphorylation was markedly reduced in *Irs2* null hepatocytes but p70S6K activation was not affected. *LivIrs2KO* mice, in contrast, did not show any difference in Gsk3β phosphorylation and p70S6K expression also was similar to controls.

Thus, the isolated deletion of *Irs2* in the liver had minimal consequences for the hepatic PI3K-associated signalling pathway. The simultaneous loss of Irs2 in other tissues, such as the brain, skeletal muscle and adipose tissue, affected the distal insulin signalling in the liver in the global *Irs2* null model. The negative findings in *LivIrs2KO* mice hence support the importance of indirect insulin effects on the downstream hepatic signalling cascade.

10.1.3 Glucose metabolism

Overall most interestingly, *LivIrs2KO* animals did not develop diabetes and the detailed analysis of glucose homeostasis detected only minor disturbances in carbohydrate metabolism. Fasted and fed blood glucose levels, as well as the response to a glucose challenge, were indistinguishable from control mice whilst maintained on a regular diet. *LivIrs2KO* mice also had essentially normal fasted insulin levels, thus excluding significant insulin resistance. Hence a challenge with high fat diet was conducted to enhance the observed mild alterations in glucose homeostasis. Fasted glucose levels were shown to be elevated in *LivIrs2KO* mice; however, this difference disappeared on feeding.

No other abnormalities of glucose homeostasis were detected on GTT or ITT. Therefore hyperinsulinaemic-euglycaemic clamp experiments were conducted to conclusively settle the question of altered insulin sensitivity. In animals on regular chow these studies showed reduced whole-body glucose utilisation, accounted for by reduced glycogen synthesis, and otherwise similar glucose infusion rates, glucose production, and glycolysis. Thus only minor disturbances in glucose metabolism were present, without significant changes in overall insulin sensitivity.

The results in *LivIrs2KO* mice contrast with the rapid development of diabetes seen in the global *Irs2* null model, where β-cell expansion in the presence of insulin resistance was markedly impaired. Irs2 has since been shown to be vital for β-cell growth, function, and survival (201, 203, 212, 261, 262). As Irs2 remained functional in all non-hepatic tissues of *LivIrs2KO* animals, the β-cell population was not affected and thus capable to respond to altered liver Irs2 signalling. However, in view of the normal insulin levels found, hypersecretion of insulin did not occur. Therefore other extra-hepatic compensation mechanisms appear to be present, perhaps most likely a CNS-mediated pathway.

Reductions in glucose utilisation and whole-body glycogen synthesis were observed in *LivIrs2KO* animals during the clamp experiments. This likely represents reduced liver glycogen synthase activity, because other glycogen-producing tissues, such as skeletal and cardiac muscle, kidney, and the intestine, retained intact insulin signal transduction. Impaired hepatic glycogen synthesis and storage has been observed in the LIRKO mouse, in liver-specific Pdk1 null mice, and in hepatocytes with downregulated Irs2 expression (128, 186, 263). The findings in *LivIrs2KO* animals thus are consistent with previous studies and support a direct role of Irs2-associated insulin signalling on glycogen metabolism, whilst endogenous glucose production and glycolysis remains unaltered.

10.1.4 Lipid metabolism

Irs2 in the liver has been implicated to preferentially regulate lipid rather than glucose metabolism. Global *Irs2* null mice developed hepatosteatosis on the background of dysregulated lipogenesis (264), and increased serum NEFA levels and hepatic TG content were reported in mice with a transient reduction of hepatic *Irs2* by RNAi knockdown (211). *LivIrs2KO* mice, however, did not display any differences in circulating levels of NEFA or TG. The finding of normal lipid homeostasis thus suggests that for long-term lipid homeostasis Irs2 in the liver is not essential, if other tissues maintain normal insulin signalling.

Global *Irs2* null mice are leptin resistant and hyperphagic (202, 264), an effect thought to be due to defective Irs2 signalling in the hypothalamus (261, 262), although there is also evidence to the contrary (212). *LivIrs2KO* mice displayed similar leptin levels on regular chow and comparable weight gain to control animals, even when offered a high fat diet. This suggests that hepatic Irs2 is not involved in the development of leptin resistance or in the regulation of long-term energy homeostasis.

10.1.5 Gene expression

The unexpectedly subtle alterations of glucose and lipid homeostasis in *LivIrs2KO* animals prompted studies to examine the expression of key regulatory genes of both pathways.

The assessment of genes regulating carbohydrate metabolism found that *G6pc* expression was elevated in fasting *LivIrs2KO* animals, whereas *Gck* levels were reduced, indicating both reduced suppression of gluconeogenesis and reduced induction of glycolysis when insulin levels were low. Following refeeding, however, both *G6pc* and *Gck* responded appropriately and were shown to reach

expression levels comparable to control mice. This indicates that the absence of Irs2 reduces, but not ablates, hepatic sensitivity to insulin to an extent that affects gene transcription in the fasted state. Higher insulin concentrations following refeeding appear to overcome this abnormality. Dysregulation of *G6pc* expression may therefore explain the finding of fasting hyperglycaemia in *LivIrs2KO* mice on high fat diet.

Gys2 expression was measured to study the regulation of glycogen synthesis during the fasted/fed transition. Results in either metabolic state showed a non-significant increase in *Gys2* mRNA in *LivIrs2KO* mice compared to controls. These findings appear to run counter to the clamp study results that showed a reduced whole-body glycogen synthesis in *LivIrs2KO* animals. However, hepatic glycogen synthase activity is not directly correlated with mRNA levels, which in addition is regulated by kinases not under insulin control (252, 265). Hence post-translational effects may in part be responsible for these discordant findings.

The lipogenic transcription factor *Srebf1* was expressed at increased levels in global *Irs2* null mice (264). This result was reproduced by short-term hepatic *Irs2* knockdown by RNAi in wild type mice and led to increased levels of *Srebf1c* and of *Fasn*, and to mild rises of serum NEFA and triglycerides, with associated mild hepatic steatosis (211). Conversely, overexpression of *Srebf1* in isolated hepatocytes suppressed Irs2 levels (263). An inverse relationship between *Irs2* and *Srebf1c*, both at mRNA and protein level, has also been shown in *ob/ob* and lipodystrophic animals. In that study, however, the rise in *Srebf1c* was considered to occur independently of an Irs2-associated pathway (204). In *LivIrs2KO* mice no difference in *Srebf1c* expression or in any other gene related to lipid metabolism was detected. A range of genes regulating fatty acid synthesis and β-oxidation (both peroxisomal and mitochondrial) were found to be expressed normally in both fasted and fed conditions. This is in keeping with the finding of comparable levels of serum NEFA and TG in *LivIrs2KO* and control

mice. Taken together, these results do not support the suggestion that Irs2 preferentially regulates fatty acid metabolism (211), but rather indicate that isolated chronic deficiency of hepatic *Irs2* has no significant effects on lipid homeostasis.

10.1.5 Liver function

Progressive hepatic dysfunction developed in mice with liver-specific ablation of *Insr*, leading to the loss of synthetic capacity (186). At the age of six months, serum albumin levels were reduced to 50% of controls. ALP and AST levels were elevated by 50% and 160%, respectively, whereas lactate dehydrogenase and ALT concentrations remained within the normal range. In another model, liver-specific *Pdk1*-deficient animals developed oedema, 50% lower serum albumin levels, and died before the age of four months (128). The activation of PKB/Akt was abolished, leading to a markedly impaired phosphorylation of p70S6K, a key enzyme for protein synthesis. In contrast, *LivIrs2KO* mice maintained normal albumin levels at the age of three months. No abnormalities in ALP and bilirubin were detected, but both ALT and AST concentrations were elevated, suggesting a mild degree of hepatocellular damage. However, at the age of six months no fall in fasted blood glucose levels and no interstitial oedema were observed, indicating that no clinically relevant progression to liver failure had occurred. These results suggest that hepatic Irs2 deficiency causes minor injury to hepatocytes but is not sufficient to cause liver failure.

10.2 Role of Irs2 in the liver

The relative lack of a phenotype in the *LivIrs2KO* model calls into question the significance of Irs2-associated hepatic insulin signalling.

As the insulin receptor rather than the Igf1 receptor signalling cascade mediates insulin effects (182, 183), and Irs1 is predominantly associated with growth rather than with metabolic regulation (197, 266), Irs2 is considered to be the main mediator of insulin's metabolic effect. Indeed, Irs2 phosphorylation was found to be essential for the insulin response of *Insr* null hepatocytes (85). The importance of Irs2 in the liver was also shown by the restoration of insulin-mediated metabolic effects on glycogen synthesis and gluconeogenesis through adenoviral re-expression of Irs2 in immortalised *Irs2*$^{-/-}$ hepatocytes (209). In a global *Irs2* null model, the normalisation of endogenous glucose production through adenoviral reintroduction of *Irs2* in the liver ameliorated hyperglycaemia, although glucose utilisation remained impaired (206). Conversely, a short-term reduction of *Irs2* expression by 75% in the livers of wild type mice by RNAi did not lead to significant changes in glucose homeostasis (211). However, since *LivIrs2KO* animals failed to express significant disturbances in lipid and carbohydrate homeostasis other than mildly impaired glycogen synthesis, mechanisms not involving hepatic Irs2 appear to be responsible for near-normal metabolic regulation. These finding thus do not support the central role in direct hepatic signalling so far assigned to Irs2, and a consistent inverse relationship between insulin resistance and *Irs2* expression in the liver has not been demonstrated.

10.3 Direct and indirect insulin effects on the liver

In two murine models reported recently, the expression of hepatic insulin receptor was altered to further clarify the relative dominance of direct or indirect insulin effects on hepatic glucose production.

By short-term systemic administration of antisense oligonucleotides directed against the insulin receptor to wild type mice, a near ablation of hepatic Insr protein expression was achieved (210). Whilst downstream signalling in the

liver was impaired, as judged by PKB/Akt phosphorylation, and a small reduction in hepatic glycogen content was observed, clamp studies failed to detect significant changes in insulin resistance or insulin-mediated suppression of glucose production. In a different experiment, a transthyretin promoter-driven insulin receptor was re-expressed in the liver of insulin receptor knockout mice but failed to restore normal hepatic insulin action during a hyperinsulinaemic-euglycaemic clamp (267). The animals displayed severe liver insulin resistance and failed to suppress glucose production. Both studies thus suggested a predominantly indirect effect of insulin to regulate hepatic glucose output. The findings in *LivIrs2KO* mice add further evidence to this concept, because even though Irs2 represents only part of the signalling cascade downstream of the insulin receptor, no compensatory increase in Irs1 was observed and following its selective ablation whole-body glucose homeostasis remained intact.

10.4 Methodological differences to other studies

The lack of significant alterations in insulin signalling, insulin sensitivity, and lipid metabolism in *LivIrs2KO* mice was unexpected. These findings contrast with some previously published observations and may in part be explained by a range of methodological and physiological differences to other models.

The global *Irs2* null model was generated by traditional gene targeting techniques leading to germ line deletion, i.e. the absence of Irs2 throughout life, including embryological development (200, 225). Similarly, the studies in embryological or neonatal hepatocytes lacking *Insr* or *Irs2* were performed in cells derived from animals with germ line mutations (85, 209). In contrast, the *LivIrs2KO* model relied on the Cre-mediated excision of a floxed *Irs2* allele that begins *in utero* and gradually occurs over the first 6 weeks of postnatal life (214). Hence all experiments were performed in mice older than this age.

During most of the intrauterine and early weaning period of *LivIrs2KO* animals, however, Irs2 would still have been present, albeit in gradually reducing levels. This process may have allowed the gradual development of compensatory mechanisms that persist into later adulthood.

In the cell culture experiments referred to earlier, *Insr* or *Irs2* deficient hepatocytes were immortalised by viral transformation with SV40. Whilst the hepatocyte lineage was confirmed by albumin production or selection achieved by incubation with arginine-free medium (85, 209), the viral infection itself interferes with the host cell metabolism. In myeloid cells and fibroblasts the SV40 transformation capability depends on Igf1r and Irs1 signalling (268, 269), and a SV40 overexpressing murine model of hepatocellular carcinoma demonstrated increased levels of Irs2, Irs1, and the inhibition of Gsk3β activity (270). At the same time, at low passage numbers hepatic cell lines continue to express liver specific genes normally and may thus suggest normal hepatic metabolism (271). Furthermore, although cell culture allows the isolated study of defined aspects of metabolism, not only the undesired influences but also the entirety of necessary physiological interactions with other tissue compartments are abolished. This may include unrelated signals that are essential for normal cellular function, and therefore conclusions must be drawn with care when generalising from the *in vitro* to the *in vivo* situation.

Two techniques aiming to silence gene expression have been used in recent studies. Systemic antisense oligonucleotides directed against *Insr* did not only lead to the near ablation of insulin receptor protein expression in the liver, but at the same time to a 65% reduction in adipose tissue (210). When studied seven days after treatment, among other results, lower levels of glycerol and NEFA were reported, which suggested an alteration of insulin signalling in fat tissue in addition to the liver. This may have given rise to indirect effects on hepatic metabolism, thus influencing the main results. Adenovirus-mediated RNAi to specifically knockdown hepatic *Irs2*, in contrast, only achieved a 75%

reduction of hepatic Irs2 protein five days after treatment (211). Whilst this failed to alter glucose homeostasis, abnormalities in lipid metabolism were reported. In order to assess how well gene silencing can be achieved by either of these techniques, their specificity of was investigated in a systematic comparison by microarray analysis (272). By targeting *Pdk1* with either approach in cell culture, the *Pdk1*-specific pattern of changes in gene expression was no longer detectable after the initial 72-hour time period. Results revealed a significant increase in non-specific gene alterations thereafter. Thus, results derived from these short-term studies with either overlapping and incomplete reduction of protein levels or with potentially non-specific changes in gene expression appear prone to interferences. This is in contrast to the permanent and complete gene deletion in *LivIrs2KO* animals from the age of 6 weeks.

Insr null mice that survived by restoring insulin receptors in the liver but failed to normalise both increased HGP and insulin resistance, also showed marked impairment of hypothalamic insulin receptor signalling, which likely reduced neuronal insulin signals to the liver (267). Thus the complex genetic make-up of this model may have led to interferences between different aspects of insulin signalling at organismal level and made an accurate interpretation of the results difficult.

Finally, there is significant strain variation documented in the glucose metabolic pathways of mice after prolonged fasting, with up to 30% difference in glucose production, which may contribute to the phenotype of genetically altered animals (273).

10.5 Comparison to LKO model

In a manuscript that was published at the same time as the work presented here, another group has described the characteristics of a hepatocyte-specific *Irs2* knockout mouse, which they named LKO (274). The animal was generated by the same Cre/*loxP* technique as the *LivIrs2KO* model.

LKO animals bred as expected and development, including the brain, was normal. Whilst Insr and Irs1 protein expression was unaltered, following insulin stimulation an increased Insr phosphorylation was documented compared to animals with floxed alleles of *Irs2*. Whilst PI3K activity appeared non-significantly reduced by 25%, PKB/Akt activation was unchanged and the MAPK cascade was unaltered. These signalling results were in keeping with findings in our *LivIrs2KO* mice.

At the age of 6 weeks, LKO animals displayed glucose levels comparable to wild type in the fasted and in the fed state, as well as during an i.p. GTT. Insulin concentrations increased 2-fold in LKO animals, which at the age of 16 weeks animals had mildly higher fasted glucose levels, albeit still remaining in the normal range. The response to an i.p. ITT at the age of 8 weeks was similar to that of floxed animals. Changes in lipid metabolism were limited to a decrease in circulating triglyceride level, whereas hepatic triglyceride content was unaltered, as were NEFA and leptin levels. Thus no major abnormalities in glucose or lipid homeostasis were detected in these studies, which is similar to the findings in our *LivIrs2KO* mice.

The liver glycogen content was reduced as assessed by histological staining with periodate, and paralleling this result was a reduced glycogen synthase activity. In keeping with normal PKB/Akt activation, however, insulin-stimulated Gsk3 phosphorylation was similar in LKO and floxed animals. These findings again closely resemble the results of the *LivIrs2KO* model, where Gsk3

phosphorylation was unchanged, but glycogen synthesis was found to be lower during the hyperglycaemic clamp studies. No clamp studies were undertaken in the LKO model and therefore a complete comparison of the metabolic phenotypes of the two mice is not possible.

The assessment of gene expression in LKO animals was performed by Affymetrix chip array with subsequent confirmation by quantitative PCR. *Pck1*, *Gck*, and *Pparg* increased approximately 2-fold, whilst otherwise few changes were found both on array and real-time PCR analysis. These results were in contrast to the observations in our *LivIrs2KO* mice, where *Pck1* and *Pparg* remained unchanged, *Gck* expression was reduced and *G6pc* increased; the latter had remained unchanged in LKO animals. Methodology and small sample numbers might in part explain this discrepancy. Samples from only two LKO mice were arrayed and the same samples appear to have been repeatedly quantified by PCR, which would lead to an apparent reduction in standard error and thus increase in statistical significance. Even with five *LivIrs2KO* animals per group in some of our real-time PCR experiments a substantial standard error remained. However, surprisingly few alterations in gene expression were found in either animal model with liver-specific deletion of Irs2.

In summary, the phenotypes of both LKO and *LivIrs2KO* mice were relatively similar. Despite the lack of hepatic Irs2, insulin signalling events in the liver showed few alterations. Diabetes did not develop and disturbances of lipid metabolism were minimal. A reduction in glycogen synthesis found during clamp studies in *LivIrs2KO* animals was consistent with reduced liver glycogen in LKO mice. Analytical differences were found in gene expression studies, but the discrepancies again were minor.

10.6 Conclusion

The characterisation of a murine model with Cre/*loxP*-mediated deletion of *Irs2* in the liver revealed only minor changes during a detailed analysis of insulin signalling events, carbohydrate and lipid metabolism, as well as gene expression. Whole-body glucose homeostasis was maintained. Irs2-associated direct insulin receptor signalling in the liver is therefore not a major determinant of hepatic insulin resistance and thus the development of type 2 diabetes. This suggests that indirect effects and/or neuronal pathways are the main mechanisms by which insulin controls hepatic metabolism in mice.

FUTURE WORK

The unexpectedly minor phenotype of the *LivIrs2KO* model demonstrated that glucose homeostasis could be maintained even in the absence of Irs2-mediated insulin signalling in the liver. Other pathways must therefore contribute to the dysregulation of hepatic gluconeogenesis that characterises type 2 diabetes. In particular, indirect mechanisms involving non-classical target tissues of insulin appear to play a larger role than previously appreciated.

A promising next step would seem to be a more detailed characterisation of insulin signalling in the hypothalamus. NIRKO mice did not develop diabetes (193). However, the depletion of Insr in the medial arcuate nucleus was shown to reduce neuronal signals, transmitted via K_{ATP} channels, that reached the liver through the autonomic nervous system. As a consequence, insulin-mediated suppression of hepatic glucose output was impaired (73-75, 77). Irs2-associated signalling in a population of arcuate neurons expressing the rat insulin promoter (RIP) has recently been described to play a role in growth and energy homeostasis (212). *RIPCreIrs2KO* animals were hyperphagic and obese, and they developed impaired glucose tolerance in the context of a concomitant Cre/*loxP*-mediated reduction in β-cell mass.

A specific reduction of Irs2 in these arcuate neurons, e.g. by RNAi or by gene targeting using a more selective promoter, could avoid the interference with β-cell survival that is known to depend on functional insulin signalling though Insr, Irs2, and Foxo1 mediated transcription events (200, 203, 275, 276). As the pancreas is densely innervated by autonomic fibres (39), the effect of central insulin signalling on islet physiology could be assessed simultaneously.

This approach could thus provide more detailed insights into the role of CNS-mediated pathways in glucose metabolism.

REFERENCES

1. **Blake, J.A., Eppig, J.T., Bult, C.J., Kadin, J.A., and Richardson, J.E. 2006.** The Mouse Genome Database (MGD): updates and enhancements. ***Nucleic Acids Res* 34:D562-567.**
2. **Atkinson, M.A., and Maclaren, N.K. 1994.** The pathogenesis of insulin-dependent diabetes mellitus. ***N Engl J Med* 331:1428-1436.**
3. **Stumvoll, M., Goldstein, B.J., and van Haeften, T.W. 2005.** Type 2 diabetes: principles of pathogenesis and therapy. ***Lancet* 365:1333-1346.**
4. **Flier, J.S. 2004.** Obesity wars: molecular progress confronts an expanding epidemic. ***Cell* 116:337-350.**
5. **Gill, G.V., Ismail, A.A., Beeching, N.J., Macfarlane, S.B., and Bellis, M.A. 2003.** Hidden diabetes in the UK: use of capture-recapture methods to estimate total prevalence of diabetes mellitus in an urban population. ***J R Soc Med* 96:328-332.**
6. **Wild, S., Roglic, G., Green, A., Sicree, R., and King, H. 2004.** Global prevalence of diabetes: estimates for the year 2000 and projections for 2030. ***Diabetes Care* 27:1047-1053.**
7. **Zimmet, P., Alberti, K.G., and Shaw, J. 2001.** Global and societal implications of the diabetes epidemic. ***Nature* 414:782-787.**
8. **Zimmet, P. 2003.** The burden of type 2 diabetes: are we doing enough? ***Diabetes Metab* 29:6S9-18.**
9. **Currie, C.J., Kraus, D., Morgan, C.L., Gill, L., Stott, N.C., and Peters, J.R. 1997.** NHS acute sector expenditure for diabetes: the present, future, and excess in-patient cost of care. ***Diabet Med* 14:686-692.**
10. **Trautner, C., Icks, A., Haastert, B., Plum, F., and Berger, M. 1997.** Incidence of blindness in relation to diabetes. A population-based study. ***Diabetes Care* 20:1147-1153.**

11. **Stengel, B., Billon, S., Van Dijk, P.C., Jager, K.J., Dekker, F.W., Simpson, K., and Briggs, J.D. 2003.** Trends in the incidence of renal replacement therapy for end-stage renal disease in Europe, 1990-1999. ***Nephrol Dial Transplant* 18:1824-1833.**

12. **Rayman, G., Krishnan, S.T., Baker, N.R., Wareham, A.M., and Rayman, A. 2004.** Are we underestimating diabetes-related lower-extremity amputation rates? Results and benefits of the first prospective study. ***Diabetes Care* 27:1892-1896.**

13. **Kwon, K., Choi, D., Koo, B.K., and Ryu, S.K. 2005.** Decreased insulin sensitivity is associated with the extent of coronary artery disease in patients with angina. ***Diabetes Obes Metab* 7:579-585.**

14. **Kaufman, F.R. 2002.** Type 2 diabetes mellitus in children and youth: a new epidemic. ***J Pediatr Endocrinol Metab* 15 Suppl 2:737-744.**

15. **DeFronzo, R.A. 2004.** Pathogenesis of type 2 diabetes mellitus. ***Med Clin North Am* 88:787-835, ix.**

16. **Maassen, J.A., Tobias, E.S., Kayserilli, H., Tukel, T., Yuksel-Apak, M., D'Haens, E., Kleijer, W.J., Fery, F., and van der Zon, G.C. 2003.** Identification and functional assessment of novel and known insulin receptor mutations in five patients with syndromes of severe insulin resistance. ***J Clin Endocrinol Metab* 88:4251-4257.**

17. **Saltiel, A.R., and Kahn, C.R. 2001.** Insulin signalling and the regulation of glucose and lipid metabolism. ***Nature* 414:799-806.**

18. **Morse, S.A., Zhang, R., Thakur, V., and Reisin, E. 2005.** Hypertension and the metabolic syndrome. ***Am J Med Sci* 330:303-310.**

19. **Alberti, K.G., Zimmet, P., and Shaw, J. 2005.** The metabolic syndrome--a new worldwide definition. ***Lancet* 366:1059-1062.**

20. **Gale, E.A. 2005.** The myth of the metabolic syndrome. ***Diabetologia* 48:1679-1683.**

21. **Kahn, R., Buse, J., Ferrannini, E., and Stern, M. 2005.** The metabolic syndrome: time for a critical appraisal. Joint statement from the American Diabetes Association and the European Association for the Study of Diabetes. ***Diabetologia* 48:1684-1699.**

22. **Trovati, M., and Anfossi, G. 2002.** Influence of insulin and of insulin resistance on platelet and vascular smooth muscle cell function. ***J Diabetes Complications* 16:35-40.**

23. **Juhan-Vague, I., Morange, P.E., and Alessi, M.C. 2002.** The insulin resistance syndrome: implications for thrombosis and cardiovascular disease. ***Pathophysiol Haemost Thromb* 32:269-273.**

24. **Marsden, P.J., Murdoch, A.P., and Taylor, R. 2001.** Tissue insulin sensitivity and body weight in polycystic ovary syndrome. ***Clin Endocrinol (Oxf)* 55:191-199.**

25. **Sartor, B.M., and Dickey, R.P. 2005.** Polycystic ovarian syndrome and the metabolic syndrome. ***Am J Med Sci* 330:336-342.**

26. **Resnick, H.E., and Howard, B.V. 2002.** Diabetes and cardiovascular disease. ***Annu Rev Med* 53:245-267.**

27. **Cherrington, A.D. 1999. Banting Lecture 1997.** Control of glucose uptake and release by the liver in vivo. ***Diabetes* 48:1198-1214.**

28. **Kimball, S.R., Siegfried, B.A., and Jefferson, L.S. 2004.** Glucagon represses signaling through the mammalian target of rapamycin in rat liver by activating AMP-activated protein kinase. ***J Biol Chem* 279:54103-54109.**

29. **Orci, L., Ravazzola, M., Storch, M.J., Anderson, R.G., Vassalli, J.D., and Perrelet, A. 1987.** Proteolytic maturation of insulin is a post-Golgi event which occurs in acidifying clathrin-coated secretory vesicles. ***Cell* 49:865-868.**

30. **Gagliardino, J.J. 2005.** Physiological endocrine control of energy homeostasis and postprandial blood glucose levels. ***Eur Rev Med Pharmacol Sci* 9:75-92.**

31. **Postic, C., Shiota, M., and Magnuson, M.A. 2001.** Cell-specific roles of glucokinase in glucose homeostasis. ***Recent Prog Horm Res* 56:195-217.**

32. **Matschinsky, F.M. 2002.** Regulation of pancreatic beta-cell glucokinase: from basics to therapeutics. ***Diabetes* 51 Suppl 3:S394-404.**

33. **Bratanova-Tochkova, T.K., Cheng, H., Daniel, S., Gunawardana, S., Liu, Y.J., Mulvaney-Musa, J., Schermerhorn, T., Straub, S.G., Yajima, H., and Sharp, G.W. 2002.** Triggering and augmentation mechanisms, granule pools, and biphasic insulin secretion. ***Diabetes* 51 Suppl 1:S83-90.**

34. **Leibiger, I.B., Leibiger, B., and Berggren, P.O. 2002.** Insulin feedback action on pancreatic beta-cell function. ***FEBS Lett* 532:1-6.**

35. **Jiang, G., and Zhang, B.B. 2003.** Glucagon and regulation of glucose metabolism. ***Am J Physiol Endocrinol Metab* 284:E671-678.**

36. **Rorsman, P., Berggren, P.O., Bokvist, K., Ericson, H., Mohler, H., Ostenson, C.G., and Smith, P.A. 1989.** Glucose-inhibition of glucagon secretion involves activation of $GABA_A$-receptor chloride channels. ***Nature* 341:233-236.**

37. **Wendt, A., Birnir, B., Buschard, K., Gromada, J., Salehi, A., Sewing, S., Rorsman, P., and Braun, M. 2004.** Glucose inhibition of glucagon secretion from rat alpha-cells is mediated by GABA released from neighboring beta-cells. ***Diabetes* 53:1038-1045.**

38. **Koeslag, J.H., Saunders, P.T., and Terblanche, E. 2003.** A reappraisal of the blood glucose homeostat which comprehensively explains the type 2 diabetes mellitus-syndrome X complex. ***J Physiol* 549:333-346.**

39. **Ahren, B. 2000.** Autonomic regulation of islet hormone secretion--implications for health and disease. ***Diabetologia* 43:393-410.**

40. **Van Schaftingen, E., Detheux, M., and Veiga da Cunha, M. 1994.** Short-term control of glucokinase activity: role of a regulatory protein. ***Faseb J* 8:414-419.**

41. **Magnuson, M.A., Andreone, T.L., Printz, R.L., Koch, S., and Granner, D.K. 1989.** Rat glucokinase gene: structure and regulation by insulin. ***Proc Natl Acad Sci U S A* 86:4838-4842.**

42. **O'Brien, R.M., and Granner, D.K. 1991.** Regulation of gene expression by insulin. ***Biochem J* 278 (Pt 3):609-619.**

43. **Kawaguchi, T., Takenoshita, M., Kabashima, T., and Uyeda, K. 2001.** Glucose and cAMP regulate the L-type pyruvate kinase gene by phosphorylation/dephosphorylation of the carbohydrate response element binding protein. ***Proc Natl Acad Sci U S A* 98:13710-13715.**

44. **Gomis, R.R., Ferrer, J.C., and Guinovart, J.J. 2000.** Shared control of hepatic glycogen synthesis by glycogen synthase and glucokinase. ***Biochem J* 351 Pt 3:811-816.**

45. **Cross, D.A., Alessi, D.R., Cohen, P., Andjelkovich, M., and Hemmings, B.A. 1995.** Inhibition of glycogen synthase kinase-3 by insulin mediated by protein kinase B. ***Nature* 378:785-789.**

46. **Lawrence, J.C., Jr., and Roach, P.J. 1997.** New insights into the role and mechanism of glycogen synthase activation by insulin. ***Diabetes* 46:541-547.**

47. **Mabrouk, G.M., Helmy, I.M., Thampy, K.G., and Wakil, S.J. 1990.** Acute hormonal control of acetyl-CoA carboxylase. The roles of insulin, glucagon, and epinephrine. ***J Biol Chem* 265:6330-6338.**

48. **Paulauskis, J.D., and Sul, H.S. 1989.** Hormonal regulation of mouse fatty acid synthase gene transcription in liver. ***J Biol Chem* 264:574-577.**

49. **Ishii, S., Iizuka, K., Miller, B.C., and Uyeda, K. 2004.** Carbohydrate response element binding protein directly promotes lipogenic enzyme gene transcription. ***Proc Natl Acad Sci U S A* 101:15597-15602.**

50. **Quinn, P.G., and Yeagley, D. 2005.** Insulin regulation of PEPCK gene expression: a model for rapid and reversible modulation. ***Curr Drug Targets Immune Endocr Metabol Disord* 5:423-437.**

51. **Pilkis, S.J., and Granner, D.K. 1992.** Molecular physiology of the regulation of hepatic gluconeogenesis and glycolysis. ***Annu Rev Physiol* 54:885-909.**

52. **Van Schaftingen, E., and Gerin, I. 2002.** The glucose-6-phosphatase system. ***Biochem J* 362:513-532.**

53. **Vander Kooi, B.T., Streeper, R.S., Svitek, C.A., Oeser, J.K., Powell, D.R., and O'Brien, R.M. 2003.** The three insulin response sequences in the glucose-6-phosphatase catalytic subunit gene promoter are functionally distinct. ***J Biol Chem* 278:11782-11793.**

54. **Witters, L.A., and Avruch, J. 1978.** Insulin regulation of hepatic glycogen synthase and phosphorylase. ***Biochemistry* 17:406-410.**

55. **Pereira, L.O., and Lancha, A.H., Jr. 2004.** Effect of insulin and contraction up on glucose transport in skeletal muscle. ***Prog Biophys Mol Biol* 84:1-27.**

56. **Aas, V., Rokling-Andersen, M., Wensaas, A.J., Thoresen, G.H., Kase, E.T., and Rustan, A.C. 2005.** Lipid metabolism in human skeletal muscle cells: effects of palmitate and chronic hyperglycaemia. ***Acta Physiol Scand* 183:31-41.**

57. **Hargreaves, M., and Richter, E.A. 1988.** Regulation of skeletal muscle glycogenolysis during exercise. ***Can J Sport Sci* 13:197-203.**

58. **Cortright, R.N., and Dohm, G.L. 1997.** Mechanisms by which insulin and muscle contraction stimulate glucose transport. ***Can J Appl Physiol* 22:519-530.**

59. **Large, V., Peroni, O., Letexier, D., Ray, H., and Beylot, M. 2004.** Metabolism of lipids in human white adipocyte. ***Diabetes Metab* 30:294-309.**

60. **Panarotto, D., Remillard, P., Bouffard, L., and Maheux, P. 2002.** Insulin resistance affects the regulation of lipoprotein lipase in the postprandial period and in an adipose tissue-specific manner. ***Eur J Clin Invest* 32:84-92.**

61. **Holm, C. 2003.** Molecular mechanisms regulating hormone-sensitive lipase and lipolysis. ***Biochem Soc Trans* 31:1120-1124.**

62. **Lam, T.K., van de Werve, G., and Giacca, A. 2003.** Free fatty acids increase basal hepatic glucose production and induce hepatic insulin resistance at different sites. ***Am J Physiol Endocrinol Metab* 284:E281-290.**

63. **Dubois, M., Kerr-Conte, J., Gmyr, V., Bouckenooghe, T., Muharram, G., D'Herbomez, M., Martin-Ponthieu, A., Vantyghem, M.C., Vandewalle, B., and Pattou, F. 2004.** Non-esterified fatty acids are deleterious for human pancreatic islet function at physiological glucose concentration. ***Diabetologia* 47:463-469.**

64. **Magnusson, I., Rothman, D.L., Katz, L.D., Shulman, R.G., and Shulman, G.I. 1992.** Increased rate of gluconeogenesis in type II diabetes mellitus. A 13C nuclear magnetic resonance study. ***J Clin Invest* 90:1323-1327.**

65. **Prager, R., Wallace, P., and Olefsky, J.M. 1987.** Direct and indirect effects of insulin to inhibit hepatic glucose output in obese subjects. ***Diabetes* 36:607-611.**

66. **Ishihara, H., Maechler, P., Gjinovci, A., Herrera, P.L., and Wollheim, C.B. 2003.** Islet beta-cell secretion determines glucagon release from neighbouring alpha-cells. ***Nat Cell Biol* 5:330-335.**

67. **Cherrington, A.D. 2005.** The role of hepatic insulin receptors in the regulation of glucose production. ***J Clin Invest* 115:1136-1139.**

68. **Ader, M., and Bergman, R.N. 1990.** Peripheral effects of insulin dominate suppression of fasting hepatic glucose production. ***Am J Physiol* 258:E1020-1032.**

69. **Giacca, A., Fisher, S.J., Shi, Z.Q., Gupta, R., Lickley, H.L., and Vranic, M. 1992.** Importance of peripheral insulin levels for insulin-induced suppression of glucose production in depancreatized dogs. ***J Clin Invest* 90:1769-1777.**

70. **Sindelar, D.K., Balcom, J.H., Chu, C.A., Neal, D.W., and Cherrington, A.D. 1996.** A comparison of the effects of selective increases in peripheral or portal insulin on hepatic glucose production in the conscious dog. ***Diabetes* 45:1594-1604.**

71. **Sindelar, D.K., Chu, C.A., Rohlie, M., Neal, D.W., Swift, L.L., and Cherrington, A.D. 1997.** The role of fatty acids in mediating the effects of peripheral insulin on hepatic glucose production in the conscious dog. ***Diabetes* 46:187-196.**

72. **Satake, S., Moore, M.C., Igawa, K., Converse, M., Farmer, B., Neal, D.W., and Cherrington, A.D. 2002.** Direct and indirect effects of insulin on glucose uptake and storage by the liver. ***Diabetes* 51:1663-1671.**

73. **Obici, S., Feng, Z., Karkanias, G., Baskin, D.G., and Rossetti, L. 2002.** Decreasing hypothalamic insulin receptors causes hyperphagia and insulin resistance in rats. ***Nat Neurosci* 5:566-572.**

74. **Obici, S., Zhang, B.B., Karkanias, G., and Rossetti, L. 2002.** Hypothalamic insulin signaling is required for inhibition of glucose production. ***Nat Med* 8:1376-1382.**

75. **Spanswick, D., Smith, M.A., Mirshamsi, S., Routh, V.H., and Ashford, M.L. 2000.** Insulin activates ATP-sensitive K+ channels in hypothalamic neurons of lean, but not obese rats. ***Nat Neurosci* 3:757-758.**

76. **Pocai, A., Morgan, K., Buettner, C., Gutierrez-Juarez, R., Obici, S., and Rossetti, L. 2005.** Central leptin acutely reverses diet-induced hepatic insulin resistance. ***Diabetes* 54:3182-3189.**

77. **Pocai, A., Obici, S., Schwartz, G.J., and Rossetti, L. 2005.** A brain-liver circuit regulates glucose homeostasis. ***Cell Metab* 1:53-61.**

78. **Taniguchi, C.M., Emanuelli, B., and Kahn, C.R. 2006.** Critical nodes in signalling pathways: insights into insulin action. ***Nat Rev Mol Cell Biol* 7:85-96.**

79. **Ullrich, A., Bell, J.R., Chen, E.Y., Herrera, R., Petruzzelli, L.M., Dull, T.J., Gray, A., Coussens, L., Liao, Y.C., Tsubokawa, M., et al. 1985.** Human insulin receptor and its relationship to the tyrosine kinase family of oncogenes. ***Nature*** **313:756-761.**

80. **Siddle, K., Urso, B., Niesler, C.A., Cope, D.L., Molina, L., Surinya, K.H., and Soos, M.A. 2001.** Specificity in ligand binding and intracellular signalling by insulin and insulin-like growth factor receptors. ***Biochem Soc Trans*** **29:513-525.**

81. **White, M.F. 2003.** Insulin signaling in health and disease. ***Science*** **302:1710-1711.**

82. **Cheatham, B., and Kahn, C.R. 1995.** Insulin action and the insulin signaling network. ***Endocr Rev*** **16:117-142.**

83. **Kido, Y., Nakae, J., and Accili, D. 2001.** Clinical review 125: The insulin receptor and its cellular targets. ***J Clin Endocrinol Metab*** **86:972-979.**

84. **Bjornholm, M., He, A.R., Attersand, A., Lake, S., Liu, S.C., Lienhard, G.E., Taylor, S., Arner, P., and Zierath, J.R. 2002.** Absence of functional insulin receptor substrate-3 (IRS-3) gene in humans. ***Diabetologia*** **45:1697-1702.**

85. **Rother, K.I., Imai, Y., Caruso, M., Beguinot, F., Formisano, P., and Accili, D. 1998.** Evidence that IRS-2 phosphorylation is required for insulin action in hepatocytes. ***J Biol Chem*** **273:17491-17497.**

86. **Anai, M., Ono, H., Funaki, M., Fukushima, Y., Inukai, K., Ogihara, T., Sakoda, H., Onishi, Y., Yazaki, Y., Kikuchi, M., et al. 1998.** Different subcellular distribution and regulation of expression of insulin receptor substrate (IRS)-3 from those of IRS-1 and IRS-2. ***J Biol Chem*** **273:29686-29692.**

87. **Fantin, V.R., Sparling, J.D., Slot, J.W., Keller, S.R., Lienhard, G.E., and Lavan, B.E. 1998.** Characterization of insulin receptor substrate 4 in human embryonic kidney 293 cells. ***J Biol Chem*** **273:10726-10732.**

88. **Sciacchitano, S., and Taylor, S.I. 1997.** Cloning, tissue expression, and chromosomal localization of the mouse IRS-3 gene. ***Endocrinology*** **138:4931-4940.**

89. **Sun, X.J., Rothenberg, P., Kahn, C.R., Backer, J.M., Araki, E., Wilden, P.A., Cahill, D.A., Goldstein, B.J., and White, M.F. 1991.** Structure of the insulin receptor substrate IRS-1 defines a unique signal transduction protein. ***Nature*** **352:73-77.**

90. **Araki, E., Sun, X.J., Haag, B.L., 3rd, Chuang, L.M., Zhang, Y., Yang-Feng, T.L., White, M.F., and Kahn, C.R. 1993.** Human skeletal muscle insulin receptor substrate-1. Characterization of the cDNA, gene, and chromosomal localization. ***Diabetes*** **42:1041-1054.**

91. **Tobe, K., Tamemoto, H., Yamauchi, T., Aizawa, S., Yazaki, Y., and Kadowaki, T. 1995.** Identification of a 190-kDa protein as a novel substrate for the insulin receptor kinase functionally similar to insulin receptor substrate-1. ***J Biol Chem*** **270:5698-5701.**

92. **Sun, X.J., Wang, L.M., Zhang, Y., Yenush, L., Myers, M.G., Jr., Glasheen, E., Lane, W.S., Pierce, J.H., and White, M.F. 1995.** Role of IRS-2 in insulin and cytokine signalling. ***Nature*** **377:173-177.**

93. **Sawka-Verhelle, D., Tartare-Deckert, S., White, M.F., and Van Obberghen, E. 1996.** Insulin receptor substrate-2 binds to the insulin receptor through its phosphotyrosine-binding domain and through a newly identified domain comprising amino acids 591-786. ***J Biol Chem*** **271:5980-5983.**

94. **Previs, S.F., Withers, D.J., Ren, J.M., White, M.F., and Shulman, G.I. 2000.** Contrasting effects of IRS-1 versus IRS-2 gene disruption on carbohydrate and lipid metabolism in vivo. ***J Biol Chem*** **275:38990-38994.**

95. **Lavan, B.E., Lane, W.S., and Lienhard, G.E. 1997.** The 60-kDa phosphotyrosine protein in insulin-treated adipocytes is a new member of the insulin receptor substrate family. ***J Biol Chem*** **272:11439-11443.**

96. **Kuhne, M.R., Zhao, Z., and Lienhard, G.E. 1995.** Evidence against dephosphorylation of insulin-elicited phosphotyrosine proteins in vivo by the phosphatase PTP2C. ***Biochem Biophys Res Commun* 211:190-197.**

97. **Lavan, B.E., Fantin, V.R., Chang, E.T., Lane, W.S., Keller, S.R., and Lienhard, G.E. 1997.** A novel 160-kDa phosphotyrosine protein in insulin-treated embryonic kidney cells is a new member of the insulin receptor substrate family. ***J Biol Chem* 272:21403-21407.**

98. **Fantin, V.R., Lavan, B.E., Wang, Q., Jenkins, N.A., Gilbert, D.J., Copeland, N.G., Keller, S.R., and Lienhard, G.E. 1999.** Cloning, tissue expression, and chromosomal location of the mouse insulin receptor substrate 4 gene. ***Endocrinology* 140:1329-1337.**

99. **Numan, S., and Russell, D.S. 1999.** Discrete expression of insulin receptor substrate-4 mRNA in adult rat brain. ***Brain Res Mol Brain Res* 72:97-102.**

100. **Liu, S.C., Wang, Q., Lienhard, G.E., and Keller, S.R. 1999.** Insulin receptor substrate 3 is not essential for growth or glucose homeostasis. ***J Biol Chem* 274:18093-18099.**

101. **Fantin, V.R., Wang, Q., Lienhard, G.E., and Keller, S.R. 2000.** Mice lacking insulin receptor substrate 4 exhibit mild defects in growth, reproduction, and glucose homeostasis. ***Am J Physiol Endocrinol Metab* 278:E127-133.**

102. **Liu, Y.F., Herschkovitz, A., Boura-Halfon, S., Ronen, D., Paz, K., Leroith, D., and Zick, Y. 2004.** Serine phosphorylation proximal to its phosphotyrosine binding domain inhibits insulin receptor substrate 1 function and promotes insulin resistance. ***Mol Cell Biol* 24:9668-9681.**

103. **Zhang, S.Q., Tsiaras, W.G., Araki, T., Wen, G., Minichiello, L., Klein, R., and Neel, B.G. 2002.** Receptor-specific regulation of phosphatidylinositol 3'-kinase activation by the protein tyrosine phosphatase Shp2. ***Mol Cell Biol* 22:4062-4072.**

104. **Asante-Appiah, E., and Kennedy, B.P. 2003.** Protein tyrosine phosphatases: the quest for negative regulators of insulin action. ***Am J Physiol Endocrinol Metab*** **284:E663-670.**

105. **Skolnik, E.Y., Batzer, A., Li, N., Lee, C.H., Lowenstein, E., Mohammadi, M., Margolis, B., and Schlessinger, J. 1993.** The function of GRB2 in linking the insulin receptor to Ras signaling pathways. ***Science*** **260:1953-1955.**

106. **Cantrell, D.A. 2001.** Phosphoinositide 3-kinase signalling pathways. ***J Cell Sci*** **114:1439-1445.**

107. **Terauchi, Y., Tsuji, Y., Satoh, S., Minoura, H., Murakami, K., Okuno, A., Inukai, K., Asano, T., Kaburagi, Y., Ueki, K., et al. 1999.** Increased insulin sensitivity and hypoglycaemia in mice lacking the p85 alpha subunit of phosphoinositide 3-kinase. ***Nat Genet*** **21:230-235.**

108. **Vanhaesebroeck, B., and Alessi, D.R. 2000.** The PI3K-PDK1 connection: more than just a road to PKB. ***Biochem J*** **346 Pt 3:561-576.**

109. **Mora, A., Komander, D., van Aalten, D.M., and Alessi, D.R. 2004.** PDK1, the master regulator of AGC kinase signal transduction. ***Semin Cell Dev Biol*** **15:161-170.**

110. **Shepherd, P.R., Withers, D.J., and Siddle, K. 1998.** Phosphoinositide 3-kinase: the key switch mechanism in insulin signalling. ***Biochem J*** **333 (Pt 3):471-490.**

111. **Brachmann, S.M., Ueki, K., Engelman, J.A., Kahn, R.C., and Cantley, L.C. 2005.** Phosphoinositide 3-kinase catalytic subunit deletion and regulatory subunit deletion have opposite effects on insulin sensitivity in mice. ***Mol Cell Biol*** **25:1596-1607.**

112. **Bi, L., Okabe, I., Bernard, D.J., Wynshaw-Boris, A., and Nussbaum, R.L. 1999.** Proliferative defect and embryonic lethality in mice homozygous for a deletion in the p110alpha subunit of phosphoinositide 3-kinase. ***J Biol Chem*** **274:10963-10968.**

113. **Bi, L., Okabe, I., Bernard, D.J., and Nussbaum, R.L. 2002.** Early embryonic lethality in mice deficient in the p110beta catalytic subunit of PI 3-kinase. ***Mamm Genome* 13:169-172.**

114. **Foukas, L.C., Claret, M., Pearce, W., Okkenhaug, K., Meek, S., Peskett, E., Sancho, S., Smith, A.J., Withers, D.J., and Vanhaesebroeck, B. 2006.** Critical role for the p110alpha phosphoinositide-3-OH kinase in growth and metabolic regulation. ***Nature*.**

115. **Asano, T., Kanda, A., Katagiri, H., Nawano, M., Ogihara, T., Inukai, K., Anai, M., Fukushima, Y., Yazaki, Y., Kikuchi, M., et al. 2000.** p110beta is up-regulated during differentiation of 3T3-L1 cells and contributes to the highly insulin-responsive glucose transport activity. ***J Biol Chem* 275:17671-17676.**

116. **Fruman, D.A., Mauvais-Jarvis, F., Pollard, D.A., Yballe, C.M., Brazil, D., Bronson, R.T., Kahn, C.R., and Cantley, L.C. 2000.** Hypoglycaemia, liver necrosis and perinatal death in mice lacking all isoforms of phosphoinositide 3-kinase p85 alpha. ***Nat Genet* 26:379-382.**

117. **Ueki, K., Yballe, C.M., Brachmann, S.M., Vicent, D., Watt, J.M., Kahn, C.R., and Cantley, L.C. 2002.** Increased insulin sensitivity in mice lacking p85beta subunit of phosphoinositide 3-kinase. ***Proc Natl Acad Sci U S A* 99:419-424.**

118. **Lemmon, M.A., and Ferguson, K.M. 2000.** Signal-dependent membrane targeting by pleckstrin homology (PH) domains. ***Biochem J* 350 Pt 1:1-18.**

119. **Burgering, B.M., and Coffer, P.J. 1995.** Protein kinase B (c-Akt) in phosphatidylinositol-3-OH kinase signal transduction. ***Nature* 376:599-602.**

120. **Alessi, D.R., James, S.R., Downes, C.P., Holmes, A.B., Gaffney, P.R., Reese, C.B., and Cohen, P. 1997.** Characterization of a 3-phosphoinositide-dependent protein kinase which phosphorylates and activates protein kinase Balpha. ***Curr Biol* 7:261-269.**

121. **Stokoe, D., Stephens, L.R., Copeland, T., Gaffney, P.R., Reese, C.B., Painter, G.F., Holmes, A.B., McCormick, F., and Hawkins, P.T. 1997.** Dual role of phosphatidylinositol-3,4,5-trisphosphate in the activation of protein kinase B. ***Science* 277:567-570.**

122. **Currie, R.A., Walker, K.S., Gray, A., Deak, M., Casamayor, A., Downes, C.P., Cohen, P., Alessi, D.R., and Lucocq, J. 1999.** Role of phosphatidylinositol 3,4,5-trisphosphate in regulating the activity and localization of 3-phosphoinositide-dependent protein kinase-1. ***Biochem J* 337 (Pt 3):575-583.**

123. **Alessi, D.R. 2001.** Discovery of PDK1, one of the missing links in insulin signal transduction. **Colworth Medal Lecture. *Biochem Soc Trans* 29:1-14.**

124. **Pende, M., Kozma, S.C., Jaquet, M., Oorschot, V., Burcelin, R., Le Marchand-Brustel, Y., Klumperman, J., Thorens, B., and Thomas, G. 2000.** Hypoinsulinaemia, glucose intolerance and diminished beta-cell size in S6K1-deficient mice. ***Nature* 408:994-997.**

125. **Kozma, S.C., and Thomas, G. 2002.** Regulation of cell size in growth, development and human disease: PI3K, PKB and S6K. ***Bioessays* 24:65-71.**

126. **Farese, R.V., Sajan, M.P., and Standaert, M.L. 2005.** Atypical protein kinase C in insulin action and insulin resistance. ***Biochem Soc Trans* 33:350-353.**

127. **Lawlor, M.A., Mora, A., Ashby, P.R., Williams, M.R., Murray-Tait, V., Malone, L., Prescott, A.R., Lucocq, J.M., and Alessi, D.R. 2002.** Essential role of PDK1 in regulating cell size and development in mice. ***Embo J* 21:3728-3738.**

128. **Mora, A., Lipina, C., Tronche, F., Sutherland, C., and Alessi, D.R. 2005.** Deficiency of PDK1 in liver results in glucose intolerance, impairment of insulin-regulated gene expression and liver failure. ***Biochem J* 385:639-648.**

129. **Sarbassov, D.D., Guertin, D.A., Ali, S.M., and Sabatini, D.M. 2005.** Phosphorylation and regulation of Akt/PKB by the rictor-mTOR complex. ***Science*** **307:1098-1101.**

130. **Cho, H., Mu, J., Kim, J.K., Thorvaldsen, J.L., Chu, Q., Crenshaw, E.B., 3rd, Kaestner, K.H., Bartolomei, M.S., Shulman, G.I., and Birnbaum, M.J. 2001.** Insulin resistance and a diabetes mellitus-like syndrome in mice lacking the protein kinase Akt2 (PKB beta). ***Science*** **292:1728-1731.**

131. **Bae, S.S., Cho, H., Mu, J., and Birnbaum, M.J. 2003.** Isoform-specific regulation of insulin-dependent glucose uptake by Akt/protein kinase B. ***J Biol Chem*** **278:49530-49536.**

132. **Zeigerer, A., McBrayer, M.K., and McGraw, T.E. 2004.** Insulin stimulation of GLUT4 exocytosis, but not its inhibition of endocytosis, is dependent on RabGAP AS160. ***Mol Biol Cell*** **15:4406-4415.**

133. **Chen, W.S., Xu, P.Z., Gottlob, K., Chen, M.L., Sokol, K., Shiyanova, T., Roninson, I., Weng, W., Suzuki, R., Tobe, K., et al. 2001.** Growth retardation and increased apoptosis in mice with homozygous disruption of the Akt1 gene. ***Genes Dev*** **15:2203-2208.**

134. **Cho, H., Thorvaldsen, J.L., Chu, Q., Feng, F., and Birnbaum, M.J. 2001.** Akt1/PKBalpha is required for normal growth but dispensable for maintenance of glucose homeostasis in mice. ***J Biol Chem*** **276:38349-38352.**

135. **Tschopp, O., Yang, Z.Z., Brodbeck, D., Dummler, B.A., Hemmings-Mieszczak, M., Watanabe, T., Michaelis, T., Frahm, J., and Hemmings, B.A. 2005.** Essential role of protein kinase B gamma (PKB gamma/Akt3) in postnatal brain development but not in glucose homeostasis. ***Development*** **132:2943-2954.**

136. **George, S., Rochford, J.J., Wolfrum, C., Gray, S.L., Schinner, S., Wilson, J.C., Soos, M.A., Murgatroyd, P.R., Williams, R.M., Acerini, C.L., et al. 2004.** A family with severe insulin resistance and diabetes due to a mutation in AKT2. ***Science*** **304:1325-1328.**

137. **Woodgett, J.R. 1990.** Molecular cloning and expression of glycogen synthase kinase-3/factor A. ***Embo J* 9:2431-2438.**

138. **Roach, P.J. 2002.** Glycogen and its metabolism. ***Curr Mol Med* 2:101-120.**

139. **Cline, G.W., Johnson, K., Regittnig, W., Perret, P., Tozzo, E., Xiao, L., Damico, C., and Shulman, G.I. 2002.** Effects of a novel glycogen synthase kinase-3 inhibitor on insulin-stimulated glucose metabolism in Zucker diabetic fatty (fa/fa) rats. ***Diabetes* 51:2903-2910.**

140. **McManus, E.J., Sakamoto, K., Armit, L.J., Ronaldson, L., Shpiro, N., Marquez, R., and Alessi, D.R. 2005.** Role that phosphorylation of GSK3 plays in insulin and Wnt signalling defined by knockin analysis. ***Embo J* 24:1571-1583.**

141. **Wang, X., Paulin, F.E., Campbell, L.E., Gomez, E., O'Brien, K., Morrice, N., and Proud, C.G. 2001.** Eukaryotic initiation factor 2B: identification of multiple phosphorylation sites in the epsilon-subunit and their functions in vivo. ***Embo J* 20:4349-4359.**

142. **Frame, S., and Cohen, P. 2001.** GSK3 takes centre stage more than 20 years after its discovery. ***Biochem J* 359:1-16.**

143. **Potter, C.J., Pedraza, L.G., and Xu, T. 2002.** Akt regulates growth by directly phosphorylating Tsc2. ***Nat Cell Biol* 4:658-665.**

144. **Nellist, M., van Slegtenhorst, M.A., Goedbloed, M., van den Ouweland, A.M., Halley, D.J., and van der Sluijs, P. 1999.** Characterization of the cytosolic tuberin-hamartin complex. Tuberin is a cytosolic chaperone for hamartin. ***J Biol Chem* 274:35647-35652.**

145. **Zhang, H., Cicchetti, G., Onda, H., Koon, H.B., Asrican, K., Bajraszewski, N., Vazquez, F., Carpenter, C.L., and Kwiatkowski, D.J. 2003.** Loss of Tsc1/Tsc2 activates mTOR and disrupts PI3K-Akt signaling through downregulation of PDGFR. ***J Clin Invest* 112:1223-1233.**

146. **Burnett, P.E., Barrow, R.K., Cohen, N.A., Snyder, S.H., and Sabatini, D.M. 1998.** RAFT1 phosphorylation of the translational regulators p70 S6 kinase and 4E-BP1. ***Proc Natl Acad Sci U S A* 95:1432-1437.**

147. **Gao, X., and Pan, D. 2001.** TSC1 and TSC2 tumor suppressors antagonize insulin signaling in cell growth. ***Genes Dev* 15:1383-1392.**

148. **Proud, C.G. 2006.** Regulation of protein synthesis by insulin. ***Biochem Soc Trans* 34:213-216.**

149. **Biggs, W.H., 3rd, Meisenhelder, J., Hunter, T., Cavenee, W.K., and Arden, K.C. 1999.** Protein kinase B/Akt-mediated phosphorylation promotes nuclear exclusion of the winged helix transcription factor FKHR1. ***Proc Natl Acad Sci U S A* 96:7421-7426.**

150. **Kops, G.J., and Burgering, B.M. 2000.** Forkhead transcription factors are targets of signalling by the proto-oncogene PKB (C-AKT). ***J Anat* 197 Pt 4:571-574.**

151. **Kaestner, K.H., Knochel, W., and Martinez, D.E. 2000.** Unified nomenclature for the winged helix/forkhead transcription factors. ***Genes Dev* 14:142-146.**

152. **Brunet, A., Bonni, A., Zigmond, M.J., Lin, M.Z., Juo, P., Hu, L.S., Anderson, M.J., Arden, K.C., Blenis, J., and Greenberg, M.E. 1999.** Akt promotes cell survival by phosphorylating and inhibiting a Forkhead transcription factor. ***Cell* 96:857-868.**

153. **Puigserver, P., Rhee, J., Donovan, J., Walkey, C.J., Yoon, J.C., Oriente, F., Kitamura, Y., Altomonte, J., Dong, H., Accili, D., et al. 2003.** Insulin-regulated hepatic gluconeogenesis through FOXO1-PGC-1alpha interaction. ***Nature* 423:550-555.**

154. **Altomonte, J., Richter, A., Harbaran, S., Suriawinata, J., Nakae, J., Thung, S.N., Meseck, M., Accili, D., and Dong, H. 2003.** Inhibition of Foxo1 function is associated with improved fasting glycemia in diabetic mice. ***Am J Physiol Endocrinol Metab* 285:E718-728.**

155. **Zhang, W., Patil, S., Chauhan, B., Guo, S., Powell, D.R., Le, J., Klotsas, A., Matika, R., Xiao, X., Franks, R., et al. 2006.** FoxO1 regulates multiple metabolic pathways in the liver: effects on gluconeogenic, glycolytic, and lipogenic gene expression. ***J Biol Chem* 281:10105-10117.**

156. **Wolfrum, C., Asilmaz, E., Luca, E., Friedman, J.M., and Stoffel, M. 2004.** Foxa2 regulates lipid metabolism and ketogenesis in the liver during fasting and in diabetes. ***Nature* 432:1027-1032.**

157. **Wolfrum, C., and Stoffel, M. 2006.** Coactivation of Foxa2 through Pgc-1beta promotes liver fatty acid oxidation and triglyceride/VLDL secretion. ***Cell Metab* 3:99-110.**

158. **Horton, J.D., Goldstein, J.L., and Brown, M.S. 2002.** SREBPs: activators of the complete program of cholesterol and fatty acid synthesis in the liver. ***J Clin Invest* 109:1125-1131.**

159. **Shimomura, I., Shimano, H., Horton, J.D., Goldstein, J.L., and Brown, M.S. 1997.** Differential expression of exons 1a and 1c in mRNAs for sterol regulatory element binding protein-1 in human and mouse organs and cultured cells. ***J Clin Invest* 99:838-845.**

160. **Fleischmann, M., and Iynedjian, P.B. 2000.** Regulation of sterol regulatory-element binding protein 1 gene expression in liver: role of insulin and protein kinase B/cAkt. ***Biochem J* 349:13-17.**

161. **Ribaux, P.G., and Iynedjian, P.B. 2003.** Analysis of the role of protein kinase B (cAKT) in insulin-dependent induction of glucokinase and sterol regulatory element-binding protein 1 (SREBP1) mRNAs in hepatocytes. ***Biochem J* 376:697-705.**

162. **Porstmann, T., Griffiths, B., Chung, Y.L., Delpuech, O., Griffiths, J.R., Downward, J., and Schulze, A. 2005.** PKB/Akt induces transcription of enzymes involved in cholesterol and fatty acid biosynthesis via activation of SREBP. ***Oncogene* 24:6465-6481.**

163. **Shimomura, I., Bashmakov, Y., Ikemoto, S., Horton, J.D., Brown, M.S., and Goldstein, J.L. 1999.** Insulin selectively increases SREBP-1c mRNA in the livers of rats with streptozotocin-induced diabetes. ***Proc Natl Acad Sci U S A* 96:13656-13661.**

164. **Zhang, Y., and Mangelsdorf, D.J. 2002.** LuXuRies of lipid homeostasis: the unity of nuclear hormone receptors, transcription regulation, and cholesterol sensing. ***Mol Interv* 2:78-87.**

165. **Hegarty, B.D., Bobard, A., Hainault, I., Ferre, P., Bossard, P., and Foufelle, F. 2005.** Distinct roles of insulin and liver X receptor in the induction and cleavage of sterol regulatory element-binding protein-1c. ***Proc Natl Acad Sci U S A* 102:791-796.**

166. **Rubinfeld, H., and Seger, R. 2005.** The ERK cascade: a prototype of MAPK signaling. ***Mol Biotechnol* 31:151-174.**

167. **Yoon, S., and Seger, R. 2006.** The extracellular signal-regulated kinase: multiple substrates regulate diverse cellular functions. ***Growth Factors* 24:21-44.**

168. **Downward, J. 2004.** PI 3-kinase, Akt and cell survival. ***Semin Cell Dev Biol* 15:177-182.**

169. **Kops, G.J., Medema, R.H., Glassford, J., Essers, M.A., Dijkers, P.F., Coffer, P.J., Lam, E.W., and Burgering, B.M. 2002.** Control of cell cycle exit and entry by protein kinase B-regulated forkhead transcription factors. ***Mol Cell Biol* 22:2025-2036.**

170. **Birkenkamp, K.U., and Coffer, P.J. 2003.** Regulation of cell survival and proliferation by the FOXO (Forkhead box, class O) subfamily of Forkhead transcription factors. ***Biochem Soc Trans* 31:292-297.**

171. **Suhara, T., Kim, H.S., Kirshenbaum, L.A., and Walsh, K. 2002.** Suppression of Akt signaling induces Fas ligand expression: involvement of caspase and Jun kinase activation in Akt-mediated Fas ligand regulation. ***Mol Cell Biol* 22:680-691.**

172. **Downward, J. 1999.** How BAD phosphorylation is good for survival. ***Nat Cell Biol* 1:E33-35.**

173. **Datta, S.R., Ranger, A.M., Lin, M.Z., Sturgill, J.F., Ma, Y.C., Cowan, C.W., Dikkes, P., Korsmeyer, S.J., and Greenberg, M.E. 2002.** Survival factor-mediated BAD phosphorylation raises the mitochondrial threshold for apoptosis. ***Dev Cell* 3:631-643.**

174. **Sabbatini, P., and McCormick, F. 1999.** Phosphoinositide 3-OH kinase (PI3K) and PKB/Akt delay the onset of p53-mediated, transcriptionally dependent apoptosis. ***J Biol Chem* 274:24263-24269.**

175. **Ogawara, Y., Kishishita, S., Obata, T., Isazawa, Y., Suzuki, T., Tanaka, K., Masuyama, N., and Gotoh, Y. 2002.** Akt enhances Mdm2-mediated ubiquitination and degradation of p53. ***J Biol Chem*** **277:21843-21850.**

176. **Rodriguez-Viciana, P., Marte, B.M., Warne, P.H., and Downward, J. 1996.** Phosphatidylinositol 3' kinase: one of the effectors of Ras. ***Philos Trans R Soc Lond B Biol Sci*** **351:225-231; discussion 231-222.**

177. **Gille, H., and Downward, J. 1999.** Multiple ras effector pathways contribute to G(1) cell cycle progression. ***J Biol Chem*** **274:22033-22040.**

178. **Li, D.W., Liu, J.P., Mao, Y.W., Xiang, H., Wang, J., Ma, W.Y., Dong, Z., Pike, H.M., Brown, R.E., and Reed, J.C. 2005.** Calcium-activated RAF/MEK/ERK signaling pathway mediates p53-dependent apoptosis and is abrogated by alpha B-crystallin through inhibition of RAS activation. ***Mol Biol Cell*** **16:4437-4453.**

179. **Hribal, M.L., Oriente, F., and Accili, D. 2002.** Mouse models of insulin resistance. ***Am J Physiol Endocrinol Metab*** **282:E977-981.**

180. **Nandi, A., Kitamura, Y., Kahn, C.R., and Accili, D. 2004.** Mouse models of insulin resistance. ***Physiol Rev*** **84:623-647.**

181. **Sauer, B. 2002.** Cre/lox: one more step in the taming of the genome. ***Endocrine*** **19:221-228.**

182. **Accili, D., Drago, J., Lee, E.J., Johnson, M.D., Cool, M.H., Salvatore, P., Asico, L.D., Jose, P.A., Taylor, S.I., and Westphal, H. 1996.** Early neonatal death in mice homozygous for a null allele of the insulin receptor gene. ***Nat Genet*** **12:106-109.**

183. **Joshi, R.L., Lamothe, B., Cordonnier, N., Mesbah, K., Monthioux, E., Jami, J., and Bucchini, D. 1996.** Targeted disruption of the insulin receptor gene in the mouse results in neonatal lethality. ***Embo J*** **15:1542-1547.**

184. **Longo, N., Wang, Y., Smith, S.A., Langley, S.D., DiMeglio, L.A., and Giannella-Neto, D. 2002.** Genotype-phenotype correlation in inherited severe insulin resistance. ***Hum Mol Genet*** **11:1465-1475.**

185. **Okamoto, H., Nakae, J., Kitamura, T., Park, B.C., Dragatsis, I., and Accili, D. 2004.** Transgenic rescue of insulin receptor-deficient mice. ***J Clin Invest*** **114:214-223.**

186. **Michael, M.D., Kulkarni, R.N., Postic, C., Previs, S.F., Shulman, G.I., Magnuson, M.A., and Kahn, C.R. 2000.** Loss of insulin signaling in hepatocytes leads to severe insulin resistance and progressive hepatic dysfunction. ***Mol Cell*** **6:87-97.**

187. **Rohilla, A.M., Anderson, C., Wood, W.M., and Berhanu, P. 1991.** Insulin downregulates the steady-state level of its receptor's messenger ribonucleic acid. ***Biochem Biophys Res Commun*** **175:520-526.**

188. **Fisher, S.J., and Kahn, C.R. 2003.** Insulin signaling is required for insulin's direct and indirect action on hepatic glucose production. ***J Clin Invest*** **111:463-468.**

189. **Bruning, J.C., Michael, M.D., Winnay, J.N., Hayashi, T., Horsch, D., Accili, D., Goodyear, L.J., and Kahn, C.R. 1998.** A muscle-specific insulin receptor knockout exhibits features of the metabolic syndrome of NIDDM without altering glucose tolerance. ***Mol Cell*** **2:559-569.**

190. **Kim, J.K., Michael, M.D., Previs, S.F., Peroni, O.D., Mauvais-Jarvis, F., Neschen, S., Kahn, B.B., Kahn, C.R., and Shulman, G.I. 2000.** Redistribution of substrates to adipose tissue promotes obesity in mice with selective insulin resistance in muscle. ***J Clin Invest*** **105:1791-1797.**

191. **Bluher, M., Michael, M.D., Peroni, O.D., Ueki, K., Carter, N., Kahn, B.B., and Kahn, C.R. 2002.** Adipose tissue selective insulin receptor knockout protects against obesity and obesity-related glucose intolerance. ***Dev Cell*** **3:25-38.**

192. **Bluher, M., Kahn, B.B., and Kahn, C.R. 2003.** Extended longevity in mice lacking the insulin receptor in adipose tissue. ***Science*** **299:572-574.**

193. **Bruning, J.C., Gautam, D., Burks, D.J., Gillette, J., Schubert, M., Orban, P.C., Klein, R., Krone, W., Muller-Wieland, D., and Kahn, C.R. 2000.** Role of brain insulin receptor in control of body weight and reproduction. ***Science*** **289:2122-2125.**

194. **Schubert, M., Gautam, D., Surjo, D., Ueki, K., Baudler, S., Schubert, D., Kondo, T., Alber, J., Galldiks, N., Kustermann, E., et al. 2004.** Role for neuronal insulin resistance in neurodegenerative diseases. ***Proc Natl Acad Sci U S A*** **101:3100-3105.**

195. **Lauro, D., Kido, Y., Castle, A.L., Zarnowski, M.J., Hayashi, H., Ebina, Y., and Accili, D. 1998.** Impaired glucose tolerance in mice with a targeted impairment of insulin action in muscle and adipose tissue. ***Nat Genet*** **20:294-298.**

196. **Tamemoto, H., Kadowaki, T., Tobe, K., Yagi, T., Sakura, H., Hayakawa, T., Terauchi, Y., Ueki, K., Kaburagi, Y., Satoh, S., et al. 1994.** Insulin resistance and growth retardation in mice lacking insulin receptor substrate-1. ***Nature*** **372:182-186.**

197. **Araki, E., Lipes, M.A., Patti, M.E., Bruning, J.C., Haag, B., 3rd, Johnson, R.S., and Kahn, C.R. 1994.** Alternative pathway of insulin signalling in mice with targeted disruption of the IRS-1 gene. ***Nature*** **372:186-190.**

198. **Ueki, K., Yamauchi, T., Tamemoto, H., Tobe, K., Yamamoto-Honda, R., Kaburagi, Y., Akanuma, Y., Yazaki, Y., Aizawa, S., Nagai, R., et al. 2000.** Restored insulin-sensitivity in IRS-1-deficient mice treated by adenovirus-mediated gene therapy. ***J Clin Invest*** **105:1437-1445.**

199. **Bruning, J.C., Winnay, J., Cheatham, B., and Kahn, C.R. 1997.** Differential signaling by insulin receptor substrate 1 (IRS-1) and IRS-2 in IRS-1-deficient cells. ***Mol Cell Biol*** **17:1513-1521.**

200. **Withers, D.J., Gutierrez, J.S., Towery, H., Burks, D.J., Ren, J.M., Previs, S., Zhang, Y., Bernal, D., Pons, S., Shulman, G.I., et al. 1998.** Disruption of IRS-2 causes type 2 diabetes in mice. ***Nature* 391:900-904.**

201. **Withers, D.J., Burks, D.J., Towery, H.H., Altamuro, S.L., Flint, C.L., and White, M.F. 1999.** Irs-2 coordinates Igf-1 receptor-mediated beta-cell development and peripheral insulin signalling. ***Nat Genet* 23:32-40.**

202. **Burks, D.J., Font de Mora, J., Schubert, M., Withers, D.J., Myers, M.G., Towery, H.H., Altamuro, S.L., Flint, C.L., and White, M.F. 2000.** IRS-2 pathways integrate female reproduction and energy homeostasis. ***Nature* 407:377-382.**

203. **Hennige, A.M., Burks, D.J., Ozcan, U., Kulkarni, R.N., Ye, J., Park, S., Schubert, M., Fisher, T.L., Dow, M.A., Leshan, R., et al. 2003.** Upregulation of insulin receptor substrate-2 in pancreatic beta cells prevents diabetes. ***J Clin Invest* 112:1521-1532.**

204. **Shimomura, I., Matsuda, M., Hammer, R.E., Bashmakov, Y., Brown, M.S., and Goldstein, J.L. 2000.** Decreased IRS-2 and increased SREBP-1c lead to mixed insulin resistance and sensitivity in livers of lipodystrophic and ob/ob mice. ***Mol Cell* 6:77-86.**

205. **Zhang, J., Ou, J., Bashmakov, Y., Horton, J.D., Brown, M.S., and Goldstein, J.L. 2001.** Insulin inhibits transcription of IRS-2 gene in rat liver through an insulin response element (IRE) that resembles IREs of other insulin-repressed genes. ***Proc Natl Acad Sci U S A* 98:3756-3761.**

206. **Suzuki, R., Tobe, K., Aoyama, M., Inoue, A., Sakamoto, K., Yamauchi, T., Kamon, J., Kubota, N., Terauchi, Y., Yoshimatsu, H., et al. 2004.** Both insulin signaling defects in the liver and obesity contribute to insulin resistance and cause diabetes in Irs2(-/-) mice. ***J Biol Chem* 279:25039-25049.**

207. **Bruning, J.C., Winnay, J., Bonner-Weir, S., Taylor, S.I., Accili, D., and Kahn, C.R. 1997.** Development of a novel polygenic model of NIDDM in mice heterozygous for IR and IRS-1 null alleles. ***Cell* 88:561-572.**

208. **Kido, Y., Burks, D.J., Withers, D., Bruning, J.C., Kahn, C.R., White, M.F., and Accili, D. 2000.** Tissue-specific insulin resistance in mice with mutations in the insulin receptor, IRS-1, and IRS-2. ***J Clin Invest*** **105:199-205.**

209. **Valverde, A.M., Burks, D.J., Fabregat, I., Fisher, T.L., Carretero, J., White, M.F., and Benito, M. 2003.** Molecular mechanisms of insulin resistance in IRS-2-deficient hepatocytes. ***Diabetes*** **52:2239-2248.**

210. **Buettner, C., Patel, R., Muse, E.D., Bhanot, S., Monia, B.P., McKay, R., Obici, S., and Rossetti, L. 2005.** Severe impairment in liver insulin signaling fails to alter hepatic insulin action in conscious mice. ***J Clin Invest*** **115:1306-1313.**

211. **Taniguchi, C.M., Ueki, K., and Kahn, R. 2005.** Complementary roles of IRS-1 and IRS-2 in the hepatic regulation of metabolism. ***J Clin Invest*** **115:718-727.**

212. **Choudhury, A.I., Heffron, H., Smith, M.A., Al-Qassab, H., Xu, A.W., Selman, C., Simmgen, M., Clements, M., Claret, M., Maccoll, G., et al. 2005.** The role of insulin receptor substrate 2 in hypothalamic and beta cell function. ***J Clin Invest*** **115:940-950.**

213. **Postic, C., Shiota, M., Niswender, K.D., Jetton, T.L., Chen, Y., Moates, J.M., Shelton, K.D., Lindner, J., Cherrington, A.D., and Magnuson, M.A. 1999.** Dual roles for glucokinase in glucose homeostasis as determined by liver and pancreatic beta cell-specific gene knock-outs using Cre recombinase. ***J Biol Chem*** **274:305-315.**

214. **Postic, C., and Magnuson, M.A. 2000.** DNA excision in liver by an albumin-Cre transgene occurs progressively with age. ***Genesis*** **26:149-150.**

215. **Schorle, H., Holtschke, T., Hunig, T., Schimpl, A., and Horak, I. 1991.** Development and function of T cells in mice rendered interleukin-2 deficient by gene targeting. ***Nature*** **352:621-624.**

216. **Perrin, C., Knauf, C., and Burcelin, R. 2004.** Intracerebroventricular infusion of glucose, insulin, and the adenosine monophosphate-activated kinase activator, 5-aminoimidazole-4-carboxamide-1-beta-D-ribofuranoside, controls muscle glycogen synthesis. ***Endocrinology*** **145:4025-4033.**

217. **Viollet, B., Andreelli, F., Jorgensen, S.B., Perrin, C., Geloen, A., Flamez, D., Mu, J., Lenzner, C., Baud, O., Bennoun, M., et al. 2003.** The AMP-activated protein kinase alpha2 catalytic subunit controls whole-body insulin sensitivity. ***J Clin Invest*** **111:91-98.**

218. **Louderback, A., Mealey, E.H., and Taylor, T.A. 1968.** A new dye-binding technique using bromocresol purple for the determination of albumin in serum. ***Clin Chem*** **14:793-794.**

219. **Bergmeyer, H.U., Scheibe, P., and Wahlefeld, A.W. 1978.** Optimization of methods for aspartate aminotransferase and alanine aminotransferase. ***Clin Chem*** **24:58-73.**

220. **Saris, N.E. 1978.** Revised IFCC method for aspartate aminotransferase. ***Clin Chem*** **24:720-721.**

221. **Bowers, G.N., Jr., and McComb, R.B. 1966.** A continuous spectrophotometric method for measuring the activity of serum alkaline phosphatase. ***Clin Chem*** **12:70-89.**

222. **Doumas, B.T., Kwok-Cheung, P.P., Perry, B.W., Jendrzejczak, B., McComb, R.B., Schaffer, R., and Hause, L.L. 1985.** Candidate reference method for determination of total bilirubin in serum: development and validation. ***Clin Chem*** **31:1779-1789.**

223. **Shimizu, S., Tani, Y., Yamada, H., Tabata, M., and Murachi, T. 1980.** Enzymatic determination of serum-free fatty acids: a colorimetric method. ***Anal Biochem*** **107:193-198.**

224. **2001.** SDS-PAGE of proteins. **In *Molecular Cloning*. J. Sambrook, and D.W. Russell, editors. New York: Cold Spring Harbor Laboratory Press. A8.40.**

225. **Kubota, N., Tobe, K., Terauchi, Y., Eto, K., Yamauchi, T., Suzuki, R., Tsubamoto, Y., Komeda, K., Nakano, R., Miki, H., et al. 2000.** Disruption of insulin receptor substrate 2 causes type 2 diabetes because of liver insulin resistance and lack of compensatory beta-cell hyperplasia. ***Diabetes* 49:1880-1889.**

226. **Grunberger, G., Taylor, S.I., Dons, R.F., and Gorden, P. 1983.** Insulin receptors in normal and disease states. ***Clin Endocrinol Metab* 12:191-219.**

227. **Yamauchi, T., Tobe, K., Tamemoto, H., Ueki, K., Kaburagi, Y., Yamamoto-Honda, R., Takahashi, Y., Yoshizawa, F., Aizawa, S., Akanuma, Y., et al. 1996.** Insulin signalling and insulin actions in the muscles and livers of insulin-resistant, insulin receptor substrate 1-deficient mice. ***Mol Cell Biol* 16:3074-3084.**

228. **Scheid, M.P., Marignani, P.A., and Woodgett, J.R. 2002.** Multiple phosphoinositide 3-kinase-dependent steps in activation of protein kinase B. ***Mol Cell Biol* 22:6247-6260.**

229. **Jonassen, A.K., Mjos, O.D., and Sack, M.N. 2004.** p70s6 kinase is a functional target of insulin activated Akt cell-survival signaling. ***Biochem Biophys Res Commun* 315:160-165.**

230. **Pullen, N., Dennis, P.B., Andjelkovic, M., Dufner, A., Kozma, S.C., Hemmings, B.A., and Thomas, G. 1998.** Phosphorylation and activation of p70s6k by PDK1. ***Science* 279:707-710.**

231. **Huang, C., Thirone, A.C., Huang, X., and Klip, A. 2005.** Differential contribution of insulin receptor substrates 1 versus 2 to insulin signaling and glucose uptake in l6 myotubes. ***J Biol Chem* 280:19426-19435.**

232. **Riccardi, G., Giacco, R., and Rivellese, A.A. 2004.** Dietary fat, insulin sensitivity and the metabolic syndrome. ***Clin Nutr* 23:447-456.**

233. **Song, S., Andrikopoulos, S., Filippis, C., Thorburn, A.W., Khan, D., and Proietto, J. 2001.** Mechanism of fat-induced hepatic gluconeogenesis: effect of metformin. ***Am J Physiol Endocrinol Metab* 281:E275-282.**

234. **Boden, G., She, P., Mozzoli, M., Cheung, P., Gumireddy, K., Reddy, P., Xiang, X., Luo, Z., and Ruderman, N. 2005.** Free Fatty Acids Produce Insulin Resistance and Activate the Proinflammatory Nuclear Factor-κ-B Pathway in Rat Liver. ***Diabetes* 54:3458-3465.**

235. **Ginsberg, H.N., Zhang, Y.L., and Hernandez-Ono, A. 2005.** Regulation of plasma triglycerides in insulin resistance and diabetes. ***Arch Med Res* 36:232-240.**

236. **Ruotolo, G., and Howard, B.V. 2002.** Dyslipidemia of the metabolic syndrome. ***Curr Cardiol Rep* 4:494-500.**

237. **Adams, L.A., Angulo, P., and Lindor, K.D. 2005.** Nonalcoholic fatty liver disease. ***Cmaj* 172:899-905.**

238. **Rossetti, L., Massillon, D., Barzilai, N., Vuguin, P., Chen, W., Hawkins, M., Wu, J., and Wang, J. 1997.** Short term effects of leptin on hepatic gluconeogenesis and in vivo insulin action. ***J Biol Chem* 272:27758-27763.**

239. **Anderwald, C., Muller, G., Koca, G., Furnsinn, C., Waldhausl, W., and Roden, M. 2002.** Short-term leptin-dependent inhibition of hepatic gluconeogenesis is mediated by insulin receptor substrate-2. ***Mol Endocrinol* 16:1612-1628.**

240. **DeFronzo, R.A., Tobin, J.D., and Andres, R. 1979.** Glucose clamp technique: a method for quantifying insulin secretion and resistance. ***Am J Physiol* 237:E214-223.**

241. **Bouche, C., Serdy, S., Kahn, C.R., and Goldfine, A.B. 2004.** The cellular fate of glucose and its relevance in type 2 diabetes. ***Endocr Rev* 25:807-830.**

242. **Hall, R.K., Yamasaki, T., Kucera, T., Waltner-Law, M., O'Brien, R., and Granner, D.K. 2000.** Regulation of phosphoenolpyruvate carboxykinase and insulin-like growth factor-binding protein-1 gene expression by insulin. The role of winged helix/forkhead proteins. ***J Biol Chem* 275:30169-30175.**

243. **O'Brien, R.M., Streeper, R.S., Ayala, J.E., Stadelmaier, B.T., and Hornbuckle, L.A. 2001.** Insulin-regulated gene expression. ***Biochem Soc Trans* 29:552-558.**

244. **Nakae, J., Biggs, W.H., 3rd, Kitamura, T., Cavenee, W.K., Wright, C.V., Arden, K.C., and Accili, D. 2002.** Regulation of insulin action and pancreatic beta-cell function by mutated alleles of the gene encoding forkhead transcription factor Foxo1. ***Nat Genet* 32:245-253.**

245. **Tontonoz, P., Kim, J.B., Graves, R.A., and Spiegelman, B.M. 1993.** ADD1: a novel helix-loop-helix transcription factor associated with adipocyte determination and differentiation. ***Mol Cell Biol* 13:4753-4759.**

246. **Varanasi, U., Chu, R., Huang, Q., Castellon, R., Yeldandi, A.V., and Reddy, J.K. 1996.** Identification of a peroxisome proliferator-responsive element upstream of the human peroxisomal fatty acyl coenzyme A oxidase gene. ***J Biol Chem* 271:2147-2155.**

247. **Tugwood, J.D., Issemann, I., Anderson, R.G., Bundell, K.R., McPheat, W.L., and Green, S. 1992.** The mouse peroxisome proliferator activated receptor recognizes a response element in the 5' flanking sequence of the rat acyl CoA oxidase gene. ***Embo J* 11:433-439.**

248. **Memon, R.A., Tecott, L.H., Nonogaki, K., Beigneux, A., Moser, A.H., Grunfeld, C., and Feingold, K.R. 2000.** Up-regulation of peroxisome proliferator-activated receptors (PPAR-alpha) and PPAR-gamma messenger ribonucleic acid expression in the liver in murine obesity: troglitazone induces expression of PPAR-gamma-responsive adipose tissue-specific genes in the liver of obese diabetic mice. ***Endocrinology* 141:4021-4031.**

249. **Lin, J., Puigserver, P., Donovan, J., Tarr, P., and Spiegelman, B.M. 2002.** Peroxisome proliferator-activated receptor gamma coactivator 1beta (PGC-1beta), a novel PGC-1-related transcription coactivator associated with host cell factor. ***J Biol Chem* 277:1645-1648.**

250. **Lin, J., Tarr, P.T., Yang, R., Rhee, J., Puigserver, P., Newgard, C.B., and Spiegelman, B.M. 2003.** PGC-1beta in the regulation of hepatic glucose and energy metabolism. ***J Biol Chem* 278:30843-30848.**

251. **Powell, D.R., Suwanichkul, A., Cubbage, M.L., DePaolis, L.A., Snuggs, M.B., and Lee, P.D. 1991.** Insulin inhibits transcription of the human gene for insulin-like growth factor-binding protein-1. ***J Biol Chem* 266:18868-18876.**

252. **Gannon, M.C., and Nuttall, F.Q. 1997.** Effect of feeding, fasting, and diabetes on liver glycogen synthase activity, protein, and mRNA in rats. ***Diabetologia* 40:758-763.**

253. **Iozzo, P., Pratipanawatr, T., Pijl, H., Vogt, C., Kumar, V., Pipek, R., Matsuda, M., Mandarino, L.J., Cusi, K.J., and DeFronzo, R.A. 2001.** Physiological hyperinsulinemia impairs insulin-stimulated glycogen synthase activity and glycogen synthesis. ***Am J Physiol Endocrinol Metab* 280:E712-719.**

254. **Pederson, B.A., Schroeder, J.M., Parker, G.E., Smith, M.W., Depaoli-Roach, A.A., and Roach, P.J. 2005.** Glucose metabolism in mice lacking muscle glycogen synthase. ***Diabetes* 54:3466-3473.**

255. **Bonnefont, J.P., Djouadi, F., Prip-Buus, C., Gobin, S., Munnich, A., and Bastin, J. 2004.** Carnitine palmitoyltransferases 1 and 2: biochemical, molecular and medical aspects. ***Mol Aspects Med* 25:495-520.**

256. **Goessling, W., and Friedman, L.S. 2005.** Increased liver chemistry in an asymptomatic patient. ***Clin Gastroenterol Hepatol* 3:852-858.**

257. **Kim, S.P., Ellmerer, M., Van Citters, G.W., and Bergman, R.N. 2003.** Primacy of hepatic insulin resistance in the development of the metabolic syndrome induced by an isocaloric moderate-fat diet in the dog. ***Diabetes* 52:2453-2460.**

258. **Schubert, M., Brazil, D.P., Burks, D.J., Kushner, J.A., Ye, J., Flint, C.L., Farhang-Fallah, J., Dikkes, P., Warot, X.M., Rio, C., et al. 2003.** Insulin receptor substrate-2 deficiency impairs brain growth and promotes tau phosphorylation. ***J Neurosci* 23:7084-7092.**

259. **Soll, A.H., Kahn, C.R., and Neville, D.M., Jr. 1975.** Insulin binding to liver plasm membranes in the obese hyperglycemic (ob/ob) mouse. Demonstration of a decreased number of functionally normal receptors. ***J Biol Chem* 250:4702-4707.**

260. **Dominici, F.P., Hauck, S., Argentino, D.P., Bartke, A., and Turyn, D. 2002.** Increased insulin sensitivity and upregulation of insulin receptor, insulin receptor substrate (IRS)-1 and IRS-2 in liver of Ames dwarf mice. ***J Endocrinol* 173:81-94.**

261. **Lin, X., Taguchi, A., Park, S., Kushner, J.A., Li, F., Li, Y., and White, M.F. 2004.** Dysregulation of insulin receptor substrate 2 in beta cells and brain causes obesity and diabetes. ***J Clin Invest* 114:908-916.**

262. **Kubota, N., Terauchi, Y., Tobe, K., Yano, W., Suzuki, R., Ueki, K., Takamoto, I., Satoh, H., Maki, T., Kubota, T., et al. 2004.** Insulin receptor substrate 2 plays a crucial role in beta cells and the hypothalamus. ***J Clin Invest* 114:917-927.**

263. **Ide, T., Shimano, H., Yahagi, N., Matsuzaka, T., Nakakuki, M., Yamamoto, T., Nakagawa, Y., Takahashi, A., Suzuki, H., Sone, H., et al. 2004.** SREBPs suppress IRS-2-mediated insulin signalling in the liver. ***Nat Cell Biol* 6:351-357.**

264. **Tobe, K., Suzuki, R., Aoyama, M., Yamauchi, T., Kamon, J., Kubota, N., Terauchi, Y., Matsui, J., Akanuma, Y., Kimura, S., et al. 2001.** Increased expression of the sterol regulatory element-binding protein-1 gene in insulin receptor substrate-2(-/-) mouse liver. ***J Biol Chem* 276:38337-38340.**

265. **Pugazhenthi, S., and Khandelwal, R.L. 1995.** Regulation of glycogen synthase activation in isolated hepatocytes. ***Mol Cell Biochem* 149-150:95-101.**

266. **Liu, J.P., Baker, J., Perkins, A.S., Robertson, E.J., and Efstratiadis, A. 1993.** Mice carrying null mutations of the genes encoding insulin-like growth factor I (Igf-1) and type 1 IGF receptor (Igf1r). ***Cell* 75:59-72.**

267. **Okamoto, H., Obici, S., Accili, D., and Rossetti, L. 2005.** Restoration of liver insulin signaling in Insr knockout mice fails to normalize hepatic insulin action. ***J Clin Invest* 115:1314-1322.**

268. **DeAngelis, T., Chen, J., Wu, A., Prisco, M., and Baserga, R. 2006.** Transformation by the simian virus 40 T antigen is regulated by IGF-I receptor and IRS-1 signaling. ***Oncogene* 25:32-42.**

269. **Sell, C., Rubini, M., Rubin, R., Liu, J.P., Efstratiadis, A., and Baserga, R. 1993.** Simian virus 40 large tumor antigen is unable to transform mouse embryonic fibroblasts lacking type 1 insulin-like growth factor receptor. ***Proc Natl Acad Sci U S A* 90:11217-11221.**

270. **Boissan, M., Beurel, E., Wendum, D., Rey, C., Lecluse, Y., Housset, C., Lacombe, M.L., and Desbois-Mouthon, C. 2005.** Overexpression of insulin receptor substrate-2 in human and murine hepatocellular carcinoma. ***Am J Pathol* 167:869-877.**

271. **Woodworth, C.D., Kreider, J.W., Mengel, L., Miller, T., Meng, Y.L., and Isom, H.C. 1988.** Tumorigenicity of simian virus 40-hepatocyte cell lines: effect of in vitro and in vivo passage on expression of liver-specific genes and oncogenes. ***Mol Cell Biol* 8:4492-4501.**

272. **Bilanges, B., and Stokoe, D. 2005.** Direct comparison of the specificity of gene silencing using antisense oligonucleotides and RNAi. ***Biochem J* 388:573-583.**

273. **Burgess, S.C., Jeffrey, F.M., Storey, C., Milde, A., Hausler, N., Merritt, M.E., Mulder, H., Holm, C., Sherry, A.D., and Malloy, C.R. 2005.** Effect of murine strain on metabolic pathways of glucose production after brief or prolonged fasting. ***Am J Physiol Endocrinol Metab* 289:E53-61.**

274. **Dong, X., Park, S., Lin, X., Copps, K., Yi, X., and White, M.F. 2006.** Irs1 and Irs2 signaling is essential for hepatic glucose homeostasis and systemic growth. ***J Clin Invest*** **116:101-114.**

275. **Kulkarni, R.N., Bruning, J.C., Winnay, J.N., Postic, C., Magnuson, M.A., and Kahn, C.R. 1999.** Tissue-specific knockout of the insulin receptor in pancreatic beta cells creates an insulin secretory defect similar to that in type 2 diabetes. ***Cell*** **96:329-339.**

276. **Okamoto, H., Hribal, M.L., Lin, H.V., Bennett, W.R., Ward, A., and Accili, D. 2006.** Role of the forkhead protein FoxO1 in beta cell compensation to insulin resistance. ***J Clin Invest*** **116:775-782.**

PUBLICATIONS

Arisen from this thesis

Simmgen M, Knauf C, Lopez M, Choudhury AI, Charalambous M, Cantley J, Bedford DC, Claret M, Iglesias MA, Heffron H, Cani PD, Vidal-Puig A, Burcelin R, Withers DJ 2006. Liver-specific deletion of insulin receptor substrate 2 does not impair hepatic glucose and lipid metabolism in mice. ***Diabetologia* 49:552-61.**

Arisen during this fellowship

Choudhury A, Heffron H, Smith MA, Al-Qassab H, Xu AW, Selman C, Simmgen M, Clements M, Claret M, MacColl G, Bedford DC, Hisadome K, Diakonov I, Moosajee V, Bell JD, Speakman JR, Batterham RL, Barsh GS, Ashford ML, Withers DJ 2005. The role of insulin receptor substrate 2 in hypothalamic and beta cell function. ***J Clin Invest* 115:940-50.**

Diabetologia
DOI 10.1007/s00125-005-0084-4

ARTICLE

M. Simmgen · C. Knauf · M. Lopez · A. I. Choudhury · M. Charalambous · J. Cantley · D. C. Bedford · M. Claret · M. A. Iglesias · H. Heffron · P. D. Cani · A. Vidal-Puig · R. Burcelin · D. J. Withers

Liver-specific deletion of insulin receptor substrate 2 does not impair hepatic glucose and lipid metabolism in mice

Received: 7 July 2005 / Accepted: 25 September 2005

Abstract *Aims/hypothesis:* Hepatic insulin resistance is thought to be a critical component in the pathogenesis of type 2 diabetes but the role of intrinsic insulin signalling pathways in the regulation of hepatic metabolism remains controversial. Global gene targeting in mice and in vitro studies have suggested that IRS2 mediates the physiological effects of insulin in the liver. Reduced hepatic production of IRS2 is found in many cases of insulin resistance. To investigate the role of IRS2 in regulating liver function in vivo, we generated mice that specifically lack *Irs2* in the liver (*LivIrs2KO*). *Materials and methods:* Hepatic insulin signalling events were examined in *LivIrs2KO* mice by western blotting. Glucose homeostasis and insulin sensitivity were assessed by glucose tolerance tests and hyperinsulinaemic–euglycaemic clamp studies. The effects of high-fat feeding upon glucose homeostasis were also determined. Liver function tests were performed and expression of key metabolic genes in the liver was determined by RT-PCR. *Results:* Proximal insulin signalling events and forkhead box O1 and A2 function were normal in the liver of *LivIrs2KO* mice, which displayed minimal abnormalities in glucose and lipid homeostasis, hepatic gene expression and liver function. In addition, hepatic lipid homeostasis and the metabolic response to a high-fat diet did not differ between *LivIrs2KO* and control mice. *Conclusions/interpretation:* Our findings suggest that liver IRS2 signalling, surprisingly, is not required for the long-term maintenance of glucose and lipid homeostasis, and that extra-hepatic IRS2-dependent mechanisms are involved in the regulation of these processes.

Keywords Insulin receptor substrate protein · Insulin resistance · Insulin signalling · Liver

Abbreviations *AlbCre* mice: albumin Cre recombinase transgenic mice · *Fasn*: fatty acid synthase · FOXA2: forkhead box A2 · FOXO1: forkhead box O1 · *G6pc*: glucose-6-phosphatase · *Gck*: glucokinase · GSK: glycogen synthase kinase · HGP: hepatic glucose production · *Insr*: insulin receptor · *Irs2lox* mice: mice with a floxed allele of *Irs2* · *LIRKO* mice: mice lacking *Insr* in the liver · *LivIrs2KO* mice: mice lacking *Irs2* in liver · MAPK: mitogen-activated protein kinase · PI3K: phosphatidylinositol 3-kinase · RNAi: RNA interference · ZBTB16: zinc finger and BTB domain containing protein 16

Introduction

Type 2 diabetes is a complex metabolic disorder characterised by skeletal muscle and adipose tissue insulin resistance coupled with pancreatic beta cell dysfunction [1, 2]. A failure to appropriately regulate hepatic glucose and lipid metabolism are also key components, but the mechanisms underlying these abnormalities are incompletely understood [2]. The liver plays a critical role in fuel homeostasis, integrating the actions of anabolic and catabolic hormones with nutrient availability and requirements. Insulin may alter hepatic glucose production (HGP) and other aspects of metabolism through direct effects upon liver enzyme activity and gene expression, and through diverse indirect effects such as the regulation of glucagon production, suppression of gluconeogenic precursor production and via the central nervous system [3]. However,

M. Simmgen and C. Knauf contributed equally to this work.

M. Simmgen · A. I. Choudhury · M. Charalambous · J. Cantley · D. C. Bedford · M. Claret · H. Heffron · D. J. Withers (✉)
Centre for Diabetes and Endocrinology, Rayne Institute,
University College London,
University Street,
London, UK
e-mail: d.withers@ucl.ac.uk
Tel.: +44-2076796586

C. Knauf · M. A. Iglesias · P. D. Cani · R. Burcelin (✉)
Centre National de la Recherche Scientifique-UMR 5018,
Paul Sabatier University,
Toulouse, France
e-mail: remy.burcelin@toulouse.inserm.fr

M. Lopez · A. Vidal-Puig
Department of Clinical Biochemistry,
University of Cambridge/Addenbrooke's Hospital,
Cambridge, UK

the contribution of intrinsic hepatic insulin receptor (INSR) signalling to normal physiology and the pathogenesis of type 2 diabetes is an area of ongoing controversy [3], fuelled in part by observations using mouse models with different manipulations of the insulin signalling pathway [4–7].

Mice lacking *Insr* only in the liver (*LIRKO* mice) have marked insulin resistance and defects in hepatic glucose metabolism and gene expression, suggesting that direct hepatic INSR signalling is required for whole-body glucose homeostasis [7]. Hyperinsulinaemic clamp studies in these mice suggest that hepatic *Insr* is required for both direct and indirect effects of insulin upon HGP [8]. However, *LIRKO* mice developed significant liver disease and have abnormal insulin clearance, which may complicate this interpretation [7]. In contrast, acute anti-sense oligonucleotide-mediated knockdown of liver *Insr* expression did not impair insulin action upon HGP [5]. Similarly, transgenic rescue of *Insr* expression in the liver but not other tissues of *Insr* global null mice, suggested that indirect effects of insulin signalling predominate in the regulation of hepatic glucose metabolism [4]. However, methodological and physiological questions have been raised about these studies [3].

Insulin receptor substrate proteins mediate the effects of the insulin receptor upon cellular and whole-body physiology [9], and therefore hepatic insulin resistance may result from defects in their function [10, 11]. Mice lacking *Irs1* display profound growth retardation and insulin resistance, but do not develop diabetes due to beta cell compensation [12]. In contrast, mice lacking *Irs2* develop diabetes due to a combination of insulin resistance and pancreatic beta cell dysfunction [12, 13]. Hyperinsulinaemic–euglycaemic clamp analysis of *Irs1* and *Irs2*-null mice demonstrated that *Irs2*-null mice have markedly impaired suppression of HGP and reduced stimulation of liver glycogen synthesis, while *Irs1*-null mice have insulin resistance predominantly in skeletal muscle and adipose tissue [14]. Reduced hepatic IRS2 production has also been observed in a number of in vivo models of insulin resistance, suggesting a role in this condition [10, 15]. Studies on transformed hepatic cell lines derived from *Irs2*- or *Insr*-null mice have also demonstrated that IRS2 is the predominant IRS protein through which insulin acts [16, 17]. Short-term adenoviral RNA interference (RNAi) strategies to cause acute knockdown of hepatic *Irs* expression have suggested that IRS2 also mediates the effects of insulin upon hepatic lipid metabolism [6]. Therefore to further understand the complex roles of IRS2 in liver metabolism, we generated a novel mouse line lacking *Irs2* specifically in hepatocytes (*LivIrs2KO* mice) and performed detailed analysis of glucose homeostasis and liver function in these mice.

Materials and methods

Mouse breeding and genotyping strategies for mice with a floxed allele of *Irs2* and for albumin Cre recombinase transgenic mice

Mice with a floxed allele of *Irs2* (*Irs2lox* mice) [18] were intercrossed with albumin Cre recombinase transgenic mice (*AlbCre* mice) obtained from The Jackson Laboratory (Bar Harbor, ME, USA) [19] to generate compound heterozygote mice. Double heterozygote mice were crossed with $Irs2lox^{+/-}$ mice to obtain wild-type, $Irs2lox^{+/+}$, *AlbCre* and $AlbCreIrs2lox^{+/+}$ mice. Mice lacking *Irs2* in *AlbCre*-expressing cells were designated *LivIrs2KO* mice. Mice were maintained on a 12-h light/dark cycle with free access to water and standard mouse chow (4% fat, RM1; Special Diet Services, Witham, Essex, UK) and housed in specific-pathogen-free barrier facilities. For high-fat diet studies, mice were fed with a diet containing 45% fat, 20% protein and 35% carbohydrate (Special Diet Services) for 3 months. Mice were handled and all in vivo studies performed in accordance with the 1986 Home Office Animal Procedures Act (Home Office, London, UK). *LivIrs2KO* mice were studied on a mixed *129Sv/C57Bl/6* background with appropriate litter-mate controls. Wild-type, *Cre* transgenic and $Irs2lox^{+/+}$ mice were phenotypically indistinguishable and balanced numbers of mice of these genotypes were used as controls. Genotyping of the mice was performed by PCR amplification of tail DNA as described previously [18].

Metabolic studies

Blood samples were collected from mice via tail vein bleeds or from cardiac puncture on terminally anaesthetised mice. Blood glucose, plasma insulin levels and leptin levels were determined as previously described [18]. Adiponectin was measured using a mouse adiponectin ELISA (R & D Systems, Minneapolis, MN, USA). NEFAs were measured using a NEFA kit (Roche Diagnostics, Lewes, UK). Serum and tissue triglyceride levels from fasted and fed animals were assayed using the GPO Trinder kit (Sigma-Aldrich, Dorset, UK). Albumin and liver function tests were measured using a Dimension RXL multi-channel analyzer (Dade-Behring, Milton Keynes, UK). Glucose and insulin tolerance tests were performed as previously described [18]. Body fat mass was determined by dual emission X-ray absorptiometry using a PIXImus densitometer (GE Healthcare, Chalfont St Giles, UK).

RNA isolation and real-time quantitative RT-PCR

RT-PCR was performed as previously described [18] using FAM/TAMRA-labelled fluorescent probes. RT primers listed in 5' to 3' orientation were: for glucokinase *(Gck)*, forward: GGTGCTTTTGAGACCCGTTTT, reverse: GA GTGCTCAGGATGTTAAGGATCTG, probe: TGTCGC AGGTGGAGAGCGACTCTG; and for glucose-6-phosphatase (*G6pc*) forward: ACTCTTGCTATCTTTCGAG GAAAGA, reverse: CCAACCACAAGATGACGTTCA, probe: AAAGCCAACGTATGGATTCCGGTGT. The relative amount of mRNA was calculated from an internal standard curve following normalisation to 18 S ribosomal RNA levels.

Hyperinsulinaemic clamp studies, whole-body glucose turnover rate, and tissue glycogen content

Hyperinsulinaemic clamp studies were performed as previously described [20]. In brief, under general anaesthesia, an indwelling catheter was placed into the left femoral vein, subcutaneously tunnelled and externalised in the interscapular region. The animals were allowed to recover for 5 days and fasted for 6 h on the day of the experiment. For 3 h D-[3-^{3}H]-glucose was infused at a rate of 11 mBq $kg^{-1}min^{-1}$ and insulin at a rate of 18 mU $kg^{-1}min^{-1}$. Euglycaemia was maintained by a variable infusion of 15% glucose. Whole blood was sampled from the tail every 10 min during the last hour for ^{3}H-Glucose enrichment, which was biochemically determined as follows. Samples were de-proteinised by precipitation with equal volumes (125 µl) of 0.1 mol/l $Ba(OH)_2$ and 0.1 mol/l $ZnSO_4$, followed by centrifugation for 5 min. Total radioactivity in the supernatant (from D-[3-^{3}H]-glucose and glycolysis-derived ^3H_2O) was measured by scintillation counting. A corresponding aliquot was evaporated to dryness to estimate D-[3-^{3}H]-glucose alone. Total glucose concentration was determined in a third aliquot by the glucose oxidase method (BioMerieux, Marcy l'Etoile, France). Glycogen content was determined in liver and quadriceps muscle using the amyloglucosidase method. In brief, tissues underwent alkaline hydrolysis at 55°C for 1 h (30 mg of liver in 200 µl 1 mol/l NaOH, 20 mg of muscle in 50 µl 1 mol/l NaOH). Equivalent volumes of 1 mol/l HCl were added for neutralisation and the samples spun at 340 g for 2 min. Aliquots of the glycogen-containing supernatant were incubated at 37°C for 1 h with α-amyloglucosidase (Roche Diagnostics) at a concentration of 0.01 mg/ml in 0.2 mol/l Na citrate buffer pH 4.8. The released glucose was determined by the glucose oxidase method (BioMerieux). Baseline hepatic glucose content was measured in an undigested aliquot and subtracted from the value obtained after α-amyloglucosidase incubation. Calculations of glucose turnover were made from parameters obtained during the last 60 min of the infusions under steady-state conditions as described previously [20].

Preparation of tissue extracts and immunoblot assays

Following an overnight fast, a bolus of insulin (5 IU) or vehicle was injected via the inferior vena cava of terminally anaesthetised mice. Tissues were removed and snap-frozen in liquid nitrogen and stored at −80°C until use. Tissues were homogenised in lysis buffer [18], solubilised for 30 min on ice and clarified by centrifugation. Supernatants were snap-frozen in aliquots and stored at −80°C. For Western blotting, 50 µg of total protein extract was immunoblotted with the indicated antibodies. For analysis of IRS protein levels and tyrosine phosphorylation or INSR β tyrosine phosphorylation, tissue extracts (2 mg of total protein) were immunoprecipitated for 2 h with the indicated antibodies. Immune complexes were collected with 100 µl of 50% slurry of protein-A or protein-G sepharose, washed with lysis buffer and resolved on 7.5% SDS-PAGE and transferred to nitrocellulose. The blots were probed with polyclonal antibodies against IRS2 and IRS1 or monoclonal antibody to antiphosphotyrosine and enhanced chemiluminescence (Amersham, Little Chalfont, UK) detection performed. Nuclear preparations were performed by homogenisation of liver samples in nuclear buffer [21] followed by centrifugation over a cushion of nuclear buffer with 1.2 mol/l sucrose and 5% glycerol. Nuclear pellets were re-suspended in nuclear buffer with 0.3 mol/l sucrose and 10% glycerol, purity analysed under a haematocytometer and aliquots frozen. Nuclear preparations were subsequently lysed in lysis buffer, solubilised for 5 min on ice, clarified by centrifugation, after which 50 µg of nuclear extract was immunoblotted with the indicated antibodies. Blots were stripped and re-probed with an antibody against zinc finger and BTB domain containing protein 16 (ZBTB16) as a nuclear loading control.

Antibodies

Sheep polyclonal antibodies to IRS1 and IRS2 were used as previously described [18]. Rabbit anti-IRS1, anti-IRS2, anti-phosphotyrosine (PY) (4G10) and anti-p85 antibodies were from Upstate Biotechnology (Dundee, UK). Anti-AKT, anti-pAKT^{Ser473}, anti-pp70S6K^{Thr389}, anti-glycogen synthase kinase (GSK)-3β, anti-pGSK3α/β$^{Ser9/21}$, anti-mitogen-activated protein kinase (MAPK), anti-pMAPK$^{Thr202/Tyr204}$, anti-forkhead box O1 (FOXO1) antibodies were from Cell Signalling Technology (Beverly, MA, USA) and anti-forkhead box A2 (FOXA2) antibody was a gift from R. I. Altaba (University of Geneva Medical School, Geneva, Switzerland). Anti-INSR β, and anti-p70^{S6K} antibodies were from Santa Cruz (Insight Biotechnology, Wembley, UK). Mouse anti-ZBTB16 was from Calbiochem-Novachem (San Diego, CA, USA). HRP-conjugated goat anti-rabbit antibody was from DAKO (Ely, UK) and HRP-conjugated sheep anti-mouse antibody was from Amersham Bioscience.

Statistical methods

All statistics were performed using GraphPad Prism4 software (Graphpad Software, San Diego, CA, USA) and paired and unpaired *t*-tests and two-way ANOVA with Bonferroni post-tests performed as appropriate. A p value of <0.05 was regarded as significant.

Results

Mice lacking *Irs2* in liver (*LivIrs2KO* mice)

LivIrs2KO mice were obtained with the expected Mendelian frequency and developed normally. To confirm the deletion of *Irs2* in liver, we performed Western blotting on IRS2 immunoprecipitates from *LivIrs2KO* and control

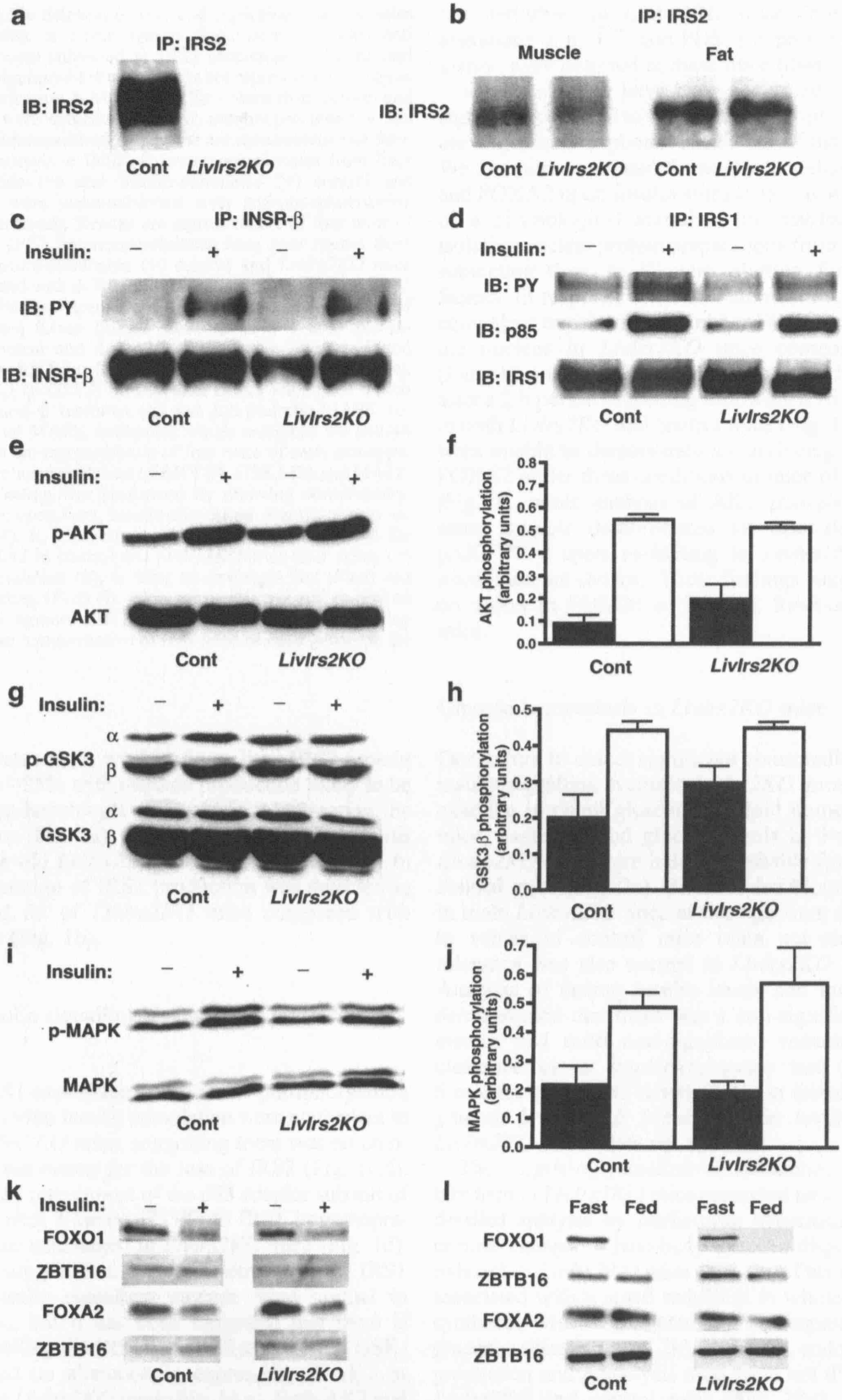
a
IP: IRS2
IB: IRS2
Cont
Livlrs2KO
b
IP: IRS2
Muscle
Fat
IB: IRS2
Cont
Livlrs2KO
Cont
Livlrs2KO
c
IP: INSR-β
Insulin:
– + – +
IB: PY
IB: INSR-β
Cont
Livlrs2KO
d
IP: IRS1
Insulin:
– + – +
IB: PY
IB: p85
IB: IRS1
Cont
Livlrs2KO
e
Insulin:
– + – +
p-AKT
AKT
Cont
Livlrs2KO
f
AKT phosphorylation (arbitrary units)
0.0
0.1
0.2
0.3
0.4
0.5
0.6
0.7
0.8
Cont
Livlrs2KO
g
Insulin:
– + – +
p-GSK3
α
β
GSK3
α
β
Cont
Livlrs2KO
h
GSK3 β phosphorylation (arbitrary units)
0.0
0.1
0.2
0.3
0.4
0.5
Cont
Livlrs2KO
i
Insulin:
– + – +
p-MAPK
MAPK
Cont
Livlrs2KO
j
MAPK phosphorylation (arbitrary units)
0.0
0.1
0.2
0.3
0.4
0.5
0.6
0.7
Cont
Livlrs2KO
k
Insulin:
– + – +
FOXO1
ZBTB16
FOXA2
ZBTB16
Cont
Livlrs2KO
l
Fast Fed Fast Fed
FOXO1
ZBTB16
FOXA2
ZBTB16
Cont
Livlrs2KO

◀ **Fig. 1** Liver-specific deletion of *Irs2* and signalling characteristics in *LivIrs2KO* mice. **a** Liver lysates from control (*Cont*) and *LivIrs2KO* mice were subjected to IRS2 immunoprecipitation and subsequent IRS2 immunoblotting. Results are representative of three independent experiments. **b** Muscle and fat lysates from control and *LivIrs2KO* mice were subjected to IRS2 immunoprecipitation and subsequent IRS2 immunoblotting. Results are representative of three mice of each genotype. **c** INSR β immunoprecipitates from liver lysates from saline (−) and insulin-stimulated (+) control and *LivIrs2KO* mice were immunoblotted with anti-phosphotyrosine (*PY*) or INSR β antibody. Results are representative of four mice of each genotype. **d** IRS1 immunoprecipitates from liver lysates from saline (−) and insulin-stimulated (+) control and *LivIrs2KO* mice were immunoblotted with 4G10 anti-phosphotyrosine (*PY*), anti-p85 or anti-IRS1 antibodies. Results are representative of four mice of each genotype. **e–j** Liver lysates from saline (−) and insulin-stimulated (+) control and *LivIrs2KO* mice were immunoblotted with anti-phospho AKT (*p-AKT*) or anti-total AKT antibodies **(e)**, anti-phosphoGSK3 (*p-GSK3*) or anti-total GSK3 antibodies which recognise the α and β isoforms **(g)** and anti-phospho-MAPK (*p-MAPK*) or anti-total MAPK antibodies which recognise the p42/44 isoforms **(i)**. Blots are representative of four mice of each genotype. Quantification of phosphorylation of AKT **(f)**, GSK3 **(h)** and MAPK **(j)** on Western blotting was performed by scanning densitometry. *Filled bars*, saline; *open bars*, insulin-stimulated. Results shown are means±SEM (n=4). **k, l** Hepatic nuclear extracts were blotted for FOXO1 and FOXA2 in control and *LivIrs2KO* mice after saline (−) or insulin (+) stimulation **(k)**, or after an overnight fast (*Fast*) and after 2 h of refeeding (*Fed*) **(l)**. Blots were stripped and re-probed with an antibody against ZBTB16 protein as a nuclear loading control. Results are representative of four mice of each genotype for each condition

mouse liver lysates. At 4 weeks of age, liver IRS2 protein was reduced by >95% with residual production likely to be occurring in non-hepatocyte cell types not expressing the *AlbCre* transgene (Fig. 1a). A similar level of deletion was seen in 12-week-old *LivIrs2KO* mice (data not shown). In contrast, no alteration of IRS2 production was detected in the muscle and fat of *LivIrs2KO* mice compared with control animals (Fig. 1b).

Analysis of insulin signalling pathways in *LivIrs2KO* mice

INSR β and IRS1 expression and tyrosine phosphorylation in response to in vivo insulin stimulation were equivalent in control and *LivIrs2KO* mice, suggesting there was no compensation by these events for the loss of IRS2 (Fig. 1c,d). Insulin-stimulated recruitment of the p85 adaptor subunit of phosphatidylinositol 3-kinase (PI3K) to IRS1 immunoprecipitates was also unchanged in *LivIrs2KO* mice (Fig. 1d). These findings suggest that proximal elements of the IRS1 limb of the insulin signalling cascade were normal in *LivIrs2KO* mice, but it has been suggested that there is differential signalling via IRS1 and IRS2 to AKT and GSK-3β. We detected no alteration in expression of AKT or GSK3α/β in the *LivIrs2KO* mice (Fig. 1e,g). Both AKT and GSK3β basal phosphorylation was mildly elevated in *LivIrs2KO* mice, but there was no defect in insulin-stimulated phosphorylation of either of these kinases (Fig. 1e–h). MAPK expression and phosphorylation were not perturbed in *LivIrs2KO* mice (Fig. 1i,j), and no alterations in $p70^{S6K}$ and PDK-1 expression and phosphorylation were detected in these mice (data not shown).

IRS1 and IRS2 have been suggested to have different signalling potential to forkhead transcription factors, which are major transcriptional mediators of insulin action [22]. We therefore examined the nuclear localisation of FOXO1 and FOXA2 upon insulin stimulation, as well as the effects of a physiological stimulus, the fast/fed transition, by isolating nuclear protein preparations from liver lysates and subjecting them to Western blotting for both of these factors. In response to insulin stimulation, we detected an equivalent translocation of either FOXO1 or FOXA2 from the nucleus in *LivIrs2KO* mice compared to controls (Fig. 1k). Likewise, FOXO1 translocated from the nucleus after a 2-h period of feeding following a 16-h overnight fast in both *LivIrs2KO* and control mice (Fig. 1l). However, we were unable to demonstrate a convincing translocation of FOXA2 under these conditions in mice of either genotype (Fig. 1), while analysis of AKT phosphorylation in the same animals demonstrated an equivalent increase in $pAKT^{Ser473}$ upon re-feeding in *LivIrs2KO* and control mice (data not shown). These findings suggest that there is no defect in FOXO1 or FOXA2 function in *LivIrs2KO* mice.

Glucose homeostasis in *LivIrs2KO* mice

Our failure to detect significant abnormalities in proximal insulin signalling events in *LivIrs2KO* mice prompted us to examine in detail glucose and lipid homeostasis in these mice. Fasting blood glucose levels in 3-month-old male *LivIrs2KO* mice were indistinguishable from those seen in control mice (Fig. 2a). Random fed blood glucose levels in male *LivIrs2KO* mice at this age were also comparable to values in control mice (data not shown). Glucose tolerance was also normal in *LivIrs2KO* mice (Fig. 2b). Analysis of fasting insulin levels and insulin sensitivity demonstrated that there was a non-significant increase in insulin and mild non-significant reduction in glucose clearance in an insulin tolerance test (Fig. 2c,d). At 6 months of age, no deterioration in fasted and fed blood glucose levels and fasting insulin levels was seen in *LivIrs2KO* mice (data not shown).

The surprisingly modest abnormalities in glucose metabolism in *LivIrs2KO* mice prompted us to undertake more detailed analysis by performing hyperinsulinaemic-euglycaemic clamps. Whole-body glucose disposal was mildly reduced in *LivIrs2KO* mice (Fig. 2e). This impairment was associated with a small reduction in whole-body glycogen synthesis, which accounted for the impaired whole-body glucose utilisation (Fig. 2h). However, endogenous glucose production and glycolysis rates were not different between *LivIrs2KO* and control mice (Fig. 2f,g). These findings suggest that *LivIrs2KO* mice have a very mild defect in whole-body insulin sensitivity, which is unlikely to be detected by glucose and insulin tolerance tests, and also does not impact on long-term glucose homeostasis.

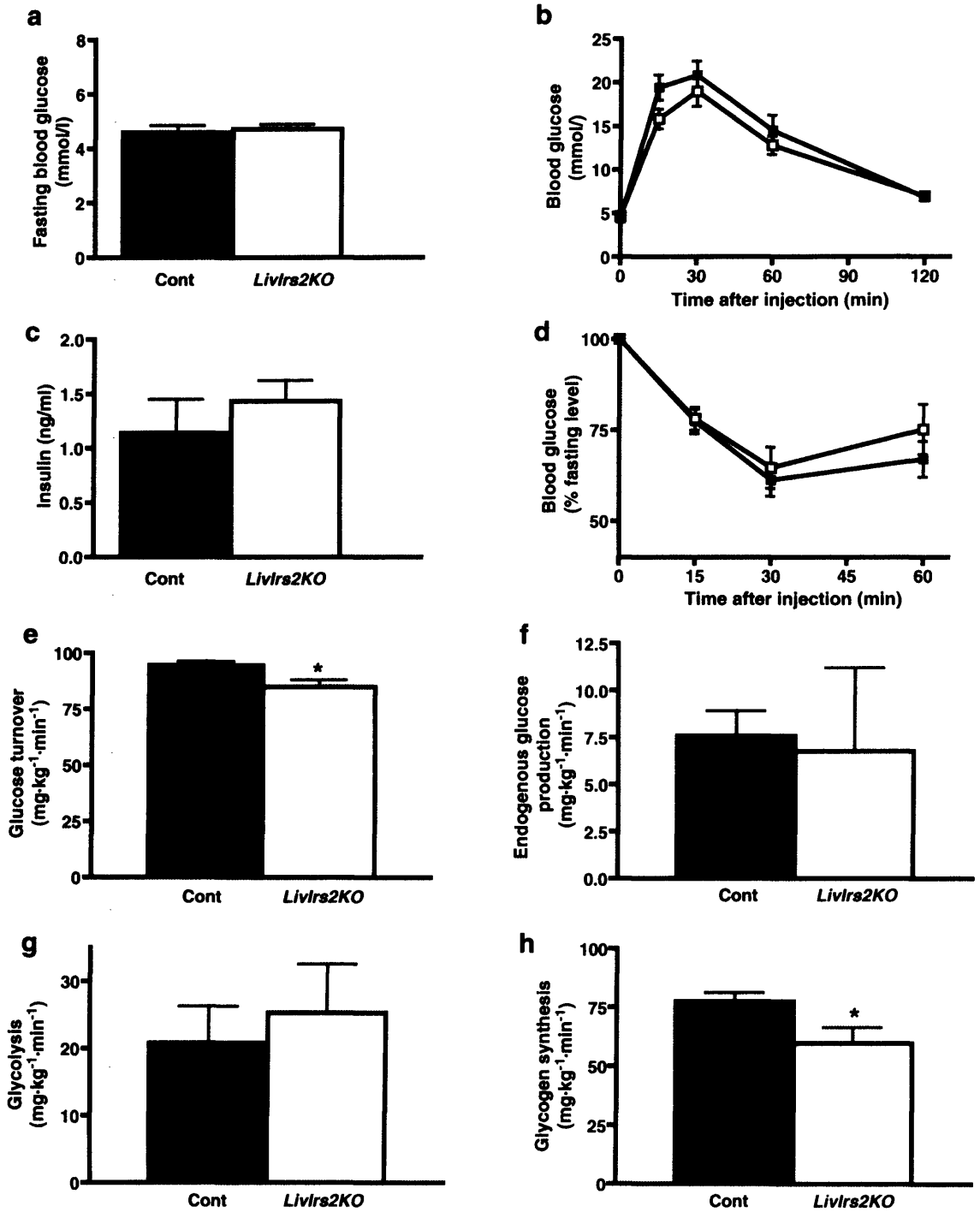

Fig. 2 Glucose homeostasis in *Livlrs2KO* mice. **a** Fasting blood glucose levels were determined on male control and *Livlrs2KO* mice at 3 months of age. Data represent the mean±SEM for six to eight animals of each genotype. **b** Glucose tolerance tests were performed on male control (*closed squares*) and *Livlrs2KO* mice (*open squares*) at 3 months of age. Data represent the mean±SEM for six to eight animals of each genotype. **c** Fasting blood insulin levels were measured on male control and *Livlrs2KO* mice at 3 months of age. Data represent the mean±SEM for six to eight animals of each genotype. **d** Insulin tolerance tests (0.75 IU/kg) were performed on 3-month-old male control (*closed squares*) and *Livlrs2KO* mice (*open squares*). Results represent blood glucose concentration as a percentage of starting value at time 0 and are expressed as mean± SEM (n=8). **e–h** Hyperinsulinaemic–euglycaemic clamps were performed on conscious mice of the indicated genotypes to determine glucose turnover (**e**), endogenous glucose production (**f**), glycolysis (**g**) and glycogen synthesis rates (**h**). Data represent the mean±SEM for eight to nine animals of each genotype. *p<0.05

Lipid homeostasis and response to high-fat diet in *LivIrs2KO* mice

IRS2 signalling may play a predominant role in hepatic lipid metabolism rather than glucose homeostasis [6], and therefore we assessed a number of parameters of whole-body lipid homeostasis in *LivIrs2KO* mice on normal chow. In both the fasted and fed states NEFA were comparable in *LivIrs2KO* and control mice (Fig. 3a). No differences in serum and liver tissue triglyceride levels were found in *LivIrs2KO* and control mice, either in the fed or fasted conditions (Fig. 3b,c and data not shown). We also found no differences in fasting leptin levels between *LivIrs 2KO* and control animals (Fig. 3d). Serum adiponectin levels were non-significantly elevated in *LivIrs2KO* mice compared with control animals (control, 6.98±0.94 μg/ml vs *LivIrs2KO*, 9.3±1.1 μg/ml, n=17, p=NS). Dual emission X-ray absorptiometry scanning at 6 months of age did not reveal alterations in fat mass in *LivIrs2KO* mice (data not shown). Taken together, these findings suggest that defects

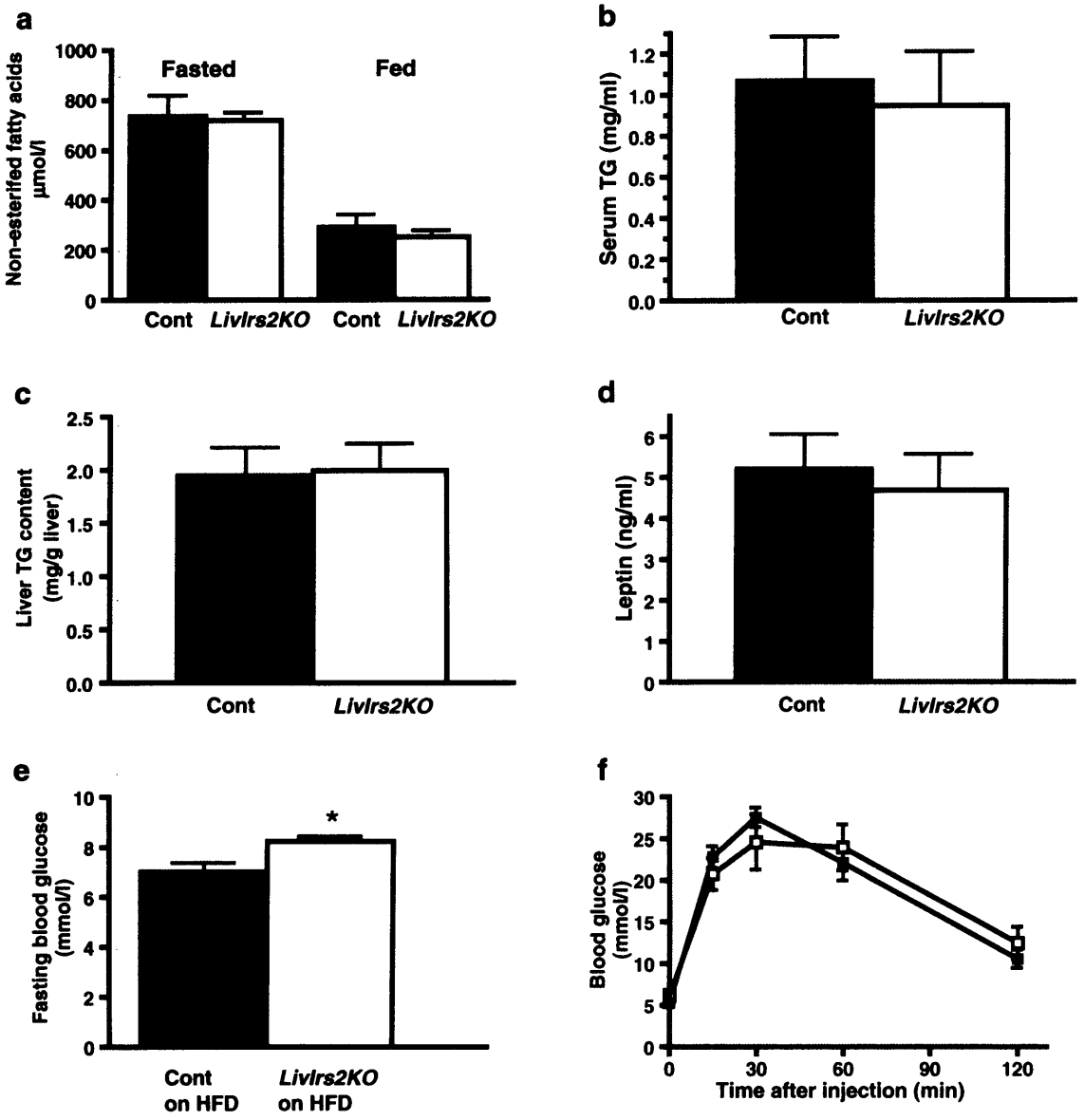

Fig. 3 Assessment of lipid metabolism and high-fat feeding in *LivIrs2KO* mice. **a** Fasted and fed serum NEFA levels were determined in 12-week-old male control and *LivIrs2KO* mice. Data represent the mean±SEM for five animals of each genotype. **b** Fed serum triglycerides (TG) in 12-week-old male control and *LivIrs2KO* mice. Data represent the mean±SEM for six animals of each genotype. **c** Triglyceride levels in liver extracts from fed 12-week-old male control and *LivIrs2KO* mice. Data represent the mean±SEM for six animals of each genotype. **d** Serum leptin levels in fasting 6-month-old male control and *LivIrs2KO* mice. Data represent the mean±SEM for five animals of each genotype. **e** Fasting blood glucose levels in 6-month-old male mice of the indicated genotypes after 3 months on a high-fat diet. Data represent the mean±SEM for four to six animals of each genotype. **f** Glucose tolerance tests were performed on 6-month-old male control (*closed squares*) and *LivIrs2KO* mice (*open squares*) after 3 months on a high-fat diet. Data represent the mean±SEM for six animals of each genotype. *p<0.05

in hepatic lipid homeostasis and fat storage in *LivIrs2KO* mice are minimal.

Hepatic insulin resistance is involved in the development of the metabolic syndrome induced by increased fat intake [23]. Therefore, we next assessed the effects of a high-fat diet upon glucose homeostasis in *LivIrs2KO* mice. Control and *LivIrs2KO* male mice fed a diet consisting of 45% fat for 3 months gained on average 25% more weight than mice on normal chow (data not shown). However, while fasting blood glucose levels in *LivIrs2KO* mice were mildly higher than in control mice (Fig. 3e), glucose tolerance was not significantly different (Fig. 3f). Fasting insulin levels and serum and liver triglyceride levels were similar in both control and *LivIrs2KO* mice subjected to high-fat diet (data not shown). These findings suggest that a high-fat diet does not result in greater insulin resistance in *LivIrs2KO* mice than in control animals.

Liver function in *LivIrs2KO* mice

Since *LIRKO* mice have been reported to display progressive liver dysfunction [7], we performed liver function tests in *LivIrs2KO* mice. At 3 months of age, albumin and bilirubin levels were indistinguishable between male control and *LivIrs2KO* (Fig. 4a). Aspartate amino-transferase and alanine amino-transferase levels were both elevated in *LivIrs2KO* mice, while alkaline phosphatase levels were not (Fig. 4b). *LivIrs2KO* mice remained healthy beyond 12 months of age and did not develop clinical evidence of progressive liver dysfunction such as oedema or morphological abnormalities in the liver (data not shown).

Hepatic gene and protein expression in *LivIrs2KO* mice

Insulin regulates hepatic metabolism partly by regulating the expression of key metabolic genes in glucose and lipid metabolism. RT-PCR analysis of liver mRNA expression revealed that in the fasted state, *Gck* expression was mildly reduced in *LivIrs2KO* mice, although in the fed state no difference was found (Fig. 4c). *G6pc* expression was mildly increased in fasted *LivIrs2KO* mice, but in the fed state no difference was found (Fig. 4d). In contrast RNA expression of a panel of other hepatic metabolic genes (notably *Pck1*, *Fasn*, *Srebf1a* and *1c*, *Acaca*, *Ppara* and *Ppargl*, *Cpt1a*, *Ppargc1b* and *Igfbp1*) were unaltered in *LivIrs2KO* mice either in the fasted or fed state (data not shown). Therefore deletion of *Irs2* in the liver had no significant effect on a number of insulin-regulated transcriptional events.

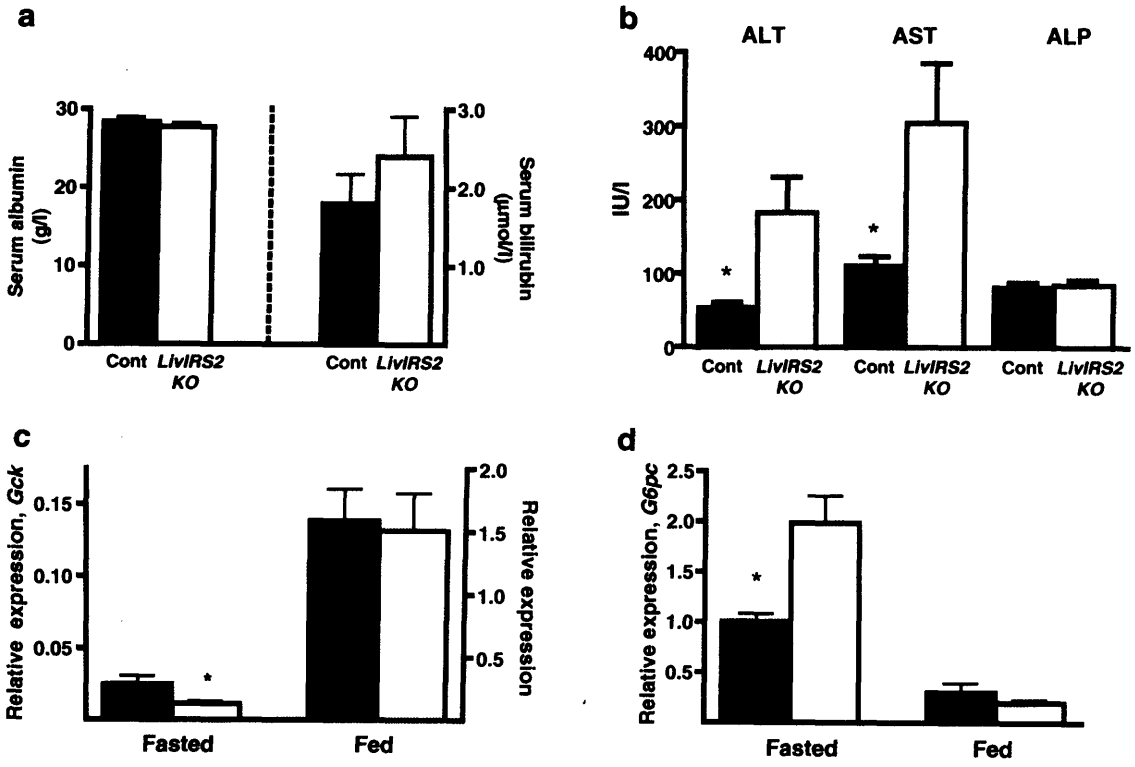

Fig. 4 Liver function tests and gene expression in *LivIrs2KO* mice. **a** Serum albumin (*left*) and bilirubin (*right*) levels in fasting 12-week-old male control and *LivIrs2KO* mice. Data represent the mean±SEM for six animals of each genotype. **b** Serum aspartate amino-transferase (*AST*), alanine amino-transferase (*ALT*) and alkaline phosphatase (*ALP*) levels in fasting 12-week-old male control and *LivIrs2*KO mice. Data represent the mean±SEM for six animals of each genotype. Hepatic glucokinase (*Gck*) (**c**) and glucose-6-phosphatase (*G6pc*) (**d**) mRNA expression in fasted and fed 12-week-old male control (*closed bars*) and *LivIrs2KO* (*open bars*) mice was determined by RT-PCR. Data represent the mean±SEM for five animals of each genotype. *$p<0.05$

Discussion

LivIrs2KO mice displayed no marked alteration in insulin receptor, IRS1 and downstream PI3K-dependent signalling events in the liver. These observations contrast with findings in mice with global deletion of *Irs2* and in *Irs2*-null transformed hepatic cell lines derived from neonatal mice. In both these models there are abnormalities in signalling events downstream of the insulin receptor. From our studies, however, it is clear that the chronic deletion of *Irs2* in the liver appears to have minimal effects upon proximal insulin signalling events in vivo. The transcription factors FOXO1 and FOXA2 are thought to play distinct roles in the regulation of hepatic carbohydrate and lipid metabolism. FOXO1, which predominantly regulates gluconeogenesis, has been reported to be phosphorylated only by the IRS2 signalling limb while FOXA2, which regulates fatty acid oxidation, was phosphorylated in response to both IRS1 and IRS2 signalling pathways [22]. However, these in vitro findings were not confirmed by our studies. In the absence of liver *Irs2*, FOXO1 translocation both in response to insulin and refeeding was normal. FOXA2 translocation in response to insulin was also comparable to that seen in control animals. Therefore, these results do not support the idea that IRS2 preferentially signals to FOXO1.

Consistent with the normal hepatic insulin signalling events, *LivIrs2KO* mice on a regular diet displayed minimal abnormalities of glucose homeostasis up to and beyond 6 months of age, which contrasts with the marked and progressive diabetes observed in *Irs2* global null mice [12]. Although we did detect decreased expression of *Gck* and increased expression of *G6pc* in the livers of fasted *LivIrs2KO* mice, suggesting some minor dysregulation of insulin-regulated gene expression in the fasted state, we did not find abnormalities in the expression of these enzymes in the fed state, suggesting that they are appropriately regulated by insulin. Interestingly, *Irs2* expression is high in the fasted state and markedly reduced by feeding and by increased insulin levels [10], and perhaps IRS2 in the liver serves to predominantly regulate the expression of particular genes in the fasted state. Taken together, these findings suggest that IRS2-dependent pathways are not essential for the long-term regulation of glucose homeostasis.

Recent studies have suggested that hepatic IRS2 is particularly involved in the regulation of lipid metabolism. RNAi knockdown of *Irs2* resulted in increased levels of the transcription factor SREBF1c and this was associated with mildly increased serum NEFA and triglyceride levels and mild hepatic steatosis [6]. Others have demonstrated a reciprocal relationship between IRS2 function and the expression of *Srebf1c* [10, 11]. We found that hepatic deficiency of IRS2 had no effects upon circulating NEFA and triglyceride or on hepatic triglyceride levels. Likewise, we found no alterations in the expression of key hepatic transcription factors and enzymes involved in the regulation of lipid metabolism or of leptin levels or of total body fat stores. We also found no differences in glucose and lipid homeostasis between *LivIrs2KO* and control mice while on a high-fat diet. These findings suggest that hepatic IRS2-dependent signalling events are not required for the long-term in vivo maintenance of hepatic lipid homeostasis.

The differences between our observations and those of others may be explained by a number of methodological and physiological factors. Differences between global and conditional deletion may reflect developmental events and are potentially related to both the timing of *Irs2* deletion as well as to the contribution of other tissues to the phenotype. *AlbCre* mice are reported to delete floxed alleles completely and this may occur at several weeks of age post-natally [19]. We found complete deletion of *Irs2* by 4 weeks of age and our subsequent physiological studies were performed on mice at older ages. Studies in immortalised cell lines do not reflect the in vivo physiological situation; moreover, the hepatocyte cell lines reported were derived from neonatal mice with germ-line deletion of either *Insr* or *Irs2* [16, 17]. For the studies involving the disruption of *Irs2* expression by RNAi, the knockdown was both relatively short-term lasting no more than 5 days and was incomplete, with a persistent 40% residual *Irs2* expression evident [6]. In contrast, our studies involve long-term complete deletion of *Irs2*, which may permit compensatory mechanisms to develop. However, we saw no increased expression of insulin signalling components in the liver and no alterations of *Irs2* expression in other tissues. Furthermore, in the *Irs2* RNAi knock-down there was an alteration in adipose tissue function, which was not apparent in our studies, but may explain the abnormalities seen in hepatic lipid homeostasis. The mechanism for this effect was not determined but it is clear that systemic as opposed to tissue-specific delivery of RNAi may abrogate gene expression in other tissues in addition to the liver [5]. Unfortunately, *Irs2* expression in adipose tissue was not reported in the liver *Irs2* RNAi model. Since insulin positively regulates lipogenesis, disruption of insulin receptor function via down-regulation of IRS signalling in the liver alone might be expected to reduce rather than increase lipogenesis. Indeed, this is seen in *LIRKO* mice and in mice with knock-down of liver *Insr* expression by anti-sense oligonucleotide [5, 7]. The mechanism of increased lipogenesis in *Irs2* RNAi knock-down mice is probably due to extra-hepatic effects or to residual insulin signalling in the liver. Our findings also call into question the suggestion that there is a physiologically relevant reciprocal relationship between IRS2 and regulators of lipid homeostasis such as SREBF1c [10, 11]. These findings were largely derived from in vitro models and in vivo models with systemic deletion of *Irs2* or with complex multi-tissue metabolic abnormalities such as *ob/ob* and lipodystrophic mice, and this may explain the differences between our observations and those of others.

Recent data from two distinct mouse models have suggested that insulin regulates hepatic metabolism largely through indirect means rather than through the liver insulin receptor and this provides a physiological explanation why *LivIrs2KO* mice have a minimal phenotype [4, 5]. While

these recent findings are at odds with those generated by studies on the *LIRKO* mice, this latter model has marked defects in hepatic function and insulin clearance that impinge upon insulin action in other tissues and may explain the differences in phenotype. Our observations in *LivIrs2 KO* mice are consistent with the idea that insulin signalling pathways are not required for the direct regulation of hepatic metabolism. While we have not abrogated other insulin receptor signalling pathways through this manipulation, hepatic *Irs2* is not required for the long-term maintenance of many aspects of hepatic function. Recently we showed that mice lacking *Irs2* only in the central nervous system develop insulin resistance and impaired glucose homeostasis, and we are exploring hepatic metabolism in this model, as it is likely that central nervous system IRS2 pathways contribute to the regulation of hepatic metabolism [18]. These findings together with those of others suggest that in mice, central nervous system pathways and other indirect effects may be the predominant mechanisms by which insulin signalling regulates hepatic metabolism.

In summary, through the generation of *LivIrs2KO* mice we have demonstrated that IRS2 signalling events in the liver are not required for the regulation of hepatic metabolism.

Acknowledgements This work was supported by grants from the Wellcome Trust (to M. Simmgen, A. Choudhury, M. Charalambous, A. Vidal-Puig and D. J. Withers), from Diabetes UK (to J. Cantley and D. Bedford), from the Medical Research Council (to A. Vidal-Puig and D. J. Withers) and from the Biotechnology and Biological Sciences Research Council (to M. Claret and H. Heffron). The work was in part performed in the Integrative Physiology Consortium for the Study of Common Metabolic Disease, which is supported by the Wellcome Trust Integrative Physiology programme (to A. Vidal-Puig), and in the Biological Atlas of Insulin Resistance (BAIR) consortium, which is supported by the Wellcome Trust Functional Genomics programme (to D. J. Withers). M. Simmgen is a Wellcome Trust Training Fellow.

References

1. DeFronzo RA (1997) Pathogenesis of type 2 diabetes: metabolic and molecular implications for identifying diabetes genes. Diabetes Reviews 5:177–268
2. Tripathy D, Eriksson KF, Orho-Melander M, Fredriksson J, Ahlqvist G, Groop L (2004) Parallel manifestation of insulin resistance and beta cell decompensation is compatible with a common defect in Type 2 diabetes. Diabetologia 47:782–793
3. Cherrington AD (2005) The role of hepatic insulin receptors in the regulation of glucose production. J Clin Invest 115:1136–1139
4. Okamoto H, Obici S, Accili D, Rossetti L (2005) Restoration of liver insulin signaling in Insr knockout mice fails to normalize hepatic insulin action. J Clin Invest 115:1314–1322
5. Buettner C, Patel R, Muse ED et al (2005) Severe impairment in liver insulin signaling fails to alter hepatic insulin action in conscious mice. J Clin Invest 115:1306–1313
6. Taniguchi CM, Ueki K, Kahn R (2005) Complementary roles of IRS-1 and IRS-2 in the hepatic regulation of metabolism. J Clin Invest 115:718–727
7. Michael MD, Kulkarni RN, Postic C et al (2000) Loss of insulin signaling in hepatocytes leads to severe insulin resistance and progressive hepatic dysfunction. Mol Cell 6:87–97
8. Fisher SJ, Kahn CR (2003) Insulin signaling is required for insulin's direct and indirect action on hepatic glucose production. J Clin Invest 111:463–468
9. Withers DJ (2001) Insulin receptor substrate proteins and neuroendocrine function. Biochem Soc Trans 29:525–529
10. Shimomura I, Matsuda M, Hammer RE, Bashmakov Y, Brown MS, Goldstein JL (2000) Decreased IRS-2 and increased SREBP-1c lead to mixed insulin resistance and sensitivity in livers of lipodystrophic and *ob/ob* mice. Mol Cell 6:77–86
11. Suzuki R, Tobe K, Aoyama M et al (2004) Both insulin signaling defects in the liver and obesity contribute to insulin resistance and cause diabetes in Irs2(−/−) mice. J Biol Chem 279:25039–25049
12. Withers DJ, Gutierrez JS, Towery H et al (1998) Disruption of IRS-2 causes type 2 diabetes in mice. Nature 391:900–904
13. Kubota N, Tobe K, Terauchi Y et al (2000) Disruption of insulin receptor substrate 2 causes type 2 diabetes because of liver insulin resistance and lack of compensatory beta-cell hyperplasia. Diabetes 49:1880–1889
14. Previs SF, Withers DJ, Ren JM, White MF, Shulman GI (2000) Contrasting effects of IRS-1 versus IRS-2 gene disruption on carbohydrate and lipid metabolism in vivo. J Biol Chem 275:38990–38994
15. Zhang J, Ou J, Bashmakov Y, Horton JD, Brown MS, Goldstein JL (2001) Insulin inhibits transcription of *IRS-2* gene in rat liver through an insulin response element (IRE) that resembles IREs of other insulin-repressed genes. Proc Natl Acad Sci USA 98:3756–3761
16. Rother KI, Imai Y, Caruso M, Beguinot F, Formisano P, Accili D (1998) Evidence that IRS-2 phosphorylation is required for insulin action in hepatocytes. J Biol Chem 273:17491–17497
17. Valverde AM, Burks DJ, Fabregat I et al (2003) Molecular mechanisms of insulin resistance in IRS-2-deficient hepatocytes. Diabetes 52:2239–2248
18. Choudhury AI, Heffron H, Smith MA et al (2005) The role of insulin receptor substrate 2 in hypothalamic and beta cell function. J Clin Invest 115:940–950
19. Postic C, Shiota M, Niswender KD et al (1999) Dual roles for glucokinase in glucose homeostasis as determined by liver and pancreatic beta cell-specific gene knock-outs using Cre recombinase. J Biol Chem 274:305–315
20. Perrin C, Knauf C, Burcelin R (2004) Intracerebroventricular infusion of glucose, insulin, and the adenosine monophosphate-activated kinase activator, 5-aminoimidazole-4-carboxamide-1-beta-D-ribofuranoside, controls muscle glycogen synthesis. Endocrinology 145:4025–4033
21. Otte K, Choudhury D, Charalambous M, Engstrom W, Rozell B (1998) A conserved structural element in horse and mouse *IGF2* genes binds a methylation sensitive factor. Nucleic Acids Res 26:1605–1612
22. Wolfrum C, Asilmaz E, Luca E, Friedman JM, Stoffel M (2004) Foxa2 regulates lipid metabolism and ketogenesis in the liver during fasting and in diabetes. Nature 432:1027–1032
23. Kim SP, Ellmerer M, Van Citters GW, Bergman RN (2003) Primacy of hepatic insulin resistance in the development of the metabolic syndrome induced by an isocaloric moderate-fat diet in the dog. Diabetes 52:2453–2460